THE UNIVERSITY
of EDINBURGH

Engineering Functional Kidney Tissue Using Human iPS cells

By

Mona Elhendawi

A Thesis submitted in fulfilment of the requirement for the degree of Doctor of Philosophy

The University of Edinburgh

2020

Declaration:

I confirm that the work presented in this thesis is my own and that it has not been submitted in any previous application for a degree. Except where stated otherwise by reference or acknowledgement, the presented work is my own.

Mona Elhendawi

Acknowledgement

First and foremost, I would like to thank Allah for being with me and helping me through all my steps and giving me the strength and patience to finish my thesis.

I would like to express my sincere appreciation to Professor Jamie Davies, for giving me the chance to join his lab and undertake such a challenging project. I would like to thank him for his continuous guidance and support during my study. I would also like to deeply thank my second supervisor Professor Norah Spears for her support, time and guidance during the project. I would like to show my appreciation to all current and former members of Jamie Davies lab for their advice and suggestions. I worked in collaboration with Dr Melanie Lawrence and Weijia Liu for part of my project. Dr Alazne Dominguez gave me advice on planning CRISPR/Cas9 experiment. I have had many useful discussions with Dr Elise Cachat, Dr. Christopher Mills, Dr. Amnah Alharbi and Julia Tarnick.

I would like to thank the Egyptian Cultural Affairs and Missions sector for funding this work. I would like to thank my professors and colleagues in the Clinical Pathology department, Mansoura University, Egypt who motivated me to undertake this project.

I must thank my sisters Mariam, Fatma and Asmaa; my brother Ahmad; and my friends Amnah, Asmaa and Hala for supporting me and helping me during my tough times.

My beloved husband; Yasser, I cannot thank you enough for all your love, patience and support. I consider myself blessed to have you in my life.

My parents, my gratitude to you is beyond the ability of my words to express. You have offered me limitless love and support throughout my life. Thank you for everything; I love you from all my heart.

My dear sons, Ammar, Ali and Omar, I apologise that you had to take that stress with me, but I want you to know that you have been my biggest source of support. Your small true love's hugs were my biggest motive to finish this work. Love you to the moon and back infinity times.

Abstract:

Recent advances in the field of stem cell research have enabled the derivation of renal organoids from hiPSCs; these organoids might be a powerful tool with important implications for regenerative medicine, but meticulous assessment of the functional abilities of the induced nephrons is key to the use of these organoids in any application. Here, I show that hiPSC-derived renal organoids possess proximal tubular transporters and receptors; I present optimised techniques to assess the function of these receptors in-vitro and show that these organoids have anion and cation uptake capacities similar to what can be seen in foetal kidney tissue or isolated proximal tubules, implying tubular functional capacity, an aspect of renal physiology that has particular importance in the renal handling of drugs and toxins.

Due to high blood flow and the primary role of the kidney in clearing toxins and metabolites, renal cells are highly vulnerable to drug toxicity. The lack of in-vitro high throughput models to screen pharmaceutical compounds for potential nephrotoxicity during drug development has always hindered the field of drug development and increased the cost of delivering drugs into the market; in this study, I demonstrate that hiPSCs-derived renal organoids are able to predict nephrotoxicity with reasonable accuracy. Combining this ability with the possibility of cryopreserving renal-differentiated cells and to the use of HMOX1 reporter cell line, to detect oxidative stress, could streamline the use of these organoids in nephrotoxicity screening and could potentially flourish the field of drug development.

While the current model of renal organoids could be used for drug screening without further manipulation, the use of such tissue for therapeutic purposes necessitates a higher degree of organisation and complexity. In-vivo kidney function is based on the complex interplay of a range of highly specialised cells together with their three-dimensional structure and organisation. Scientists are adopting different strategies to build kidney tissue, from hiPSCs, that could be suitable for use in therapeutic applications. Common to any of these strategies is the need to generate the correct cell types in sufficient numbers and purity, and most important, in the right location. I aim in this study to isolate correctly differentiated ureteric bud (UB) structures from surrounding cells and to induce branching from single UB-like structure to recapitulate branching morphogenesis in-vitro. I conjugated GDNF protein to a fluorophore and

used it to label the UB structures and isolate them. I show that the combination of GDNF, FGF1, CHIR99021 and RA was able to induce branching in the isolated UB-like structures. The ability to isolate pure differentiated UB structures from surrounding contaminant tissue and to induce them to branch forming contiguous collecting duct tree could be a step further towards engineering a more realistic kidney tissue with single continuous collecting duct system, yet optimising culture conditions and techniques to build such a tissue is still needed.

Lay abstract

Current advances in stem cell research have had considerable impact on the field of regenerative medicine and raised the hope that obtaining lab-grown organs might be possible one day. Recent research has enabled the generation of miniature kidney-like structure from stem cells, albeit with poor overall structural organisation. The function of these structures, has not, however, been evaluated; I have conducted experiments to examine some functional aspects of these structures to evaluate how similar they are compared to the normal organ; I show that the mini kidney-like tissue is not only structurally similar to the kidney tissue, but it can also perform some of the function of a kidney.

Kidneys are normally at high risk of drug toxicity; due to the lack of proper models to test the toxic potential of pharmaceutical compounds before getting access to the market, the process of drug development becomes very expensive and slow; I demonstrate that these kidney-like structures, being structurally and functionally similar to the kidney, might be a useful high throughput in-vitro model for predicting nephrotoxicity and thus could enhance the process of drug development and help in protection against one of the major causes of renal failure; drug toxicity.

Our kidneys are complex organs comprised of a variety of different types of cells, the intricate arrangement of which is crucial for the proper function of the organ in-vivo; for example for a kidney to function in a normal way, the excretory part of the kidney should be connected all through the organ and it should lead to a single exit path through which the urine comes out of the kidney. Despite showing structural and functional similarity to the kidney tissue, the miniature kidney-like structures that could be obtained from stem cells so far lack that intricate 3D macroscale organisation; one main pre-requisite for the use of these structures in therapeutic purposes is the ability to obtain pure cell types to arrange them in a realistic way. For that purpose, I developed a technique to isolate cells responsible for forming the excretory part of the kidney, the collecting duct system, and developed technique to evaluate the ability of the isolated cells to grow into single, branching and contiguous collecting duct tree, like what we see in a normal organ. These developed techniques could be one way to obtain pure collecting duct cells and thus might be a step toward organising the current model of stem cell derived kidney-like tissue.

Contents

Abbreviations

AIM	Anterior intermediate mesoderm
AQP1	Aquaporin1
ASP	4-(4-Dimethylaminostyryl)-1-methylpyridinium iodide
ATP	Adenosine triphosphate
BMP	Bone morphogenetic protein
BSA	Bovine serum albumin
CAA	Chloroacetaldehyde
CD	Collecting duct
CDH1	Cadherin 1 (Ecadherin)
CDS	coding sequence
Cited1	Cbp/p300-interacting transactivator 1
CM	Cap mesenchyme
COX	Cyclo-oxygenase
CS	Carnegie stage
DAPI	4′,6-diamidino-2-phenylindole
DCT	Distal convoluted tubule
DMEM	Dulbecco's modified eagle medium
DMSO	Dimethyl sulfoxide
DNA	Deoxyribonucleic acid
DSB	Double-strand DNA break
E8 medium	Essential 8 Medium
EB	Embryoid bodies
EC	Embryonal carcinoma cells
EG	Embryonal germ cells
EGF	Epidermal growth factor
EPCAM	Epithelial cell adhesion molecule
ER	Endoplasmic reticulum
ERK	Extracellular signal regulated kinase
ESCs	Embryonic stem cells
FACS	Fluorescence-activated cell sorting
FBS	Fetal bovine serum
FGFRs	Fibroblast growth factor receptors
FGFs	Fibroblast growth factors
FIAU	1-(-2-deoxy-2-fluoro-1-b-D-arabino-furanosyl)-5-iodouracil
FOXD1	Forkhead Box D1
GBM	Glomerular basement membrane
GDNF	Glial derived neurotropic factor
GFR	Glomerular filtration rate
GFRM	Growth factor reduced Matrigel

GO	Gene ontology
gRNA	Guide RNA
GSH	Glutathione
GSK-3	Glycogen synthase kinase-3
HDR	Homology Directed Repair
hESCs	Human embryonic stem cells
HGF	Hepatocyte growth factor
hiPSCs	Human induced pluripotent stem cells
hiUBs	hiPSCs-derived UBs
HMOX1	Heme oxygenase1
HOX	Homeobox containing gene
ICM	Inner cell mass
IL	Interleukin
IM	Intermediate mesoderm
INHBE	Inhibin Subunit Beta E
iPSCs	Induced pluripotent stem cells
JAK	Janus Kinase
JAG1	Jagged 1 protein
KIM	Kidney injury molecule
LDN	Low dose naltrexone
LHX1	LIM Homeobox1
LIF	Leukemia inhibitory factor
LTA	Lipoteichoic acid
LTL	Lotus tetragonolobus lectin
MATE	Multi drug and toxin extrusion transporter 1
MATE2K	human kidney-specific multidrug and toxin extrusion transporter
MEFS	Mouse embryonic fibroblasts
MESC	Mouse embryonic stem cell
MET	Mesenchymal-to-epithelial transition
miUBs	Induced mESC-derived UBs
MM	Metanephric mesenchyme
mRNA	Messenger RNA
MRP	multidrug-associated resistance proteins
NCAM	Neural cell adhesion molecule
NEPH1	Nephrin-like protein
NHEJ	Nonhomologous End joining
NP	Nephron progenitor
NPHS1	Nephrin
NSAID	Non-steroidal anti-inflammatory
nm	Nanometre
OATP	Organic anion transporter polypeptides
OATs	Organic anion transporters

OCT4	Octamer-binding transcription factor 4
OCTN	Organic cation/carnitine transporter
OCTs	Organic cation transporters
OSR	Odd skipped related
PAM	Protospacer adjacent motif
PAX	Paired box
PCR	Polymerase chain reaction
PFA	Paraformaldehyde
PIM	Posterior intermediate mesoderm
PNA	Peanut agglutinin
PS	Primitive streak
Puro	Puromycin N-acetyltransferase
RA	Retinoic acid
RARs	Retinoic acid receptors
RET	Receptor tyrosine kinase
RNA	Ribonucleic acid
RNA-Seq	RNA sequencing
ROCK	Rho-associated kinase
ROS	radical oxygen species
RT-PCR	Reverse transcription polymerase chain reaction
SIX	Sine oculis related homeobox
SLC	Solute carrier family
∧Tk	Truncated version of herpes simplex virus type 1 thymidine kinase
TGF-β	Transforming growth factor beta
TIMP-1	Tissue inhibitors of metalloproteinase-1
TPA	Tetrapentylammonium
UB	Ureteric bud
URAT1	Uric Acid Transporter1
UV	Ultraviolet
VEGF	Vascular endothelial growth factor
WD	Wolffian duct
WNT	Wingless signalling pathway
WT1	Wilms’ tumour1

Chapter 1

1 Introduction

Introduction:

End-stage renal disease is a serious medical problem that necessitates renal function replacement either by renal transplantation, from a donor, or dialysis. In the UK alone, patients on the donor waiting lists who are waiting for a kidney donor represent around 80% of the total patients in the lists, and around 60% of death among patients while waiting for a donor occurs in kidney patients. These percentages are for kidney-only patients and the numbers are even higher if kidney plus another organ is considered (NHS, 2018).

After receiving a transplant, except from a monozygotic twin, patients are kept under immunosuppressive drugs which puts them under high risk of infection and expose them to higher morbidity and mortality rates (Gupta and Lam, 2016). Furthermore, despite the current advance in allograft survival, the ten year graft survival estimate is 68-86% (NHS, 2018), this especially becomes a problem in paediatric patients indicating that one-off kidney transplantation could be insufficient to last a normal lifetime in a considerable percentage of patients who experience transplant failure and are therefore either shifted to dialysis or considering re-transplantation. Dialysis remains as a life-saving solution for those who do not find a donor. Nonetheless, it is inefficient in filtering the blood from waste products with uremic retention solutes left behind predisposing to atherosclerosis (Masereeuw and Stamatialis, 2017a). In addition, dialysis does not compensate for the renal endocrinal function, namely Erythropoietin synthesis and Vitamin D activation; chronic kidney disease patients usually suffer from chronic anaemia and osteomalacia; generally, dialysis decreases the patient's quality of life (Gupta and Lam, 2016; Moon *et al.*, 2016).

There is therefore an increasing need to find new therapeutic modalities for end stage renal disease. Researchers are adopting different strategies to tackle the problem, spanning regeneration of the damaged kidney in-situ, engineering a new organ in-vitro and then transplanting it to the patient, and engineering Bio-artificial kidneys that can replace kidney function. For researchers who are trying to regenerate the damaged kidney in-situ, choosing the type of cells used to induce regeneration has been a big question and different types of cells have been shown to induce regeneration, reverse inflammation and fibrosis, and/or induce new vessel formation (thus rescuing the remaining nephrons). Cells used for this purpose include: renal progenitors obtained

either by dissociation of embryonic kidneys, isolation from adult kidney (they are present in very low percentage in adult kidneys), differentiation from pluripotent cells, or by direct reprogramming from renal tubular cells (Kaminski *et al.*, 2016; Lagies *et al.*, 2018). Cells used for regeneration of the damaged kidney are not restricted to renal types of cell; endothelial progenitor cells have been shown to reverse the inflammation and fibrosis, induce new vessel formation, and improve the kidney (Chade *et al.*, 2009). As well mesenchymal stem cells or their conditioned media (van Koppen *et al.*, 2012) and bone marrow derived cells and their conditioned media (Golle *et al.*, 2017) have also been demonstrated to induce regeneration. However, the engraftment efficiency in most of the studies so far was low and most of the effect is believed to be achieved by humoral factors.

Techniques that work to engineer new transplantable kidney tissue are also diverse. One option is to repopulate a decellularized renal matrix (Gifford, 2015). Nevertheless, this approach still needs an adult kidney to use as a scaffold. 3D bioprinting of a kidney is another option (Murphy and Atala, 2014); however, bioprinting a complex structure, like the kidney, that has different types of cells performing different functions and has cortico-medullary zonation, could be very challenging and sophisticated. Another option aims at engineering foetal kidneys from human induced pluripotent stem cells (hiPSCs), using optimised differentiation protocol to obtain renal-differentiated cells and renal organoids from them, applying techniques previously developed in mouse to organise the structure and obtain a tissue that resembles foetal kidney with a ureter, and then allowing that tissue to mature and develop by grafting into a host thus ending by tissue that could be transplanted to the patient (Davies and Chang, 2014; Mills *et al.*, 2017).

Recent advances in optimising protocols to obtain renal cells and renal organoids from iPSCs could reshape the future of regenerative medicine and pave the way for patient-tailored immune-competent therapy; one of the major advantages of hiPSCs is that they could be generated from any individual and thus they will evade the allogenic rejection that occurs upon transplanting from a donor and would eliminate the need for immunosuppressive drugs (Gupta and Lam, 2016).

hiPSC-derived renal cells hold remarkable promise not only for regenerative medicine but also for drug discovery and pharmaceutical purposes. Kidneys are highly vulnerable to drug toxicity due to their essential role in handling drugs and toxins (Pazhayattil and Shirali, 2014; Nigam *et al.*, 2015). During the process of drug discovery, potentially therapeutic compounds have to go through a meticulous process of assessment to exclude toxic compounds, however, current models for nephrotoxicity screening are inefficient with some drugs show unexpected toxicity after their release into the market (Davies, 2018). This hinders the process of drug discovery and increases its cost; hence there is an increasing need to develop new models for evaluating drug efficacy and toxicity and hiPSC-derived renal tissue represents a promising potential model. This thesis investigates different aspects of the current model of hiPSC-derived renal tissue and possible ways for improving it.

1.1 Kidney structure and function:

Exploring the constituting components of the renal tissue, their complex organisation within the organ, and the importance of that complexity for a proper function is a pre-requisite to all engineering trials.

Kidneys are paired retro-peritoneal organs that have excretory function. Together with the ureters, the urinary bladder and the urethra they constitute the urinary system. Each kidney has a collecting duct tree plumbing into the ureter that conveys urine from the kidney to the urinary bladder from where it is excreted out of the body through the urethra.

The kidney is enclosed within a fibrous capsule; its medial concave surface contains the renal hilum which is the site of entry of the renal artery and nerves and also the site of exit of the renal vein, lymphatic vessels and the ureter. The renal parenchyma can be divided into an outer renal cortex and an inner medulla. There is no physical boundary between the cortex and medulla, but the difference in their appearance makes it possible to distinguish the cortico-medullary boundary visually (Hallgrimsson, Benediktsson and Vize, 2003). The human kidney medulla is formed of multiple conical pyramids, the tips of these pyramids are known as papillae. Urine flows out of

the papillae into the minor calyces which converge to form major calyces. In turn, the major calyces also converge to form the renal pelvis which continues as a narrower tube; the ureter (figure 1.1a).

The nephron is the functional and structural unit of the kidney; it is composed of different domains and it is the part responsible for blood filtration and urine production. Each mouse kidney contains between 12,000 and 16,000 nephrons with the number of nephrons varying according to the mouse strain (Short *et al.*, 2014). There is also a wide range of variability in human regarding the number of nephrons per kidney; studies suggest that the number ranges between 200,000 and 1,800,000 with an average of 1,000,000 nephron per kidney (Sariola and Philipson, 1999; Hughson *et al.*, 2003; Bertram *et al.*, 2011). Nephron endowment seems to be dependent on many factors and has a great impact on disease/health state with higher nephron number thought to be protective against renal diseases (Bertram *et al.*, 2011; Walker *et al.*, 2012).

The nephron can be divided into two main components; the renal corpuscle and the renal tubule, to which it connects (figure 1.1b). The renal corpuscle is the site where blood filtration takes place. It is at the proximal end of the nephron and is composed of Bowman's capsule into which an afferent arteriole invades and forms a knot of leaky glomerular tuft capillary; the glomerulus, from the other side of which the blood exits through the efferent arteriole. The Bowman's capsule is itself formed of a visceral layer, lined with specialized cells known as podocytes, a parietal layer, and a capsular space between them. The podocytes lining the visceral layer of Bowman's capsule together with the glomerular basement membrane and the fenestrated endothelium lining the glomerular capillary form the three core constituents of the glomerular blood filtration barrier that separates between blood in the glomerular capillary and the filtrate in the capsular space of Bowman's capsule and controls filtration into the renal corpuscle. Water and small sized molecules filter freely through this barrier, while it retains large molecules as proteins. It also exerts a charge selectivity with the negatively charged molecules being held back (Menon, Chuang and He, 2012).

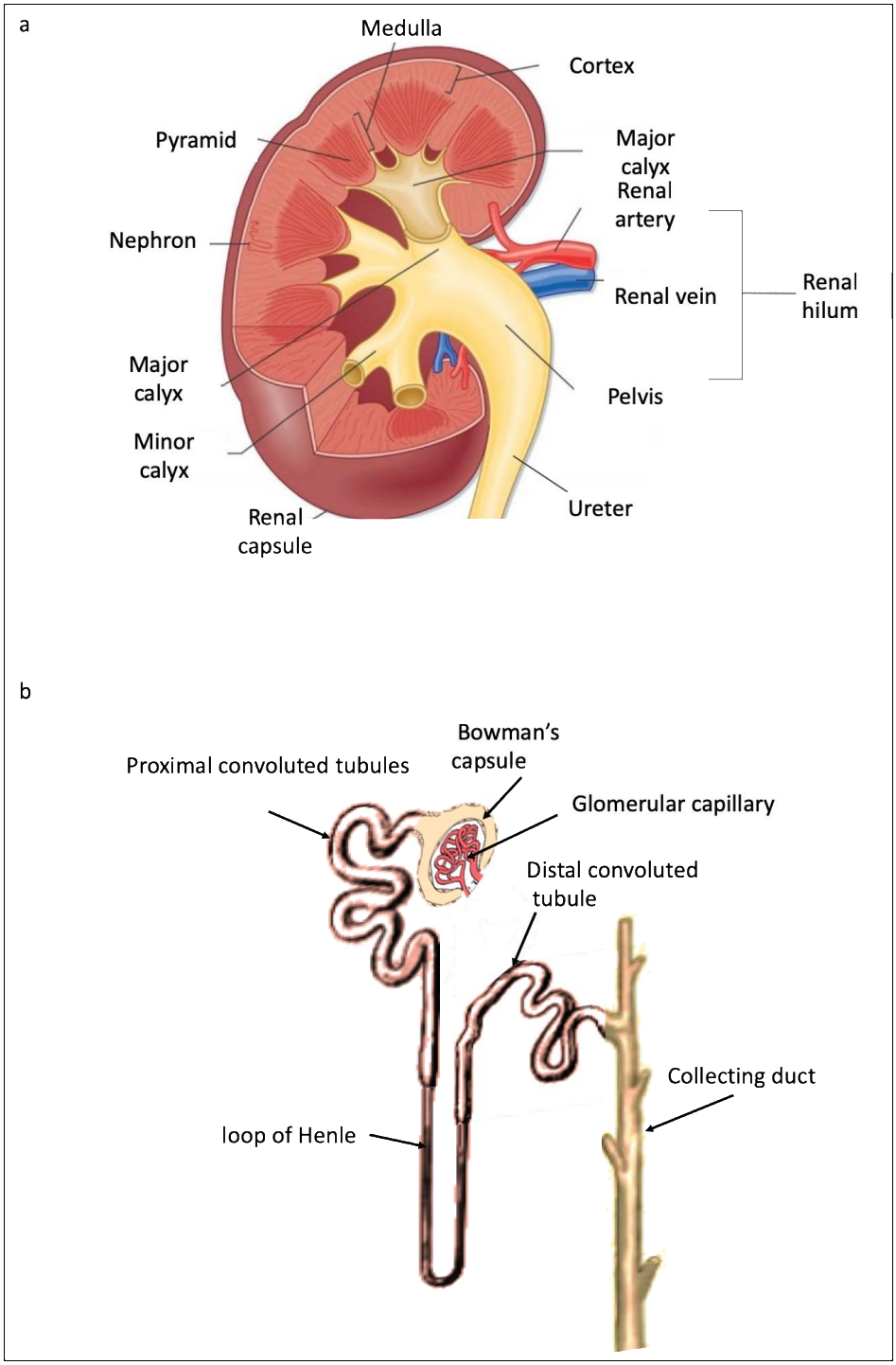

Figure 1.1. a) Cross section in the kidney demonstrating the overall structure of the organ (adapted from https://airfreshener.club/quotes/kidney/-calyx-pelvis-renal.html). b) Illustration of the different segments of the nephron and the collecting duct.

The vascular endothelial cells represent the first layer of the glomerular filtration barrier. These endothelial cells are characterized by having fenestrations of 50-100 nm size. The endothelial surface is covered by a glycocalyx that functions to retain the cellular component of the blood and the large molecules (Hallgrimsson, Benediktsson and Vize, 2003; Satchell and Braet, 2009).

The glomerular basement membrane is the middle layer of this barrier; it is an acellular, thick, highly specialized matrix. Both the endothelial cells and the epithelial podocytes contribute to its synthesis. Also, the mesangial cells have been shown to contribute to its turnover. Type Ⅳ collagen, β2-Laminin and sulphated proteoglycans are its main constituents. (Abrahamson, 1985; Abrahamson *et al.*, 2009; Menon, Chuang and He, 2012; Miner, 2012).

The podocytes are the mesenchymal-derived epithelial cells that line the visceral layer of Bowman's capsule. They extend what is known as foot processes; these foot processes interact at their joining surfaces to form the slit diaphragm and the spaces between them are known as filtration slits. The slit diaphragm is composed of proteins which are known for their importance in tight junction and adherence junction (e.g. Zona occludens-1, Catenin and P-cadherin). Podocytes lie on top of the GBM and the interaction between β2-Laminin from the GBM and α3 β1 integrin on the basal surface of the podocytes plays an important role in anchoring podocytes to the GBM (Adler and Chen, 1992). The luminal surface of the podocytes is covered with anionic glycocalyx; the main constituent of which is Podocalyxin (Kerjaschki, 1984). Nephrin (NPHS1); a transmembrane protein that is found in the slit diaphragm, interacts with either Nephrin or Nephrin-like protein (NEPH1) from the adjacent podocyte and with other regulatory proteins through its intracellular domain facilitating actin polymerization which is key for foot process architecture. Mutations in its coding gene result in foot process abnormality and cause congenital Nephrotic syndrome which is characterized by massive proteinuria. Foot process effacement, a condition in which the foot processes are abnormally flattened and their architecture is distorted, is a leading cause to glomerular proteinuria (Ruotsalainen *et al.*, 1999; Wartiovaara *et al.*, 2004; Menon, Chuang and He, 2012; Miner, 2012).

The ultrafiltrate in the Bowman's space then passes to the tubular epithelium which can be divided into four main segments: the proximal tubule, the loop of Henle, the

distal tubule and the connecting tubule. The proximal tubule is the tubular segment that connects to Bowman's capsule and is marked by the transition of the epithelial lining from the simple squamous epithelium of Bowman's capsule to the cuboidal type (Bulger, Cronin and Dobyan, 1979; Haensly *et al.*, 1982). The proximal tubule itself can be further subdivided into three segments S1, S2 and S3. The renal corpuscle and the first two segments of the proximal tubule (S1, S2) lie in the renal cortex, while the S3 segment lies in the outer medulla (Mcmahon, 2016). The luminal surface of the proximal tubules stands by its brush border that is formed of densely packed microvilli which function to increase the surface area available for reabsorption (Heidrich *et al.*, 1972). Also, the cytoplasm of these cells is rich in mitochondria to supply energy needed for the active transport across the epithelial membranes. A myriad of apical and basolateral transmembrane channels and transporters within the proximal tubule function to reabsorb and recover salt, glucose, amino acids and vital molecules from the ultrafiltrate into the surrounding vascular capillaries (Sekine *et al.*, 2012; Yin and Wang, 2016). (More details about the proximal tubular transporters and their functions will be detailed in a later section).

The ultrafiltrate then passes to the loop of Henle which dips deep into the medulla before it loops and reverses its direction back to join the distal tubule in the cortex (Hallgrimsson, Benediktsson and Vize, 2003). The primary function of the loop of Henle is to concentrate the urine through maintaining high interstitial salt concentration in the medulla. The thick ascending limb does not have aquaporin proteins and is impermeable to water while it actively transports sodium. This increases the interstitial fluid osmolality which helps osmotic water reabsorption from the descending limb and the collecting ducts. The thin descending limb of the loop of Henle is highly permeable to water but has limited permeability to sodium and urea (Kokko, 1970, 1972). In contrast, the thin ascending limb has relatively high permeability to sodium and urea but is water-impermeable (Imai and Kokko, 1974, 1976). The Counter-current configuration of flow inside the loop of Henle is thought to multiply the osmolality difference between the fluid that flows in the ascending limb and the surrounding tubules and vessels establishing a cortico-medullary osmotic gradient that increases progressively from the cortico-medullary junction to the papillary tip in the inner medulla (Pallone *et al.*, 2003; Sands and Layton, 2009, 2014).

The distal convoluted tubule (DCT) is the shortest segment of the nephron; it spans only 5 mm in human. Cells in the distal convoluted tubules are characterised by the positioning of their nuclei close to their apical sides and by the deep infoldings extending from their basolateral membrane. The DCT regulates sodium, potassium, calcium and magnesium reabsorption under the control of aldosterone and parathyroid hormones and shares in maintaining water balance under the control of vasopressin hormone (Subramanya and Ellison, 2014). The DCT and the connecting tubule are together referred to as the distal tubule; the DCT can be further subdivided into DCT1 and DCT2. DCT2 together with the connecting tubule and the collecting ducts are known to be aldosterone-sensitive distal nephron, as it is inferred from the term, they represent the site of action of the aldosterone hormone.

The distal tubules connect to the collecting ducts (CDs). The CDs form a highly arborized tree that derives from a distinct developmental origin than that of the contiguous nephron tubule (see details in section 1.2.4). The lining cells of the collecting ducts are divided into principal cells, the more abundant cell type that is mainly involved in sodium retention, and intercalated cells, a rarer type of cell that is involved in acid-base regulation through transporters that secrete hydrogen ions and bicarbonate (Al-Awqati, 2013; Pearce *et al.*, 2015). The collecting ducts then drain the urine through the renal papillae into the minor calyces which in turn convey urine to the major calyces then down the ureter to the urinary bladder.

This brief overview of kidney structure and function demonstrate how complex the kidney is; its function necessitates the integrative interaction between mesenchymal-derived different specialised epithelial cells, a highly branched connected collecting duct tree that drains into a single ureter, a tightly regulated vascular system, and different types of interstitial cells, and makes it clear that building up a realistic organoid from stem cells that contains all these different types of cells interacting together in a correct way, crucial for producing and excreting urine, is an intricate process that probably would need different steps of maturation, organisation and assessments.

1.2 Early stages of embryonic development:

Differentiating iPSCs or ESCs into renal cells requires the recapitulation of natural developmental processes in-vitro. Therefore, understanding how a single totipotent cell (the zygote) undergoes different cell specification processes to end in a whole organism, consisting of different body systems and organs, is a pre-requisite.

Embryonic development would need a whole literature review, so in this overview, early stages of embryonic development are summarized only within the context of renal specification.

Mammals, in general, share common developmental processes with inter-species differences. I will focus on the human and mouse embryonic development and, wherever possible, I will try to highlight the inter-species differences between them.

In the 3rd week of human embryonic development, a very major event takes place; gastrulation, that converts the embryo into a trilaminar disc formed of the three germ layers: ectoderm, mesoderm and endoderm (Solnica-Krezel and Sepich, 2012; Moore, Persaud and Torchia, 2015; Schoenwolf *et al.*, 2015) (figure 1.2).

Gastrulation starts by formation of the primitive streak in the midline of the caudal part of the epiblast. The primitive streak (PS) is formed of a thickening of cells with a central groove known as the primitive groove, the cranial end of the groove is continuous with the primitive pit which is a depression inside the expanded primitive node. After formation of the PS, the main embryo's body axes will be defined: the cranio-caudal axis (the primitive streak develops on the caudal part of the epiblast), the medio-lateral axis (as the PS develops in the midline) and the dorso-ventral axis (the epiblast becomes dorsal) (Robb and Tam, 2004; Solnica-Krezel and Sepich, 2012).

During gastrulation, cells undergo an epithelial-to-mesenchymal transition. In their epithelial state cells are regularly shaped and are tightly connected, while mesenchymal cells are irregular in shape and detach from each other as they extend pseudopodia, filopodia and lamellipodia. During epithelial-to-mesenchymal transition, the cells upregulate the transcription factor SNAIL and downregulate or even lose E-cadherin (ECAD or CDH1) from their surfaces (Solnica-Krezel and Sepich, 2012; Schoenwolf *et al.*, 2015; Yamamoto *et al.*, 2018).

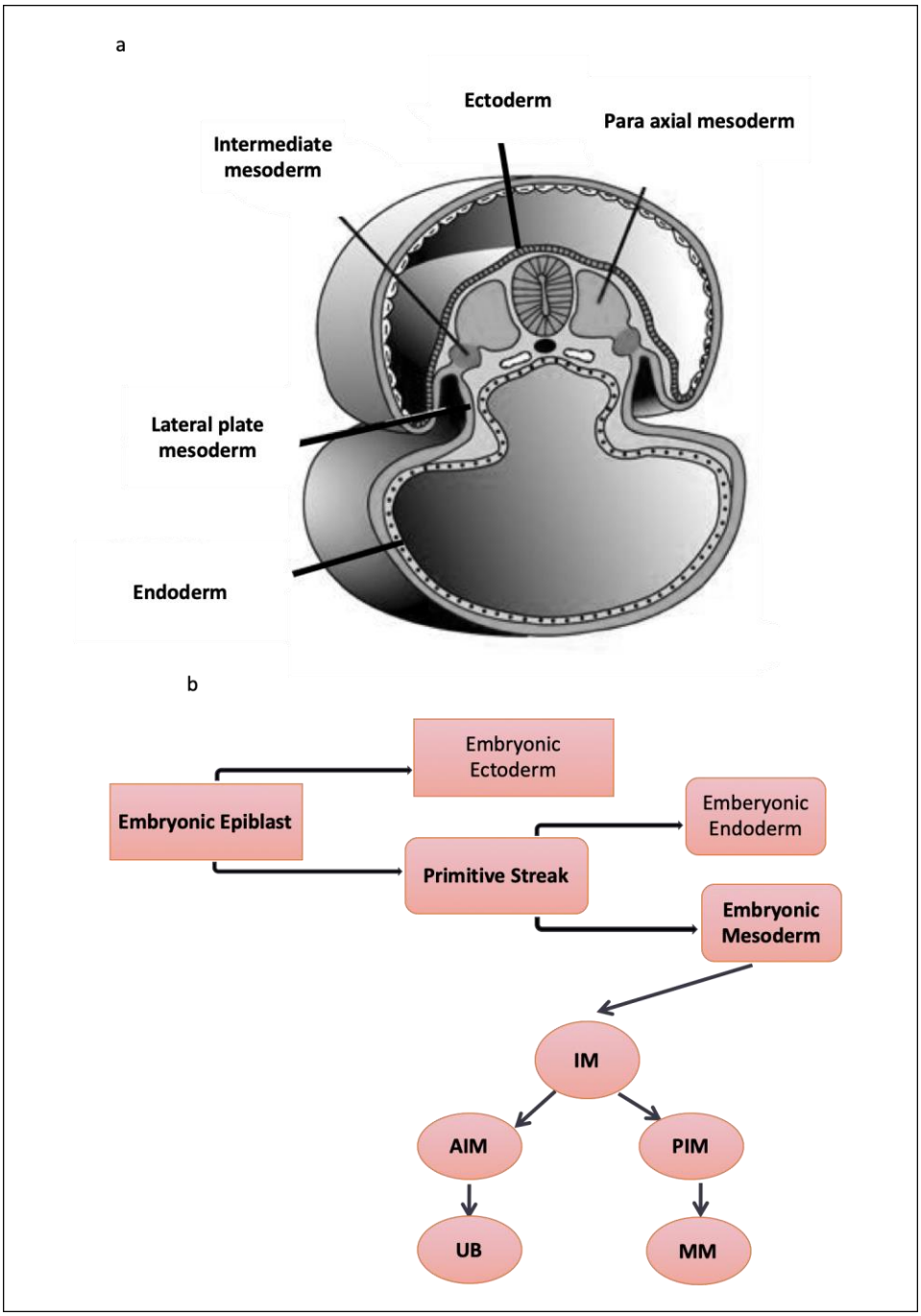

Figure 1.2. a) Section in the gastrulating embryo demonstrating the three embryonic germ layers (the ectoderm, the mesoderm and the endoderm). b) Schematic illustration of the metanephric kidney specification starting from the epiblast stage of the embryo (pluripotent cells). Cells from the epiblast migrate through the primitive streak to form embryonic endoderm and mesoderm. The intermediate mesoderm is the part of the embryo that gives rise to the two main renal progenitors, the UB and MM. IM: intermediate mesoderm; AIM: anterior intermediate mesoderm; PIM: posterior intermediate mesoderm; UB: ureteric bud; MM: metanephric mesenchyme.

Once the PS is formed, the epiblast cells migrate through it into the inside of the embryo. The first-migrating cells displace the hypoblast layer to form the endoderm layer of the embryo. The cells that remain in the epiblast and do not migrate through the primitive streak will form the ectodermal layer of the embryo. While the mesoderm layer is formed by cells that migrate through the primitive streak and reside between the epiblast and the endoderm layer (figure 1.2). The mesodermal cells divide into five main subdivisions: the cardiogenic mesoderm, the notochord (also known as the midline or axial mesoderm) and on both sides of the notochord from medial to lateral direction the mesoderm is divided into: para-axial mesoderm, intermediate mesoderm (IM; it is the part of the embryo that gives rise to all the nephrogenic structures and is therefore called the nephrotome) and the lateral plate mesoderm (Schoenwolf et al., 2015).

1.2.1 Mesoderm patterning:

Here, I will focus on mesodermal medial-lateral specification and the morphogens that control the intermediate mesoderm specification, as these actions are responsible for generating renal structures.

Fate mapping studies in animals reveal that cells in different regions of the epiblast migrate through different parts of the PS and take a different fate in the mesoderm. At the mid PS stage, cells of the notochord migrate through the most cranial end of the PS in the midline to form the notochordal process. Cells of the para-axial mesoderm, IM and the lateral plate mesoderm migrate in a cranial-to-caudal succession through the PS with the para-axial mesoderm cells migrating through the cranial part and the lateral plate mesoderm migrating through the caudal part (Smith, Gesteland and Schoenwolf, 1994; Parameswaran and Tam, 1995; Kinder, Loebel and Tam, 2001).

With the definition of the dorsal-ventral axis of the embryo, the notochord becomes the most dorsal mesoderm and the lateral plate mesoderm becomes the most ventral mesoderm. Interaction between dorsalising factors and ventralising factors generates gradients of morphogens over the embryonic disc during gastrulation and promotes dorsal-ventral patterning of the mesoderm; low, intermediate or high concentrations of specific morphogens induce specification of particular mesodermal fate (De Robertis

and Kuroda, 2004). Studies in mice have shown that mutations affecting *Fgfr1* can interfere with para-axial mesoderm formation (Yamaguchi *et al.*, 1994). Similarly, loss of WNT3A signalling also leads to defects in the para-axial mesoderm (Yoshikawa *et al.*, 1997). In contrast, *Bmp4* is expressed in the posterior part of the primitive streak (the part from which the ventral mesoderm, IM and lateral plate mesoderm, emerges) and is known to be a ventralizing factor; loss of its function leads to defects in ventral mesoderm development (Winnier *et al.*, 1995). Studies performed on chicken, zebrafish and xenopus embryos have provided evidence that BMP molecules are necessary for IM specification and gene expression.

The IM is further patterned along its anterior-posterior axis. The definitive kidney develops from two main progenitors: the metanephric mesenchyme (MM) and the ureteric bud (UB), both of which have been shown to drive from the IM (Mugford *et al.*, 2008). It was first thought that the two progenitors originated from anterior (cranial) specified IM that extends posteriorly (caudally) and commits to the two different types of progenitors. However, fate-mapping studies using *Osr1* (expressed in the IM) and *Brachyury* (*T;* a marker of gastrulation and transient mesodermal marker) genes have shown that these two progenitors arise from different parts of the IM. The anterior IM gives rise to the Wolffian duct (WD), the UB precursor, prior to E8.5 in mouse and they develop into T^- state earlier. While the MM develops later from the posterior IM and is maintained in T^+ state for a longer period (Attia *et al.*, 2012; Atsuta *et al.*, 2013; Taguchi *et al.*, 2014).

1.2.2 Wolffian Ducts:

The Wolffian duct (WD) is so named after the German scientist Casper Friedrich Wolff who first described it in 1774; it is also known as the nephric duct. It is the first urogenital epithelial structure that develops from the IM. It develops as a cellular thickening arising from the most cranial part of the IM (the prospective pronephric region) that undergoes epithelisation and then elongates and extends caudally through mesenchymal-to-epithelial transition of their tip cells. While migrating, the WD induces the formation of three paired nephric structures from the nearby IM in a cranial-caudal sequence: the pronephros, the mesonephros and the metanephros (the

last one to develop and the progenitor for the definitive kidney) (Saxén, 1987; Saxén and Sariola, 1987; Costantini and Kopan, 2010).

Molecular mechanisms underlying the specification of the WD within the IM and involved in its further development and elongation to reach the urogenital sinus have been investigated through mouse knock out models; the transcription factors PAX2, PAX8, LHX1 and GATA3 have been shown to be important players (Dressler *et al.*, 1990; Fujii *et al.*, 1994; Bouchard *et al.*, 2002; Grote *et al.*, 2006).

1.2.3 The Pronephros and the mesonephros:

The pronephroi develop from the nephrogenic cord as small mesenchymal condensations. The pronephroi do not function in mammals including human; they degenerate by the fourth week of gestation (Vetter and Gibley, 1966; Dressler, 2006); however, they represent the primary filtering structures for lower vertebrates including Larva fish (Drummond *et al.*, 1998) and Xenopus embryos (Vize *et al.*, 1997).

In contrast, the mesonephroi have been demonstrated to produce urine in mammals during embryogenesis (Torres *et al.*, 1995). In mouse, the mesonephros is composed of around 18 pairs of tubules which could be subdivided into cranial tubules and caudal tubules (Vetter and Gibley, 1966; Sainio, 2003). The cranial tubules acquire connection to the WD at 4-6 sites through short connecting segments that develop from the WD, they have rudimentary glomeruli and some of them form branches from their distal segments (Croisille, Gumpel-Pinot and Martin, 1976; Sainio, Hellstedt, *et al.*, 1997; Sainio, 2003). The caudal tubules, which represent most of the mesonephros, do not connect to the WD (Sainio, Hellstedt, *et al.*, 1997; Davidson, 2008). Like the pronephros, the mesonephros finally regresses except for some of the cranial tubules which become modified in males to form the rete testis (Vetter and Gibley, 1966; Buehr, Gu and McLaren, 1993).

1.2.4 Metanephric kidney development:

Among the three pairs of kidneys that develop during the embryonic stage, the Metanephros represents the precursor for the adult functional kidney. It is the last pair that develops chronologically and is the most caudal (posterior) one (Bremer, 1916).

The Metanephric kidney develops from two main progenitors; the ureteric bud (UB) and the metanephric mesenchyme (MM). While the MM and the UB are both derivatives of the IM, the two have distinct spatial origin (as mentioned earlier); the UB develops as an outgrowth of the Wolffian duct, which itself is a derivative of the anterior IM, and the MM develops from the posterior nephrogenic cord (Fraser, 1920; Grobstein, 1955; Vetter and Gibley, 1966; Taguchi *et al.*, 2014) (figure 2b).

The MM blastema first appears at around day E10.5 in mouse as an aggregate of mesenchymal cells derived from the IM adjacent to the caudal part of the WD. It is to be noted that once the MM blastema is specified from the IM, the cells already have a predetermined kidney-making determination and experiments showed that in no case will other embryonic cells at that stage of embryonic development be able to make metanephric nephrons or other specific metanephric structures (Saxén, 1970, 1999).

At around day E10.5 in mouse (week 4 in human), the caudal end of the WD responds to inductive signals emanating from the adjacent MM by localized cellular outgrowth to form the UB. Early studies in which the MM and UB were separated and then cultured either isolated, recombined in-vitro, or combined with other kinds of tissues provided a strong evidence that there are reciprocal inductive signals between the two progenitors and that this interaction is crucial for the metanephric kidney development. The UB emits signals that induce the MM to condense around its tip and undergo mesenchymal-to-epithelial transition to start nephrogenesis; and on its turn, the MM induces the UB outgrowth and its subsequent branching (Grobstein, 1953; Grobstein, 1955; Saxén, 1987). Studies showed that these inductive signals could also be provided, at least in part, by a number of other heterologous tissues, for example co-culture of the isolated MM with the dorsal spinal cord decreases apoptosis and induces nephron formation (Grobstein, 1955; Lehtonen *et al.*, 1983; Saxén and Lehtonen, 1987). On the other hand, studies mixing the UB with different mesenchymal tissues also showed that UB arborisation could be seen upon mixing with lung mesenchyme;

however, the branching pattern was more like that of the lung than that of the kidney (showed more lateral branching) suggesting similarity in the signals inducing branching to the UB and the lung buds and also suggesting a mesenchymal influence on the pattern of branching (Kispert *et al.*, 1996; Lin *et al.*, 2001) .

The nature of the inductive signals between the UB and the MM is now fairly understood thanks to experiments involving transgenic mice knock-outs and in-vitro culture and manipulation to embryonic kidney rudiments. Glial derived neurotropic factor (GDNF) produced from the MM and the co-receptor GFRα1 (expressed in both WD and MM) stimulate the tyrosine kinase receptor c-RET (expressed in the WD) to induce localized cellular proliferation and migration to form the UB. GDNF-soaked beads are able to induce the formation of multiple buds from the WD projecting towards the beads (Sainio, Suvanto, *et al.*, 1997; Tang *et al.*, 1998). The signal produced from the UB to induce differentiation and maturation of the MM was also a subject for meticulous investigations. In 1995, Davies and Garrod observed that treatment with lithium chloride, a WNT agonist, was able to induce tubulogenesis in cultured isolated mouse MM (Davies and Garrod, 1995). Later, it was proved that WNT9B, secreted from the UB, acting through the canonical WNT/β-Catenin pathway, induces MM condensation and initiates mesenchymal to epithelial transition (Carroll *et al.*, 2005).

The advances that have been made to understand the signalling pathways involved in metanephric kidney development and morphogenesis not only widen our understanding of kidney organogenesis, but also provide developmental cues that could be used to direct cells in a progenitor state towards more specialised cells forming highly specialised structures and participating in a complex way to perform different kidney functions (more details about important molecular mechanisms involved in metanephric kidney development are discussed in section 1.2.5).

1.2.4.1 Ureteric bud outgrowth and branching

Once inside the MM, the UB: grows and differentiates into tip cells and stalk cells, undergoes a process of repeated branching and patterning morphogenesis, and continues to induce the MM to condense around its tips and form nephrons (Michos, 2010).

The branching process implies a repeated process of: proliferation of the UB tip cells to form expanded ampulla, splitting of the ampulla forming new branches and then elongation of these branches (Lin *et al.*, 2003; Watanabe and Costantini, 2004).

In mouse, the UB undergoes ten generations of iterative branching after which the branching slows down and the collecting ducts elongate before giving one to two rounds of branching before birth (Srinivas *et al.*, 1999; Cebrián *et al.*, 2004). Terminal bifurcation is believed to be the main way of branching (Saxen *et al.*, 1965; Saxen and Wartiovaara, 1966) with the first branching described to be occurring at an angle of 180^{o} to give a T-shaped structure and the following ones at more acute angle to give Y-shaped bifurcations (Saxen *et al.*, 1965) less commonly trifurcations are also described. A time-lapse study performed on transgenic mice expressing green fluorescent protein marking their UB branches (under the control of *Hoxb7* gene; the expression of which is restricted in the kidney to the UB and its branches) concluded that lateral branching also takes place in UB branching and it could be a way to fill the gaps left by terminal bifurcations (Srinivas *et al.*, 1999).

In human, consistent with earlier studies, a recent study on human kidney organogenesis describes the first appearance of the UB as a globular outgrowth from the WD at around Carnegie stage (CS) 13. According to the same study, the first one to two branches are observed by CS16 with the first branch most likely to be trifurcation. Between CS16-CS22 the branching tips have either T or Y-shape; CS23 - week16 the tips adopt a V-shaped morphology. They also describe an expanded tip morphology with a prominent lumen between CS23 and week9, the expansion extends to the stalk region and that morphology is distinct from the other stages examined in their study. Matching this morphology with their findings that predict the glomerular filtration to start at CS23, they suggested that this could be because of active glomerular filtration occurring before the ureter connects to the urinary bladder.

Unlike the mouse UB, they described the first branches of the human UB between CS13 and CS19 to have a pseudo-stratified tip epithelium (Potter, 1972; Lindström *et al.*, 2018).

1.2.4.2 Mesenchyme condensation and nephron formation

After penetration of the UB, the loose mesenchymal cells condense around the tip forming densely packed cap mesenchyme (CM). As the UB grows and undergoes branching, the MM continues to form new caps around each newly formed tip and the process of nephron formation undergoes different steps of growth, differentiation and patterning. The CM forms pretubular aggregates from which the first epithelial structure, the renal vesicle, develops. The renal vesicle is a polarized structure that remains in contact with the UB tip at one side (Saxén, 1987; Georgas *et al.*, 2009). Morphological changes then take place; a single cleft forms at one end of the vesicle changing its morphology into a comma-shaped body which then changes into an S-shaped body after a second cleft is formed at the other end (Jokelainen, 1963). The S-shaped body has a distinct proximal-distal pattern, with its distal end joining the UB and finally forming a continuous lumen between the CD and the nephron (Georgas *et al.*, 2009) (figure 3c).

The S-shaped body further elongates and differentiate; ultimately giving rise to various specialised cell types arranged in distinct specialised domains of the mature nephron each with a unique expression pattern:

Bowman's capsule: which is the most proximal part of the nephron. It has a parietal layer and a visceral layer; the visceral layer is lined with podocytes which express the characteristic transcription factors Wilms tumour1 (WT1) and PODXL1; the specific transmembrane protein NPHS1, and secrete the Vascular endothelial growth factor (VEGF) that recruits the vascular endothelial cells to invade the capsule and form the glomerular capillary loop (Kreidberg *et al.*, 1993; Kitamoto, Tokunaga and Tomita, 1997; Ruotsalainen *et al.*, 1999).

Proximal convoluted tubules: which express Aquaporin1 (AQP1) and Jagged1 and bind Lotus tetragonolobus lectin (LTL) (Hennigar, Schulte and Spicer, 1985; Barresi, Tuccari and Arena, 1988; Cheng *et al.*, 2003; Bauchet *et al.*, 2011).

Loop of Henle: it has a thin descending limb that expresses AQP1 and a thick ascending limb which expresses Uromodulin (Bauchet *et al.*, 2011).

Distal convoluted tubules: the distal most part of the nephron which connects to the CD and is expressing the adhesion molecule ECAD (Lee *et al.*, 2013).

At E10.5 the mouse MM is already divided into 2 main sub-populations: central $SIX2^+$ nephron progenitor cells that condense around the invading UB forming CM and outer stromal $FOXD1^+$ cells (Kobayashi *et al.*, 2008). Lineage tracing studies have shown that cells expressing *Six2* are multipotent self-renewing cells that give rise to all cell types incorporated in the nephron epithelium (Kobayashi *et al.*, 2008).

Nephrogenesis does not occur as a single burst where all the MM undergoes mesenchymal-to-epithelial transition (MET) and forms nephron tubules, but rather proceeds in a repeated radial pattern around the dividing UB tips. For this to happen, there should be a balance between differentiation and self-renewal of the progenitor cells. Studies have shown that the transcription factor SIX2 plays a key role in maintaining this balance (Self *et al.*, 2006). More details about SIX2 function and its interaction with other signalling pathways to maintain the balance between differentiation and self-renewal will be discussed in the following section.

Signals emanating from renal stromal cells have also been demonstrated to fine-tune this balance; destroying stroma with diphtheria toxin disrupts WNT9B signalling and leads to thickened mesenchymal caps and reduced nephron formation (Das *et al.*, 2014). Mutations affecting *Foxd1* are also associated with arrest of differentiation and expansion of the nephron progenitors caused by the high level of proteoglycan decorin, its level is normally high in the medullary interstitium but not in the cortical interstitium (where nephrogenesis takes place), which antagonizes the effect of BMP7 (Fetting *et al.*, 2014).

1.2.5 Important genes involved in embryonic kidney development:

Detailed information about molecular mechanisms and the important genes implicated in kidney development would need many more pages to be fully covered, however, I would like to highlight the importance of the following genes in kidney development with three main aims:

1- To understand basic pathways and mechanisms underlying metanephric kidney development and branching morphogenesis.
2- Growth factors encoded by some of these genes will be used throughout the thesis either to induce renal differentiation or UB branching.
3- The expression of these genes will be used to verify the differentiation of the cells to a specified renal fate.

Paired-box transcription factors PAX2 and PAX8

PAX2 and PAX8 are 2 important interconnected transcription factors the function of which is important for the specification and development of the kidney. The two transcription factors have an important role in IM specification. Their expression is restricted to the IM, unlike LHX1 or OSR1 which extend to the lateral plate mesoderm (Bouchard *et al.*, 2002). They are also co-expressed in the WD, the UB and later in the CD (Dressler *et al.*, 1990).

Their function seems to be inter-connected and partially redundant as *Pax8* mutants do not exhibit any renal abnormalities; *Pax2* mutants can still develop WD but they degenerate before reaching the urogenital sinus and, consequently, the UB does not develop (Torres *et al.*, 1995; Brophy *et al.*, 2001; Soofi, Levitan and Dressler, 2012). The initial development of the WD in *Pax2* deficient mice is probably due to overlapping function of *Pax8* during the early stage of development (Torres *et al.*, 1995). Nonetheless, *Pax2/Pax8* double mutants fail to develop WD from the IM and fail to express the WD markers LHX1, c-RET (Bouchard *et al.*, 2002) and GATA3 (Grote *et al.*, 2006). As a consequence, the double mutant embryos do not develop pronephroi or any other nephric structures and the IM undergoes apoptosis (Bouchard *et al.*, 2002).

In addition, *Pax2* is also expressed in the nephrogenic cord, the MM and the differentiating nephrons (Dressler *et al.*, 1990). In the MM, it stimulates the expression of important kidney development regulators including: LHX1, SIX2 and GDNF (Ranghini and Dressler, 2015). PAX2 stimulates the UB outgrowth into the MM by stimulating the expression of the GDNF (Brophy *et al.*, 2001; Ranghini and Dressler, 2015). It has also been shown that PAX2 plays an important role in segregating the nephron progenitor cells from the surrounding renal interstitial cells; the conditional

inactivation of *Pax2* in nephron progenitors leads to their trans-differentiation into renal stromal-like cells (Naiman *et al.*, 2017).

As the CM undergoes mesenchymal to epithelial transition, the maturing nephrons downregulate *Pax2* expression (Ryan *et al.*, 1995). Reactivation of its expression is demonstrated in adult kidneys after exposure to injury, suggesting a role in kidney regeneration (Villanueva, Céspedes and Vio, 2006; Kusaba *et al.*, 2014).

LHX1:

LHX1 belongs to the LIM family of transcription factors. It plays important roles in different stages of kidney development and is expressed in different nephric structures including the WD, UB, pretubular aggregates, renal vesicles, comma-shaped and S-shaped developing nephrons; and also, in the maturing podocytes (Karavanov *et al.*, 1998; Sariola, 2002; Kobayashi, 2005).

In earlier stages of embryonic development, it is expressed all-over the IM and lateral plate mesoderm while by E9.5 the expression becomes restricted to the WD that develops within the IM and then it becomes expressed in the mesonephric tubules and the developing metanephros (Barnes *et al.*, 1994; Carroll and Vize, 1999; Kobayashi, 2005). LHX1 is involved in the specification of different renal progenitors from the IM and its over expression during the early stage of kidney specification leads to expansion of the kidney field (Cirio *et al.*, 2011). Loss of function mutations of *Lhx1* lead to necrotic degeneration of caudal part of the WD and renal agenesis as a consequence (Tsang *et al.*, 2000; Pedersen, Skjong and Shawlot, 2005).

During metanephric kidney development it plays a key role in regulating ureteric bud growth and morphogenesis (Kobayashi, 2005; Pedersen, Skjong and Shawlot, 2005), and in renal vesicle patterning (Kobayashi, 2005). PAX2/8 are important to maintain LHX1 expression, which is downregulated in *Pax2/8* double mutant (Bouchard *et al.*, 2002).

GDNF/RET:

As briefly mentioned before, the GDNF-RET-GFRα1 pathway plays an important role in inducing UB formation. Early events of the metanephric kidney development

involves signalling of the GDNF protein via GFRA/RET receptor complex to induce localised outgrowth from the caudal end of the WD forming the UB. The GDNF protein is initially, before induction by the UB, expressed all over the specified metanephric mesenchyme then the expression undergoes progressive restriction to the caudal part, correlated to the precise site where the UB forms, after the outgrowth of the UB the expression becomes more restricted to the CM surrounding the growing ureteric tips. Similarly, RET expression is initially found all-over the WD and later it becomes localised to the growing tips (Marose *et al.*, 2008).

Cells of the growing UB could be divided into tip cells expressing RET and stalk cells which are RET negative (Shakya *et al.*, 2005; Costantini and Shakya, 2006). The undifferentiated MM around the tip cells are thought to produce factors that promote growth and branching while the growing nephron epithelia around the stalk cells induce elongation and stop branching (Sweeney, Lindstrom and Davies, 2008). As the GDNF has a chemo-attractive property it is suggested that attraction of the tip cells towards sources of GDNF induces branching (Sariola and Saarma, 2003). Blocking of the GDNF activity in *in-vitro* cultures using anti-GDNF antibodies yields smaller kidneys with fewer UB tips (Vega *et al.*, 1996).

GDNF stimulation of the RET receptors further upregulates *Ret* expression at the tip cells (Pepicelli *et al.*, 1997; Costantini, 2012). In addition, GDNF stimulates *Wnt11* expression in the UB tips which in turn acts, through a paracrine action, to maintain *Gdnf* expression in the CM (Majumdar *et al.*, 2003; Mcmahon, 2016).

The fact that the WDs in response to GDNF beads would form multiple ectopic buds shows that tight regulation of the GDNF expression is essential for proper positioning of the ureter and for preventing supernumerary ureters. FOXC1 and FOXC2 are two closely related transcriptional factors; they have an overlapping pattern of expression in different types of embryonic tissue, and they were shown to be important in regulating GDNF expression. Mouse embryos with *Foxc1* homozygous mutations show anterior expansion of *Gdnf* expression which leads to double ureters and double kidneys with the ectopic ureters anteriorly located to the normal position (Kume, Deng and Hogan, 2000). Likewise, Greishammer and colleagues showed that mutations affecting the signalling pathway SLIT2/ROBO2 lead to anterior expansion of *Gdnf*

expression in the MM and cause supernumerary anterior located ureters (Grieshammer *et al.*, 2004) (figure 1.3a).

Michos and colleagues showed that UB can grow and branch in absence of the GDNF/RET pathway when its negative regulator SPRY1 is also absent. *Gdnf*-/-; *Spry*1-/- or *Ret*-/-; *Spry*1-/- mice developed normal sized kidneys with branching UBs and normal nephrogenesis; the pattern of branching however was altered suggesting important role of the GDNF in branch patterning and revealing that beside GDNF there are other factors participating in inducing UB branching (Michos, 2010). Consistent with this, GDNF alone is not sufficient to support growth and branching in isolated cultured UB, addition of extracellular matrix and either MM conditioned medium or combination of other growth factors is necessary (Sakurai, Bush and Nigam, 2005; Yuri *et al.*, 2017).

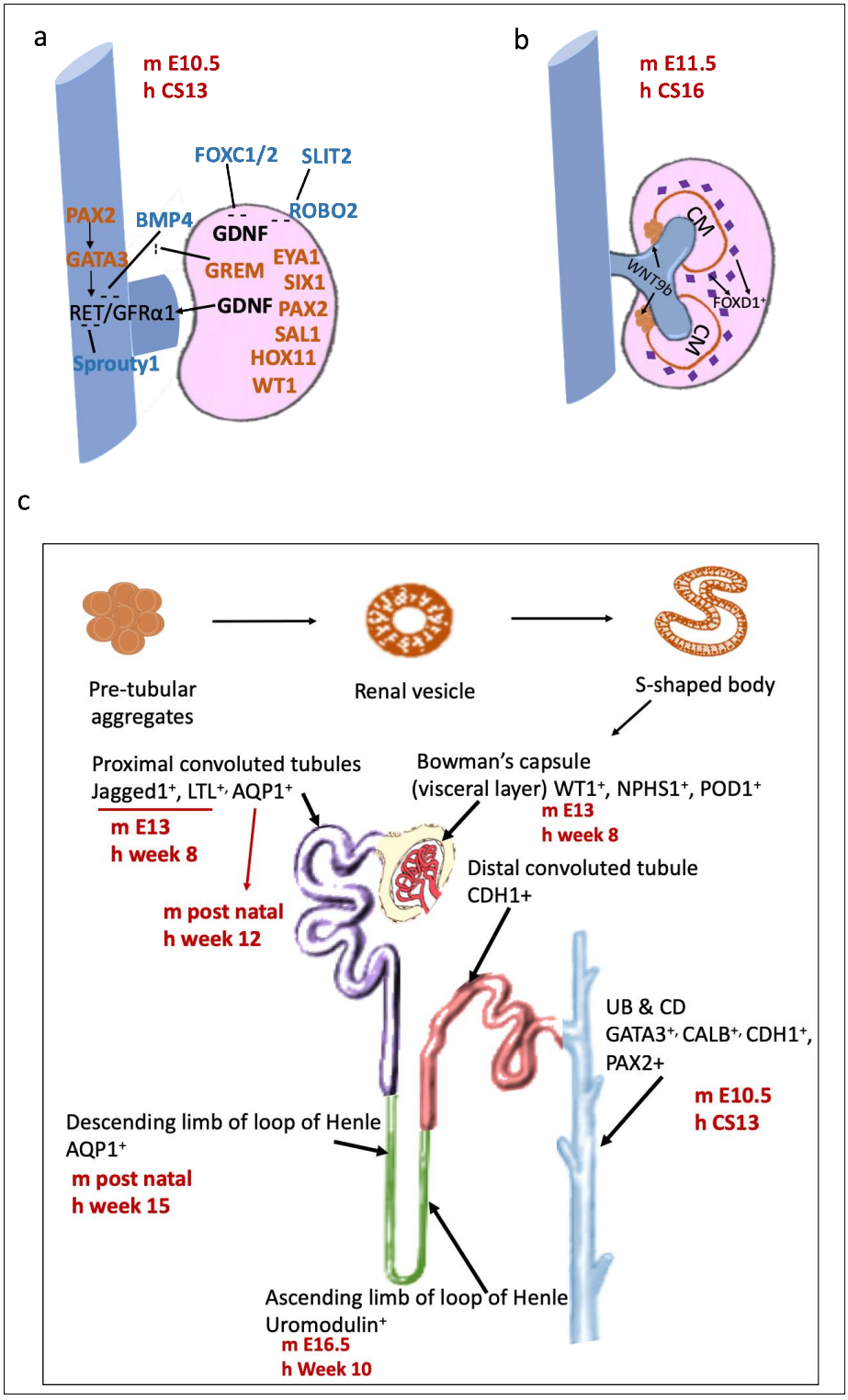

Figure 1.3. Illustration of the metanephric kidney development. a) The specified MM expresses GDNF protein and the transcriptional factors EYA1, SIX1, PAX2, SALL1, HOX11 and WT1. The Wolffian duct express the tyrosine kinase receptor RET, which respond to the GDNF protein secreted from the metanephric mesenchyme by localized cellular proliferation and migration to form the ureteric bud (UB). The GDNF/RET pathway is tightly regulated along the anterior-posterior axis to prevent supernumerary and ectopic ureters. Enhancers of the GDNF/RET pathway are shown in brown and inhibitors are shown in blue. b) The UB penetrates the MM and starts bifurcation. WNT9B, secreted from the UB, stimulates the MM to condense and form the cap mesenchyme which forms aggregates close the ureteric stalk (the pre-tubular aggregates). C)

Different stages of nephron formation and the particular pattern of expression of the different segments of the nephron and the collecting duct. The embryonic age at which the presented markers is detected is shown in red. m: for indicating the mouse embryonic age; h: for indicating the human embryonic age. CM: cap mesenchyme; UB: ureteric bud; CD: collecting duct. Adapted from (Elhendawi and Liu, 2018; for references see section 1.2.4 , 1.2.5, and table 2.1).

Retinoic acid (RA) signalling through Retinoic acid receptors (RARs):

Similar to the paracrine signalling between the nephrogenic mesenchyme and the UB, through the GDNF/RET pathway, an important interplay between the renal stroma and UB also exist. Renal stromal cells produce RA which acts on RARs in UB cells to regulate *Ret* expression, UB growth and further branching (Rosselot *et al.*, 2010).

RA is the active form of vitamin A; deficiency of vitamin A has been linked to renal abnormalities, in the form of fewer nephrons and abnormal UB branches, of varying degrees related to the degree of deficiency (Bhat and Manolescu, 2008). RARs belong to a family of transcription factors that regulates the expression of different genes. Three genes, *Rara*, *Rarb* and *Rarg*, are responsible for encoding members of the RAR family. *Rara* and *Rarb2* double homozygous mutants were demonstrated to have abnormally small kidneys, low nephron no and abnormal few UB branches. Further analysis of the developing embryos showed downregulation of RET receptors in the UB and the developing CD system (Mendelsohn *et al.*, 1999). Forced expression of *Ret* in *Rara*/*Rarb2* double mutants reverses the effect of the mutation and rescues the kidney which confirms the role of RA in regulating *Ret* expression (Batourina *et al.*, 2001).

It was first thought that RA, secreted from stromal cells, bind to RARS present in stromal cells, in an autocrine pathway, to stimulate retinoid response elements that on turn regulate *Ret* expression in the UB (Mendelsohn *et al.*, 1999). Later, it has been shown that RARs are also expressed in the UB and experiments on isolated UBs (cultured in gel; in absence of the surrounding MM) showed that when GDNF or RA was added alone to the culturing media, the cultured UBs downregulate *Ret* expression and do not show branching, while adding RA with GDNF induces branching (Rosselot et al., 2010). That experiment has shown that RA works on RARs expressed in the UB, in a paracrine pathway, and that both GDNF and RA both act independently to induce branching; while RA induces the expression RET receptors, GDNF is important for their activation. Furthermore, conditional expression of

homozygous mutant form of *Rara* in the ureteric bud leads to severe renal hypoplasia and agenesis in some conditions which were attributed to the loss of *Ret* expression (Rosselot et al., 2010).

GATA3:

One of the members of the GATA family of transcription factors; members of this family have high similarity in their zinc finger DNA binding domain (Ko and Engel, 1993). In the human kidney GATA3 expression is demonstrated in the WD, collecting ducts of the mesonephros until their involution, the UB, CDs and mesangial cells of both mesonephros and metanephros (Labastie *et al.*, 1995).

Haploinsufficiency of the *GATA3* gene in human leads to hypoparathyroidism, deafness and renal anomalies; a condition known as HDR, indicating its importance in the development of the parathyroid, inner ear and kidney (Van Esch *et al.*, 2000). The renal anomalies in HDR vary between renal dysplasia, hypoplasia, vesico-ureteric reflux, glomerulonephritis and renal aplasia; these renal anomalies are sometimes accompanied by female genital malformations (Van Esch and Devriendt, 2001; Hernández *et al.*, 2007).

Likewise, conditional inactivation of the *Gata3* gene in mouse, in the developing ND, has been linked to a variety of renal anomalies including renal agenesis, aplasia and severe renal dysplasia; it was also associated with genital anomalies. *Gata3* is a direct target of PAX2/8 working downstream to them (Grote *et al.*, 2006). It has also been demonstrated that WNT/β-catenin pathway activates the expression of *Gata3* which on turn activates *Ret* expression in the ND and UB (Grote *et al.*, 2008). I tried in this work to construct a GATA3-reporting hiPSC line to track the expression of GATA3 in renal organoids and isolate the induced UBs (details about this work are described in chapter 6)

Wingless signalling pathway (WNT):

WNT proteins belong to a family of lipid-modified signalling proteins that are implicated in several developmental events throughout embryogenesis. Binding of WNT protein to its receptor complex FRZ/LRP inhibits the destruction complex GSK3/APC/Annexin (in absence of WNT, that complex destructs the transcription factor β-Catenin and

keeps its cytoplasmic level low) and increases the concentration of β-Catenin (Logan and Nusse, 2004). WNT signalling through the canonical β-Catenin pathway has been shown to regulate crucial steps in kidney development and is involved both in UB branching (Bridgewater *et al.*, 2008) and MM condensation and nephrogenesis (Park, Valerius and McMahon, 2007).

Several WNT proteins have been shown to be expressed in the metanephric kidney including WNT4, WNT2B and WNT5A in the metanephric mesenchyme and WNT9, WNT11, WNT6, WNT7B, WNT5A and WNT5B in the UB and the developing CD system. WNT4 was shown to have role in nephrogenesis (Stark *et al.*, 1994; Kispert, Vainio and McMahon, 1998); at E11.5 it is expressed in the mesenchyme condensing around the T-bud; that pattern of expression is maintained in every newly formed CM afterwards, and then it continues to be expressed in pre-tubular aggregates, the renal vesicle and the comma-shaped body, while its expression starts to regress in the S-shaped body where it is restricted to its distal limb before the expression is lost after fusion with the CD. Homozygous targeting of *Wnt4* results in embryos with small agenic kidneys in which the MM forms CM but it fails to differentiate further and does not develop pretubular aggregates, thus WNT4 was identified as an auto inducer that is expressed in the CM to induce nephrogenesis (Stark *et al.*, 1994).

It has long been known that inductive signal from the UB is crucial for inducing nephrogenesis and, as WNT4 is expressed in the MM itself, it has been proposed that its nephron-inducing effect works downstream of another inducer from the UB. Eventually, WNT9B was identified as the UB-derived nephrogenesis inducer (Carroll *et al.*, 2005). *Wnt9b* is expressed in the WD and continues to be expressed in its derivative; the UB. Within the UB, *Wnt9b* is strongly expressed in the stalk and downregulated in the tip cells, unlike *Wnt11* which is mainly expressed in the tip cells. This pattern of expression, which does not extend to the tips, is maintained within the UB as it branches to form CD tree. Renal vesicles appear correlated to and preceded by the *wnt9b* expression below the tips of the UBs.

Moreover, WNT9B secreting cells can induce nephrogenesis in isolated MM. Knockout of *Wnt9b* results in downregulation of *Wnt11* in the UB tips and *Gdnf* in the MM, as a consequence, the UB branching is disturbed after the T-bud stage; in

addition, the expression of WNT4, FGF8, PAX2 and LHX1 (which represent early markers of tubulogenesis) is not detected in the mesenchyme (Carroll *et al.*, 2005).

More recently, the importance of the β-Catenin pathway in renal stromal cells was demonstrated through conditional knock-out of *β-Catenin* in stromal cells, which caused marked renal defects including reduction in the condensing cap mesenchyme with decreased cell proliferation and loss of *Cited1* expression; the expression of *Wnt9b* in UB cells was also downregulated. In contrast, overexpression of *β-Catenin* in stromal cells upregulates *Wnt9b* expression and increases the CM population (Boivin *et al.*, 2015).

Fibroblast growth factors (FGFs):

Another family of proteins with essential role in kidney development is the FGF family signalling through FGF receptors (FGFRs) which belong to the receptor tyrosine kinase family. Among the members of FGFRs FGFR1 and FGFR2 have been demonstrated to be expressed in both the UB and MM.

Signalling through this pathway was shown to induce UB branching (Qiao *et al.*, 1999, 2001). Zhao et al showed that conditional deletion of *Fgfr2* in the UB leads to abnormal thin stalks, aberrant few branches, and smaller abnormal shaped kidneys (Zhao *et al.*, 2004). Similar branching defects are also seen in mutants of *Fgf7* and of *Fgf10* (Qiao *et al.*, 1999; Ohuchi *et al.*, 2000; Revest *et al.*, 2001); FGF7 and FGF10 are expressed by the CM cells to induce the FGFR2B expressed in the ureteric epithelial cells and stimulate branching. Knock out of *Fgf7* leads to reduced branches and as a result, fewer nephrons (Walker, Sims-Lucas and Bates, 2016).

Furthermore, it was shown that FGFR signalling could compensate for the loss of GDNF/RET signalling; the key RTK pathway involved in UB budding and branching, when combined with inactivation of BMP/Activin signalling (Maeshima *et al.*, 2007; Michos, 2010). A more recent study has shown that *Fgfr2* is expressed all-over the WD where it plays an important role in its maintenance in the caudal mesonephros. Upon specific inactivation of the receptor in the WD, the study showed WD regression and obstruction of the WD in the area of caudal mesonephros (Okazawa *et al.*, 2015).

On the other hand, the importance of FGFs signalling in MM development was also investigated. FGF2 has been demonstrated to prevent apoptosis in the isolated MM and induce mesenchymal condensation (Perantoni, Dove and Karavanova, 1995; Barasch *et al.*, 1997). Conditional deletion of either *fgfr1* or *fgfr2* in the MM does not lead to any renal abnormalities but simultaneous deletion of the two receptors causes renal aplasia suggesting redundancy in the function of the two receptors; the MM fails to condense and analysis of the MM rudiments shows preserved expression of *Eya1* and *Six1* but absence of SIX2, SALL1 and PAX2. The UB does form in these mutants but fails to elongate or undergo branching, consistence with this *Gdnf* is expressed at E10.5 but falls dramatically afterwards (Poladia *et al.*, 2006).

FGF9 and FGF20 have also been demonstrated to promote survival, induce proliferation while maintaining stemness of nephron progenitors in the CM; this finding was demonstrated *in-vivo* either through knock-out studies of both *Fgf9* and *Fgf20* in mice or by demonstrating that mutation in *FGF20* in human leads to renal agenesis. In addition, FGF9 or FGF20 is able to maintain isolated MM cell in *in-vitro* cultures and retain their ability to form nephrons in response to WNT agonist for up to 5 days (Barak *et al.*, 2012).

In contrast, FGF8 is expressed in pretubular aggregates and induces the differentiation to renal vesicles; it works in conjunction with WNT4 in response to WNT9B signals from the UB. Its function is upstream to WNT4, however, WNT4, through a positive feedback effect, maintains its expression (Grieshammer *et al.*, 2005; Perantoni *et al.*, 2005).

WT1:

Wilms Tumour1 (WT1) is a zinc finger transcription factor; mutation in its encoding gene was identified as the leading cause of the paediatric Wilm's tumour, after which the gene was named, that affects the renal progenitor cells resulting in uncontrolled proliferation and abnormal differentiation (Mierau, Beckwith and Weeks, 1987; Cowell *et al.*, 1991; Hohenstein and Hastie, 2006).

Wt1 is expressed in the early mesonephric tubules and then in the specified uninduced MM; after induction from the UB its expression increases in the MM and becomes

specifically higher in the CM. It continues to be expressed in the proximal part of the developing nephrons and the podocytes. It is widely expressed by other mesoderm-derived tissues; however, its expression becomes restricted to renal podocytes by E20 in mouse (Armstrong *et al.*, 1993). That pattern of expression, which is restricted to the podocytes, is maintained afterwards and is seen in normal adults suggesting a role of WT1 in maintaining normal podocyte phenotype. *Wt1* mutations cause Wilm's tumour, genitourinary defects, and immature podocyte phenotypes which are involved in genetic causes of glomerulosclerosis including Denys Drash and Fraiser syndromes (McTaggart *et al.*, 2001; Patek *et al.*, 2003; Srichai *et al.*, 2004).

Wt1 mutants maintain the expression of *Gdnf* (Donovan *et al.*, 1999) but fail to recruit UBs (Kreidberg *et al.*, 1993) or start nephrogenesis upon recombination with normal UB. The block of nephrogenesis could be explained by the finding that *Wnt4* is controlled by WT1 (Essafi *et al.*, 2011). WT1 is also required for the survival of the progenitor cells; *Wt1* mutants undergo spontaneous apoptosis. This has been shown to be mediated through regulating a balance between FGF and BMP/pSMAD signalling; Inhibiting pSMAD or inducing FGF stops apoptosis in nephron progenitors in *Wt1* mutants (Motamedi *et al.*, 2014). Another recent study has investigated the effect of conditional *Wt1* knockout in different developmental stages, before and after MET. According to that study, loss of *Wt1* function before the MET leads to expansion of the MM and severe disruption of mesenchymal condensation and subsequent epithelization, while loss of *Wt1* function after MET disturbs glomerulogenesis and tubular maturation. They also compared the genome-wide pattern of expression of the mutant mouse models to that of human Wilm's tumour cases carrying either wild-type or mutant *WT1.* Interestingly, they found that the expression pattern of the mutant mouse kidneys in which *Wt1* loss of function occurs after MET closely resembles human wild-type *WT1* cases, while kidneys in which loss of function occurs after MET resemble in their expression pattern human mutant *WT1* cases (Berry et al., 2015).

SIX1/SIX2:

In mouse metanephros *Six1* is expressed early and has a role in the specification of MM within the IM at E10.5 before UB induction and its expression is transient; it supports the survival of MM cells and in its absence the MM undergoes apoptosis and the formed UB fails to branch (Xu *et al.*, 2003; Nie *et al.*, 2011; Xu and Xu, 2015).

SIX2 plays a key role in the maintenance and renewal of nephron progenitor cells. It is expressed in the CM cells and its deletion leads to abrupt premature epithelisation of CM and early cessation of nephrogenesis which ultimately causes severe reduction in nephron number (Self *et al.*, 2006; Kobayashi *et al.*, 2008). In response to WNt9B induction from the UB, a subset of $SIX2^{+ve}$ cells relatively lower their *Six2* expression and express *Wnt4* together with other nephrogenesis markers including FGF8, PAX8 and BMP7 (Kobayashi *et al.*, 2008; Mugford *et al.*, 2009; Park *et al.*, 2012). On the opposite side, a separate population of SIX2 positive cells, which is co-expressing CITED1 ($Cited1^{+}/Six2^{+}$), is refractory to WNT9B induction and does not participate in nephrogenesis, but rather, engages in self renewal of the nephron progenitor cells (Mugford *et al.*, 2009; Park *et al.*, 2012; Brown *et al.*, 2013). BMP7 signalling through the SMAD pathway has been demonstrated to drive the cells from the refractory CITED1+/SIX2+ state into a $CITED1^{-}/SIX2^{+}$ state that is responsive to induction to start nephrogenesis (Brown *et al.*, 2013).

The function of SIX2 comes downstream to SIX1 as demonstrated by reduced SIX2 levels in *Six1* mouse mutants (Xu, 2003; Xu *et al.*, 2003). The expression pattern, transcriptional targets and function of SIX2 is highly conserved between human and mouse (O'Brien *et al.*, 2016). While the expression and function of *Six1* and *Six2* seem to be well separated in mouse, *Six1* is expressed earlier and function to support the MM cell survival whereas *Six2* expression follows and is maintained throughout nephrogenesis in the CM to support self-renewal of the progenitor cells, a recent study showed that there is an overlap between them in human; and surprisingly *SIX1* was demonstrated as a target gene for SIX2. *Six1* expression disappears in mouse after the first round of UB branching while in human *SIX1* continues to be expressed in overlap with *SIX2* in CM (O'Brien *et al.*, 2016).

$Calbindin_{28KD}$:

$Calbindin_{28KD}$ is a cytoplasmic, vitamin D-dependent calcium-binding protein. In adult kidney *Calbindin* is mainly expressed in the distal convoluted tubules where it plays a key role in active calcium transport. It interacts with the apical calcium transporting channel TRPV5 and buffers any free calcium released to the inside of the cell to prevent negative feedback effect of the free intracellular calcium on the channel

(Lambers *et al.*, 2006), it has also recently been shown that it regulates the expression of DCT calcium transport molecules including TRPV5 and TRPV6 (Lee *et al.*, 2016).

During kidney development however, *Calbindin* expression is quite different; $Calbindin_{28KD}$ is detected in the mesonephric WD and the mesonephric connecting tubules but not in mesonephric nephrons. In the developing metanephros it is expressed in the UB and the collecting ducts; it is also expressed in the most distal part of the nephron. In-vitro culture models have shown that the expression in the UB/ collecting ducts is constitutive and is detected from the point the UB outgrows from the WD. The expression extends to the UB branches and the collecting ducts. $Calbindin_{28KD}$ expression in distal tubules is however dependent on the presence of vitamin D and on the developmental age. In absence of vitamin D, $Calbindin_{28KD}$ expression remains confined to the UB/CD system and is considered as a reliable CD marker in standard culture conditions (Davies, 1994).

ECAD:

ECAD is a cellular adhesion molecule, belongs to the cadherin family, that functions to maintain the integrity and polarity of renal epithelial cells. The transmembrane proteins of the Cadherin family belong to adherens junction and desmosome proteins. Disturbance in adhesion proteins has been linked to different renal diseases (Molitoris and Nelson, 1990; Prozialeck and Edwards, 2007). Various members of the cadherin family are expressed in the kidney; the most abundant are ECAD and N-cadherin (Lee *et al.*, 2013). The renal expression of ECAD is subject to inter-species difference; being expressed in mouse and rabbit in all tubular segments (Piepenhagen *et al.*, 1995; Thomson and Aronson, 1999), while in human, monkey, rat and pig the expression of ECAD is mainly in the distal convoluted tubules and the collecting ducts, it is also expressed in the thick ascending limb of loop of Henle in both human (Kirk *et al.*, 2010) and rat but not in pigs (Lee *et al.*, 2013). N-cadherin is the main expressed cadherin in the proximal tubules in human, rat and pig, and ECAD is not expressed (or expressed in very low levels) in that segment (Nouwen *et al.*, 1993; Prozialeck, Lamar and Appelt, 2004; Lee *et al.*, 2013).

1.3 Renal Organoids:

An organoid is an in-vitro grown tissue-like structure in which cells of different types are organised in a 3-D way that yields histology similar to that of the natural tissue. Techniques upon which organoid construction is based have their origin long ago. The experiment done by H.V Wilson was the first to show that single cells in an organism have all the information needed to re-construct a multicellular structure when he dissociated a sponge into single cells and then was able to reconstruct a viable sponge from the dissociated cells after re-aggregating them (Wilson, 1910). Decades after, several studies were performed to investigate the self-organisation ability of the more complex vertebrates and mammals. In 1952 Moscona and Moscona demonstrated the ability of dissociated chick mesonephroi to self-organise, after re-aggregation and incubation, into epithelial tubules surrounded by mesenchymal derived stroma (Moscona and Moscona, 1952). Similar work was conducted on metanephric kidney Aurbach and Grobstein dissociated metanephric kidney mesenchyme into single cells, re-aggregated the cells and cultured them either alone or in the presence of inducer. While the cells died when cultured alone, they formed nephrons when cultured with inducer which was in that experiment embryonic spinal cord as the natural inducer; the UB cells died upon dissociation (Auerbach and Grobstein, 1958).

In 2010, Unbekandt and Davies showed that a single cell suspension of renal progenitors, obtained at that time by dissociating mouse embryonic kidneys, have the ability to self-organise and could be used to re-construct renal tissue. The re-constructed tissue contained all the correct components of the normal renal tissue: nephrons, stromal cells and collecting ducts. That was the first production of what we call today renal organoids (Unbekandt & Davies 2010) (more details about this technique and the steps that were developed to improve it are discussed in chapter 6). Those renal organoids were obtained from dissociated embryonic kidneys as there were no defined protocols, at that time, for obtaining renal progenitors from pluripotent stem cells and embryonic kidneys were the only reliable source for renal progenitors. Recent studies have succeeded in differentiating human pluripotent stem cells towards renal progenitors which provided the suitable starting cells to make human renal organoids using the self-organising ability of renal progenitors (Taguchi *et al.*, 2014; Morizane *et al.*, 2015; Takasato *et al.*, 2015).

1.4 Development of pluripotent cells:

Embryonal Carcinoma Cells:

The first described pluripotent cells that could be propagated in culture were embryonal carcinoma (EC) cells, proliferative undifferentiated cells that were isolated from teratocarcinoma; a multilineage tumour that contains different tissues, commonly including teeth and hair. Kleismith and Pierce demonstrated that single EC cells when injected into mouse brain were able to regenerate the multilineage teratocarcinoma, which means that these cells have, individually, the ability to differentiate into all cell types constituting the tumour (Kleinsmith and Pierce, 1964). Indeed, EC cell lines retained the capacity to differentiate into derivatives of all three germ layers; pluripotent (Kleinsmith and Pierce, 1964; Martin and Evans, 1975). Nevertheless, differentiated cells within the teratocarcinoma were not able to do the same (Martin, 1980). Transplanting foetal germ cells into adult tissues effectively induced the production of these cells. However, their characteristics differed from those of germ cells, they rather resembled the early embryonic cell stages prior to gastrulation. Consequently, cells from the early embryonic stages were isolated and transplanted into extra-uterine tissue, similarly, they formed teratocracinoma (Diwan and Stevens, 1976).

The EC cells were able to produce chimeric embryos when injected to developing blastocysts, although with poor efficiency and poor contribution, with the EC-derived cells detected in different tissues of the embryo (Papaioannou, Waters and Rossant, 1984; Rossant and Papaioannou, 1985).

Embryonic Stem Cells:

Two studies performed independently at almost the same time by Evans and Kaufman (University of Cambridge), and Martin (University of California) reported the first successful derivation of mouse embryonic stem cell lines from the inner cell mass of blastocyst stage embryos. Evans and Kaufman used the term EK cells to describe these cells while Martin gave the name Embryonic stem cells (ESCs) (Evans and Kaufman, 1981; Martin, 1981). ESCs show similar morphology and gene expression pattern to EC cells, also they form teratocarcinoma when injected in-vivo.

Mouse ESCs are derived from the inner cell mass of the blastocyst stage of embryonic development and they have some defining criteria: they have the ability of self-renewal and can proliferate indefinitely in-vitro, they can differentiate into cells corresponding to all the three germ layers thus generating all body cell types, they form teratoma when injected in-vivo, XX-lines do not show X-inactivation, they could be clonally selected and expanded, and they can form chimera (in which they highly contribute to all germ layers) capable of germline transmission (Bradley *et al.*, 1984; Smith, 2001). Germ line transmission means that ESCs could be used as a tool for genetic manipulation in mice; knock-out mutation carrying mice, generated by gene targeting of ESCs, was first reported in 1989 (Thompson *et al.*, 1989).

ESCs are best described as pluripotent cells as they can integrate with blastocysts to form either chimera (in diploid complementation) or purely ESCs-derived embryos (in tetraploid complementation), however, they do not form de novo blastocysts neither do they produce trophoblast. Therefore, the term totipotent is restricted for the zygote and the blastomeres of the early developing embryo (Smith, 2001).

Ten years after the first report of developing ESCs, it was found that a proliferative stem cell state could be obtained under specific culture conditions from primordial germ cells, these cells were called embryonal germ (EG) cells. Apart from their origin, from the primordial germ cells rather than the ICM, these cells were indistinguishable from ES cells (Matsui, Zsebo and Hogan, 1992; Resnick *et al.*, 1992).

For years later, researchers tried to isolate the equivalent human cells to mESCs. It was not until 1998 that Thomson and his colleagues succeeded in the isolation and maintenance of the first hESCs line (Thomson *et al.*, 1998). Because of their properties, scientists had expectations that hESCs would be a useful tool for studying pathogenesis of different diseases, drug and toxicity screening, and most ambitious, providing replacement therapies for various diseases. Nonetheless, the use of hESCs faced ethical debate. The debate arose from the fact that ESCs are obtained from the ICM of an embryo, which leads to the destruction of the embryo. Furthermore, they are not patient-specific.

Induced Pluripotent Cells:

An early experiment done by John Gurdon demonstrated that transferring the nucleus of somatic fully differentiated frog cells into the cytoplasm of unfertilized eggs reprogrammed the somatic cells back to an embryonic state and generated tadpoles (Gurdon, 1962). A few decades later, Ian Wilmut and colleagues used the nuclear transfer technique to report the first somatic cloning of a mammal, generating the well-known Dolly the sheep (Wilmut *et al.*, 1997). The group of Takashi Tada showed that ESCs, like the oocyte, also can reprogram the nuclei of somatic cells (Tada *et al.*, 2001). These experiments clearly showed that the terminally differentiated somatic cell nuclei still enclosed all the genetic information needed to derive a whole organism and that there are factors, provided by the oocyte or the ESCs, that can reprogram them back to a pluripotent state (Yamanaka, 2012).

In 2006, a breakthrough happened when Yamanaka and Takahashi succeeded in reprogramming mouse skin fibroblasts into a pluripotent state by the forced expression of four transcriptional factors (OCT3/4, SOX2, KLF4 and C-MYC). This achievement was a great leap forward in the field of regenerative medicine (Takahashi and Yamanaka, 2006a). These cells were designated as induced pluripotent stem cells (iPSCs) and were described as being indistinguishable from ESCs.

The ability to generate viable fertile mouse from iPSCs, using the tetraploid complementation technique, reprogrammed from adult somatic cells was the most rigorous test of pluripotency and the best proof for the principle that iPSCs can be differentiated into all cell types, tissues, organs and even a whole viable organism (Zhao *et al.*, 2010; Boland *et al.*, 2012).

The introduction of strategies to reprogram human somatic cells into induced pluripotent stem cells (iPSCs) (Takahashi, Okita, *et al.*, 2007; Yu *et al.*, 2007) has strongly encouraged the field of regenerative research and created a second surge of interest after the field had been slowed by the ethical restrictions on the use of embryonic pluripotent stem cells (Yokoo, Kawamura and Kobayashi, 2008).

1.4.1 Maintenance of mouse pluripotent cells:

The ability of ES cells to self-renew indefinitely in culture together with their potency to differentiate into all germ layers are what make these cells unique. At the beginning of ESCs research, the exact factors that enable them to self-renew without differentiation (i.e. maintain pluripotency) were not known. Culture on a feeder layer of fibroblasts in the presence of serum was considered essential for the maintenance of pluripotency and self-renewal. The putative interaction of the feeder cells and serum with the ESCs to maintain pluripotency was unobscured by a group of studies. Culturing ESCs on gelatine coat in absence of feeder cells leads to its differentiation; adding feeder cells conditioned medium was able to delay the onset of differentiation (Koopman and Cotton, 1984). Smith and Hooper then demonstrated that conditioned medium obtained from buffalo rat liver cells allowed long term maintenance of ES cells without differentiation in absence of feeder cells (Smith and Hooper, 1987).

The cytokine Leukemia inhibitory factor (LIF) was identified as the differentiation inhibitory factor secreted from these cells (Williams et al. 1988, Smith et al. 1988). Consistent with that, fibroblast feeder cells that lack functioning *Lif* gene are not able to maintain the undifferentiated state of ESCs (Stewart et al., 1992). However, ESCs cultured in LIF and serum, unlike those cultured on feeder cells, look morphologically heterogeneous and usually show some differentiated cells which probably means that feeder cells supply factors other than LIF to support pluripotency (Martello and Smith, 2014). LIF binding to its receptors activates JAK which in turn recruits STAT3 to the LIF/receptor binding site and activates it through phosphorylation (Boeuf *et al.*, 1997; Niwa *et al.*, 1998; Matsuda *et al.*, 1999).

When ESCs are cultured without serum, they tend to differentiate after a short period of time, despite the presence of LIF, which infers that LIF/STAT3 is not sufficient to maintain self-renewal and that serum contains other undefined factor/s essential for maintaining the undifferentiated state. As the auto-differentiation tends to be towards neural precursors, Ying et al used a neuronal differentiation antagonist, BMP, in ES cultures and concluded that combining BMP with LIF could replace serum and maintain the self-renewal undifferentiated state of the ESCs (Ying *et al.*, 2003). However, BMP alone is not enough to maintain self-renewal, instead it induces differentiation to non-neuronal fate (Wiles and Johansson, 1999; Malaguti *et al.*, 2013).

On the other hand, a group of other factors is implicated in ESCs differentiation. As described above, LIF acts through activation of JAKs; ERK is a downstream effector of JAK. Activation of ERK, however, seems to oppose self-renewal as it has been shown that mutant LIF receptors that do not activate the ERK pathway show promoted self-renewal ability (Burdon *et al.*, 1999). FGF4 is actively expressed in ESCs together with its receptor FGFR2. It was first thought that FGF4 acts as an autocrine factor to support self-renewal, nonetheless, *Fgf4* deletion (*Fgf4*-/-) suggested a role in growth and survival of differentiated cells (Wilder *et al.*, 1997). FGF4 is a major activator of ERK; consistent with the previous studies, Kunath et al demonstrated that FGFF4 stimulates ERK1/2 which stimulates ESCs to stop self-renewing and start lineage commitment. Furthermore, ERK2 mutant cells resisted differentiation and LIF was sufficient to maintain their self-renewal (Kunath *et al.*, 2007).

The WNT antagonist, GSK3 has also been shown to induce ESCs differentiation (Sato *et al.*, 2004; Doble and Woodgett, 2007). Using FGFR/ERK specific inhibitors or GSK3 specific inhibitors in combination with LIF allows long term maintenance of ES cells without differentiation. Moreover, the combination of the two inhibitors (2i) PD0325901 and CH99021 that specifically inhibit ERK and GSK3 pathways respectively inhibited differentiation and supported self-renewal in absence of LIF and serum. Upon that, it was proposed that ESCs are in a “ground state” of pluripotency that they will maintain as long as they are properly shielded from differentiation inducing stimuli (Silva and Smith, 2008; Silva *et al.*, 2008; Ying *et al.*, 2008).

1.4.2 Culture conditions for maintaining human pluripotent cells:

Human pluripotent cells (hPSCs: hESCs and hiPSCs) need quite different conditions from those needed to maintain the murine pluripotency. While the mESCs are known to be naive pluripotent cells, the human pluripotent cells are described as primed pluripotent cells (Ying *et al.*, 2008; Nichols and Smith, 2009). One important difference between mESCs and hPSCs is that it is possible to passage mESCs as single cells effectively without affecting their growth, whereas hPSCs tend to die progressively when dissociated into single cells and prefer to stay in clumps. The specified factors that have been proved to support the maintenance of mESCs, LIF and BMP, were not enough to maintain hESCs (Xu *et al.*, 2002). Studies demonstrated that interaction between different signalling pathways is important to maintain self-renewal and

pluripotency in human cells including Activin/Nodal, FGF2, TGF-β, and Noggin (Chen *et al.*, 2014). So, the different nature of hPSCs necessitates different culture conditions to support their growth.

Feeder cells:

Feeder cells provide suitable adhesion surface to hPSCs as well as secrete some growth factors that contribute to their growth and maintenance. MEFs have classically been the feeder cells used to culture hPSCs (Thomson *et al.*, 1998; Mallon *et al.*, 2006). Different human alternatives have been tested to replace the xenogenic contaminants in the culture system. Fibroblast feeder cells from human foetal or adult sources proved to be suitable for supporting long-term maintenance of hPSCs (Richards *et al.*, 2002, 2003). Different other types of cells from foetal, neonatal and adult sources including foreskin, endometrium cells and Fallopian tube cells were also used to expand and maintain hPSCs (Richards *et al.*, 2003). However, feeder-dependent culture adds to the workload and is a time-consuming way of maintaining hPSCs and even the use of human feeder cells still has the risk of immunogenicity. Besides, it adds undefined culture conditions which lead to variability in results (Mallon *et al.*, 2006).

Feeder free conditions:

Several extracellular surfaces have been used to provide adhesion surface to hPSCs including:

Matrigel: Matrigel is a widely used extracellular matrix to support hPSCs cultured in a feeder-free condition. It is composed of solubilized basement membrane components extracted from Engelbreth-Holm-Swarm sarcoma cells. It includes Laminin, Collagen, Heparin sulfate proteoglycans and growth factors (Kleinman *et al.*, 1982; Mackay *et al.*, 1993).

Recombinant Vitronectin and recombinant Laminin-511 both are defined xeno-free extracellular matrix surfaces that are suitable for long-term maintenance of hPSCs (Braam *et al.*, 2008; Rodin *et al.*, 2010).

Synthetic surfaces: some synthetic surfaces can support the maintenance of hPSCs (Kolhar *et al.*, 2010; Melkoumian *et al.*, 2010; Villa-Diaz *et al.*, 2010). Most interesting, however, was the use of UV/Ozone radiation to modify the cell culture plastic making it convenient surface for hPSCs culture without the need of any matrices, peptides or

polymer coat (Saha *et al.*, 2011). Compared to feeder-based cultures, this study showed 3 times increase in cell number.

Suitable maintenance media for hPSCs

The first attempts for culture and propagation of hESCs usually used a feeder layer of MEFs and added foetal bovine serum (FBS) to the media. Since the first isolation and culture of hESCs the components of the growth media used for their culture has changed a lot. The goal of such continuous dynamic adjustment and changing was to set conditions to suit their use for therapeutic purposes later on. The aim was to achieve a chemically defined condition that is free of animal products and serum, still suitable for supporting pluripotency.

A group of studies have been performed to find replacements for the animal products in the culture system (Genbacev *et al.*, 2005; Li *et al.*, 2005; Vallier, Alexander and Pedersen, 2005).

Ludwig and colleagues developed TeSR1; a chemically defined medium that contained a combination of amino acids, trace elements, inorganic salts, lipids, vitamins, 2-mercaptoethanol and some growth factors and proteins including: FGF2, TGF beta and human serum albumin. This media was able to support maintenance of hPSCs in a feeder free condition (Ludwig *et al.*, 2006). Although TeSR1 originally depended on cloned human albumin as an albumin source, its relative high cost made most of the labs replace it with bovine serum albumin (BSA) which means that the source of albumin in the media is still derived from animal source, besides, the variation between albumin batches has led to inconsistency of results using TeSR1 media. A modified version of that media, Essential 8 (E8) media, was then developed in the same lab. A major advantage for the E8 media over TeSR1 media is that it did not have serum albumin in its components. Initial removal of albumin from TeSR1 media caused toxicity to the cells but when they removed 2-mercaptoethanol together with albumin they found that albumin became no longer essential (Chen *et al.*, 2011). In comparison to TeSR1 media that contained 18 components added to the DMEM/F12 basal media, the E8 media has only 8 components described as being essential for the maintenance of hPSCs.

More recently however, a study reported that cells cultured in either E8 or TeSR1 media show changes in nucleolar morphology and number, higher levels of radical oxygen species (ROS) and higher mitochondrial potential compared to cells cultured in KSR medium. According to that study, maintaining cells in E8 or mTeSR media induces double-stranded DNA breaks, higher sensitivity to gamma-irradiation and increases the expression of P53, a transcription factor that increases in response to DNA damage. Furthermore, cells cultured in these media have a higher potential of single nucleotide variations in their genomic DNA; having a normal karyotype is not enough to judge the genomic integrity of the cells. They concluded that the currently used parameters to evaluate different media rely only on pluripotency markers and the functional ability of the cells to differentiate into all three germ layers, however, these criteria do not measure the cellular stress or the genotoxic effect of the media (Prakash Bangalore *et al.*, 2017).

Improving hPSCs survival after passaging and cryopreservation:

The addition of the Rho-associated kinase (ROCK) inhibitor Y-17632 has been shown to protect cells from dissociation-induced apoptosis and enhance the survival of hPSCs after dissociation into single cells both in feeder cultured cells and in feeder-free culture condition using Matrigel-coated plates and MEF-conditioned medium. Using ROCK inhibitor increased the cloning efficiency and enabled subcloning of hPSCs after genetic manipulation (Watanabe *et al.*, 2007). The use of ROCK inhibitor also proved to enhance the revival of hPSCs after cryopreservation and increased single cells cloning after thawing (Li *et al.*, 2008).

1.4.3 iPSC genomic instability:

Reports on chromosomal abnormalities and genetic mutations in different iPSC lines have raised concerns regarding the use of these cells in therapeutic applications (Yoshihara *et al*, 2017; Henry *et al*, 2019). A clinical trial to implant hiPSC-derived retinal cells was halted in 2015 after detecting genetic mutations in three different genes (Garber, 2015).

Methods for detecting genomic instability:

G-banded karyotyping is one of the commonly used methods to detect numerical aberrations, including aneuploidy and polyploidy, and large structural aberrations that are few megabases in size (Meisner and Johnson, 2008). Array-based technologies such as comparative genomic hybridization and single nucleotide arrays investigate chromosomal copy number variations at higher resolution and can detect genomic abnormalities at the level of individual genes, however, they do not detect balanced translocation or inversion (Le Scouarnec and Gribble, 2012). More recently, the development of next-generation sequencing (such as whole-genome sequencing and whole-exome sequencing) has enabled genome-wide detection of mutations at single-nucleotide resolution. Several studies reported a considerable load of single-nucleotide variants in different iPSC lines using whole genome sequencing or whole-exome sequencing (Bahutani *et al*, 2016; Abyzov *et al*, 2017; Kown *et al*, 2017).

Origin of iPSC genomic variations:

Genomic instability in iPSCs has different causes. Studies that performed sequencing analysis for iPSCs and compared the result to that of their parental fibroblast cells have shown that some of the mutations had their origin in the fibroblasts (Abyzov *et al*, 2012; Gore *et al*, 2011). In this case, low frequency somatic variants in fibroblasts become selected and expanded as a result of clonal selection during iPSC generation (Yoshihara *et al*, 2017).

Another fraction of genetic variations in iPSCs is caused by reprogramming-induced mutations. Using whole genome sequencing, Sugiura et al assessed mouse iPSC lines and ESC lines against their corresponding parental cells. They found a remarkably higher number of point mutations, that were not detected in the parental cells, in iPSCs compared to ESCs. In addition, they investigated the variant allele frequencies and investigated the heterogenicity of point mutation profiles within a one iPSC clone through subcloning. They concluded that a considerable number of point mutations occur during the generation of the iPSCs, particularly at the initiation steps (Sugiura *et al*, 2014).

iPSCs could also acquire mutations as a result of prolonged culture (i.e., passage-induced mutations). A study that compared the sequencing analysis of one iPSC line

at early and late passages found four passage-induced point mutations in the late passages (Gore *et al*, 2011).

1.4.4 iPSCs and ESCs differentiation:

Removal of the essential factors that maintain the pluripotent state of the ESCs or iPSCs results in their spontaneous differentiation. If no specific factors were used to purposely direct the cells toward a particular cell fate, the pluripotent cells would differentiate to form Embryoid bodies (EB) in *in-vitro* cultures or result in teratoma formation if injected *in-vivo*. Both teratoma and EB contain heterogenous types of differentiated cells (obtained from the three different germ layers) including neuronal, heart, kidney, skin etc. In contrast to that type of differentiation, directed differentiation uses information obtained from developmental studies to purposely direct the cells to a particular cell fate, i.e. recapitulating the natural signalling events that specifically occur during the development of the organ of interest in-vitro. Directed differentiation usually implies sequential multi-step protocols. While the efficiency of obtaining any particular cell fate through spontaneous differentiation is low, the directed differentiation aims at increasing the efficiency and the yield of the cells of interest.

1.4.4.1 Differentiation towards renal progenitors and renal organoids:

Early studies to differentiate pluripotent cells into renal progenitors were also based on murine cells. Injecting tagged mESCs into the metanephric kidney of E12 and E13 embryos demonstrated that ESCs, in response to the embryonic developmental signals, were integrated into tubular structures that showed positive reaction to lotus tetragonolobus lectin (LTL) and expressed Na/K ATPase. The same study also showed seldom integration of individual cells into the glomerular tufts (Steenhard *et al.*, 2005). Yamamoto et al showed the expression of WD and UB markers: PAX2, LHX1, RET and EMX2; and the MM markers: WT1, SALL1, WNT4 and GDNF in EB outgrowths; when cells taken from EB outgrowths were injected retroperitoneal, they resulted in teratoma formation. These teratomas were excised and analysed to show the expression of the same genes by RT-PCR. Nevertheless, histochemical analysis showed that the majority of the teratoma components were either neuronal tissue, skeletal muscle or smooth muscle; structures with positive renal progenitor markers were limited and the found nephrons resembled the mesonephric nephrons more than

the metanephric ones (Yamamoto *et al.*, 2006). These early studies demonstrated the potential of mESCs to yield renal progenitors. That pattern of differentiation, however, was a spontaneous or stochastic differentiation with limited efficiency to produce renal progenitors.

A group of studies tried to recapitulate the sequence of molecular events that drives the differentiation of renal progenitors from pluripotent cells in-vitro, using kidney development as paradigm, to achieve directed differentiation towards renal structures with higher efficiency. RA, BMP, WNT signalling, FGF, and Activin are all factors that have been demonstrated to be essential for mesodermal specification, IM differentiation and metanephric kidney development. Using different combinations and concentrations of these factors different studies have succeeded in step-wise differentiation of mESCs and/or miPSCs into renal progenitors (Kim and Dressler, 2005; Bruce *et al.*, 2007; Morizane, Monkawa and Itoh, 2009; Nishikawa *et al.*, 2012).

The study performed by Batchelder et al was the first to extrapolate data from mouse to human; they used RA, Activin-A and BMP4 or BMP7 to direct the differentiation of hESCs towards renal progenitors (Batchelder *et al.*, 2009). Recently, there have been some published protocols using different growth factors for stepwise directed differentiation of human induced pluripotent stem cells (hiPSCs) toward UB and/or MM, then using the obtained renal progenitors to make renal organoids.

In 2013, Xia et al showed that mesodermal cells and subsequently UB progenitors could be obtained from human ESCs and hiPS cells by using BMP4 and FGF2 to differentiate the pluripotent cells to mesodermal cells followed by treatment with retinoic acid, activin A and BMP2 to drive the cells toward IM and UB renal progenitors. The researchers then mixed the obtained cells with dissociated mouse embryonic kidney cells, reaggregated the cells, cultured the pellet in 3D, and showed the integration of their UB differentiated cells into the collecting ducts of the self-organised formed organoid (Xia *et al.*, 2013).

Using a 9-day differentiation protocol, Morizane et al, were able to obtain MM nephron progenitors expressing SALL1, SIX2, PAX2 and WT1. Those nephron progenitors were able to form renal vesicles that matured to give different parts of the nephron (Morizane and Lam, 2015).

Takasato et al. (2014); published a protocol for simultaneous generation of both UB and MM cell types from PSCs in 18-day differentiation protocol using CHIR99021 followed by FGF9 and heparin (Takasato *et al.*, 2014). This protocol was striking as the UB and the MM have different developmental origin; the MM originates from the posterior IM while the UB originates from the anterior IM (Taguchi et al., 2014).

A year later, the same group modified their published protocol and proposed a theory that shorter period of initial CHIR99021 treatment (3 days) would lead to anterior IM fate and would end by more UB directed fate and longer period of initial CHIR99021 treatment (5 days) differentiates cells toward posterior IM fate and would end by more MM directed fate while midway between both directions using 4 days of initial CHIR99021 would differentiate iPSCs into both renal progenitors simultaneously. The CHIR99021 treatment was followed by a period of FGF9 treatment which ends by the simultaneous induction of UB and MM progenitors. The differentiated renal progenitors when dissociated and cultured in a 3D environment were able to form renal organoids showing positivity to different renal structures including nephrons with positive markers to Podocytes: WT1 and NPHS1, Proximal tubules: LTL and AQP1, Loop of Henle: UMOD, and distal tubules: ECAD; CDs positive to PAX2, ECAD and GATA3; renal stromal cells and renal vascular progenitors (Takasato *et al.*, 2015).

Taguchi and colleagues used a backward developmental approach in which they isolated T+ posterior IM cells from mouse embryos and defined the growth factors that induce their differentiation into MM. They used their findings to define factors to differentiate mESCs and hiPSCs, in a five steps protocol, into MM cells expressing OSR1, WT1, SIX2, HOX11, PAX2. Apart from the length of the differentiation protocols (14 days for human cells and 8.5 days for mouse cells), the protocols for driving renal progenitors from hiPSCs and mESCs were similar. The induced nephron progenitors from mESCs upon culture with mouse spinal cord showed stimulation of nephrogenesis and formation of 3-D renal tubular structures (Taguchi *et al.*, 2014).

More recently, using the same backward developmental study, Taguchi and Nishinakamura developed a 7-step differentiation protocol to obtain UBs from both mESCs and hiPSCs. The backward developmental study means that they started by identifying factors that induce maturation in a specified developmental stage, used these identified factors to recapitulate that stage of maturation from an earlier one, and

then they moved to earlier then earlier stages to repeat the same process. After that, they use the defined factors to establish a step-wise differentiation protocol to obtain UB (or NP) from mESCs and then applied the protocol to hiPSCs (after adjusting the timing of each stage to suit the longer developmental periods for human embryos) (Taguchi and Nishinakamura, 2017).

The establishment of directed differentiation protocols to obtain renal progenitors from hiPSCs has enabled the formation of renal organoids (figure 1.4). Yet, meticulous assessment of the functional capacity of the induced nephrons is still needed. In addition, the obtained renal organoids lack the organisation and complexity of the normal organ and there is an obvious anatomical difference between organoids and the native kidney; rather than having nephrons arranged around a single collecting duct tree with a clear exit, the organoid consists of dispersed multiple non-connected collecting ducts. There is an increasing interest in organising the organoid structure and increasing its complexity (Davies, 2017; Oxburgh *et al.*, 2017).

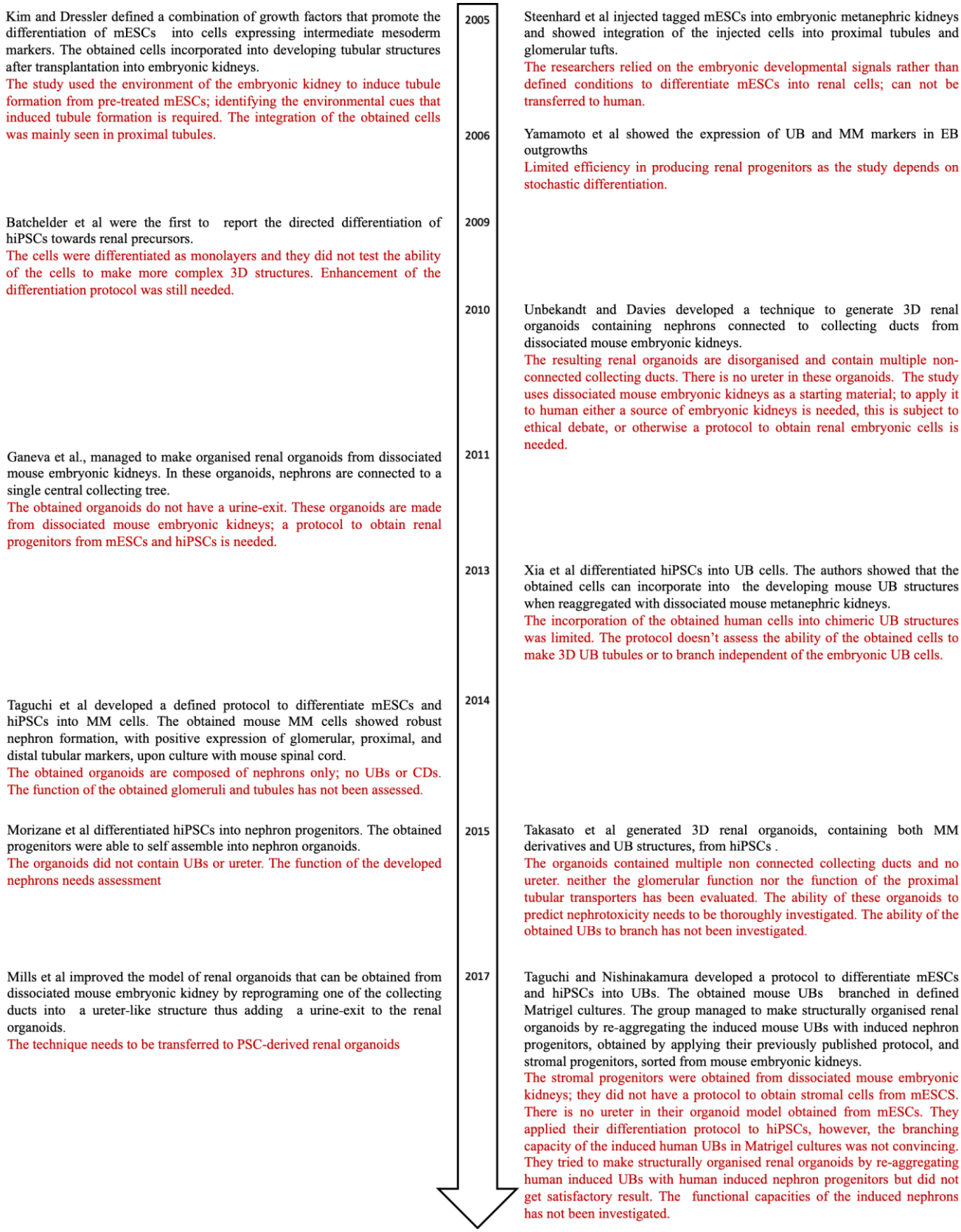

Figure 1.4. Schematic summary of the main protocols and techniques that enabled the generation of renal organoids. The main achievement of each protocol or technique is shown in black and the limitations are shown in red.

1.5 Aims:

This project builds on the current advances in stem cell research which allowed the generation of renal organoids from hiPSCs and has two main areas of focus:

First, to evaluate the currently available model of hiPSC-derived renal organoids by

- Investigating the efficiency of some of the available protocols at differentiating hiPSCs into nephron progenitors and ureteric bud progenitors.

- Exploring the ability of hiPSC-derived renal organoids to perform renal tubular function; an aspect of renal function which is involved in eliminating uremic toxins and of particular importance in renal drug handling.

- Assessing their suitability as a platform to predict nephrotoxicity. This is important as nephrotoxicity screening is commonly performed on animal models and monolayer cultures both of which have disadvantages and are not really predictive, hence it will be extremely useful if renal organoids could be employed for that purpose.

The second main focus is trying to improve that model and increase its complexity and anatomical realism, which is important for improving the functional capacity of these organoids, through:

- Developing and optimising techniques for isolating correctly differentiated UBs; this is an essential step towards in-vitro engineering strategies which necessitate obtaining pure cell populations to be used in a controlled way to build an organised structure.

- Studying signals involved in stimulating proliferation and inducing branching in embryonic UBs to use the obtained information to optimise a technique to test the ability of those UBs to branch and form 3D collecting system.

Chapter 2

2 Materials and Methods

2.1 hiPSC cultures

2.1.1 Coating culture plates with Matrigel:

Before thawing a vial of hiPSCs, culture plates were first coated with Matrigel (Corning, 354277). Matrigel was always handled on ice and was aliquoted using chilled pipettes and tips to avoid its solidification. When receiving a new bottle of Matrigel, it was thawed on ice in a 4°C fridge overnight. The Matrigel was then aliquoted into 15 mL Falcon tubes according to the batch dilution factor; the dilution factor is lot specific and is provided in the certificate of analysis. The dilution factor typically ranges between 270-350 µL and is used to prepare 25 mL of working Matrigel solution. As I never used 25 mL of Matrigel working solution at a time, I usually prepared aliquots of 67.5-87.5 µL (quarter of the recommended dilution factor; to avoid repeated freezing and thawing of the Matrigel aliquots). The Matrigel aliquots were kept in -20°C. To prepare Matrigel working solution, an aliquot of Matrigel was thawed on ice, then 6.25 mL of cold Kockout DMEM medium (KO-DMEM; Thermofisher, 10829018) were transferred to the Matrigel-containing tube and the solution was pipetted up and down gently. To coat culture plates, 1 mL of working solution was used per 1 well of a 6-well plate. Coated plates were either used immediately or sealed and stored at 4°C for up to one week.

2.1.2 Thawing of cells:

hiPSCs were obtained from Lonza Walkersville inc (clone SFC-AD3-01). They had been reprogrammed from human adult fibroblasts using Sendai virus to force the cells to express the four reprogramming factors, OCT3/4, SOX2, KLF4, c- MYC (Fusaki *et al.*, 2009).

A 6-well Matrigel-coated plate was allowed to warm at room temperature for 1 hr to allow solidification of the Matrigel. A cryo-vial of hiPSC was taken from the liquid nitrogen and was thawed rapidly in a 37°C water bath. The cell suspension was transferred to a 15 mL falcon tube containing 5 mL of pre-warmed KO-DMEM medium. The cell suspension was dispensed gently drop by drop to the wall of the tube to avoid osmotic shock. Cells were then centrifuged at 180 x g for 5 minutes. The supernatant was discarded, and the cells were re-suspended in 2 mL of Essential 8 (E8) medium (life Technologies, cat. A1517001) (Chen et al., 2011) containing 10 µM ROCK inhibitor Y-27632 (Tocris cat. 1254; to improve the recovery of the cryopreserved cells)

(Claassen, Desler and Rizzino, 2009). Excess medium was aspirated from the Matrigel-coated well. The cell suspension was mixed gently and then transferred to the Matrigel-coated well. Cells were cultured at 37°C in a humified incubator with 5% CO2.

2.1.3 hiPSCs culture and maintenance:

hiPSCs were maintained by daily change of the spent medium with fresh E8 medium. When cells reached about 85% confluency, dissociation and passaging into new plates was performed. 1 hour before passaging, ROCKI Y-27632 was added to the cells in a concentration of 10 μM to prevent dissociation induced apoptosis (Kurosawa, 2012). After that, spent medium was removed and cells were washed in pre-warmed Dulbecco's PBS (DPBS). EDTA, 0.5 mM in DPBS, was then added to the cells to release them from the Matrigel and the cells were incubated for 5 min at 37°C. After removal of the EDTA, E8 medium + ROCKI was pipetted up and down to dissociate colonies. Cells were then re-plated on the surface of new Matrigel coated plates at a seeding density ranging from 1:5 to 1:10 (cells from one well were split into 5- to 10-wells); the split ratio depended on the passage number of the cells. Higher seeding density was required for lower passages and lower seeding density was required for higher passages (cells proliferate faster with higher passages). Next morning, medium was changed with E8 complete medium (and ROCKI was removed) with daily changing of the medium thereafter.

2.1.4 Cryopreserving hiPSCs:

hiPSCs were expanded and a stock of cells was cryopreserved in liquid nitrogen. For cryopreservation, cells were dissociated as with regular passaging. Cells from 1 well of a 6-well plate were re-suspend in 1.8 mL of E8 medium plus ROCK inhibitor and were transferred to two cryovials, 0.9 mL/1 cryovial. 0.1 mL of DMSO was then added to each cryovial. Cryovials were then placed in an isopropanol box (Mr. Frosty) and were transferred to -80°C. Next day, cells were transferred to liquid nitrogen.

2.2 hiPSCs differentiation using the Takasato protocol:

To start differentiation, iPSCs were dissociated using EDTA, as described with regular passaging. They were then further split into a single cell suspension (through pipetting the cell suspension up and down 10-15 times using 5 mL pipette) then seeded on the surface of Matrigel coated 6, 24 or 96 well plates at a seeding density of approximately 15,000 cells/cm^2 and were kept in E8 complete medium + ROCKI for overnight. Next morning, differentiation was started using the published protocol of Takasato et al., 2015. APEL medium (STEMCELL Technologies; 05210) containing 8 μM CHIR99021 was used for three days without changing the culture media during those three days (as the cells tended to detach with changing media; for details see chapter 3). After the period of CHIR treatment, cells were treated with FGF9 (in a concentration of 200 ng/mL) and heparin (in a concentration of 1μg/mL) until day 12 of differentiation. After that, all growth factors were withdrawn, and cells were kept in APEL medium without any growth factors until day 20-25. From the point of shifting the media to APEL + FGF9+ Heparin until the end of the differentiation, the medium was changed every other day (figure 2.1). For the experiments that were set to compare between the three different timings of initial CHIR99021 treatment, the same described method was followed with the difference that CHIR treatment was added for 3, 4, or 5 days. For the 4- and 5-days treatment, 50% of the media was replaced with fresh media on day three. Changing the media during CHIR treatment and the first 3-4 days of FGF9+ Heparin treatment was carried out gently as the cells used to detach during this period.

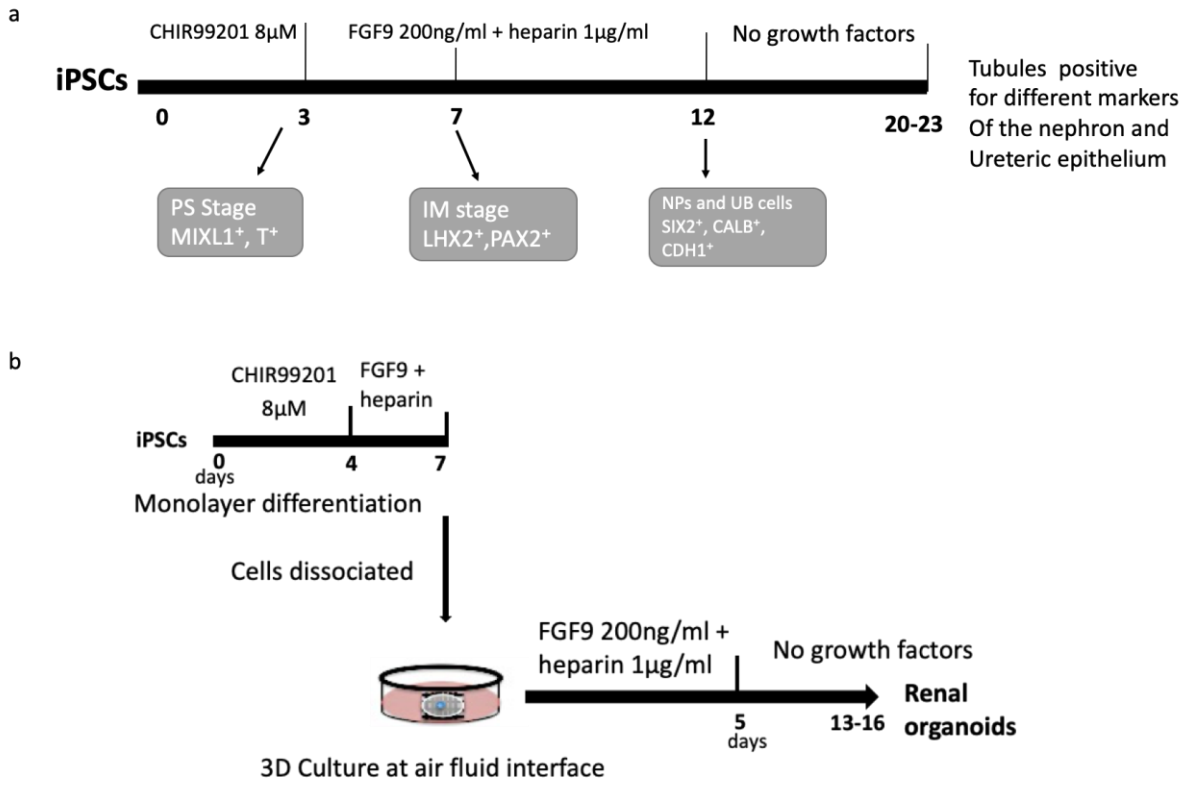

Figure 2.1. Schematic of the Takasato differentiation protocol

2.2.1 Monolayer immunostaining:

Immunostaining was performed on samples from different stages of the differentiation protocol to detect the stepwise direction of differentiation from pluripotency through the primitive streak, IM stage and renal differentiation.

To perform the immunofluorescence staining, the culture medium was aspirated, and cells were washed in PBS, then fixed using 4% PFA in PBS for 15 minutes at room temperature, after which cells were washed three times in PBS for 3 min each. Then a permeabilization/blocking step using 2% BSA and 0.3% Triton x100 in PBS solution was performed for 1 hr.

Cells were then washed in PBS and incubated with primary antibodies overnight at 4°C. After incubation with the primary antibodies, cells were washed in PBS three times for 15 minutes each and incubated with secondary antibodies for 2 hrs at room temperature. At the end, cells were washed in PBS three times for 15 minutes each

and then were kept in PBS. Images were taken using Zeiss Axiovert fluorescence microscope.

Working dilutions of the used antibodies are shown in table 2.1 (for the used primary antibodies), table 2.2 (for the used secondary antibodies). Antibody solutions were prepared using PBS containing 1% BSA.

Table 2.1 Primary antibodies

Primary antibodies	working dilutions	Company (catalogue number)	Marker for	Reference
Oct3/4	1:100	BD Biosciences (611202)	Pluripotency	Yamanaka and Takahashi, 2006
Rabbit anti-MIXL1	1:100	GeneTex (GTX60273)	Primitive streak	Davis *et al*., 2008
Rabbit anti-human Pax2	1:200	Biolegend (PRB- 276P-200)	IM, UB, MM and renal vesicle	Bouchard *et al*., 2002 Torres *et al*., 1995
Goat anti-human LHX1	1:100	SC (sc-19341)	IM and early renal marker	Tsang *et al*., 2000
Mouse anti-human Six2	1:100	Abnova (H000 10736-M01)	MM and nephrogenic progenitors	Kobayashi *et al*., 2008 Self *et al*., 2006
Rabbit anti-human Calbindin	1:200	CHEMICON (AB1778)	Ureteric buds and CD	Davies, 1994
Rabbit anti-human WT1	1:200	Santa Cruz Biotechnology (sc-192)	MM, Cap mesenchyme and podocytes	Kreidberg *et al*., 1993

Mouse anti-CDH1	1:300	BD Bioscience (610181)	Epithelial marker that marks CD and distal convoluted tubules	Lee *et al*., 2013
Goat anti-TROP2	1:100	R&D(AF650)	Ureteric trunk marker	Tsukahara *et al*., 2011
Sheep anti-NPHS1	1:200	R&D Systems (AF4269)	Podocyte marker	Ruotsalainen *et al*., 1999
Rabbit anti-T Brachyury	1:100	Santa Cruz Biotechnology (SC-20109)	Primitive streak and early stage mesoderm	Rivera-Perez Magnuson, 2005 Beddington *et al*., 1992
Pan-Uroplakin	1:500	A generous gift from Tung-Tien Sun Lab (New York University)	Urothelium	Hu *et al*., 2000 Brenner-Anantharam *et al*., 2007

Table 2.2 Secondary antibodies

Secondary antibodies	Working dilution	Company (catalogue number
Horse AMCA anti-mouse	1:100	VECTOR (C1-2000)
Donkey anti-mouse	1:500	Alexa fluor
Donkey anti-rabbit Alexa- 594	1:500	Alexa fluor (A-21207)
Donkey anti-goat Alexa-488	1:500	Alexa flour (A-11055)
	1:100	SIGMA (116K6098)

Table 2.3 lectins

Lectin	Working dilution	Company (catalogue number)	Marker for	Reference
FITC lotus tetragonolobus lectin	1:100	Vector laboratories	Proximal convoluted tubules	Barresi *et al*.,1988 Hennigar et al., 1985
Rhodamine conjugated- peanut agglutinin	1:500	Vector laboratories (RL-1072)	Distal convoluted tubules and β intercalated cells of the CD	Engel *et al*., 1997 Barresi *et al*.,1988

2.2.2 Organoid formation and culture:

For 3D cultures, cells from the monolayer were trypsinized after 7 days of differentiation and were dissociated into single cells, then re-aggregated by spinning down at 800 x g for 3 min. Cells were used at a density of 300,000 cells/ pellet.

Pellets were then cultured on the surface of Transwell inserts (Costar, 0.4µm polyester membrane) at the gas-liquid interface. 1.5 mL of culture medium was added underneath the filter membrane.

Pellets were cultured in APEL medium containing FGF9 (200ng/mL) and heparin (1µg/mL). Medium was changed every 2 days and careful attention was paid that the medium did not overflow the filter membrane. After 5 days of organoid culture (12 days of total differentiation), growth factors were removed, and organoids were kept in APEL medium without any growth factors for further 8-13 days to achieve a total differentiation period of 20-25 days.

2.2.3 Immunostaining of the organoids:

The same method was used as for monolayers, with some differences made for better penetration of the antibodies and better staining results:

- Methanol was used for fixation; the fixation step was performed overnight at -20°C and before staining organoids were rehydrated in PBS for 1 hour.
- The permeabilization/ blocking step was performed overnight instead of 1 hour.
- The secondary antibodies were kept for overnight at 4°C instead of 2 hours at room temperature.

2.3 Physiological uptake assays

2.3.1 Functional anion uptake test:

20 day-differentiated Organoids (total differentiation including the initial period of monolayer culture) were tested for the proximal tubular function anion uptake test using 6-Carboxyfluorescein (6-CF; Invitrogen, C1360). Pellets were first washed with PBS then incubated with rhodamine conjugated peanut agglutinin (PNA) to outline the tubular structures (using a final concentration of 20 µg/mL; Vector Laboratories; RL-1072) and 6-CF (1 µM) in PBS for 40 min at 37°C. for the inhibitor treated samples, Probenecid (2.5 mM) was added simultaneously with the 6-CF. After that, pellets were washed in PBS and incubated with 8 mM probenecid for 10 min at 37°C to prevent 6-CF efflux. Pellets were washed once in PBS, transferred to a microscope slide, covered with a drop of PBS to prevent dryness, and were imaged immediately.

2.3.2 Cation Uptake assay

20 day-differentiated organoids were incubated overnight with biotin-conjugated LTL (Vector Laboratories; B-1325; using a final concentration of 20 µg/mL in APEL medium) in the culture medium to outline the proximal tubular structures. The organoids were then washed three times in culture media for 10 minutes each. Streptavidin Alexa Fluor 350 was added (Thermofisher; S11249; using a final concentration of 10 µg/mL) to the culture media and the organoids were incubated for 1 hour at 37°C. After that organoids were washed once for 5 minutes and then

incubated with 4-(4-(dimethylaminostyryl)-N-methylpyridinium iodide (ASP; 10 µM; D288, Invitrogen) for 30 minutes. For the inhibitor treated organoids, the OCT2 inhibitor tetrapentylammonium chloride (TPA; 10 mM; 258962, Sigma) was first incubated with the organoids for 10 minutes and then ASP was added (still in the presence of TPA) for 30 more minutes. Organoids were then washed in ice cold PBS and transferred to a microscope slide and covered with one drop of ice-cold PBS and imaged immediately.

2.4 Cryopreservation of the differentiated cells:

To test the ability of the differentiated cells to survive cryopreservation, differentiated cells after 12 days or 18 days of differentiation were trypsinized and dissociated. After that the trypsin was neutralized using APEL medium and cells were centrifuged at 180 x g for 5 min. Cells were suspended in APEL medium + ROCK inhibitor, 10% DMSO was added and cells were transferred to cryovials and were frozen in - 80°C using slow freezing method (Miyazaki, Nakatsuji and Suemori, 2014).

2.4.1 Thawing, culture, and organoid formation from cryopreserved cells:

Once removed from -80°C cells were rapidly thawed and transferred to a 15 mL tube containing 5 mL of APEL medium, mixed gently and spun down by centrifugation for 5 min at 180 x g. After spinning down, the supernatant was aspirated, and cells were suspended in fresh APEL medium containing 10 µM ROCKI. Cells were counted and seeded on the surface of Matrigel-coated plates at a density of 300,000 cells/well of a 24-well plate as monolayers. Next morning, medium was changed for APEL medium without any growth factors.

For organoid formation the same described steps were followed but after spinning down the cells, the pellets were directly cultured on the surface of Transwell inserts at the gas-liquid interface using APEL medium + ROKI for overnight. Next morning, medium was changed as followed with monolayer culture.

2.4.2 Cisplatin treatment for the cryopreserved cells:

12 day-differentiated cells were cryopreserved as described above. After thawing the cells were used to make organoids and were cultured for 10 days before the treatment. Organoids were treated with 0, 5, 10, 30 µM Cisplatin for 24 hrs. Organoids were then fixed in methanol and stained for ECAD, LTL and Cleaved caspase 3 (Cell Signalling Technology; 9661S). Images were taken using Zeiss epifluorescence microscope.

2.5 Molecular Biology:

2.5.1 RNA extraction:

RNA was isolated using Rneasy mini kit (Qiagen; 74104) following the company instructions. On-column DNase1 treatment (RNase-Free DNase Set; Qiagen; 79254) was performed to remove contaminant DNA. The obtained RNA concentration was determined by measuring the absorbance at 260 nm using Nanodrop and A260/280 ratio was calculated to evaluate the quality of the RNA (all samples had a ratio of 1.7-2).

2.5.2 cDNA synthesis (reverse transcription) for RT-PCR:

A semi-quantitative reverse transcription was performed using 700 ng total RNA from each sample. For first strand cDNA synthesis, 0.5 µg (1µL) of Oligo DT 15 primers (Promega; C1101) was added to the RNA and the total volume was adjusted to 12.5 µl using RNase free water, the tubes were heated to 70°C for 10 minutes to anneal the primers then the tubes were transferred to ice. M-MLV-Reverse transcriptase enzyme (Promega; M1701), M-MLV 5X reaction buffer, dNTPs, rNasin RNAse inhibitor (Promega, N251A) and nuclease free water were added to the annealed primer/template as shown in table 2.4 (one reaction= 25 µL total volume). The reaction was then mixed, and an extension step was performed by incubating the mixture at 42°C for 1 hr. the product was stored at -20°C until used in PCR reaction

Table 2.4 Reagents used for reverse transcription:

Reagent	Final concentration used (volume)
M-MLV 5X reaction buffer	1x (5 µL)
dNTPs	1 mM (2.25 µL)

rNasin RNAse inhibitor	25 units (0.625 µL)
M-MLV-Reverse transcriptase enzyme	200 units (1 µL)
Annealed primer/template	12.5 µL
RNAase- DNAase-free water	3.625 µL

2.5.3 PCR for gene expression:

Primers for OAT1 (SLC22A6), OCT2 (SLC22A2), and β-actin were kindly provided by Dr. Melanie Lawrence; their design was spanning an intron (hence the cDNA product had a different length from the genomic DNA). β-actin primers were included in each PCR reaction, with the primers for the target gene, as a control. 2.0 µL of the obtained cDNA were used in a PCR amplification reaction (total volume for one reaction= 25 µL); 30 cycles were run using an annealing temperature of 58°C. PCR product was analysed by running agarose gel electrophoresis (table 2.5; 2.6) (using 1% agarose in TAE buffer; the reaction was run at 80 volts for 40 minutes) and bands were visualised under a UV lamp and were photographed.

The primer design was as follows:

SLC22A6 (OAT1; product size 209 bp)

Forward primer: AGTCCTTGTACATGGTGGGG
Reverse primer: CATGCAGTTGAGGGAGATGC

SLC22A2 (OCT2; product size 184 bp)

Forward primer: CCGTAAGCTCTGCCTCCTAA
Reverse primer: TGTTCTCCGATATCTCCGCC

Table 2.5 Reagent list for RT-PCR reactions

Component	Volume (final concentration)
cDNA	2 µL
Go Taq green reaction buffer	5 µL (1x)
dNTP mix 10mM	0.5 µL (0.2 mM)
B-actin F primer	0.4 µL
B-actin R primer	0.4 µL
Transporter gene F primer	1.1 µL (0.5 µM)
Transporter gene R primer	1.1 µL (0.5 µM)
Go Taq G2 DNA polymerase	0.25 µL (1.25U)
dsH20	14.25 µL
total	25 µL

Table 2.6 Thermocycling conditions for RT-PCR

Step	Temperature	time
Initial denaturation	95°C	2 min
Denaturation	95°C	30 s
Annealing	58°C	30 s

Extension	72°C	1 min
final extension	72°C	7 min

2.5.4 RNAseq analysis

RNAseq, and trimming, filtering and normalization of raw data, was performed by Edinburgh Genomics. 1 ug of total RNA/sample was used for sequencing library preparation using Illumina TruSeq stranded mRNA kit. Sequencing was performed using Novaseq S1 50 Paired-end run to produce 50-64 million read pairs/sample. Reads were trimmed using Cutadapt (version cutadapt-1.9.dev2) and were aligned to the Homo Sapiens reference genome (GRCh38; from Ensembl) using STAR (version 2.5.2b). The annotation used for counting was the standard GTF-format annotation for the reference genome (annotation version 84). Reads were assigned to features of type ‘exon’ in the input annotation grouped by gene_ID in the reference genome using featureCounts (version 1.5.1). The raw count data were filtered to remove very low expressed genes (genes consisting predominantly of near-zero counts), filtering was performed on counts per million to avoid artefacts due to library depth. Reads were normalised using the weighted trimmed mean of M-values method. Differential analysis (comparing the low-treated group to the control group, or the high-treated group to the control group) was carried out using edgeR4 (version 3.20.1). Fold changes were estimated as per the default behaviour of edgeR, to avoid artefacts which occur with empirical calculation. Statistical assessment of differential expression was carried out with the quasi-likelihood (QL) F-test.

To analyse the upregulated genes in the high-treated versus the control contrast, I first filtered the differentially expressed genes by the lowest FDR, selected the 400 most significant genes, and then picked the 100 most upregulated genes (out of the 400 most significant genes) and used them for downstream analysis. I used these 100 most significant upregulated genes to performed PANTHER Overrepresentation Test using the annotation version GO Ontology database (release date 2018-10-08). For the functional classification, the same list of genes was used in a Panther functional classification analysis selecting the ontology Biological Process and the ontology Molecular Function.

2.5.5 CRISPR-Cas9 editing of HMOX1 gene in hiPSCs

The targeting vector was designed to contain a 2A-peptide-mCherry-STOP cassette flanked by homologous 5' and 3' arms upstream (500bp) and downstream (1049bp) of the endogenous stop codon of the HMOX-1 gene in the hiPSCs. The vector was synthesized by IDT company and then subcloned into pUC18 for transfection (Addgene, cat. no. 50004). Guide RNAs (gRNAs) were designed using the Zhang lab resource (crispr.mit.edu). Undifferentiated hiPSCs were co-transfected in equimolar amounts with the Cas9-GFP (pCas9_GFP; Addgene, cat. no. 44719) and gRNA plasmids together with the targeting vector containing the repair template. After letting the cells recover and proliferate for 72h, cells were treated with hydrogen peroxide to induce oxidative stress (0, 25 or 150mM; Fisher Scientific, cat. no. BP2633-500) and then sorted using FACS to isolate the mCherry-targeted population. Control hiPSCs (wt) that had not been targeted were used as a control for gating. The enriched populations were recovered and expanded for a further 7 days. The low but detectable basal level of HMOX-1 expression in undifferentiated hiPSCs allowed the sorting of single, weakly mCherry-positive hiPSCs into wells of a 96-well plate without needing to first induce oxidative stress. Wild type (untargeted) hiPSCs (AD3) were again used for gating. After a further 7 days, 24 clonal populations from the single-cell sorting by FACS had survived and expanded. These were further expanded into individual wells of a 6-well plate. PCR, using primers designed to span the targeted region, was used to confirm that the reporter cassette had been integrated. The product size without cassette insertion is 1654bp, whereas product size with insertion is 2428bp, as expected. Clones were sequenced using primers spanning the homologous arms and the inserted cassette (the design and production of this cells line was done by Shuwan Liu; an MSC student in our lab, with the help of Dr. Melanie Lawrence).

2.5.6 GATA3 gene targeting strategy:

For details about the design of the gRNA and the repair template plasmid see chapter 6, section 6.3

2.5.6.1 Genomic DNA extraction from hiPSCs:

hiPSCs were dissociated from an 80% confluent well of a 6-well plate using the regular dissociation steps described earlier. The obtained cells were centrifuged at 300 x g for 5 minutes, the supernatant was discarded, and cells were re-suspended in 200 µL PBS. DNA isolation was then performed using DNeasy Blood and Tissue Kit (Qiagen, 69504) according to the manufacturer protocol. The obtained DNA concentration was measured using a Nanodrop and was stored at -20°C for PCR.

2.5.6.2 Targeting plasmid design and primer design:

GATA3 cDNA sequence was obtained from Ensemble (www.ensembl.org). The repair template was designed with the help of Geneious Prime software. The primers for the upstream segment (segment 1), the downstream segment (segment 5) and the antibiotic selection cassette segment (segment 4) were designed using NEB builder assembly tool (nebuilder.neb.com). The Gibson assembly master mix settings were used. The primer design included overhang areas to amplify overlapping segments to be assembled in Gibson reaction. Selected primers for segment 1 and 5 were checked for unspecific binding with BLASTn (after excluding the overhang areas) (segment 4 was amplified from a plasmid). The list of primers used for this work is shown in table 2.7

Table 2.7 list of primers used for amplifying the constructing segments of the GATA3 targeting plasmid

Segment	Primer sequence	Product size
Segment 1	FP: AAGCTTGCATGCCTGCAGGTCGACTAGACGGGGCTGTAATCTGG RP: CGTGGTCAGCATGTGGCTG	477 bp
Segment 4	FP: TCATATCCCCTATTTAACCCTAGAAAGATAGTCTG RP: ACTAGAGACCCTGTTAACCCTAGAAAGATAATCATATTG	3262 bp
Segment 5	FP: TTTCTAGGGTTAACAGGGTCTCTAGTGCTGTG RP: TTCGAGCTCGGTACCCGGGGATCCTCATCTTTTCTTATTTTGGTGCTTTG	519 bp

Segment 2 and segment 3 were synthesised by IDT and were obtained as gBlocks. (the cDNA sequence for the GATA3 gene, the sequence for the PMSC-AAT-PB-PGK plasmid, from which segment 4 was amplified, and the sequence for the designed segments and the cloning vector are included in the appendix of this thesis). The PCR reaction was performed using Q5 high fidelity enzyme (NEB, M0492L). The PCR reaction reagent list and concentrations are shown in table 2.8. The obtained amplified products were gel purified using QIAquick Gel Extraction Kit (Qiagen, 28704) according to the manufacturer instructions and the purified segments were measured using a Nanodrop instrument.

Table 2.8 Reagent list and concentrations for PCR reactions to amplify the GATA3 targeting plasmid segments

Component	**Volume (final concentration)**
Q5-high fidelity 2x master mix	25 µL (1 x)
Forward primer	2.5 µL (0.5 µM)
Reverse primer	2.5 µL (.05 µM)
Template DNA	Variable (50 ng)
Nuclease free water	To achieve a total volume of 50 µL

2.1.1.1. Gibson assembly:

The DNA segments were included in a cloning reaction using Gibson assembly master mix (NEB, E2611S). The reaction was performed following the kit instructions. The vector was used in a concentration of 100 ng. The number of pmols were calculated for each fragment using NEB calculator (http://nebiocalculator.neb.com). The vector was used in a concentration of 100 ng (0.057 pmols) and the segments were used in a 2-3-fold of excess with the shorter segments being used in a higher ratio (as

recommended by the company). The fragments were mixed with 10 µL of the Gibson assembly master mix and the total volume was adjusted to 20 µL using deionised water. The reaction was incubated at 50°C for 1 hr, then was stored at -20°C and was used for transformation.

2.1.1.2. gRNA design and cloning

Two gRNAs were designed using the Zhang lab resources ((https://zlab.bio/guide-design-resources). The sequence of the selected gRNAs was as follows:

gRNA1 sequence: GATGGCGGGTGCATCGGCGTGGG
gRNA2 sequence: ACCCATGGCGGTGACCATGCTGG

The selected sequence was sent to IDT for synthesising as gBlock following the addgene gRNA synthesis protocol (media.addgene.org). The obtained gBlocks were shortly spun down for 15 seconds then TE buffer was added, to achieve a final concentration of 25 ng/mL. The mixture was vortexed for 15 seconds then incubated at 50°C for 20 minutes to resuspend the pellet. The reconstituted gBlock was vortexed for 15 seconds then centrifuged at 800 x g for 3 minutes. The reconstituted gBlocks were then cloned into PCR-Blunt II-TOPO (Thermofisher, K280040). Blunt II-Topo cloning is a Topoisomerase I-based ligation that is designed to clone blunt-ended DNA fragments. The cloning reaction was performed according the company instructions and was as follows: 2 µL of the reconstituted gBlock were mixed with 2 µL of water, 1 µL of salt solution (provided in the kit) and 1 µL of the Blunt II-Topo vector. The reaction mixture was incubated for 5 minutes at room temperature and then was used in a bacterial transformation reaction.

2.5.6.3 Bacterial transformation and plasmid purification:

Top 10 chemically competent E-coli (Thermofisher, C404003) were used for transforming the cloned Blunt II-Top vector (after the insertion of the gRNA gBlocks). 5-alpha Competent E. coli (NEB, C2987H) were used for the transformation of the Gibson-cloned targeting plasmid. For both cases the protocol was the same. The bacterial cells were thawed on ice for 10 minutes. 2 µL of the plasmid DNA (~ 50 ng) were added to the tube of the bacterial cells. The tubes were gently flicked to mix the DNA and the bacterial cells. The tube was incubated on ice for 30 minutes, then heat-shocked at 42°C for 30 seconds and was placed back on ice for two minutes. Afterwards, 250 µL of SOC media were added to the bacterial cells (with no antibiotic

added) and the cells were incubated at 37°C for 1 hr in a shaking incubator (to allow the bacteria to develop the antibiotic resistant encoded on the plasmid before plating on antibiotic selection agar plates). The bacterial suspension was then spread over the surface of 10 cm LB agar plates (containing the selection antibiotic encoded on the transformed plasmid; Kanamycin in the case of the Blunt II-Topo vector, and Ampicillin in the case of the Gibson-cloned plasmid). Two plates were inoculated with different densities of the bacterial cells to give better chance for getting single colonies. One plate was inoculated with 100 µL of the bacterial suspension and the other plate was inoculated with 10 µL of the bacterial suspension diluted with 90 µL LB medium. The bacterial plates were incubated overnight at 37°C.

In the morning, single colonies were picked from the bacterial plates and each colony was resuspended in 50 µL water. Of these 50 µL bacterial suspension, 45 µL were inoculated into 4 mL LB medium (containing the selection antibiotic encoded on the transformed plasmid) and the remaining 5 µL were used in a PCR reaction to check for the incorporation of the gRNA gBlocks (in the case of Blunt II-Topo) or a middle segment of the GATA3 targeting plasmid (in the case of the Gibson-assembled targeting plasmid). The 4 mL of LB medium that have been inoculated with the 45 µL bacterial suspension were incubated in a shaking incubator at 37°C overnight. In the morning, the bacterial suspensions were used in a miniprep reaction (Qiagen, 27104) to purify the plasmid (following the company instruction), the obtained plasmid was then analysed using restriction enzyme analysis. For the gRNA-Blunt II-Topo cloned-plasmid, I obtained positive results both from the PCR reaction and from the miniprep purification and the restriction analysis, so, one colony for each gRNA-Blunt II-Topo cloned-plasmid was further amplified in a 200 ml of LB medium containing the selection antibiotic and the plasmid was purified using Maxiprep kit (Qiagen, 12963). The purified plasmid was analysed using restriction enzymes (EcoR I, cuts on both sides of the gRNA gBlock insert and Sal I, cuts in the plasmid backbone) and gel electrophoresis which.

2.6 Nephrotoxicity compound screening:

A panel of 7 compounds was used for the blind-coded validation, selected and supplied by an industrial company without revealing their identities, and was as follows: Cidofovir (cat no C5874), Cisplatin (cat no C2210000), Dexamethasone (cat

no D1756), Gentamicin (cat no G1264), Ifosfamide (cat no I4909), Ketoprofen (cat no K1751) and Puromycin (cat no P7255); all from Sigma-Aldrich. The compounds were divided into 3 groups based on their therapeutic Cmax values (Sjögren *et al.*,2018) and concentration ranges were designed accordingly: 0.375-24 µM for Dexamethasone and Puromycin, 6-384 µM for Cisplatin, Gentamycin and Ketaprofen, 24-1536 µM for Cidofovir and Ifosfamide. These concentrations were also in accordance with what have been used in other toxicological studies (see discussion of chapter 5 and references in there). A four-fold dilution series was prepared for each compound (obtained lyophilized) and HMOX1-mCherry-hiPSC-derived renal cells (2D and 3D) were incubated in these dilutions for either 24h or 72h. Untreated control samples were included for each compound, time-point and culture type (2D or 3D).

2.7 GDNF conjugation:

Microscale protein labelling kit was used for the conjugation (Thermofisher Scientific; Alexa fluor 488, A30006). Carrier-free GDNF protein (R&D; 212-GD-050/CF) was reconstituted to a concentration of 1mg/mL in PBS and the labelling was done following the instruction of the protein labelling kit. 45 µL of the GDNF was transferred to a reaction tube and 4.5 µL of 1 M sodium bicarbonate was added. 7 µL of freshly prepared Alexa fluor 488 TFP esters (11.3 nmol/µL stock solution) was added to the reaction tube and the reaction mixture was incubated for 25 minutes at room temperature. Afterwards, the reaction mixture was transferred to a spin filter with resin bed and was centrifuged at 16,000 x g for 1 min to purify the conjugated protein and remove the unreacted dye.

To determine the concentration of the recovered protein, I first used Nanodrop 2000 spectrophotometer to measure A280 of the protein before and after conjugation (to be used in this equation: Protein concentration (in mg/mL) = (A280 – 0.11(A494)) / (A280 of protein at 1 mg/mL), however A280 of the protein at 1mg/ml was very low and so was difficult to determine accurately using the Nanodrop (0.38±0.2). Alternatively, the concentration of the recovered protein was estimated based on the expected % yield of the protein based on its molecular weight using this equation: concentration of the labelled protein (in mg/mL) = (mass (mg) starting protein × % yield) / (volume of the recovered protein in mL). The estimated concentration of the conjugated protein was

400 µg/mL. The degree of labelling was calculated using this equation: DOL = A494 / (71,000 × protein concentration (M)). The obtained degree of labelling was approximately 2.5 moles of dye/mole of protein.

For testing the efficiency of labelling, mouse embryonic kidneys were treated with 100 ng/mL conjugated protein in the culture media and were incubated for 1 hr, 4 hrs, or overnight. The embryonic kidneys were then washed three times in culture media for 5 minutes each and were imaged.

For tagging the UB-differentiated structures, 22-25 day-differentiated cells were treated overnight with 100 ng/mL conjugated GDNF in the culture media at 37°C, then they were washed three times for 5 minutes each and imaged using Zeiss Axiovert fluorescence microscope.

The live-stained UB-like structures were then dissected under fluorescent microdissection microscope and were used either for re-aggregation with sorted nephron progenitors or for testing branching competence (explained in section 2.11)

2.8 Embryonic UB isolation and culture in gel:

2.8.1 Dissection of mouse embryonic kidneys:

The uterine horns of E11.5 pregnant mice (CD1) were collected (the morning of the vaginal plug appearance is counted as E0.5) and transferred to a 10 cm Petri dish that contains minimum essential media (MEM; Sigma-Aldrich, M5650). Embryos were extracted from the uteri using forceps and a surgical blade. Further dissection was carried out under microdissection microscope (Zeiss Stemi-2000) using 25-gauge needles attached to 1 mL syringes. First the embryos were decapitated. The decapitated embryos were then cut horizontally between the upper limb buds and the hind limb buds. The caudal parts of the embryos were transferred to a new petri dish with a fresh medium and the tails were removed. Then the rear-end fragments were cut along the midline into right and left sides to expose the metanephric kidney rudiments. Kidney rudiments were identified and dissected out carefully (figure 2.3).

2.8.2 Isolation and culture of embryonic UBs

Isolated metanephric kidney rudiments were transferred to a 30 mm Petri dish containing Trypsin EDTA and were incubated at 37°C for 5-7 minutes. Afterwards

metanephric kidney rudiments were transferred to a 60 mm petri dish containing kidney culture medium (KCM: MEM medium containing 10% foetal bovine serum and 1% penicillin/streptomycin) to stop the enzymatic action of the trypsin. The UBs were dissected free of the surrounding MM using fine needles. The isolated UBs were collected in a 30 mm petri dish containing fresh medium and were cut into single tips. The separated UB tips were then transferred to 96-well plate containing GFRM (Corning 354230; 60 µl/well) and were cultured suspended in Matrigel (after transferring the UB tip to the Matrigel, the plate was carefully turned upside down for ~ 30 sec -1 min to prevent the tip from sinking to the bottom of the well (as this alters the pattern of branching); the Matrigel stayed as a hanging drop when the plate was inverted). Adding the Matrigel to the wells and transferring the isolated tips to the Matrigel containing wells was performed one well at a time to avoid solidification of the Matrigel before transferring the isolated tip. After transferring all the UB tips to the Matrigel, the plate was incubated at 37°C for 10 minutes to allow for Matrigel solidification. After solidification of the Matrigel, branching basal medium containing the indicated tested growth factors was added to the Matrigel-suspended UB tips. The branching basal medium composition was as follows: Ad DMEM/F12 (Thermofisher, 12634010) containing 1X antibiotic antimycotic (Gibco 15240-096), 1X B27 minus vitamin A (Gibco 12587-010), 1X N2 supplement (Gibco 17502-048) and 1mM nicotinamide (Sigma). The following growth factors were added as indicated in chapter 7 (section 7.3.1): 125 ng/mL GDNF (Peprotech, 450-10), 250 ng/mL FGF1 (Peprotech, 450-33A), 1 µM CHIR99201 (Tocris, 4423)**,** 0.5 µM RA (Sigma) and 0.5 µM 9-cis-retinol (Sigma).

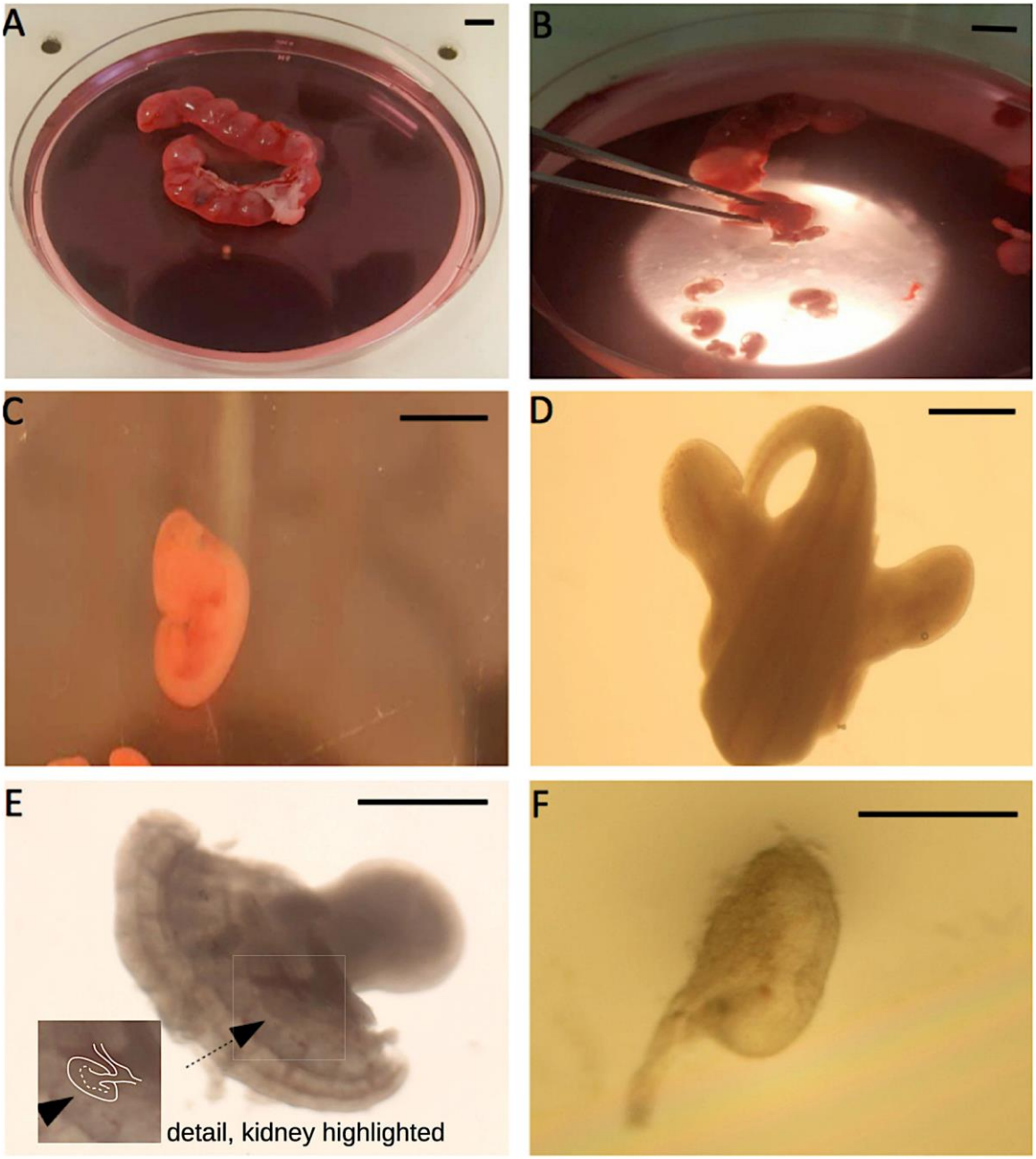

Figure 2.2. Illustration of metanephric kidney rudiments isolation. a) Uterine horn. b) Embryos are being extracted from the uterine horn. c) An extracted E11.5 embryo. d) The rear-end of the embryo after decapitation and removing the upper part of the embryo. e) The rear-end fragment of the embryo after cutting it in the midline into right and left halves; the arrow points to the metanephric kidney rudiment. f) An isolated E11.5 metanephric kidney. Scale bar is 5 mm for (a-c), 1mm for (d,e), and is 0.5 mm for f. adapted from (Elhendawi and Davies, 2018).

2.9 hiPSC differentiation towards UB progenitors using the Taguchi protocol of differentiation:

Accutase enzyme (Thermofisher, A1110501) was used to dissociate hiPSCs. The dissociated cells were suspended in step 1 medium and were cultured at a density of 10,000 cells/well of a V-bottom 96-well low cell attachment plate (Alphalaboratories, MS-9096V). The differentiation basal medium was composed of Ad DMEM/F12 containing 1X B27 supplement minus vitamin A supplement, 2 mM L-Glutamine, 1% ITS, 1%NEAA, 90 µM 2-mercaptoethanol and 1% antibiotic antimycotic. For step 1 differentiation, the following growth factors were added to the differentiation basal media: 10 µM Y27632, 10 ng/mL Activin A and 1 ng/mL BMP4. After 24 hrs, the re-aggregated cells were transferred to a new U-bottom 96-well plate and step 2 medium was added (differentiation basal medium with 1 ng/mL BMP4 and 10 µM CHIR99021). Cells were kept in step 2 differentiation medium for 36 hrs and were then switched to step 3 medium (0.1 µM RA, 100 ng/mL FGF9, 100 µM SB431542, and 100 nM LDN193189 in differentiation basal medium). Cells were kept in step 3 differentiation medium for 48 hrs and then the medium was changed to step 4 differentiation medium containing 0.1 µM RA, 100 ng/mL FGF9, 5 µM CHIR and 30 nM LDN193189. After 42 hrs, spheroids were dissociated and CXCR+/KIT+ cells were FACS sorted (see section 2.10 for details of the FACS-sorting). The sorted cells were suspended in step 5 medium and were cultured in V-bottom 96-well low attachment plates in a density of 5,000 cells/well. Step 5 medium contained the following growth factors: 10 µM Y27632, 0.1 µM RA, 1 µM CHIR, 5 ng/mL FGF9, 100 ng/mL FGF1, 10 nM LDN and 10% GFRM. After 48 hrs, medium was changed to step 6 medium containing 10 µM Y27632, 0.1 µM RA, 3 µM CHIR, 5 ng/mL FGF9, 100 ng/mL FGF1, 10 nM LDN, 1 ng/mL GDNF, and 10% GFRM. Spheroids were cultured in step 6 medium for 48 hrs and were then switched to step 7 medium containing 10 µM Y27632, 0.1 µM RA, 3 µM CHIR, 100 ng/mL FGF1, 10 nM LDN, 2 ng/mL GDNF, and 10% GFRM (figure 2.4). At the end of the differentiation protocol the spheroids showed outgrowing buds. Single buds were dissected from the periphery of the spheroids using fine needles and were suspended in Matrigel and cultured in branching inducing medium (see section 2.11 for more details about the culture procedure).

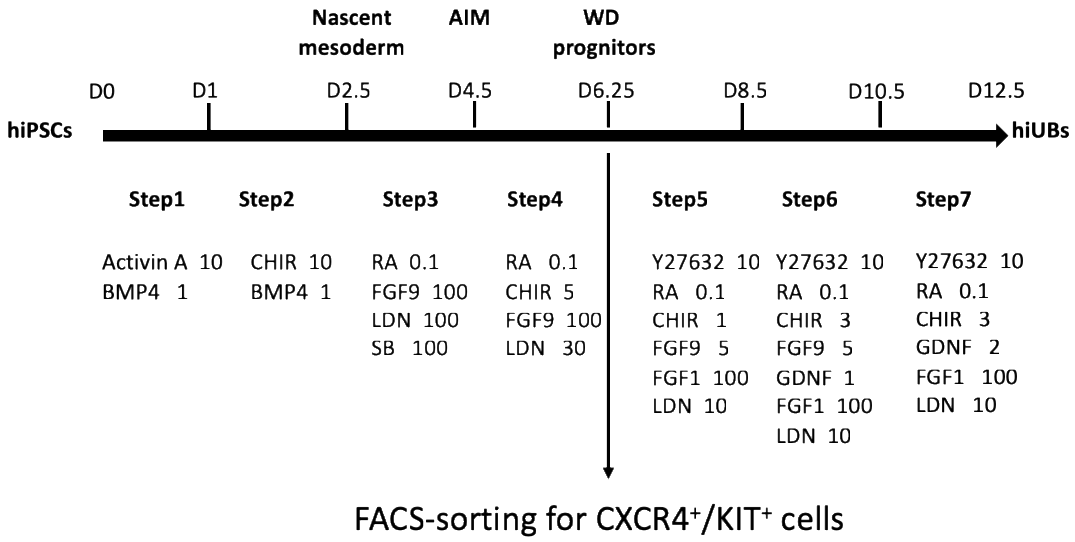

Figure 2.3. Schematic the Taguchi differentiation protocol for obtaining hiUBs

2.10 Maintenance and passaging of mESCs:

E14 mESCs were obtained from Professor John Mason lab. The cells were maintained in feeder-free culture conditions on the surface of gelatine-coated plates. Six-well plates were coated with 0.1% gelatine in PBS (1mL/ well) and were kept in room temperature for 1 hr before using to allow for polymerisation of the gelatine. Cells were seeded on the surface of gelatine-coated plates and were maintained in Glasgow minimum essential medium (GMEM; Sigma Aldrich, G5154) containing 10% FBS, 1X non-essential amino acids, 1X Glutamax, 1X sodium pyruvate, 0.1 mM 2-mercaptoethanol, 1 % penicillin/streptomycin and 1 U/µl leukaemia inhibitory factor (LIF; Santa Cruz, SC-4989). Spent medium was changed daily and cells were split when they reached 80-90% confluence. For passaging mESCs, cells were washed once in PBS and were then incubated with Accutase enzyme (Thermofisher; A1110501) for 5 minutes at 37°C. Cells were then detached by pipetting up and down. The cell suspension was added to mESC maintenance medium (containing 10% serum) to stop the enzymatic reaction. The cell suspension was centrifuged at 180 x g for 5 min. The supernatant was discarded and cells were re-suspended in fresh mESC maintenance medium and were seeded on the surface of gelatine-coated plates.

2.10.1 mESC differentiation towards UB progenitors using the Taguchi protocol of differentiation:

mESCs were dissociated using Accutase enzyme and were cultured at a density of 2,000 cells/well of a 96-well U-bottom low cell-binding plates to form EBs in the differentiation basal medium. The differentiation basal medium was composed of 75% IMDM (Thermo Fisher scientific 12440-046) and 25% HAM's/F12 (Thermo fisher, 11765054) containing: 0.5X N2 supplement (Gibco 17502-048**),** 0.5X B27 supplement without vitamin A (Gibco 12587-010**),** 1X Antibiotic/Antimycotic (Gibco 15240-096**),** 0.05% BSA (Gibco 15260-037**),** 2mM L-glutamine, 0.5mM Ascobic Acid (Sigma A4403), and 4.5 X 10^{-4} M 1-thioglycerol (Sigma M6145-25mL**).**

After 48, the medium was changed to differentiation medium containing 10 ng/mL Activin A (R&D, 338-AC; Step 1) and spheroids were cultured for 24 hrs. Afterwards, the culture medium was changed to Step 2 medium (differentiation medium containing 0.3 ng/mL BMP4 (R&D 314-BP-010) and 10 µM CHIR (Tocris, 4423) which was kept for 36 hrs. The medium was then switched to Step 3 medium (composed of differentiation medium containing 0.1 µM RA (Sigma, R2625), 100 ng/mL FGF9 (R&D, 273-F9) and 10 µM SB431542 (Tocris, 1614)). After 24 hrs, step 4 medium was added (differentiation medium containing 0.1 µM RA, 100 ng/mL FGF9 and 5 µM CHIR) and spheroids were cultured in that medium for 18 hrs. Afterwards, $CXCR^+/KIT^+$ cells were FACS-sorted (see section 2.10 for details of the FACS-sorting) and the obtained cells were suspended in step 5 medium (containing 10 µM Y27632 (Tocris, 1254), 0.1 µM RA, 1 µM CHIR, 5 ng/mL FGF9, and 10% growth factor reduced Matrigel (GFRM; Corning, 354230)) and were cultured in U-bottom 96-well plates at a density of 3,000 cells/well for 24 hrs. Cells were then switched to step 6 media (differentiation media containing 10 µM Y27632, 0.1µM RA, 3 µM CHIR, 5ng/mL FGF9, 1 ng/mL GDNF and 10% GFRM) and were cultured for 24 hrs. Medium was then changed to step 7 medium containing 10 µM Y27632, 0.1µM RA, 3 µM CHIR, 2 ng/mL GDNF and 10% GFRM. After step 7, spheroids were obtained and single buds were dissected from the periphery of the spheroids and were suspended in Matrigel and cultured in branching inducing medium.

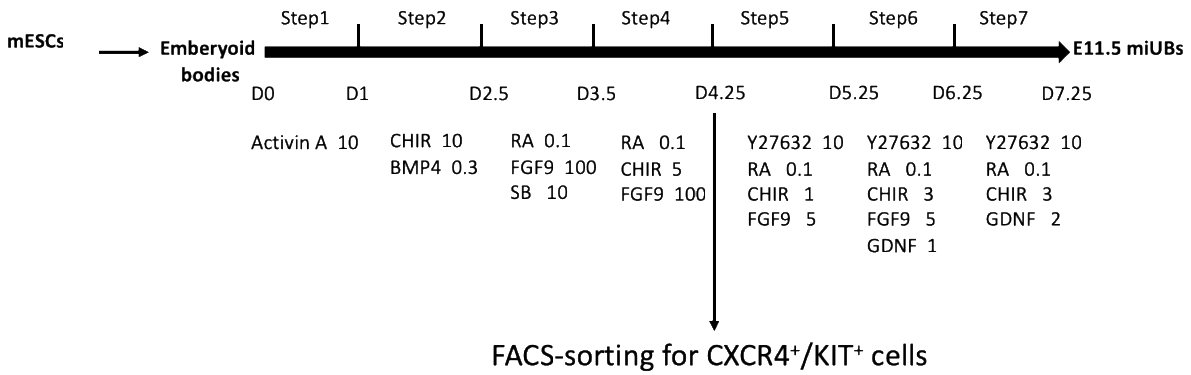

Figure 2.4. Schematic for the Taguchi differentiation protocol for obtaining miUBs

2.11 FACS-sorting of mESC-derived and hiPSC-derived WD progenitors:

At the end of step 4, the obtained spheroids (both from the mouse and the human protocols) were collected, washed once in PBS then transferred to a 30 mm petri dish containing 1X Trypsin EDTA and were incubated at 37° C for 5 minutes. The trypsinized spheroids were moved to a 15 mL falcon tube containing PBS + 5% foetal bovine serum (to stop the trypsin action) and were dissociated into single cells by pipetting up and down several times. The cell suspension was then passed through a cell strainer to ensure single cell suspension. The Cell suspension was spun down, the supernatant was discarded, and a blocking step was performed by incubating the cells in PBs containing 5% BSA at room temperature for 15 minutes. Cells were incubated with the surface markers CXCR4 (in case of mouse cells: Biolegend, 146507; used dilution: 0.5 ug/100 µl volume. In the case of human cells: Biolegend, 306510) and c-Kit (in the case of mouse cells: Bioscience, 12-1171-82; 0.125 ug/100 µl volume. In the case of human cells: Biolegend, 313204) for 20 minutes on ice protected from light. PBS containing 1% BSA was used as the staining buffer. After staining, cells were washed twice with the staining buffer. The stained cells were then FACS analysed and the $CXCR4^+$/c-KIT^+ were sorted. The double positive cells were collected and were cultured as described above.

2.12 Testing branch-competence of human induced UBs (hiUBs) and mouse induced UBs (miUBs):

Single isolated hiUBs (obtained either using the Takasato protocol of differentiation or the Taguchi protocol of differentiation) and miUBs (obtained using the Taguchi protocol for differentiating mESCs) were dissected (as described above) and were embedded in GFRM (as described above in section 2.7.2). After solidification of the Matrigel, branching basal media (see above) containing the following growth factors were added to the Matrigel-embedded UBs: 125 ng/mL GDNF, 250 ng/mL, 1 µM CHIR, 0.5 µM RA, and 0.5 µM 9-cis-retinol. The medium was changed every other day. hiUBs (both obtained using the Takasato protocol or the Taguchi protocol) were kept in culture for 14 days. miUBs were kept in culture for 7 days. The cultured UBs were imaged every other day during the duration of treatment. At the end of the culture period some of the obtained branched structures were extracted from the Matrigel and were fixed and stained (using the staining protocol described in 2.2.3).

For propagating miUBs in Matrigel, branched miUBs (1^{st} generation miUBs) were extracted from the gel, after 7 days of gel-culture, and single buds were dissected from their periphery and were embedded in Matrigel and cultured following the same procedure described above (2^{nd} generation miUBs). The whole process was repeated after 7 days of gel-culture and 3^{rd} generation miUBs were obtained and cultured embedded in Matrigel treated with branching inducing growth factors.

2.13 Examining the ability of miUBs to induce nephron formation by aggregation with embryonic MM:

Embryonic E11.5 metanephric kidney rudiments were dissected as described in section 2.7.1. The obtained metanephric rudiments were trypsinized for 2 minutes at 37°C and were then transferred to a 60 mm Petri dish containing KCM medium to stop the trypsin action. The MM was isolated from the embryonic UB using fine needles. Only kidneys that I was able to isolate and remove their UBs as intact whole T buds were used to avoid having embryonic UB cells within the mesenchymal cells. The mesenchymal cells were collected in an Eppendorf containing KCM medium and were dissociated by pipetting up and down several times. The cell suspension was then passed through a cell strainer to ensure obtaining single cells. Mesenchymal cells obtained from six metanephric kidney rudiments were used for constructing one

kidney organoid after re-aggregation with miUB. Single isolated miUBs were obtained by dissection either from a spheroid after the end of step 7 differentiation (as described in section 2.9.1) or from a branched 1st generation miUB extracted from the Matrigel (as described in section). In the case of extracting a branched 1st generation miUB from Matrigel, the dissected isolated miUB tips were cleaned from the surrounding Matrigel as much as possible using fine needles. The isolated single miUB tips were transferred to a U-bottom 96-well ultra-low attachment plate, 1 miUB tip/well, in KCM medium. The single cell suspension of the MM cells was centrifuged at 800 x g for 3 min. The obtained pellet was picked and was transferred to the 96-well that contains the isolated miUB tip. The mesenchymal cells and the miUB tip were cultured in the U-bottom 96-well plate for 24 hrs to aggregate and form a spheroid. After 24 hrs, the aggregated spheroid was transferred to the surface of a transwell insert and was cultured in KCM for 4-7 days. The constructed kidney organoid was then fixed in ice-cold methanol for 20 minutes at room temperature and was stained.

2.14 Reprograming miUBs into urothelial fate:

Branched 1st generation miUBs was extracted from the Matrigel after 7days of culture in the branching inducing medium. Single miUB tips were isolated from their periphery and were embedded in Matrigel and cultured as 2nd generation miUBs (as described in section 2.11). The miUBs were divided into two groups, the control group which was cultured in branching inducing medium (as described in 2.11), and the BMP4-treated group which was cultured in branching inducing medium to which 100 ng/mL BMP4 was added. miUBs from both groups were cultured for 7 days during which the culture medium was changed every other day. At the end of the treatment duration, miUBs from both groups were extracted from Matrigel and were fixed in ice-cold methanol for 20 minutes at room temperature then they were stained for Uroplakin (UP) and Gata3.

2.15 Imaging and fluorescence quantification:

2.15.1 Microscopes:

Images were taken using either a Zeiss Axiovert epifluorescence microscope, a Zeiss AxioObserver D1 inverted fluorescence microscope or a Nikon A1 R confocal microscope.

2.15.2 Image processing:

Image processing including splitting channels, channel merges, quantification, image adjustments, producing z-project from a stack image was performed using fiji (fiji.sc).

2.15.3 Fluorescence quantification:

All images used for fluorescence intensity analysis, within one experiment, were taken with identical exposures and settings.

For quantifying Cleaved Caspase 3, in cryopreserved organoids in response to Cisplatin treatment, first images were split into separate channels. The channel for ECAD and LTL were then merged and were converted into grey scale, then a threshold was set on that channel using the default adjustment setting (that marked all the tubular structures in the organoids). A selection was then created on the marked area and that selection was transferred to the Cleaved Caspase 3 channel; the fluorescence in the selected area was quantified (that corresponded to all the Cleaved Caspase 3 signal inside the tubular structures of the organoid and excluded all the signal in the interstitium). This was done to limit the quantification to the inside of the tubular structures as a variable number of apoptotic interstitial cells could be seen in untreated organoids (Takasato *et al.*, 2015) which would affect the total fluorescence if no selection was done. This method of quantification excludes Cisplatin-induced apoptosis in the interstitial cells; however, the main aim was to measure the response of the induced renal tubules to the toxic drug. An example of the quantification is shown in (figure 2.2).

For quantifying fluorescence as a measure of HMOX1 expression, in the nephrotoxicity screening experiment, fluorescent images were taken after 24h or 72h of treatment. Each sample was imaged either 5 times with 4 replicates (2D cultures, 24h), once with 10 replicates (2D cultures, 72h), once with 3 replicates (3D organoids, 24h) or 3 times with 3 replicates (3D organoids, 72h). To quantify fluorescence, a macro was used with a threshold value of 400-4059 to exclude the dark pixels, and the total fluorescence was measured. Before applying the macro, a random sample of images of each compound, both 2D and 3D, were manually tested for the threshold value to make sure that this value covered all the fluorescent signal in the image.

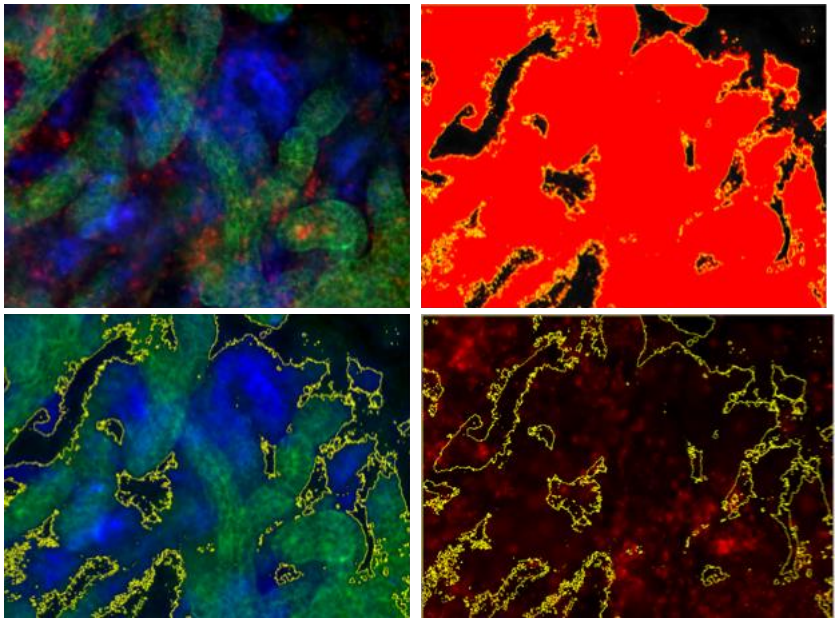

Figure 2.5. Illustration of the fluorescence quantification method: CDH1^{+ve} and LTL^{+ve} tubules were selected and then Caspase 3 total fluorescence was measured inside this area (excluding fluorescence outside tubular structures).

2.16 Statistical analysis:

Data analysis and producing graphs was performed using Prism 8 (GraphPad Prism Software Inc., La Jolla, CA, US). Normality of the data was confirmed using Kolmogorov-Smirnov's test and Shapiro-Wilk's test. To compare between different treated groups, one-way ANOVA Welch was used with Dunnett's multiple comparisons post-test correction to compare data between three or more groups. To compare between two groups, an unpaired t test with Welch's correction was performed. Welch's modification corrects for unequal variance and it is advised to be performed when the compared groups have different standard deviation. When data do have equal variance ANOVA Welch also have equal power to one-way ANOVA or t test (Welch, 1951; Ruxton, 2006). Data are presented as mean ± SD.

For analysing categorical data (absence or presence of UB fate or UB branching) 95% confidence interval was calculated and data are presented as mean, upper and lower limit of the confidence interval. The 95% confidence interval is a method to quantify the uncertainty of observations. When an experiment that has two possible outcomes (success and failure, or presence and absence of a specific feature) is repeated a

specific number of times, the result, of success or failure, is expressed as a proportion. This proportion is the observed binomial proportion. The observed proportion is obtained from random sampling (each observation denotes a sample of the population); the confidence interval predicts the true proportion in the whole population. The 95% confidence interval estimates a range of possible proportions; the probability of observing a value outside this range is less than 0.05. There are different formulas to calculate the confidence interval of a proportion; although the aim is to obtain 95% confidence interval, the actual coverage probability (obtained from any given formula) differs depending on the specific value of *n* (number of trials) and *p* (the observed sample proportion). The Wilson score interval is a commonly used formula (Wilson, 1927); the actual confidence interval of this formula equals, on average, the requested one (95% interval in this case). An exception to this is when *p* is close to 0 or 1 where the coverage shows downward spikes (Wallis, 2013; Brown, Cai and Dasgupta, 2001). The Wilson/Brown interval is a modified Wilson interval that uses one-sided Poisson approximation to remove the downward spikes when *x* (the number of successful trials) is very close to 0 or *n* (Brown, Cai and Dasgupta, 2001). I used Prism 8 to compute the 95% interval and produce the graphs using the Wilson/Brown method.

Chapter 3

3 hiPSC differentiation into renal cells and renal organoids

3.1 Introduction:

Several protocols have recently been published to differentiate hiPSCs toward renal cells and organoids (Taguchi *et al.*, 2014; Takasato *et al.*, 2014; Xia *et al.*, 2014; Morizane *et al.*, 2015; Takasato and Little, 2015; Taguchi and Nishinakamura, 2017).

Takasato et al, 2014 was one of the approaches that described obtaining both types of renal progenitors, UB and MM, simultaneously. The researchers described three-step protocol for directing the differentiation of hESCs into renal cells and renal organoids. In the first step of the protocol, hESCs are treated with high concentration of CHIR for two days to induce posterior primitive streak differentiation, the progenitor population for the IM. CHIR stimulates WNT/β-Catenin signalling by inhibiting GSK-3 enzyme (Wu *et al.*, 2015; Tran and Zheng, 2017). The role of Canonical WNT signalling in inducing primitive streak differentiation has been highlighted in different studies (Gadue *et al.*, 2006; Sumi *et al.*, 2008; Yamamoto *et al.*, 2018). The second step aims to differentiate the induced posterior primitive streak cells into IM by treating the cells with FGF9 for 4 days. FGF9 has been shown to be transiently expressed in the IM; that expression is lost upon segmentation of the IM into mesonephros, metanephros and genital ridge (Colvin *et al.*, 1999). It has also been shown that FGF9 is expressed in the nephrogenic niche and the adjacent UB cells; it functions to promote survival of the MM and maintain the progenitor state in the nephrogenic niche (Barak *et al.*, 2012). In the third step of the differentiation protocol, treatment with FGF9 is continued for 6 days to drive the differentiation of MM and UB cells. Afterwards, all the growth factors are withdrawn, and the obtained cells are kept in culture for 6 more days to allow maturation of the progenitor cells.

The researchers have shown that they obtained ureteric epithelium and early nephron markers. They also have shown that after 18 days of differentiation, cells could be dissociated, re-aggregated and cultured in a 3D condition; this allowed self-organisation, nephron patterning, and segmentation yielding 3D renal organoids with all major cellular components of the kidney tissue (Takasato *et al.*, 2014).

This protocol was paradoxical as the two main renal progenitors, UB and MM, have different spatial origin from the IM; the MM originates from the posterior IM while the

UB originates from the anterior IM (Taguchi *et al.*, 2014) (for more details see Chapter 1 section 1.2.4). Through a fate mapping study, Taguchi and Nishinakamura suggested that the anterior IM commits earlier than the posterior IM. According to that study, the posterior IM is maintained in the posterior end of the embryo in a Brachyury $(T)^+$ state and commits at a later stage of development after the extension of the body axis is completed (Taguchi *et al.*, 2014).

In 2015, Takasato and colleagues published a modification for their protocol. They hypothesized that the anterior IM mesoderm develops from early migrating cells which are exposed to FGF9 at an early stage. While the posterior IM cells are maintained under the high WNT signalling for longer duration (posteriorizing condition) and are exposed to FGF9 at a later stage. Based upon this, they described three slightly different versions of their protocol. The difference between them was in the duration of the initial CHIR treatment. They concluded that the shorter initial CHIR treatment (3 days) and the early exposure to FGF9 induces more anterior IM fate and ends by more UBs while the longer treatment (5 days) gives more posterior IM fate (MM), midway between both, the 4 days treatment ends by a balance between the two fates (Takasato *et al.*, 2015).

3.2 Aims:

My aim in this section was to adopt and evaluate a protocol for differentiating hiPSCs into renal progenitors. I choose to reproduce and evaluate the Takasato protocol. The reason of choosing this protocol was that, unlike other protocols which produce either UB or MM but not both, this protocol is reported to yield the two types of renal progenitors simultaneously in a physiological-like manner which allows each of the renal progenitors to induce further development of the other. I wanted to test the efficiency of that protocol in producing renal progenitors and to test the effect of different CHIR99021 treatment timings on the fate commitment of the iPSCs.

3.3 Results:

3.3.1 hiPSCs maintenance:

The original protocol, Takasato et al, 2015, maintained the hiPSCs on feeder cells but because the feeder-based culture condition is laborious, I used feeder free, animal free culture conditions in which the cells were maintained on Matrigel coated dishes using E8 medium (Chen *et al.*, 2011). Addition of the Rock inhibitor Y-27632 for overnight when cells were passaged enhanced the cell survival post dissociation (Watanabe *et al.*, 2007) (figure 3.1; for more details about culture conditions that support hiPSC maintenance see chapter 1, section 1.4.2).

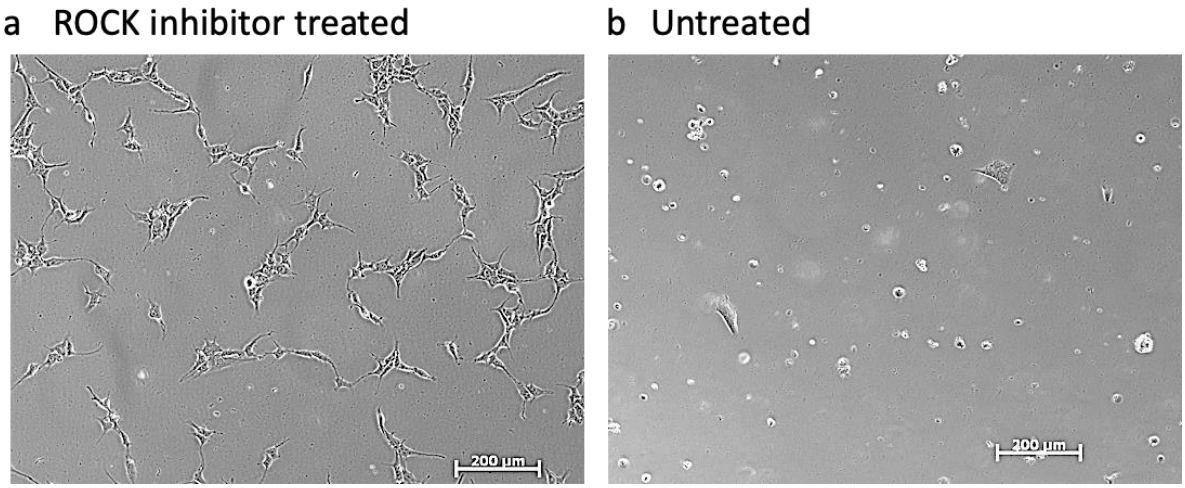

Figure 3.1. Bright field images taken after an overnight culture of recently passaged cells in presence (a) or absence (b) of ROCK inhibitor. Cells were seeded in the same density with the only difference being the ROCK inhibitor treatment. Scale bar is 200 µm.

The passage number of the cells was kept under 25 passages from original derivation to avoid possible mutations that could come to dominate the population with higher passages. The cells were regularly tested for pluripotency markers by immunostaining for OCT4 and NANOG (Takahashi and Yamanaka, 2006b; Takahashi, Tanabe, *et al.*, 2007), and assaying for alkaline phosphatase (Loh *et al.*, 2006; Štefková, Procházková and Pacherník, 2015) throughout the period of their maintenance (every 5-7 passages) (figure 3.2). The cells were generally well maintained under these conditions except for an accidental problem of cell detachment, increased cell debris and death upon passaging which led to loss of cells (figure 3.3). New vials of cryopreserved cells were thawed but the same problem happened repeatedly and the

cells were lost. The temperature inside the incubator was calibrated; the CO_2 level and the humidity were also checked. Parallel to these cells, I had cultures of mESCs maintained in the same incubator and were looking healthy with no apparent abnormality. This probably indicates that the culture conditions inside the incubator were appropriate. To exclude possible bacterial contamination of the cells that might be causing their detachment and death, the spent medium was collected and spread over the surface of a nutrient agar plate. The plate was cultured for three days with no observed growth. Cells were also tested for Mycoplasma infection (Mycoalert, Lonza) and were negative. The problem was solved after changing the lot number of the E8 medium (lot no 1896992) which suggests possible lot to lot variation in E8 medium that could severely affect the cells.

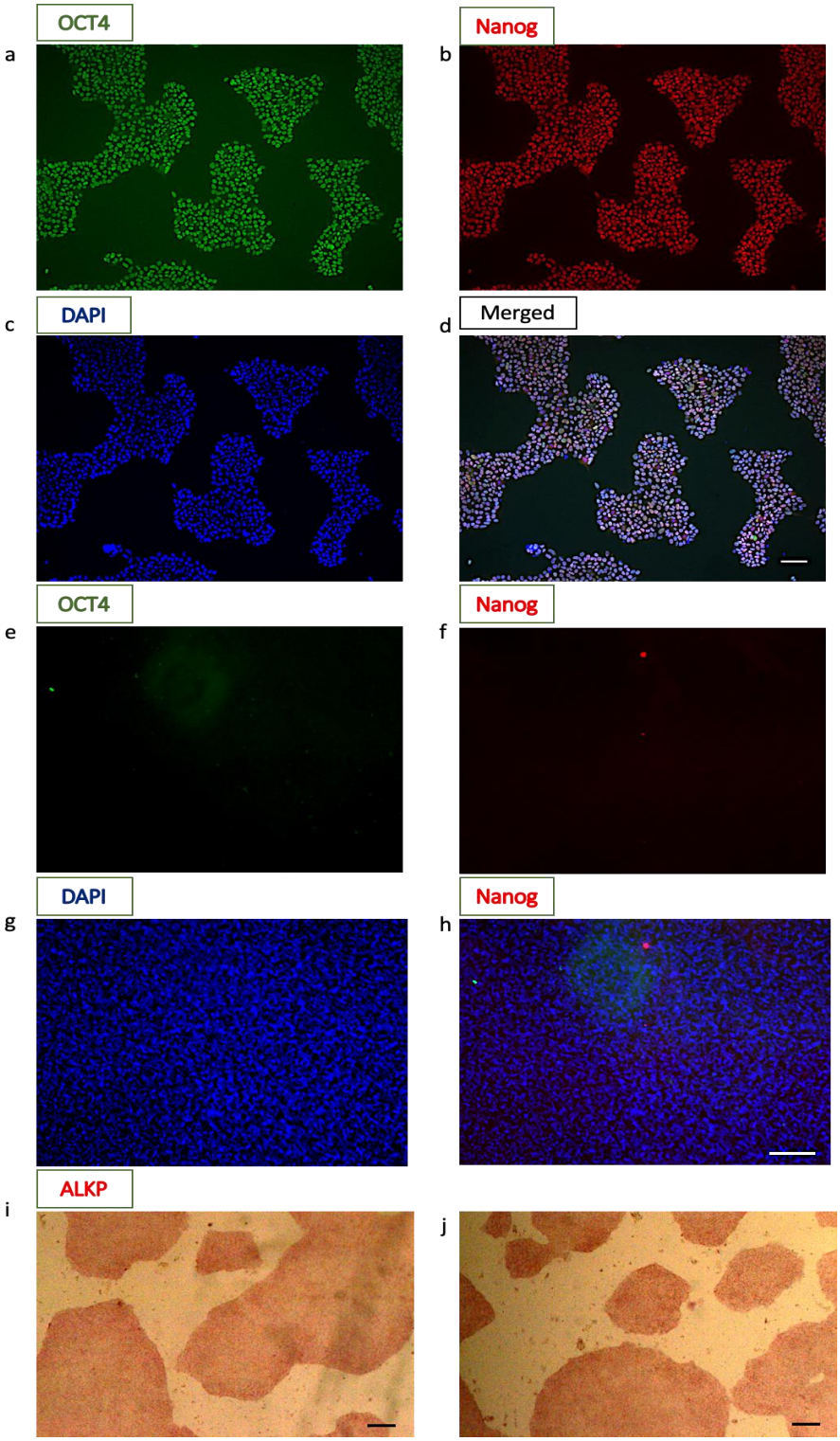

Fig. 3.2. Immunostaining of hIPSCs to the pluripotency markers OCT4 and NANOG (a-c) separate channels for OCT4, NANOG and DAPI; d) merged. e-h) differentiated cells used as a negative control for the antibodies. i-j) Increased Alkaline phosphatase activity in hiPSCs as a test for pluripotency. Scale bar is 100 μm.

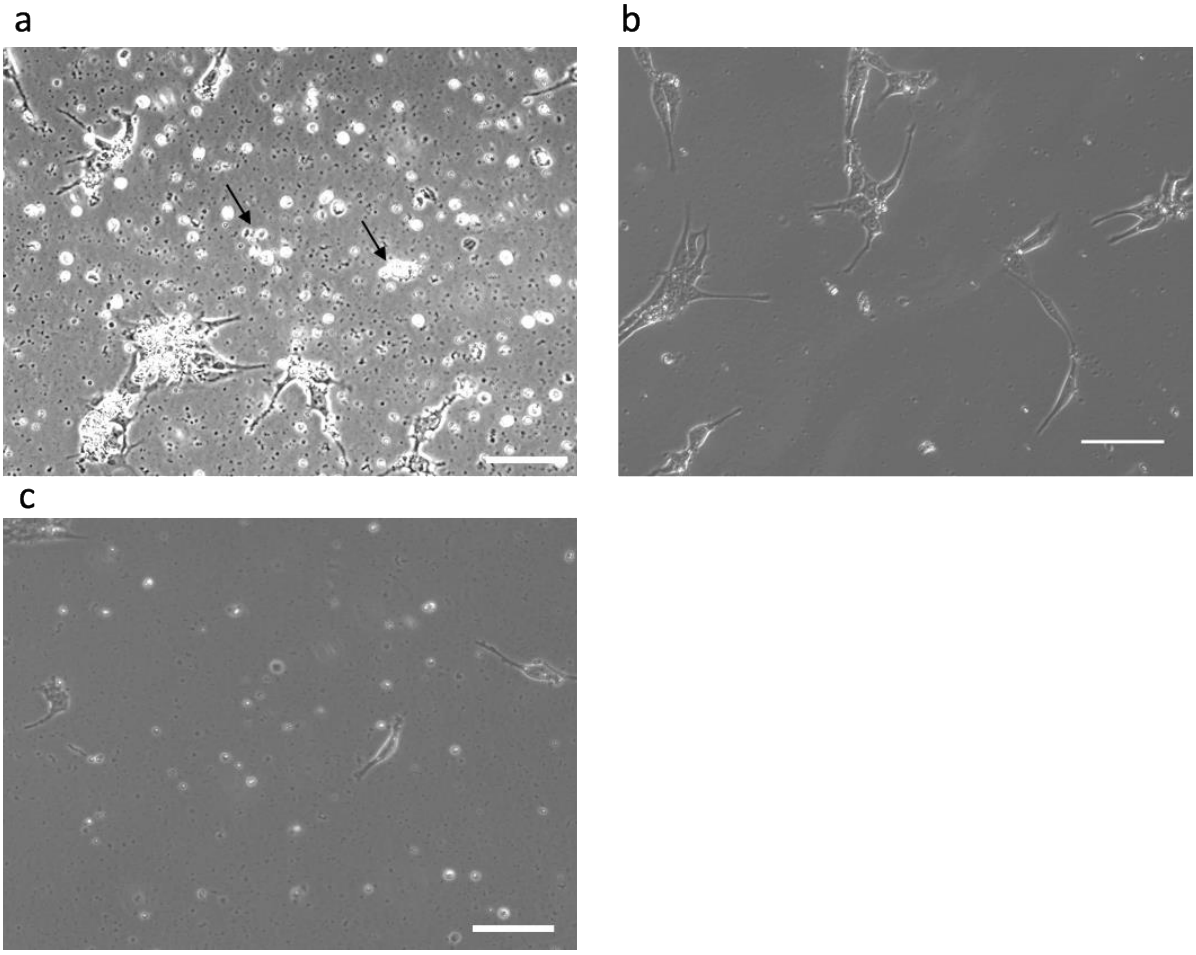

Fig. 3.3. a,b) Bright field images for the hiPSCs one day after passaging a) shows increased cellular debris and dead cells that appeared with particular lot number of the E8 medium b) the normal appearance of the cells after passaging and overnight culture. (c) an image for cells shown in (a) taken one day later showing fewer attached cells; the cells were lost afterwards. Scale bar is 100 μm.

When thawing a new vial of cryopreserved hiPSCs two passages (average 10 days) were needed to allow for cell recovery before starting a new differentiation run. Optimising the seeding density of the cells to start differentiation was important. Cells were seeded in a density that gives around 40-50% confluence on the next morning (day 0 differentiation) (approximately 15,000 cells/cm^2 were used and that number was adjusted depending on the growth rate of the cells). Cultures starting with higher cell density did not differentiate properly and did not develop structures at the end of differentiation suggesting overconsumption of the growth factors, while starting with lower density mostly ended by losing most of the cells at an early stage of differentiation and not having enough cells to continue differentiation (figure 3.4).

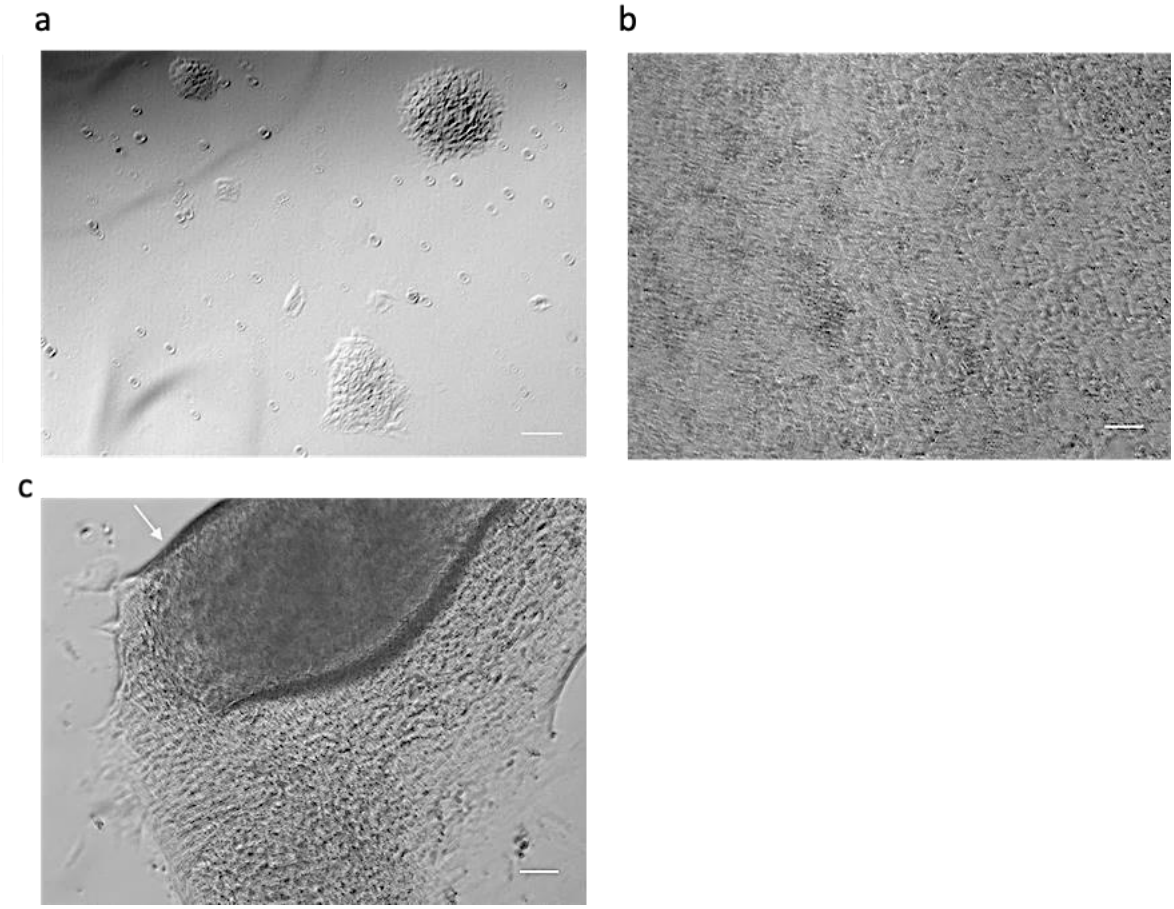

Figure 3.4. Bright field images for 7 days differentiated monolayers a) when starting with low cell density; most of the cells detached with only few separated remaining colonies b) when starting with the right density of cells (see text); cells formed a confluent monolayer sheet c) sometimes the sheet of cells was seen peeling off. Scale bar is 100 μm.

3.3.2 The differentiation process:

3.3.2.1 Primitive streak and intermediate mesoderm stages:

The Takasato protocol directs the differentiation of the hiPSCs through different intermediate stages to end by renal cells. As I explained earlier Takasato and colleagues described three slightly different versions of their protocol, with the difference being in the duration of the initial CHIR99021 treatment. Here, I started by reproducing the three-day CHIR treatment protocol. In this protocol cells are first treated with CHIR for three days to induce posterior primitive streak differentiation. Achievement of this stage is verified by the expression of *MIXL1* and *T* (Beddington, Rashbass and Wilson, 1992; Rivera-Pérez and Magnuson, 2005; Davis *et al.*, 2008). Cells are then treated with FGF9 and Heparin for nine days. After four days of FGF9 treatment (7 days of total differentiation) cells achieve the IM stage which is marked by the co-expression of LHX1 and PAX2 (Torres *et al.*, 1995; Tsang *et al.*, 2000; Bouchard *et al.*, 2002). At the end of FGF9 treatment (12 days total differentiation) cells commit into NP and UB fate. At this stage, cells express the MM markers SIX2 and WT1 (Armstrong *et al.*, 1993; Kreidberg *et al.*, 1993; Self *et al.*, 2006; Kobayashi *et al.*, 2008). At the same time the development of epithelial structures that show positivity to ECAD (Lee *et al.*, 2013), PAX2, GATA3, and CALB (Davies, 1994) marks the simultaneous development of ureteric epithelium. Afterwards, growth factors are withdrawn from the culturing media and cells are kept in culture for maturation. By day 18 of differentiation, they described obtaining elongated $ECAD^{+}$ tubules surrounded by clumps of $SIX2^{+}$, $WT1^{+}$, $PAX2^{+,}$ and $JAG1^{+}$ (Jones, Clement-Jones and Wilson, 2000; Cheng *et al.*, 2003) cells, a pattern that suggests obtaining ureteric epithelial tubules surrounded by early nephrons/renal vesicles (Takasato *et al.*, 2014, 2015) (figure 3.5; for more details about the expression of different markers involved in metanephric kidney development see chapter1 section 1.2.5).

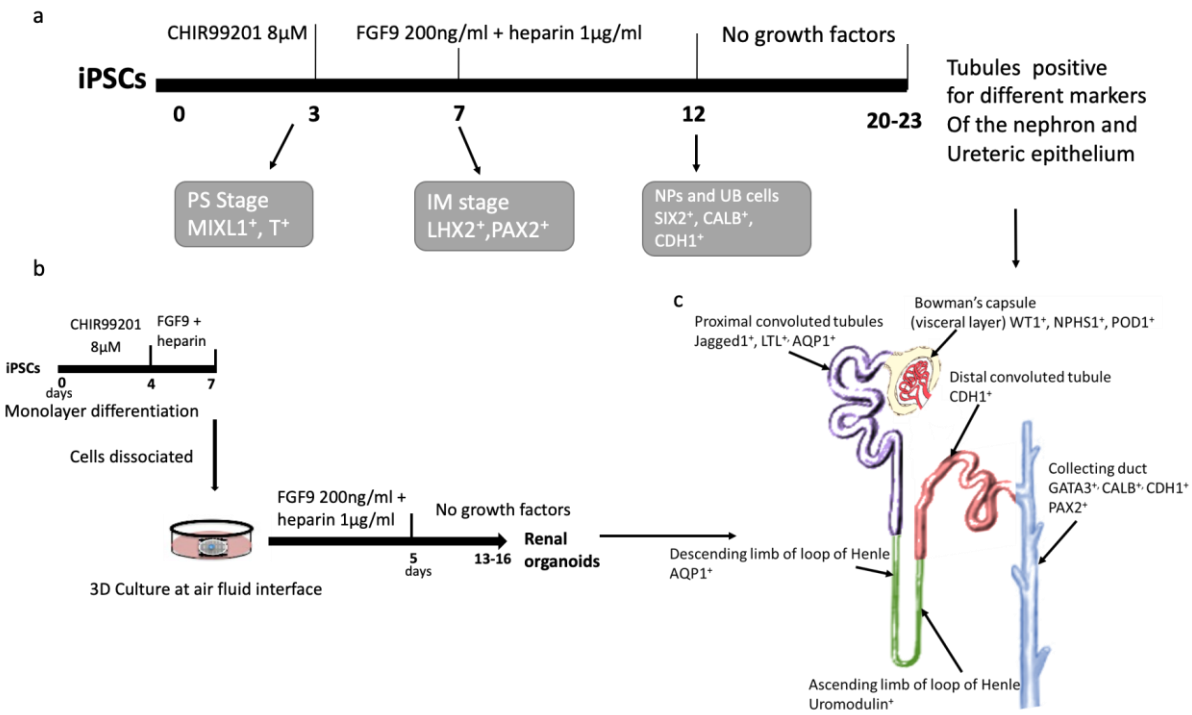

Figure 3.5. a) Schematic of the differentiation protocol illustrates the various intermediate stages and their expression markers. b) Illustration of organoid formation and culture. c) diagram showing the different segments of the nephron and the collecting duct and their specific expression markers.

Verifying the achievement of the intermediate stages was necessary to confirm that the cells were going into the right direction. After 3 days of CHIR99021 treatment, most of the cells were positive for the primitive streak markers MIXL1 and T (n = 9 independent samples) and the expression of the pluripotency marker OCT3/4 was lost (figure 3.6). This suggested successful differentiation towards primitive streak.

It was notable that at this stage the differentiated cells started to detach from the plate and lost their adherence to each other (starting from the 3rd day of CHIR99021 treatment and continuing for 2 days of FGF9 treatment; figure 3.4). When the detached cells were collected and re-plated on freshly prepared Matrigel-coated plates they adhered and were able to continue differentiation which excludes cell death as the cause of detachment. In order to test if this detachment was caused by proteases, which might be produced from the differentiated cells, that digest the Matrigel coat I added the protease inhibitor TIMP1 (SIGMA, SRP 3173) to the cells but the cells continued to detach in its presence.

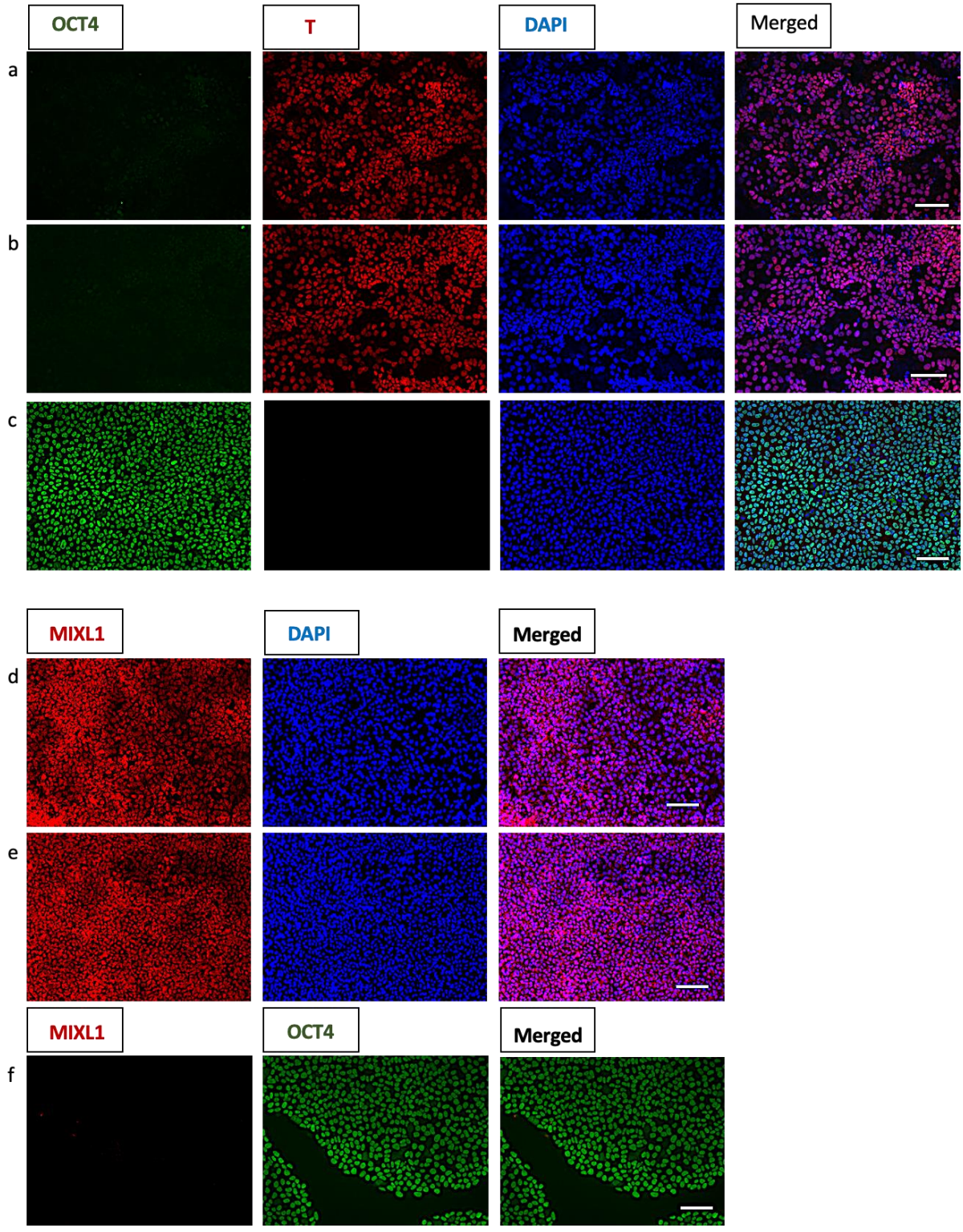

Fig. 3. 6. Immunostaining for the first stage of differentiation; the primitive streak stage a,b) 3 days differentiated cells lost the expression of the pluripotency marker OCT4 and expressed the primitive streak stage marker T (Brachyury); c) Undifferentiated hiPSCs that were used as a negative control to the T antibody; the cells expressed OCT4 and were T^-. d, e) Show $MIXL1^+$ antibody staining after 3 days of differentiation. f) Undifferentiated cells as negative control for MIXL1 antibody. Scale bar is 100 µm.

During normal development, after formation of the primitive streak, gastrulation starts during which cells undergo an epithelial to mesenchymal transition. In their epithelial state cells are regularly shaped and are tightly connected to each other, while mesenchymal cells are irregular in shape and detach from each other. The detachment and loss of adherence of the cells could be explained by simulation to the gastrulation process that happens in normal development. The process of primitive streak formation and gastrulation is regulated by several signalling pathways, the Canonical and non-Canonical WNT (Skromne and Stern, 2001; Yamamoto *et al.*, 2018) and the FGF signalling pathways are important players (Hardy *et al.*, 2011)**.** It was also observed that this state of loss of adherence was more prolonged if the cells were exposed to the longer duration of CHIR treatment (five days CHIR-treated cells) compared to the three days CHIR-treated cells. This might be explained by that, cells which were kept for longer duration in CHIR treatment were maintained in gastrulation-like state for longer period (as CHIR is a Canonical-WNT agonist), while cells which started earlier treatment of FGF9 differentiated earlier towards IM. As mentioned before optimising the density of the cells to reach around 40-50% (or 60% in the case of 5 days CHIR treatment) confluence before starting differentiation was important not to lose the cells at this stage and to ensure enough cells to continue differentiation, also gentle dispensing of the media, on the wall of the well, during feeding was necessary to minimise the detachment.

After 4 days of FGF9 treatment (7 days of total differentiation) the cells co-expressed LHX1 and PAX2 (n = 9 independent samples) both of which are IM and early renal markers (fig. 3.7 a,b). Control of hiPSCs that were seeded and kept in the same conditions but not exposed to the same treatment did not express these markers (figure 3.7 c).

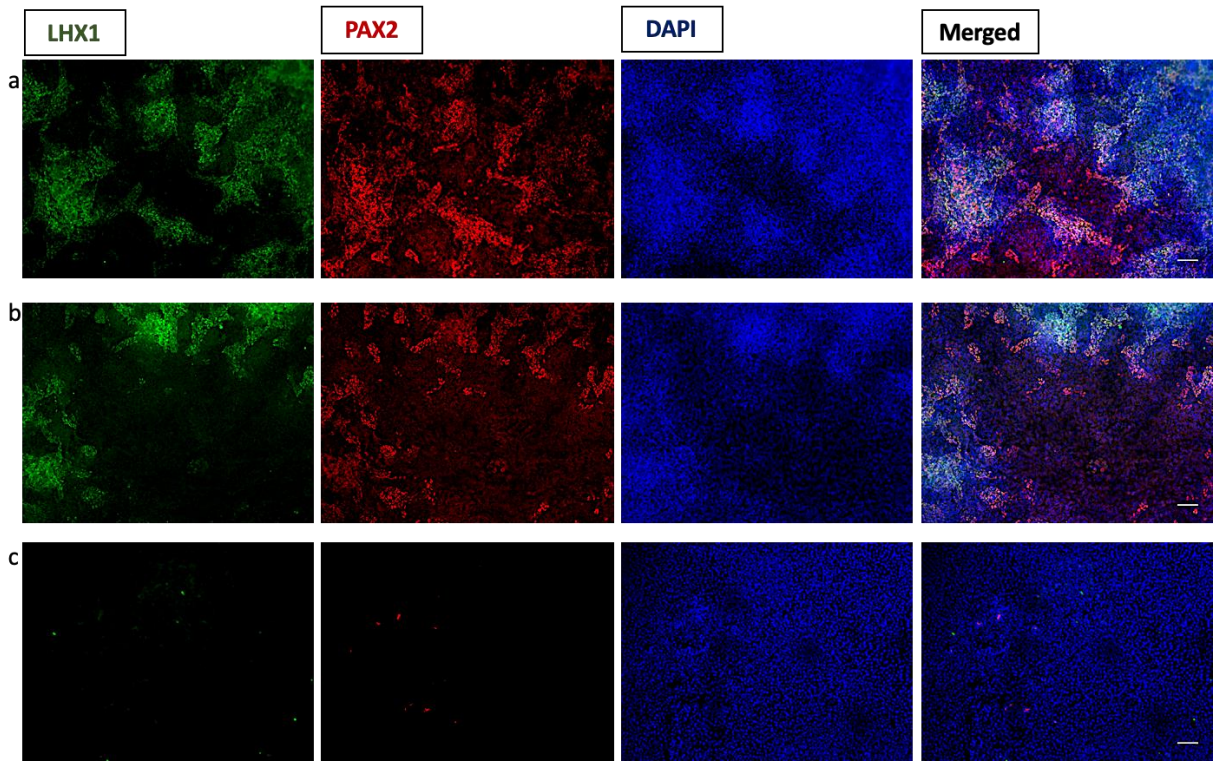

Fig. 3.7. Immunostaining for intermediate mesoderm markers after 7 days of differentiation a,b) show $LHX1^{+}$, $PAX2^{+}$ cells suggesting achieving intermediate mesoderm stage. c) Undifferentiated cells stained for these two markers as negative control. Scale bar is 100 μm.

3.3.2.2 Renal progenitors and early nephron markers:

At the end of the FGF9 treatment (total differentiation of 12 days) small spherical structures started to develop in the monolayers and could be noticed in bright field images; the cells showed positive expression of the early renal progenitor markers CALB1 (UB and collecting duct marker) and SIX2 (nephron progenitor marker) (figure 3.8).

At the end of the differentiation protocol (18-21 days) obvious tubules were seen in the monolayers. These tubules were tested for the expression of different renal markers: the cap mesenchyme and podocyte marker WT1, the more specific glomerular marker NPHS1, the proximal tubular markers JAG1 and LTL, the distal tubular and epithelial marker ECAD (figure 3.9 A), the UB/Collecting duct markers CALB and GATA3 (figure 3.9 B); these markers were all detected in the formed tubules. Obtaining tubular structures with characteristic expression pattern to developing nephrons and to the UB/Collecting duct cells suggested successful differentiation of the hiPSCs into renal-like cells.

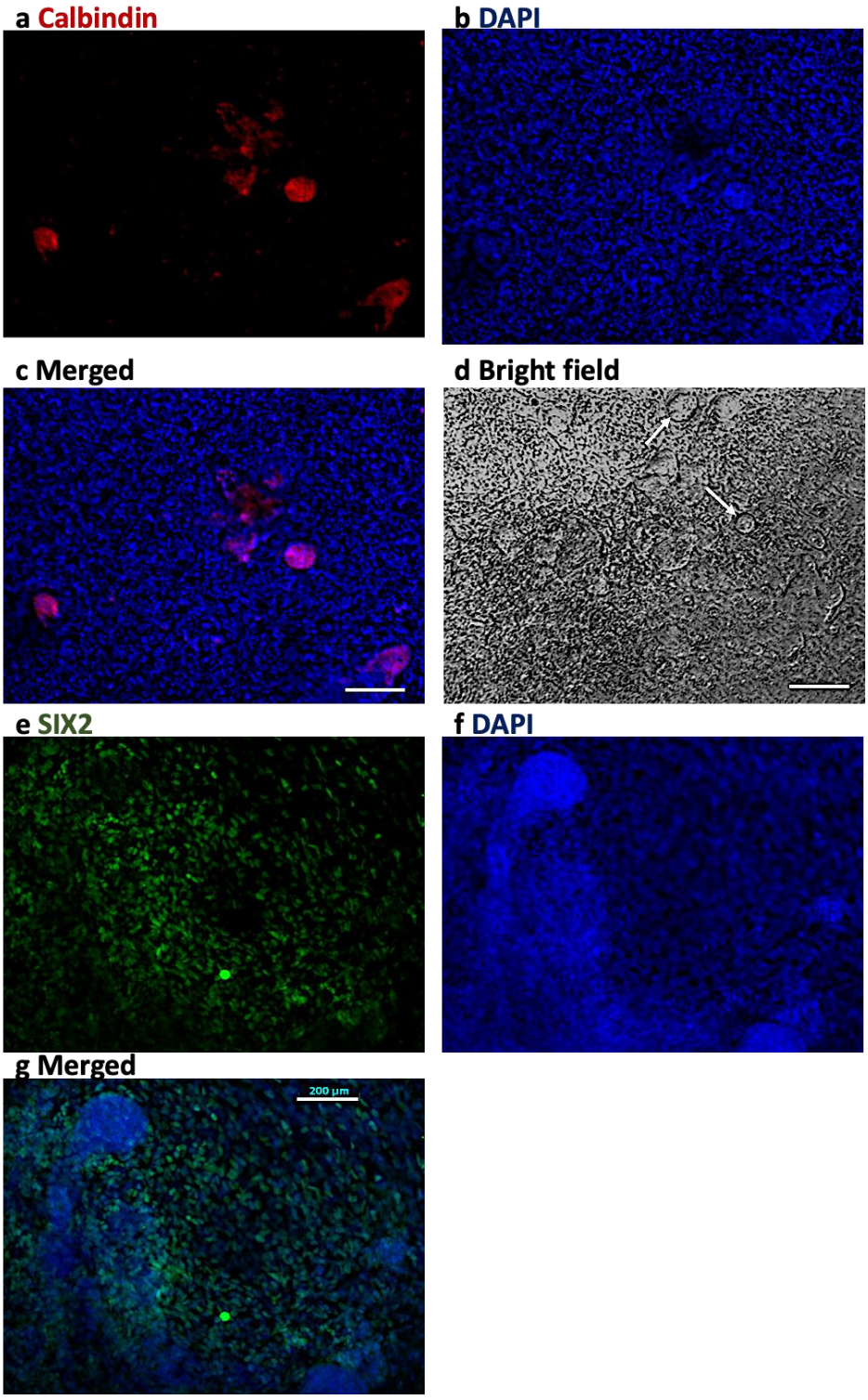

Figigure 3.8. Immunostaining for 12 days differentiated monolayers which showed spherical structures that stained positive to Calbindin (a-c); d) these spherical structures were also seen in bright field images. At the same stage the nephron progenitor marker SIX2 was also positive (e-g). scale bar is 100 µm for c and d, and 200 µm for g.

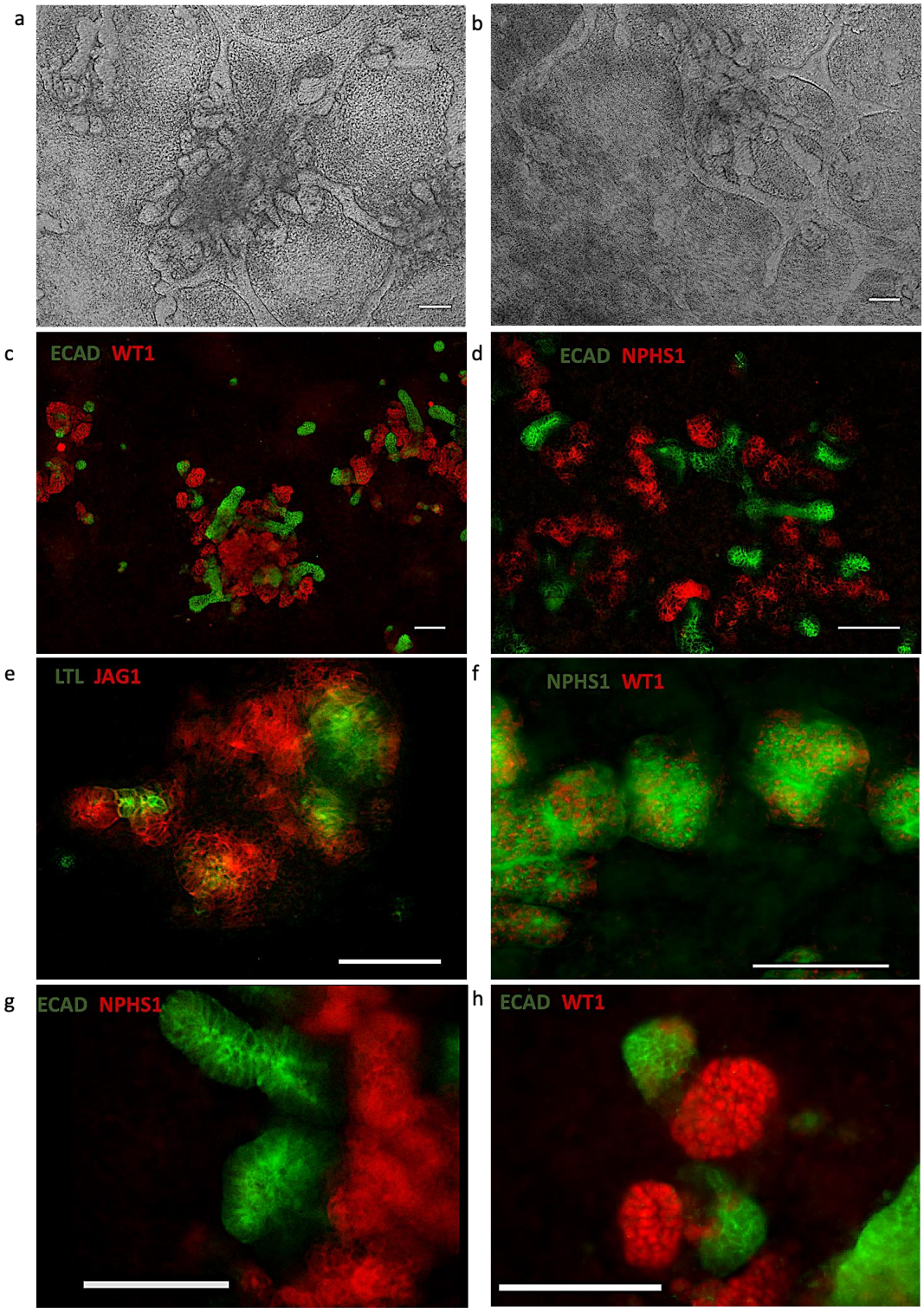

Figure 3.9 A. 21 day-differentiated monolayers a,b) bright field images showing branching tubules that developed in the monolayer cultures. c-h) Immunostaining for different nephron markers c) stained for WT1 (MM and podocyte marker, shown in red) and ECAD (distal tubule and collecting duct marker, shown in green). d) Stained for NPHS1 (podocyte marker, shown in red) and ECAD (green). In both (c) and (d) the ECAD stained structures separate from those stained with WT1 (c) or NPHS1 (d) e) shows immunostaining for LTL and JAG1 (both are proximal tubular markers) f) stained for WT1 and NPHS1; NPHS1 stained membranous protein while WT1 stained the nuclei of the same cells which matches their co-expression in the podocytes. (g, h) Are zoomed in images to show the pattern of expression of ECAD and NPHS1 (g) or ECAD and WT1. (h) Scale bar is 100 µm.

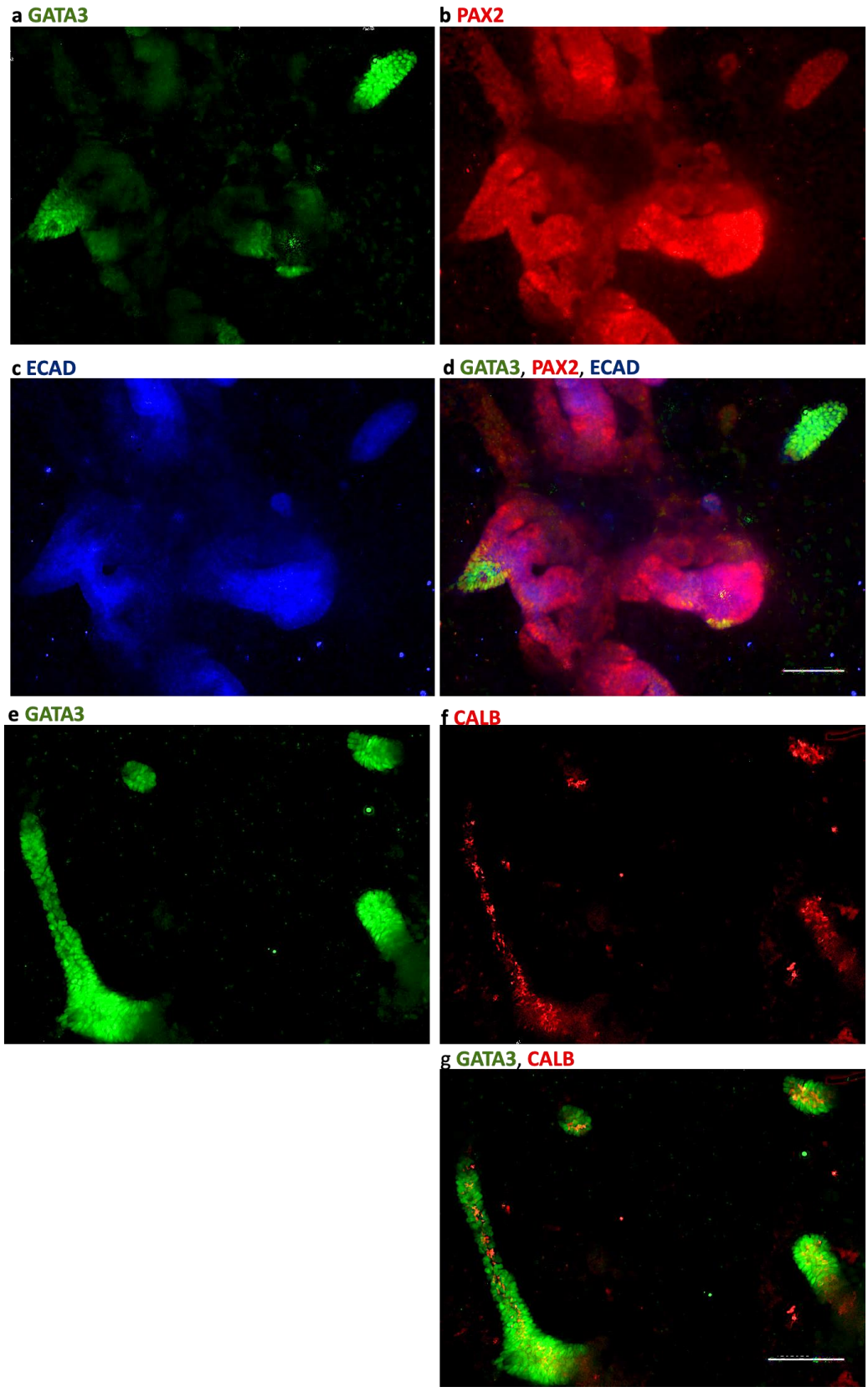

Figure 3.9 B. 21 day-differentiated monolayer stained for UB and CD markers a-d) shows the co expression of GATA3, PAX2 and ECAD; the co-localisation of the three of them indicates CD. E-g) stained for GATA3 and CALB and is showing the co-expression of these two markers. Scale bar is 100 µm.

3.3.2.3 3D Organoid culture:

Earlier studies have shown that if a single cell suspension of renal progenitor cells is pelleted, by centrifugation, and the obtained pellet is cultured in a 3D environment, cells can self-organise and form complex renal organoids that contain branched collecting ducts and segmented nephrons (Unbekandt and Davies, 2010). Takasato and colleagues examined the self-organising ability of their obtained renal cells after 18 days of differentiation (Takasato *et al.*, 2014) and at an earlier stage (after 7 days of differentiation) (Takasato *et al.*, 2015). They reported that the self-organising property allowed the cells to take particular patterns in relation to each other and enhanced the formation of more complex structures (Takasato *et al.*, 2014). In their protocol that was published in 2015, they focused more on making organoids at the early stage (after 7 days of differentiation) and showed that the 3D condition allowed for better maturation of the renal structures with evidence of proximal-distal patterning of the nephrons.

I aimed to examine the ability of the obtained cells to self-organise and form more complex 3D renal organoids. For this purpose, cells were dissociated after 7 days of differentiation, pelleted then cultured at on the surface of a filter membrane at gas-liquid interface until the end of the differentiation protocol. The 3D environment enhanced tubulogenesis and allowed for the development of more densely packed structures compared to the 2D cultures (figure 3.10). The resulting 3D organoids were investigated for the expression of different renal markers; ECAD positive tubules (marker for distal tubules and CD) were detected and appeared connected to LTL^+ tubules (proximal tubular marker) and surrounded by clusters of cells that stained positive for WT1 and NPHS1 (podocyte markers). Organoids also had tubules which stained positive for the UB markers CALB and GATA3 (figure 3.11). Collectively the data suggested successful obtaining of renal organoids.

Immunostaining allowed not only for detecting if these markers were expressed or not, but it also showed the pattern of expression, the co-localisation of some markers or the expression of other markers in separate populations which were collectively taken to evaluate the differentiation. ECAD, LTL and WT1 were expressed in separate populations (figure 3.11 c) which matches their specificity to different parts of the nephron; WT1 and NPHS1 (both stain for podocytes) were co-localised (figure 9A f).

The co-localisation of GATA3, ECAD and PAX2 or GATA3 and CALB were taken as an indicator of UB development (figure 11 e,f).

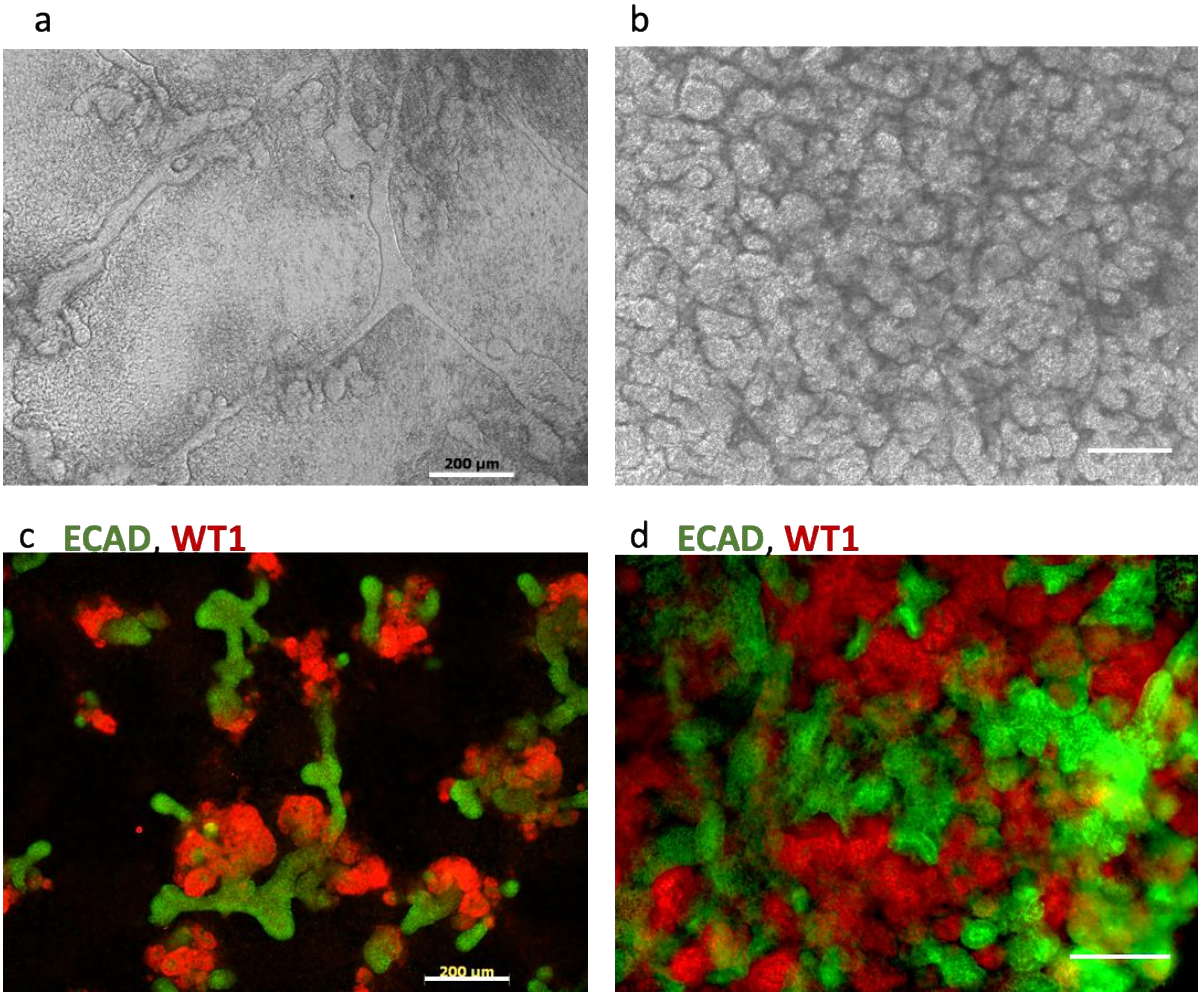

Figure 3.10. a,b) Bright field images showing differentiated monolayer (a) or organoid (b); some tubular structures developed in isolated areas of the monolayer culture, however the organoid developed into densely packed tubular structure. c,d) Immunofluorescence staining for ECAD and WT1 in monolayer (c) or organoid (d) showing robust tubulogenesis in the organoid. Scale bar is 200 µm.

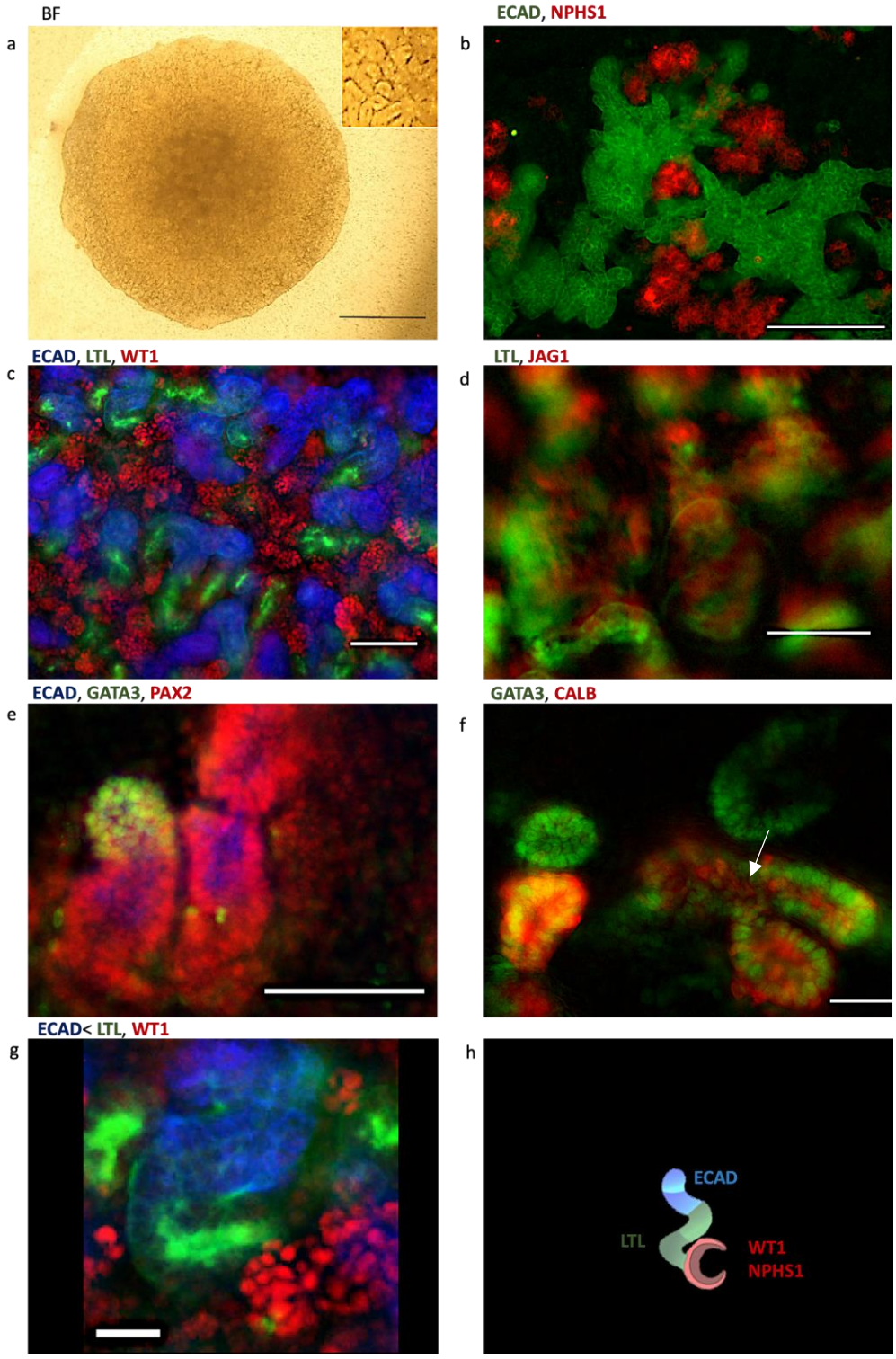

Figure 3.11. 21 day-differentiated organoids. a) Shows brightfield image of the organoid. b) Immunostaining for the distal tubular and the CD marker ECAD and the glomerular marker NPHS1 which shows expression of these two markers in separate populations. c) Shows expression of WT1 (staining podocytes), LTL (staining proximal tubules) and ECAD (staining distal tubules and CDs) in separate populations. d) The proximal tubular markers LTL and JAG1 are co-expressed in the organoids e) Shows the co-expression of ECAD, GATA3 and PAX2 in one of the tubules. f) Shows co-expression of CALB, and GATA3; the arrow points to a branching structure suggesting branching UB g) Zoomed in image for the expression of WT1, LTL and ECAD. (a) Scale bar is 1 mm, (b-f) scale bar is 100 um and (g) scale bar is 25 µm.

3.3.3 Variable results:

As mentioned before, the co-expression of GATA3 with CALB or the co-expression of GATA3, ECAD and PAX2 (or GATA3 + ECAD) were taken as positive indication of UB and collecting duct differentiation; ECAD is expressed both in the distal tubules and the UBs, and PAX2 is expressed in the IM and the early renal structures including MM, UB and renal vesicle (Bouchard et al., 2002 Torres et al., 1995) and only their co-expression with GATA3 (Grote *et al.*, 2006, 2008) was taken as a marker of UB. Both ECAD and PAX2 were always present in all the organoids or monolayers tested for them, however in some of the runs GATA3 was either negative or expressed surrounding the $ECAD^{+}/PAX2^{+}$ tubules (i.e. in between the tubules). In cases where the GATA3 expression was seen in the interstitial cells, in between the tubules, CALB staining was also negative, which precludes obtaining UB and CD fate in these runs (figure 3.12). Achieving UB differentiation was confirmed either by the co-expression of GATA3 and CALB or the co-expression of GATA3, ECAD and PAX2. From a total of 41 tested organoids 22 showed negative UB differentiation and 19 organoids were positive for UBs; all tested samples were positive for the different markers of the different parts of the nephron.

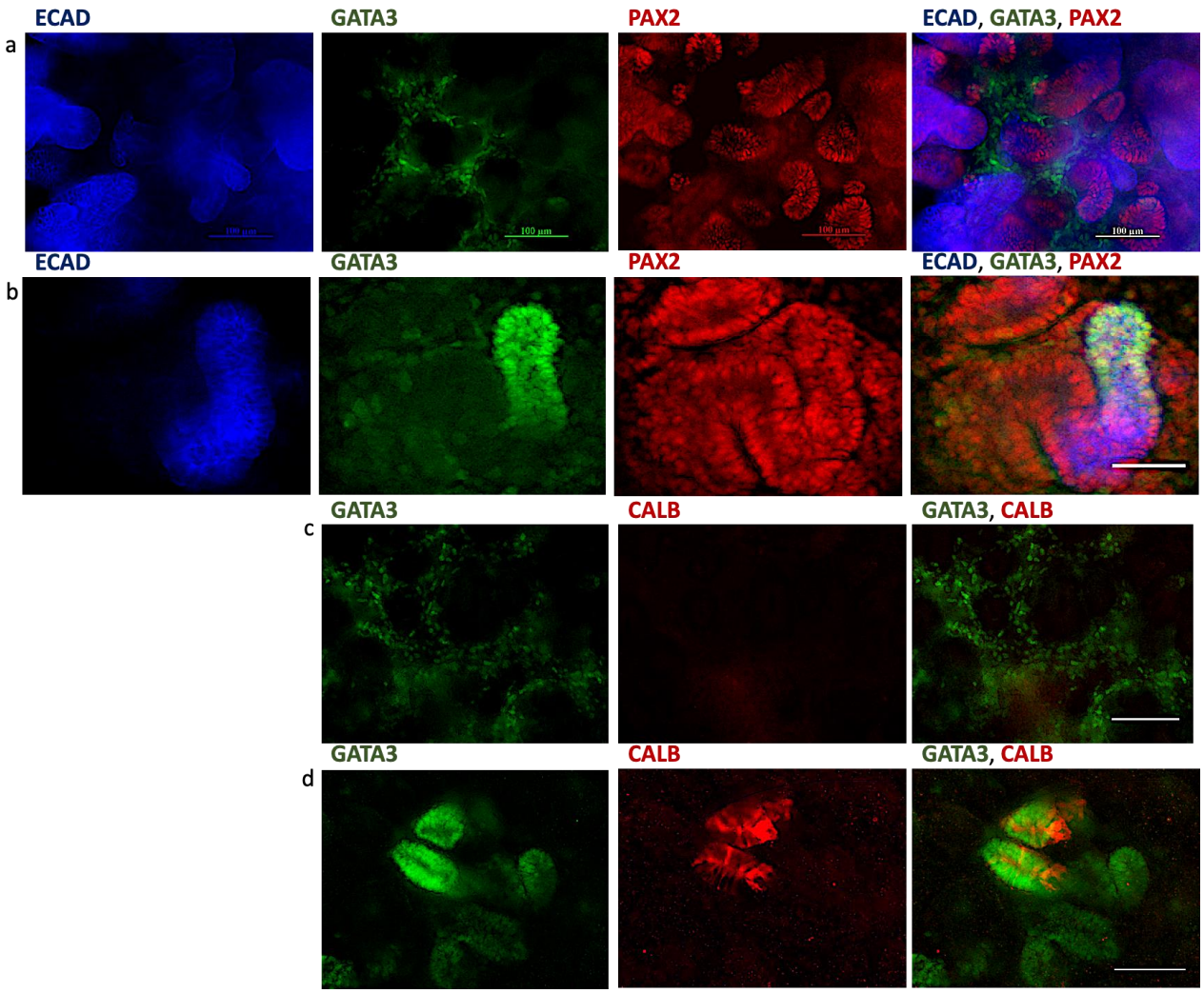

e **95% confidence interval for obtaininig UB fate**

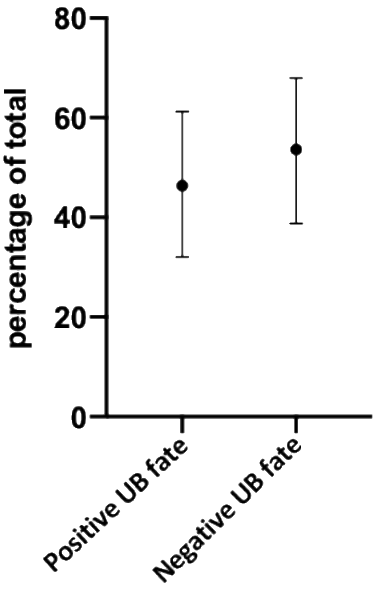

Fig. 3.12. Shows the variability in GATA3 expression in a) GATA3 is only seen in interstitial cells surrounding the ECAD^{+}, PAX2^{+} tubules and does not appear inside tubules while in b) GATA3 co-localises with ECAD and PAX2 in one of the tubules. c) shows GATA3+ interstitial cells that do not localise inside tubular structures and CALB was not expressed in that organoid while d) shows GATA3+ tubules that are co-expressing CALB in some parts. Scale bar is 100 μm. e) Shows the 95% confidence interval (Wilson/Brown) for obtaining positive or negative UB fate in organoids obtained by using the Takasato protocol; a total of 41 samples were tested for the presence or absence of the UB fate (taking the co-expression of GATA3, ECAD and PAX2 or the co-expression of CALB and GATA3 as markers for positive UB fate) 19/41 samples were positive for the UB fate while 22 /41samples were negative.

3.3.4 Comparing the three different timings of initial CHIR99021 treatment

The Takasato protocol compared between three different timings of initial CHIR99021 treatment; 3days, 4 days and 5 days and concluded that the shorter period of CHIR99021 treatment yields more UBs at the end of differentiation and that the longer CHIR99021 treatment gives more MM fate, while midway between them; the 4 days initial treatment makes a balance between the UB fate and the MM fate.

I had quite variable results in the UB direction, despite using the treatment that should give more UB fate according to the study. I wanted to check the difference between the different timings and whether any of them could give more consistent differentiation towards UB. Four different runs were differentiated and evaluated for UB markers, the three different timings of CHIR treatment were set parallel to each other at the same time to minimise causes of technical variability. Organoids from the three different timings all formed tubular structures and were all expressing nephron markers (WT1, LTL, and ECAD) with some variability in-between the different organoids in the percentage of the area that stained positive for each marker compared to the total area of the organoid (Figure 3.13). Neither of the different timings of CHIR treatment included in this comparison showed co-expression of GATA3 and CALB (figure 3.13) which suggests variability between runs in obtaining UB fate in my results rather than an effect of the duration of CHIR99021 treatment.

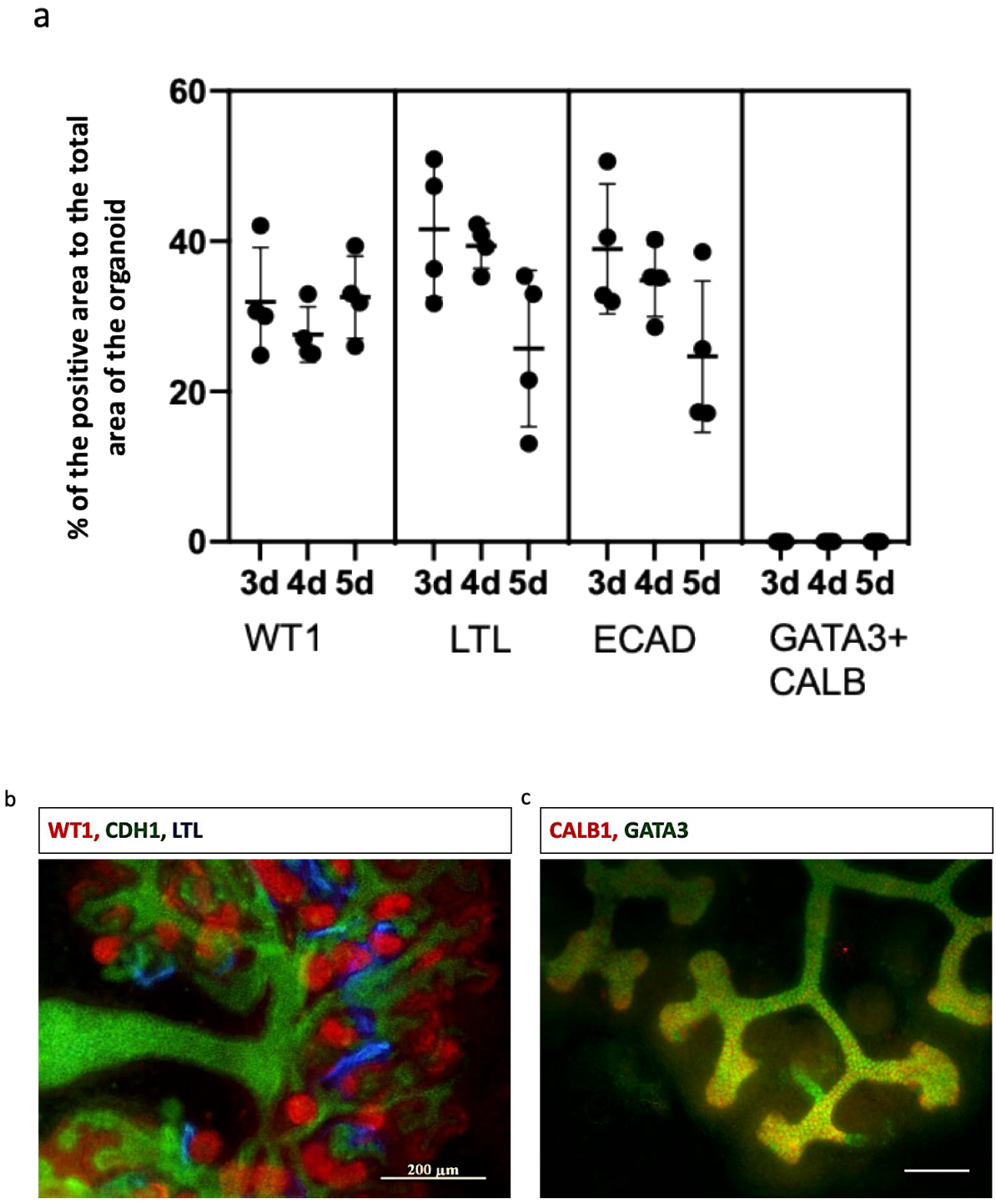

Figure 3.13. comparing between the three different initial CHIR treatment duration. a) Shows the % area stained positive for WT1, LTL, ECAD, or GATA3 and CALB to the whole area of the organoid compared between the three different durations of initial CHIR treatment (for GATA3/CALB 8 different organoids obtained from 4 different differentiation runs, 2 organoids/run, were included for each of the different CHIR treatment durations and were all negative. For the rest of the markers four different organoids obtained from 4 different differentiation runs were included for each marker in each of the different CHIR treatment). b,c) Mouse embryonic kidney stained for

ECAD, WT1, and LTL (b) or GATA3 and CALB1 (c) to show the expression of these markers in mouse kidney.

3.3.5 Possible cell death during the process of organoid formation:

Data presented in section 3.3.3; 3.3.4 were obtained from 3D organoids. I then observed that some of the examined differentiation runs showed $GATA3^{+}/ECAD^{+}$ tubules in the 2D cultures but not in the 3D organoids that were set in parallel. This suggested that anoikis of the early UB progenitor cells during the process of dissociation/re-aggregation of the cells to form organoids might be the reason for not obtaining UB-differentiated structures. The study that was done by Unbekandt and Davies, in 2010, has shown that when the embryonic mouse kidneys are dissociated into single cells then pelleted and cultured as 3D re-aggregate, many cells die unless ROCK inhibitor is added to the culture for 24 hrs. A recent study has also shown that dissociated embryonic UBs need ROCK inhibitor treatment to survive and form colonies (Yuri *et al.*, 2017). ROCK inhibitor is known to inhibit anoikis and has been shown to increase the efficiency of hPSC single cell survival (Watanabe *et al.*, 2007).

I set out experiment to compare between organoids cultured in presence or absence of ROCK inhibitor (for the initial 24 hrs of organoid culture); the organoids were cultured in the same conditions afterwards until the end of the differentiation protocol and were then stained for the UB markers. 3/10 of the organoids cultured without adding the ROCK inhibitor showed positive UB structures while 5/10 of the organoids that were treated with ROCK inhibitor showed positive UB structures. The number of obtained UB-like tubules was also higher in the ROCK inhibitor treated organoids (figure 3.14 a, b). 2D cultures were also set in parallel to these organoids; 6/10 of the 2D cultures showed positive UB markers. This result supports the idea that the UB progenitor cells might undergo dissociation induced apoptosis during the process of organoid formation but still does not exclude a source of variability in obtaining UB fate using the Takasato protocol. Therefore, I wanted to isolate these UB-like structures to further evaluate them (this will be discussed in chapter 6 and 7).

Adding the ROCK inhibitor to the culture media for the first 24 hrs of organoid culture and longer culture duration of the differentiated cells (20-23 days instead of 18 days in the original protocol) were the only modifications I did to the Takasato protocol and were applied to all the downstream experiments.

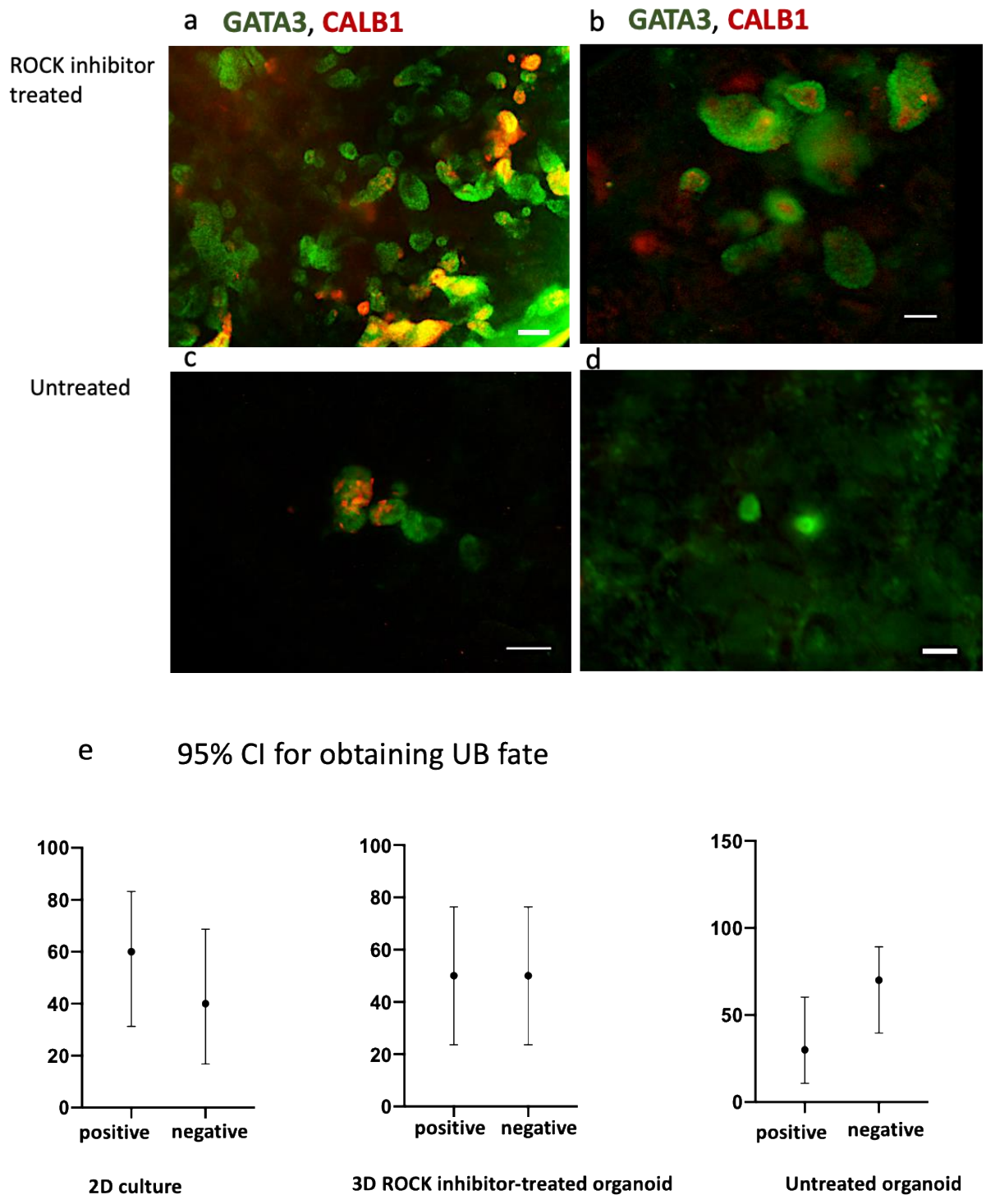

Figure 3.14. Comparing between ROCK inhibitor treated (a,b) and untreated (c,d) organoids in obtaining UB-like structures; the treated organoids developed more UB-like structures. d) Developed few UB-like structures; (c) Is negative for UB fate. e) shows the 95% confidence interval for obtaining UB fate in each group (see section 2.16); n = 10 for each group.

3.4 Discussion

Here, I reproduced the Takasato protocol of differentiation; I achieved stepwise differentiation of the hiPSC into nephron progenitors and showed the development of entities reminiscent to developing nephrons. I also evaluated the formation of 3D organoids by dissociating the cells and culturing them as 3D aggregates. The results indicate that the 3D environment enhanced the development of the renal-like tubules.

Markers for different segments of the nephron were consistently obtained but results for the UB and CD fate were quite variable. The Co-expression of GATA3 and CALB1 or GATA3 and ECAD (or $GATA3^{+}ECAD^{+}PAX2^{+}$) was taken as a marker for obtaining UB fate. Some of the organoids showed the expression of GATA3 only in interstitial cells, but not in tubular epithelial structures. GATA3 is an important transcription factor that is expressed in the WD and the UB where it plays an important role in kidney development and its deficiency in mice leads to renal agenesis (Grote *et al.*, 2008; Michos, 2010). A recent study has shown that GATA3 is also expressed in glomerular mesangial cells where it plays an important role in maintaining renal glomerular function (Moriguchi *et al.*, 2016). The pattern of GATA3 staining interstitial cells might be due to the differentiation of some cells into mesangial-like cells. ECAD and PAX2 showed positive expression in all the tested samples, however, ECAD is expressed in the distal tubules, connecting tubules, CD and UB (Lee *et al.*, 2013). PAX2 is also expressed in the IM, MM, renal vesicle and UB (Torres *et al.*, 1995; Bouchard *et al.*, 2002) and so ECAD and PAX2 are not specific to UB cells; only their co-expression with GATA3 was taken as a marker for UB and CD. CALB1 is a more specific marker for the UB and CD; a recent study has shown that in human fetal kidney between 8-11 weeks CALB1 was only detected in the CDs and was not seen in any nephron segments (Lindström *et al.*, 2018). Like GATA3, CALB1 expression in the obtained organoids was variable. 21/41 tested organoids were negative for UB fate and only 19/41 showed positive criteria for obtaining UB fate.

I also compared between the effect of the three different timings of initial CHIR treatment. The effect of the initial CHIR treatment duration in determining cell fate commitment was not as clear in my results as Takasato and colleagues described. None of the tested samples (8 organoids for each of the compared CHIR treatment duration, obtained from 4 different differentiation runs) showed co-expression of

GATA3 and CALB1. All the samples obtained from the different CHIR treatments did show positive nephron markers, albeit with, individual variation in the amount of each positive marker in relation to the total area of the organoid (Fig. 3.13). Collectively, the data suggests variability between runs in the ability to obtain UB-differentiated cells

In a recent study, Taguchi and Nishinkamura developed a protocol for differentiating mESCs and hiPSCs mainly to UB cells; they found that obtaining UB fate needed “a rigid time window for AIM induction” which was achieved by 1.5 days of CHIR treatment and according to their results the UB fate was not induced when longer durations of CHIR treatment was used (Taguchi and Nishinakamura, 2018).

A very recent study published by the same group that published the Takasato protocol; the Melissa Little group, performed single-cell transcriptomic analysis to investigate congruence and difference between their obtained organoids and human fetal kidney (Combes *et al.*, 2019). Interestingly, they reported that they did not find distinct cluster of cells that represents ureteric identity in either the organoids or the fetal kidneys. The absence of ureteric epithelial cell cluster in the fetal kidney led the researchers to suggest that the cells of the ureteric epithelium are resistant to single cell dissociation. However, they also mentioned that immunofluorescence staining for those particular set of organoids, which were included in the profiling experiment, did not show ureteric structures, or that they were present in low frequency. The study concluded that the GATA3^{+ve} epithelial structure require further studies to investigate the identity of these structures.

In my results, the UB fate was seen in some of the samples; some of the tubules that co-expressed GATA3 and CALB showed branching (Fig. 3.11 f) which suggests that these tubules might be UB-like structures despite the variability in obtaining these structures. It is likely that early UB progenitor cells undergo dissociation induced apoptosis during the process of organoid formation as the possibility of obtaining UB fate was increased when the organoids were treated with ROCK inhibitor for the first 24 hrs of organoid culture. death of the UB cells upon dissociation into single cells has been reported in previous studies. These studies have also shown that ROCK inhibitor treatment increases the survival of the dissociated UB cells (Unbekandt and Davies, 2010; Yuri *et al.*, 2017). However, a source of variability in obtaining UB fate using the Takasato protocol could not be excluded; 2D cultures, which are kept without

dissociation throughout the differentiation protocol, still show variable results in obtaining UB-like structures. Optimising conditions to minimise this variability and more characterisation for these structures is still required.

In conclusion, the MM fate and its derivatives (different segments of the nephron) were efficiently obtained in all the tested samples, so in the next chapters (chapter 4, 5), I try to investigate some functional capacities of these cells and to evaluate their possible suitability for use in nephrotoxicity screening. The UB fate was variable, so in following chapters (chapter 6, 7), I try to isolate the UB-like structures for further characterisation and assessment.

Chapter 4

4 Investigating aspects of renal tubular physiology in hiPSC-derived renal organoids

4.1 Introduction:

Despite lacking the intricate cortico-medullary zonation and the correct anatomical arrangement of nephrons around a single central collecting duct tree, compared to the normal organ, hiPSCs-derived renal organoids are quite similar to embryonic kidneys at the micro-scale anatomy level, as shown by their expressing specific markers for different segments of the nephron and for the collecting ducts. While correct macro-scale anatomy is important for the use of these organoids in regenerative medicine and transplantation purposes, it is important, before going on to engineer a more anatomically realistic tissue and trying to organise these structures, to test whether the developing nephrons are functional; having functioning nephrons growing in culture could have many implications including their use for screening drugs for potential nephrotoxicity, which could be an early application of organoids as it does not require correct macro-scale anatomy.

Research aim:

In this chapter, I wanted to evaluate some physiological aspects of the renal-differentiated organoids.

4.2 Proximal tubular transporters and their role in kidney function and drug toxicity:

Kidneys receive 20-25% of the cardiac output; 20% of the renal plasma flow is filtered at the glomeruli while the remaining blood circulates through the efferent arteriole to the peritubular capillaries. This makes a glomerular filtration rate of (GFR) of approximately 160-170 L/day; the composition of the primary filtrate being almost the same as plasma excluding plasma proteins. The high GFR necessitates intensive reabsorption mechanisms to prevent water and electrolyte disturbance, pH disturbance, and nutrient loss. Proximal tubules reabsorb almost all of the filtered glucose and amino acids, 60-70% of the filtered water and NaCl, and most of the filtered $NaHCO_3$ (Zhuo and Li, 2013).

In addition to reabsorbing valuable components of the ultrafiltrate, proximal tubules also play a key role in secreting metabolic waste products and xenobiotics into urine. This is specifically important for eliminating protein-bound substances that do not

cross the glomerular filtration barrier (Wang and Kestenbaum, 2018). Tubular secretion was first proposed by Heidenhain who assumed that tubular epithelial cells mainly perform a secretory function (Heidenhain, 1874). Marshall and Vickers were the first to provide a proof of tubular secretion; they demonstrated the uptake of phenol red by proximal tubules and observed that the elimination of that protein-bound dye was far more than what could be achieved through glomerular filtration (Marshall and Vickers, 1923). Later on, Smith and colleagues showed that Phenol red clearance could be used to measure the effective renal blood flow and the tubular excretory mass (Smith, Goldring and Chasis, 1938).

Together with glomerular filtration, tubular secretion and reabsorption are key to the clearance of toxins, metabolic waste products and drugs (Dickson *et al.*, 2014; Suchy-Dicey *et al.*, 2016; Wang and Kestenbaum, 2018).

4.2.1 Molecular mechanisms of trans-epithelial tubular transport:

While glomerular filtration depends on passive diffusion regulated by hydrostatic pressure, trans-epithelial tubular transport mostly requires the function of transporters located on the basolateral or the apical membranes of the tubular epithelial cells. Transporters are membrane proteins that mediate the uptake or efflux of specific substrates into or out of the cells; they tend to have charge-selectivity either to anions or cations, nevertheless, some studies suggest a degree of overlap (Pritchard and Miller, 1996; Sanjay K Nigam, 2015; Nigam *et al.*, 2015; Yin and Wang, 2016).

4.2.1.1 Basolateral membrane transporters:

On the basolateral membrane of the proximal tubules the main transporters responsible for the uptake of organic anions and cations are organic anion transporters (OATs) and organic cation transporters (OCTs) respectively (Burckhardt, 2012; Wang and Kestenbaum, 2018). Both types of transporters are members of the SLC22 family (figure 4.1).

In humans, three OCT isoforms have been identified; OCT1-3. OCT2 is the main cation transporter expressed in the kidney (Koepsell *et al.*, 1998), where it is localised to the basolateral membrane of the three segments of proximal tubules S1, S2, S3 (Motohashi *et al.*, 2002; Motohashi and Inui, 2013). OCT1 is mainly found in liver

(Zhang *et al.*, 1997), and OCT3 is widely expressed in different organs including placenta, skeletal muscle, heart and salivary glands (Kekuda *et al.*, 1998; Koepsell, Lips and Volk, 2007b; R. W. S. Li *et al.*, 2013).

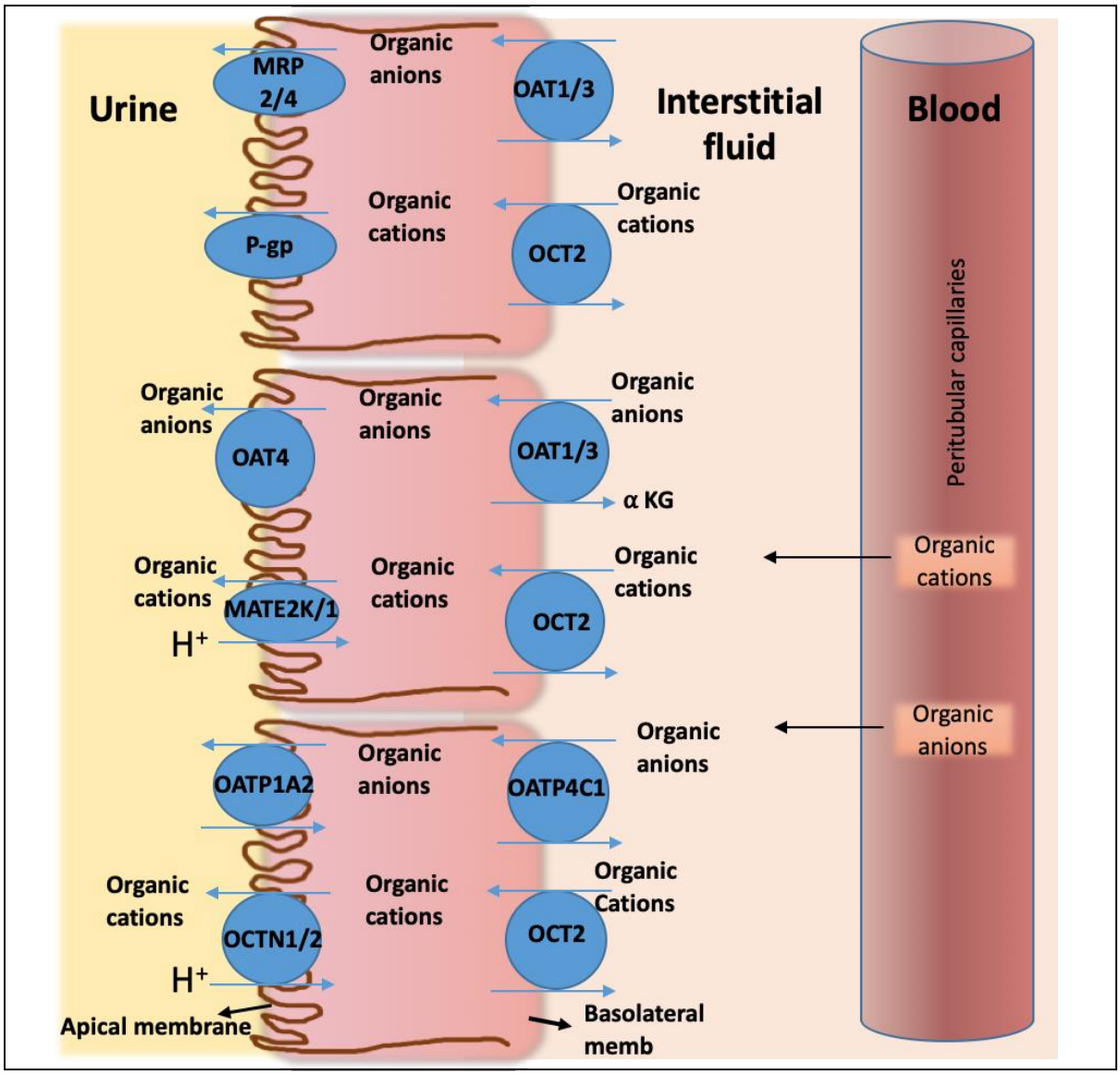

Figure 4.1. Schematic illustration of tubular transport for organic anions and cations mediated through proximal tubular transporters. Organic cations and anion are taken into the proximal tubular cells through the basolateral membrane transporters and then the apical transporters mediate their secretion into the tubular lumen.

OCT2 takes up cations from the circulation into the tubular cells, thus mediating the first step of cation secretion (Motohashi *et al.*, 2002, 2013; Fujita *et al.*, 2006). OCT2 transports cations down an electrochemical gradient, created by the inside-negative membrane potential of the tubular cells, via facilitated diffusion (Motohashi and Inui, 2013; Wang and Kestenbaum, 2018). Rat and mouse kidneys show strong expression of *Oct1* while the human kidney expresses it only in small amounts (Koepsell, Lips and Volk, 2007a)

Common substrates for OCT2 include:

- Drugs of different categories: the chemotherapeutic drugs Cisplatin (Yonezawa *et al.*, 2006; Filipski *et al.*, 2009; Ciarimboli *et al.*, 2010; More *et al.*, 2010) and Ifosfamide (Ciarimboli *et al.*, 2011); the oral hypoglycemic drug metformin (Nies *et al.*, 2011; Ren *et al.*, 2015); the anti-hypertensive drug atenolol (Ren *et al.*, 2015; Yin *et al.*, 2015); the H_2 receptor blockers Famotidine, Cimetidine and Ranitidine (Nies *et al.*, 2011); and the anti-Parkinsonian drug amantadine (Li *et al.*, 2017).
- Toxins: the mycotoxin AflatoxinB1, the herbicide Paraquat and the commonly used fluorescent nucleic acid stain Ethidium bromide (Nies *et al.*, 2011).
- Endogenous substrates: creatinine is an important substrate for OCT2. Creatinine clearance is usually used to estimate GFR, however, because of the tubular secretion of creatinine this usually gives false higher estimates of GFR so creatinine tubular secretion should be considered carefully in patients with glomerular disorders (Urakami *et al.*, 2004).
- Model cations: including ASP, TEA, TPA, N1-methylnicotinamide and MPP (Pietruck *et al.*, 2006).

OAT1 and OAT3 are the main organic anion transporters on the basolateral membrane (Sekine *et al.*, 1997; Burckhardt, Wolff and Bahn, 2002; Motohashi *et al.*, 2002). They mediate the first step of organic anion secretion in the renal proximal tubules by taking anions from blood into tubular cells in exchange with the dicarboxylic acid α-ketoglutarate (Sweet *et al.*, 2003, 2006; Burckhardt, 2012). They contribute to the secretion of a wide range of drugs and toxins in the renal proximal tubules thus protecting from putative toxic compounds. There is considerable overlap between

OAT1 and OAT3 regarding their substrate specificity, with some substrates having higher affinity to one over the other (Burckhardt, 2012; Huo and Liu, 2018).

Substrates for OAT1 and OAT3 include:

- Endogenous substrates such as Urates thus OAT1 and 3 contribute to purine metabolite excretion (Koepsell, 2013).
- Drugs of different categories including antibiotics as tetracyclines and cephalosporins, antineoplastic drugs as methotrexate (OAT3 binds to methotrexate with much higher affinity than OAT1), antiviral drugs as acyclovir and cidofovir (Zhou and You, 2007; Huo and Liu, 2018).

Another important basolateral membrane transporter involved in anion uptake is OATP4C1 transporter which transports larger and more hydrophobic anions; it also transports some neutral and even positively charged substrates (Suzuki *et al.*, 2011).

4.2.1.2 Apical membrane transporters:

Members of the ABC family; the multidrug-associated resistance proteins (MRP) 2 and 4 (also known as ABCC2 and ABCC4) are the main apical surface transporters involved in efflux of the anions that are taken into the tubular cells by OAT1 and 3; OAT4 and URAT1 are other transporters that also have role in apical efflux (Hediger *et al.*, 2005; Miyazaki *et al.*, 2005; Nigam *et al.*, 2015) (figure 4.1).

Transporters involved in cation apical efflux include the multi drug and toxin extrusion (MATE) transporter 1, the human kidney-specific multidrug and toxin extrusion transporter (MATE2K), and the organic cation/carnitine transporter (OCTN) 1 and 2 (Masuda *et al.*, 2006; Tanihara *et al.*, 2007; Nigam *et al.*, 2015; Wang and Kestenbaum, 2018). In addition to their role in efflux, MATEs have been shown to be also involved in cation uptake depending on the cation concentration gradient (Yonezawa and Inui, 2011a, 2011b).

4.2.2 Results:

Transport of organic anions and cations cannot take place without transporters, so my first step in assessing functional capacity of the organoids was to test the expression of selected proximal tubular transporters; adequate expression of these transporters is fundamental for the use of those cells for nephrotoxicity screening purposes.

4.2.2.1 Testing the expression of OAT1 and OCT2 using RT-PCR:

OAT1 expression is detected in the proximal tubules of the 14-16 week human foetal kidney (Lindström *et al.*, 2018) but little is known about when exactly these transporters first start to be expressed in the human foetal kidney. 3D Organoids were tested at two different maturation points; 11 day and 20 day differentiated organoids. Also, the expression was tested in 20 day differentiated 2D monolayers. A clear band was seen for both OAT1 and OCT2 in 20 day-differentiated 3D organoids indicating their expression at this point of maturation, however, OAT1 and OCT2 were not detected in the 20 day-differentiated 2D cells (n=2) (Figure 4.2 I).

4.2.2.2 Transporter functional assays:

I next wanted to see if the expressed transporters were truly functional. Recently, some studies used renal-differentiated organoids, made using the Takasato protocol, for in-vivo functional assessment after their transplantation in experimental animals (Bantounas, Ranjzad, Tengku, Silajdžić, Forster, M.-C. Asselin, *et al.*, 2018; van den Berg *et al.*, 2018). Neither of these studies examined the expression and function of the proximal tubular transporters. While testing glomerular filtration needs existing vascular system in the organoids with active blood circulation, testing tubular transporter function does not require blood flow (Lawrence, Elhendawi and Davies, 2019) and transporter functional assays can be performed on in-vitro organoid culture models and can be used as a way to assess some functional aspects of the hiPSC-derived renal organoids without the need for transplanting them into experimental animals.

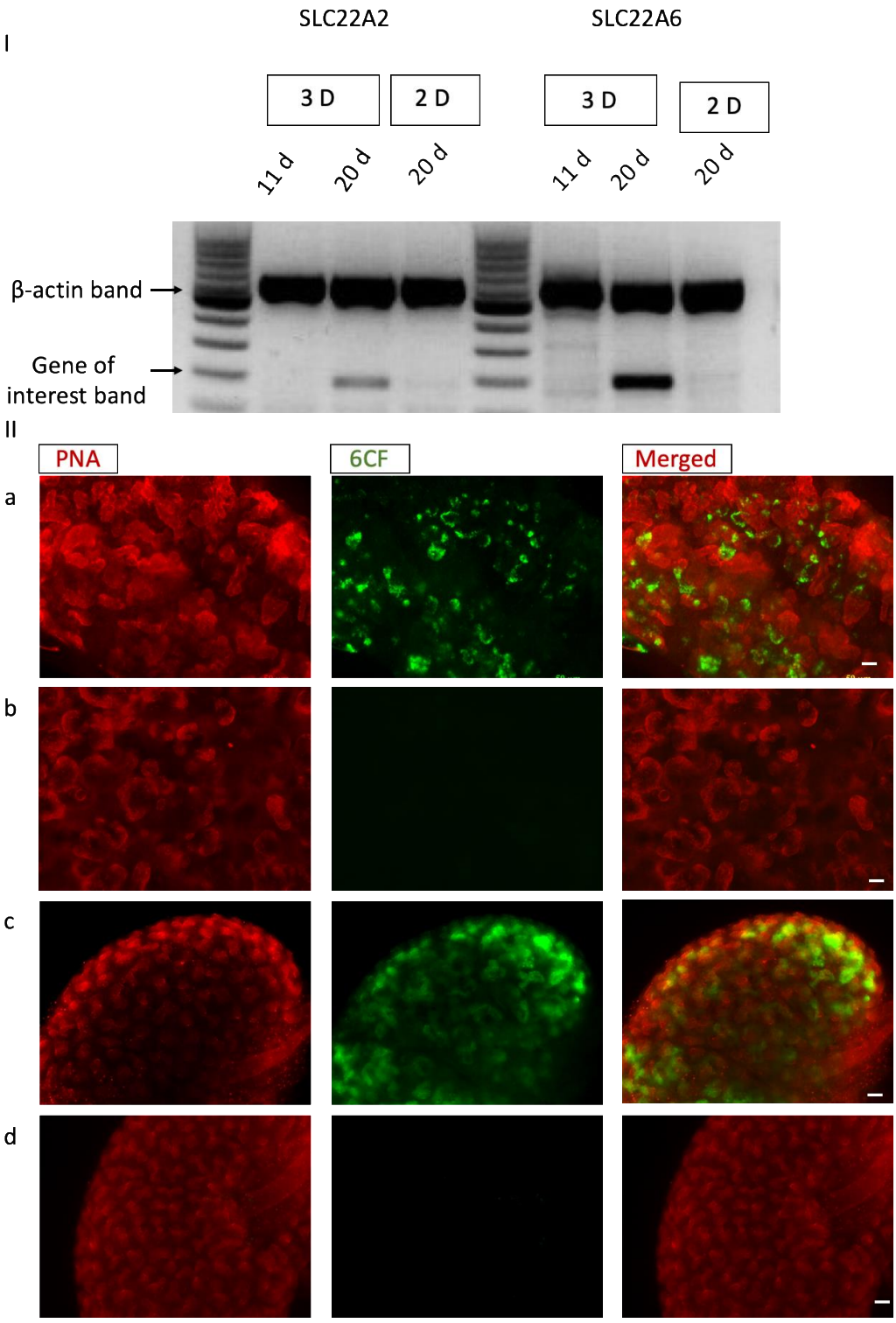

Figure 4.2. I) RT-PCR result showing expression of OCT2 (SLC22A2) and OAT1 (SLC22A6) in 20 day differentiated 3D organoids. II) a,b) functional uptake assay for the organic anion 6-CF in 20 day differentiated 3D organoid a) in absence of and b) in presence of the transporter inhibitor, Probenecid; c, d) 6-CF uptake in E15.5 mouse kidney as a control of the experiment showing uptake of 6-CF into the proximal tubules in c) where there is no inhibitor added but not in d) that was treated with the inhibitor (Probenecid). Scale bar is 100 μm.

4.2.2.2.1 Anion uptake assay:

A group of fluorescent and radiolabelled model substrates have been used in *in-vitro* metanephric cultures for testing OAT function. 6-CF was chosen as a fluorescent anion to avoid the risk of using a radiolabelled substrate and at the same time it could be imaged easily to assess the uptake. 6-CF is taken into the proximal tubular cells through the basolateral anion transporters in a Na-dependant manner (mediated by OAT1 and OAT3) and its efflux into the lumen is mediated uphill through the apical membrane transporters (mostly through MRP2 and 4) (Miller, Letcher and Barnes, 1996; Masereeuw *et al.*, 1999; Breen *et al.*, 2001; Sweet *et al.*, 2006; Lawrence, Chang and Davies, 2015b).

Uptake was tested by incubating living iPSC-derived renal organoids with the 6CF anion for 40 minutes; in some samples probenecid, a potent anion transporter inhibitor, was applied simultaneously with 6-CF to test the specificity of the uptake. After 40 minutes of incubation with 6-CF, in the absence or presence of probenecid, both conditions were washed and kept in PBS containing 8 mM probenecid to prevent efflux of the 6-CF thus, trapping the fluorophore and allowing for imaging. PNA was used as a pan-tubular marker to mark the tubules (figure 4.2 II). E15.5 mouse kidneys were used as a positive control for the whole experiment as their ability to take up 6-CF and the inhibition of the uptake with Probenecid is already known (Sweet *et al.*, 2006; Lawrence, Chang and Davies, 2015b).

As expected, 13 day differentiated organoids did not show 6-CF accumulation, indicating that at this stage nephrons had not acquired functioning transporters. Consistent with the RT-PCR results which showed that OAT1 was expressed in the 20d differentiated organoids, 6-CF accumulated in tubular structures within these organoids. Probenecid treatment inhibited the uptake of 6-CF in the organoids, indicating that the uptake was inhibitor sensitive (n = 5 independent samples). The inhibitor-sensitive uptake of 6-CF suggests functional anion transporters in the renal-differentiated organoids.

4.2.2.2.2 Cation uptake assay:

For testing the function of the cation transporters, I used 4-(4-dimethylamino-styryl)-N-methylpyridinium (ASP); ASP is a fluorescent substrate for renal organic cation transporters (Pietruck *et al.*, 2006). TPA, which is another cation substrate (Schophuizen *et al.*, 2013), was used as a competitive inhibitor for the uptake of ASP in the inhibitor-treated samples. LTL was used to live-stain the proximal tubule cells before starting the uptake experiment. The inhibitor-treated samples were incubated with TPA for 20 min prior to ASP treatment, after that both conditions (test samples and inhibitor treated samples) were treated with ASP (still in presence of the inhibitor in case of the inhibitor treated-samples) and incubated for 20 minutes to allow for the uptake; the fluorescent dye was taken up by LTL-marked tubules, suggesting uptake inside the proximal tubular cells. ASP uptake was much lower in the organoids treated with TPA compared to the test samples; in addition, ASP uptake decreased with increasing concentration of the TPA (Figure 4.3). The ability of organoids to transport ASP in an inhibitor-sensitive way (n = 5 independent samples) confirms the presence of physiological functioning organic cation transporters in the iPSCs-derived organoid model.

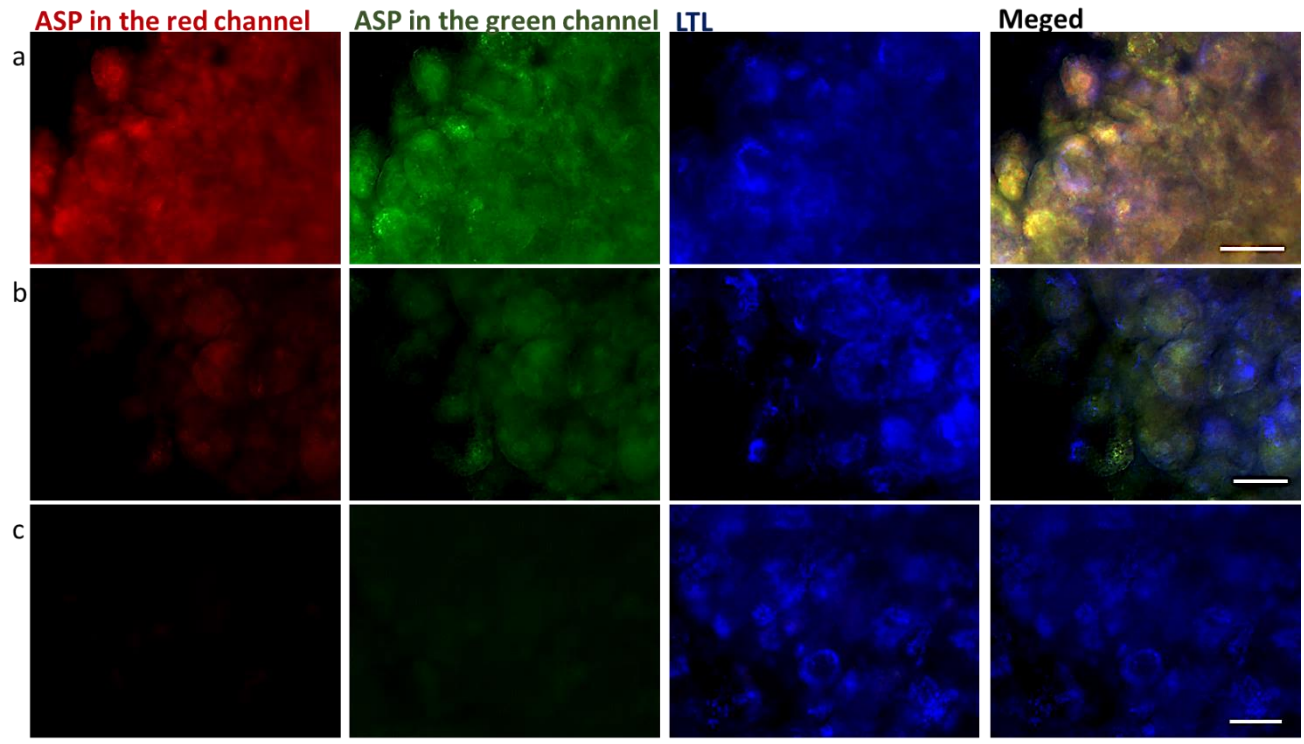

Figure 4.3. Cation uptake assay using the fluorescent cation ASP. a) Shows uptake of ASP into LTL labelled proximal tubules; no inhibitor was added. b) Shows decreased ASP uptake in an organoid that was treated with low dose of TPA (competitive ASP inhibitor). c) Shows almost no uptake in organoid treated with higher dose of the inhibitor; TPA. Scale bar is 100 µm.

4.3 Can renal-differentiated cells be cryopreserved?

Having demonstrated that the cells obtained by applying the Takasato protocol of differentiation develop into renal-like structures (chapter 3) and can perform some renal tubular functions (section 4.2.2 of this chapter), I wanted to investigate whether the differentiated cells could survive cryopreservation and retain their ability to self-organize, to form renal-like tubules, and to perform tubular function. The differentiation protocol takes 20-23 days to obtain renal-differentiated organoids from hiPSCs, plus the need to maintain, passage the iPSCs and regularly test them for pluripotency; all these requirements make the process of making renal organoids laborious. In addition, maintaining hiPSCs in culture could be a cause of variability (Takasato *et al.*, 2016) and mutations can be problematic, especially with high passages. I therefore wanted to assess the possibility of cryopreserving and reviving renal-differentiated cells. Recent studies have shown the possibility of cryopreserving cardiomyocyte-differentiated, and brain endothelial cell-differentiated hPSCs (Xu *et al.*, 2011; Wilson *et al.*, 2016). If this proved feasible with renal-differentiated hiPSCs, it could save a lot of time and effort and it could be of specific importance for the use of those cells in nephrotoxicity screening where high throughput model is needed.

4.3.1 Cryopreserving and reviving 12 days differentiated cells:

I tried to dissociate and cryopreserve renal-differentiated cells at day twelve of the differentiation protocol. In the differentiation scheme, cells achieve renal progenitor stage around day 12 of differentiation. After that point, cells are kept in culture medium without the need of adding any growth factors, therefore cells at that stage requires less manipulation and saves considerable time. So, I trypsinised 12 day differentiated cells and dissociated them into single cells to evaluate the possibility of cryopreserving and reviving them. The dissociated cells were suspended in culture media that contains 10 µM ROCK inhibitor + 10% DMSO and were cryopreserved at – 80 ° C. ROCK inhibitor was added to prevent anoikis (Watanabe *et al.*, 2007). When thawing the cells after cryopreservation, the viability was assessed using trypan blue stain and cells were counted on a haemocytometer. 95%± 2% of the cells were viable. Afterwards, cells were either seeded on Matrigel coated culture dishes and grown as monolayers or aggregated as pellets and cultured in 3D culture system as organoids. The attachment of the cells to the culture dishes was assessed in the presence and

absence of ROCK inhibitor (10 μM) for the first 24 hrs post-thawing. When cells were thawed without adding ROCK inhibitor for the first 24 hrs post-thawing, most of the cells did not attach and died afterwards (figure 4.4). Similarly, only 3D cultures that were treated with ROCK inhibitor for the first 24 hrs developed and showed tubular structures at the end of the culture period. Without it, they either remained unattached and died (in monolayers) or did not develop or form any structures (in the 3D culture system). After the first 24 hrs post-thaw, the ROCK inhibitor was removed, and the differentiation protocol was continued as usual without any further addition of growth factors figure 4.5 a).

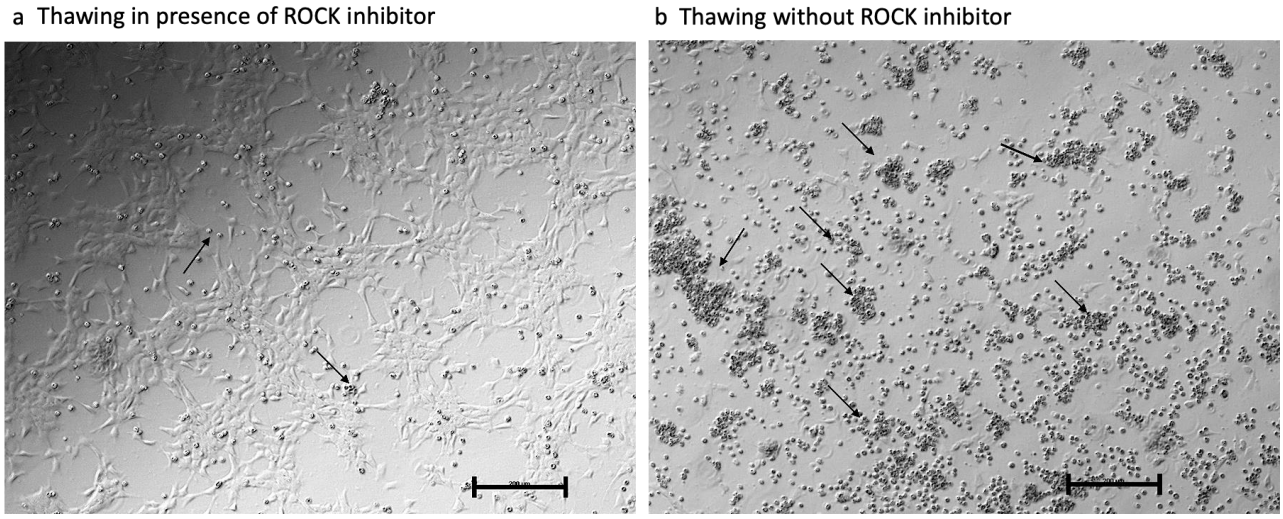

Figure 4.4. Shows the importance of adding ROCK inhibitor for the first 24 hr of culture post thawing; a) cultured in presence of ROCK inhibitor b) in absence of ROCK inhibitor; very few cells attached to the culture dish. The arrows point to unattached cells which formed aggregates in untreated cells. Scale bar is 200 μm.

4.3.1.1 Verification for the ability of the cells to revive and form renal structures:

Cells that were cultured after a period of cryo-storage continued to differentiate in mostly the same way as regular differentiated monolayers and organoids did. Cryopreserved cells that were cultured as monolayers after thawing developed tubular structures at the end of the differentiation (9 days post thawing). When these 2D cultures were fixed and stained they showed positive expression for different renal markers, ECAD1, WT1 and NPHS1, indicating the development of nephron structures

(figure 4.5) (for more details about these expression markers see chapter 3 section 3.3.2.2 and 3.3.2.3). Similarly, all the pellets formed from cryopreserved cells succeeded in forming complex 3D organoids that showed $ECAD^+$ tubules (in the distal tubules and collecting ducts) connected to LTL^+ tubules (proximal tubules) and surrounded by clusters of $WT1^+$ and $NPHS1^+$ cells (both expressed in podocytes); collectively that expression pattern suggested the development of patterned nephrons. Organoids also showed positive expression of GATA3 and Calbindin, which suggests obtaining UB/CD tubules (fig. 4.6; for more details about the differentiation markers and the obtained structures see section 3.2).

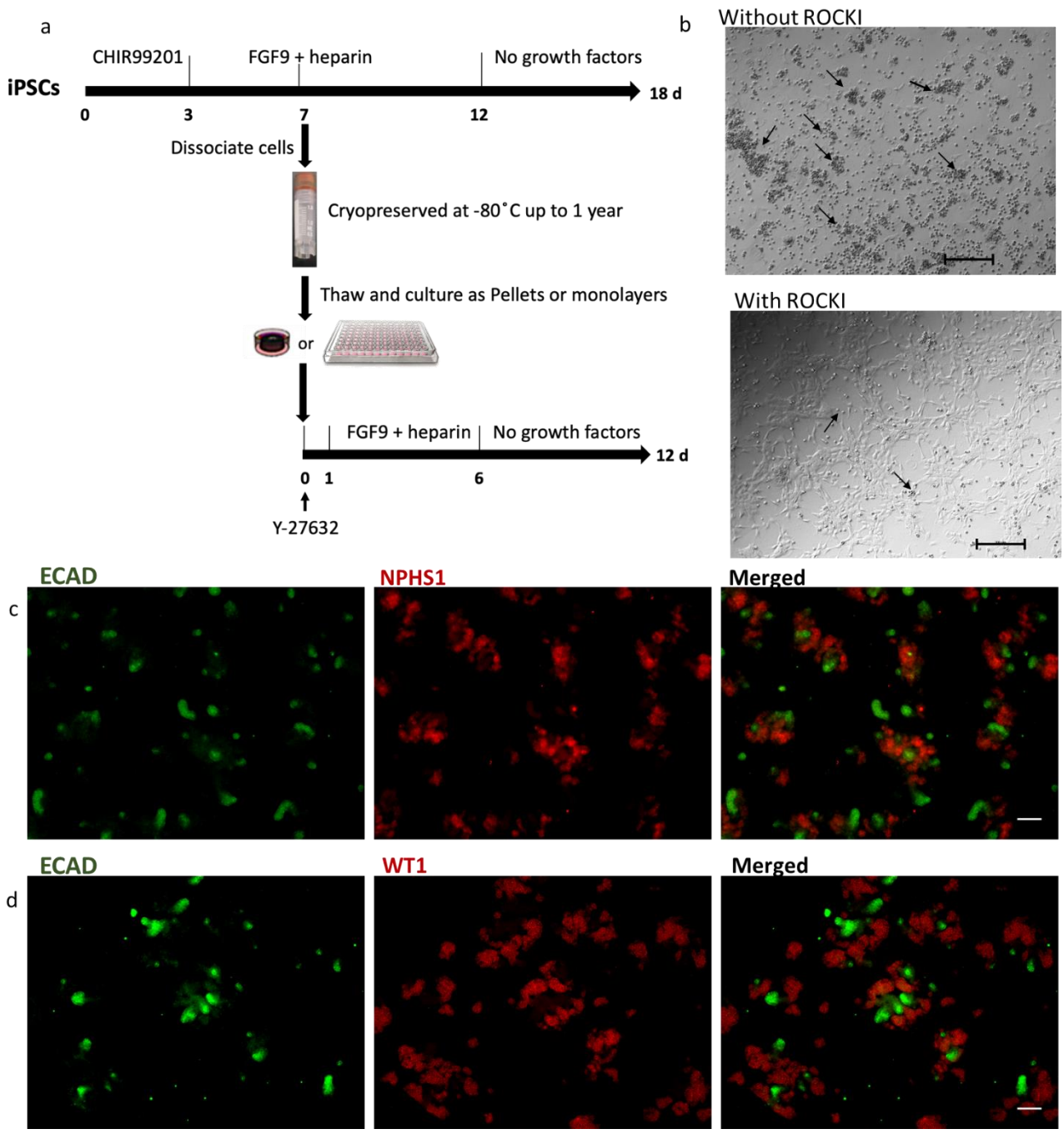

Figure 4.5. a) Schematic illustration of the cryopreservation, thawing and culture of the cells. b,c) Monolayer immunostaining of the cryopreserved cells after 9 days post-thawing b) stained for NPHS1 and ECAD, c) stained for WT1 and ECAD. Scale bar is 100 µm.

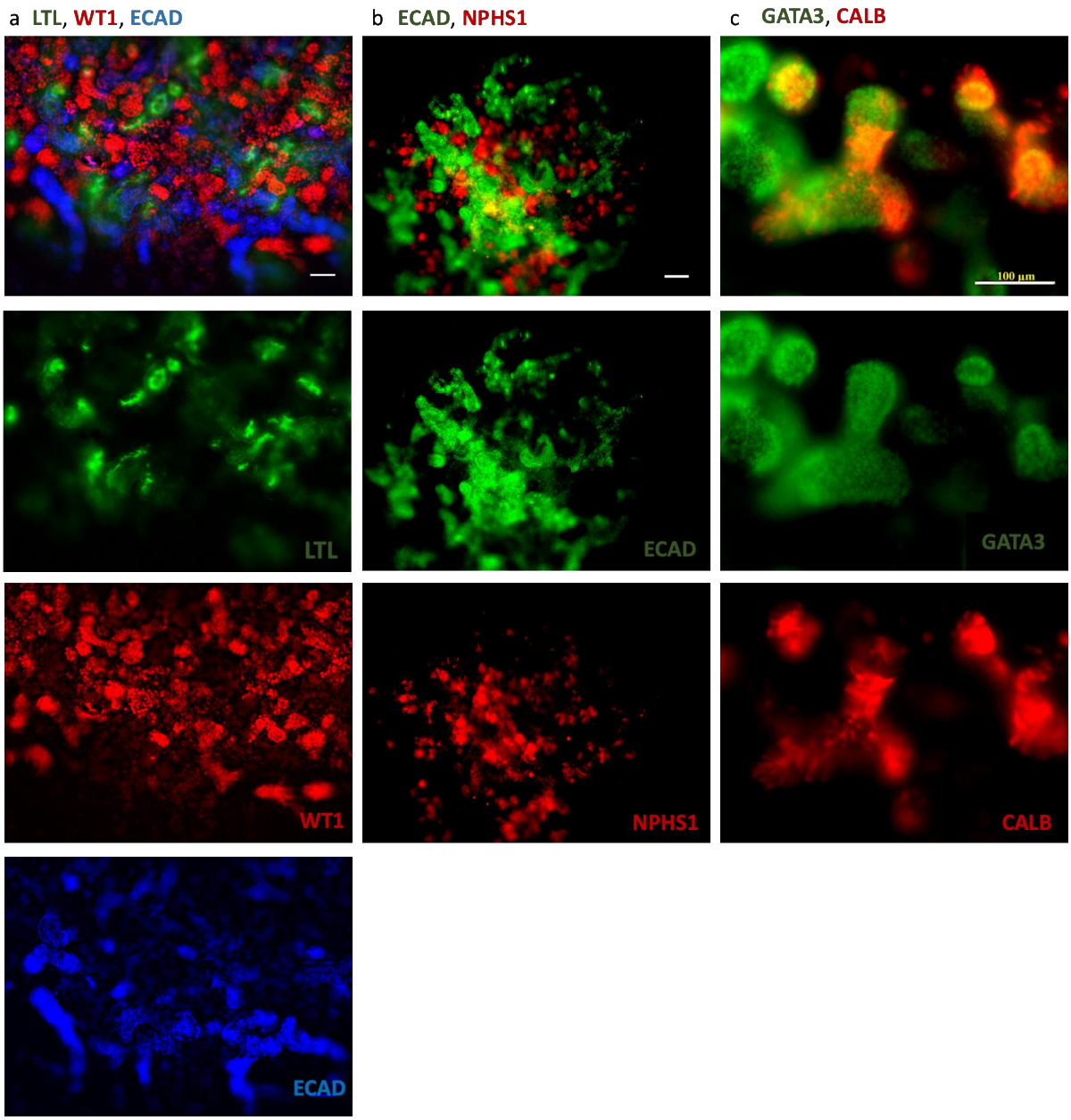

Figure 4.6. Immunostaining for organoids made from cryopreserved cells showing their ability to make 3D renal organoids that express different renal markers a) stained for the glomerular marker WT1, the proximal tubular marker LTL and the distal tubular and the collecting duct marker ECAD; b) stained for the specific glomerular membrane marker NPHS1 and ECAD; c) showing the co-localisation of the collecting duct markers CALB1 and GATA3 in branching tubular structures. Scale bar is 100 µm.

4.3.1.2 Functional assessment of the organoids obtained from cryopreserved differentiated cells

Next I used the functional assays described in section 4.2.2 to assess if organoids obtained from cryopreserved differentiated cells possess functional anion and cation transporters. The 3D organoids were examined for the uptake of 6-CF and ASP, after 10 days of post thawing culture, in presence or absence of inhibitor (as described earlier in section 4.2.2). The organoids showed positive uptake of 6-CF and ASP; that uptake was inhibitor sensitive in both cases which suggests the presence of functional proximal tubular transporters (figure 4.7).

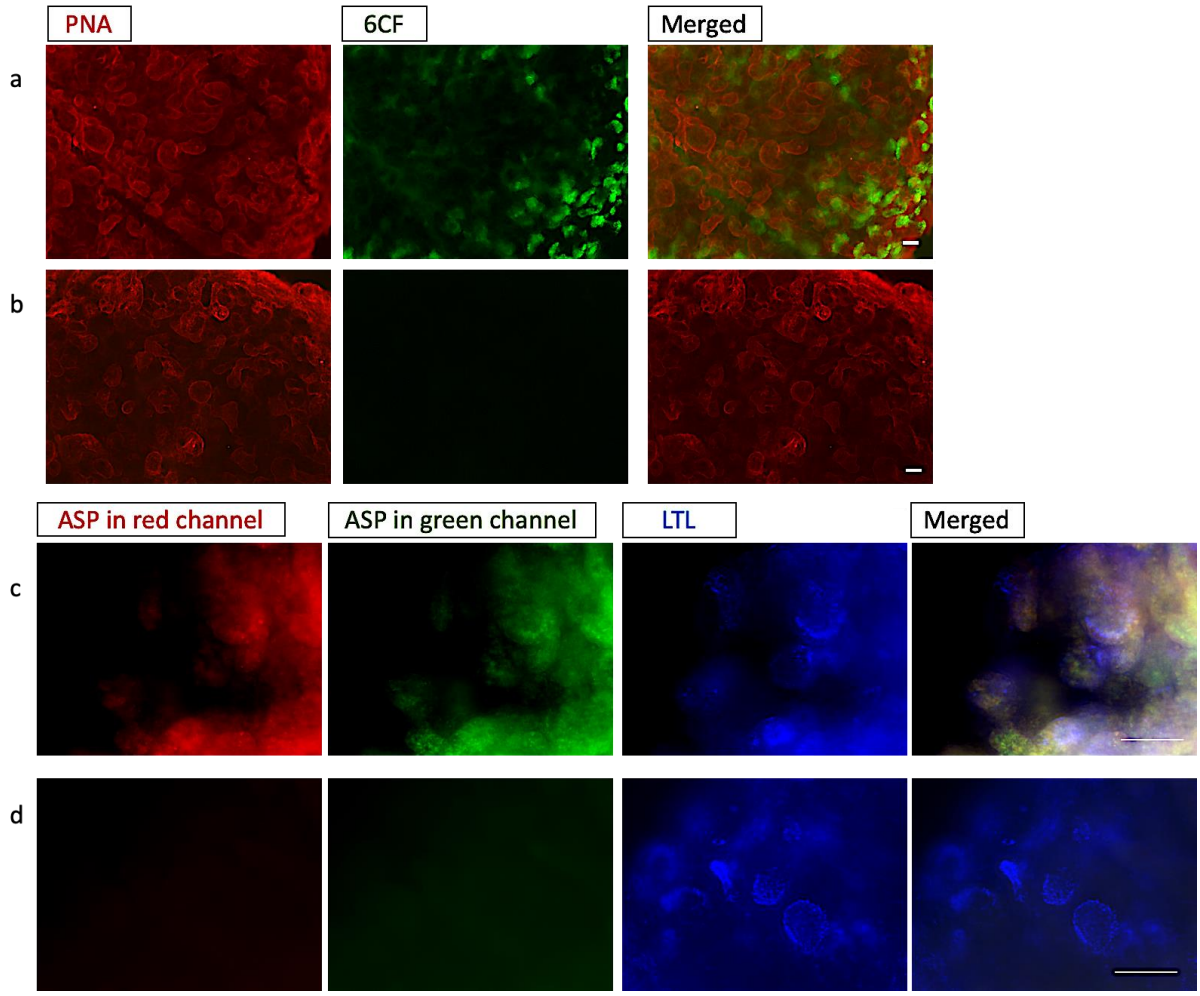

Figure 4.7. Functional uptake assays for the 3D organoids made from cryopreserved cells a,b) show 6-CF uptake in absence of (a) or presence of (b) probenecid as an inhibitor of the organic anion transporters. c, d) Show the uptake of the fluorescent cation ASP in absence of (c) or presence of (d) TPA, a competitive inhibitor of ASP. Scale bar is 100 µm.

4.3.1.3 Test the ability of renal organoids made from cryopreserved cells to detect nephrotoxicity:

To further assess the function of the proximal tubular cation transporters in the cryopreserved cells and to assess whether they can detect nephrotoxic compound in a predicted way, I used Cisplatin. Cisplatin is a chemotherapeutic drug; its nephrotoxicity is a major drawback for its clinical use. Cisplatin nephrotoxicity primarily affects proximal tubular cells. It accumulates in the proximal tubular cells mainly via OCT2 uptake where it interferes with DNA synthesis and causes DNA damage and results in dose dependent apoptosis and necrosis to the tubular cells (Yonezawa and Inui, 2011b; Volarevic *et al.*, 2019). Organoids obtained from cryopreserved cells were treated with increasing doses of Cisplatin after 10 days of post-thawing culture (0, 5, 10 and 30 µM) for 24 hrs. The treated organoids were then fixed and immuno-stained for ECAD1, LTL and Caspase3, an apoptosis marker. The toxic response was assessed by quantifying Caspase3 inside the organoid tubular structures. Increase in Caspase3 inside the proximal tubules was seen indicating dose-related apoptosis of the proximal tubular cells in response to Cisplatin treatment (Figure 4.8).

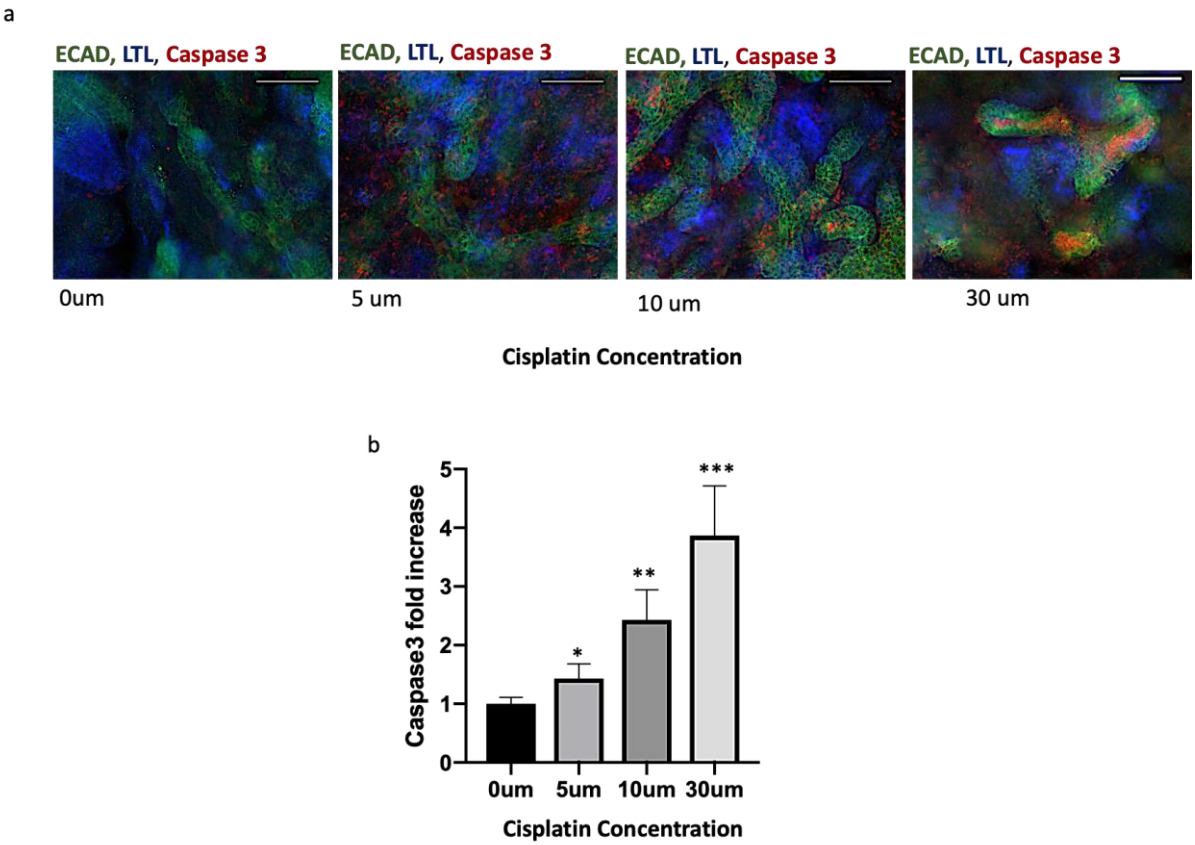

Figure 4.8. Response of the 3D organoids derived from cryopreserved cells to treatment with increasing concentrations of Cisplatin a) shows increase in the apoptotic marker Caspase 3 in response to the treatment; scale bar is 100 μm. b) Graph shows the relative increase in caspase 3 in the treated groups compared to the control, untreated cells, using total fluorescence quantification of Caspase 3 in stained organoids (n=5 for the 10 μM group and = 6 for the other groups; p *= 0.03, **= 0.01, ***= 0.002)

4.3.2 Test the possibility of cryopreserving fully differentiated cells:

Finally, I wanted to see if cells were dissociated and cryopreserved after being differentiated as monolayers until the end of the differentiation protocol (18 days) will still be able to form organoids after thawing. The fully differentiated cryopreserved cells were aggregated after thawing and cultured as pellets in presence of ROCK inhibitor for the first 24 hrs and without any additional growth factors or inducers for three more days, after which they were fixed and stained (figure 4.9). The organoids showed development of tubular structures with positive expression of ECAD1, WT1 and LTL indicating developing nephrons (for more details about see section 3.3.2.2 and section 3.3.2.3). Moreover, these organoids showed 6-CF uptake when live-incubated with it (using the same functional assays described in section 4.2.2.2.1) suggesting functional anion transporters and suggesting successful revival of differentiated cells (figure 4.9 C, D). I have to clarify that I cryopreserved only one run of differentiation after the end of the differentiation protocol, and successfully revived samples of it on three different occasions, while I investigated cryopreserving the cells after 12 days of differentiation more thoroughly and was able to revive them successfully for up to one year of cryo-storage.

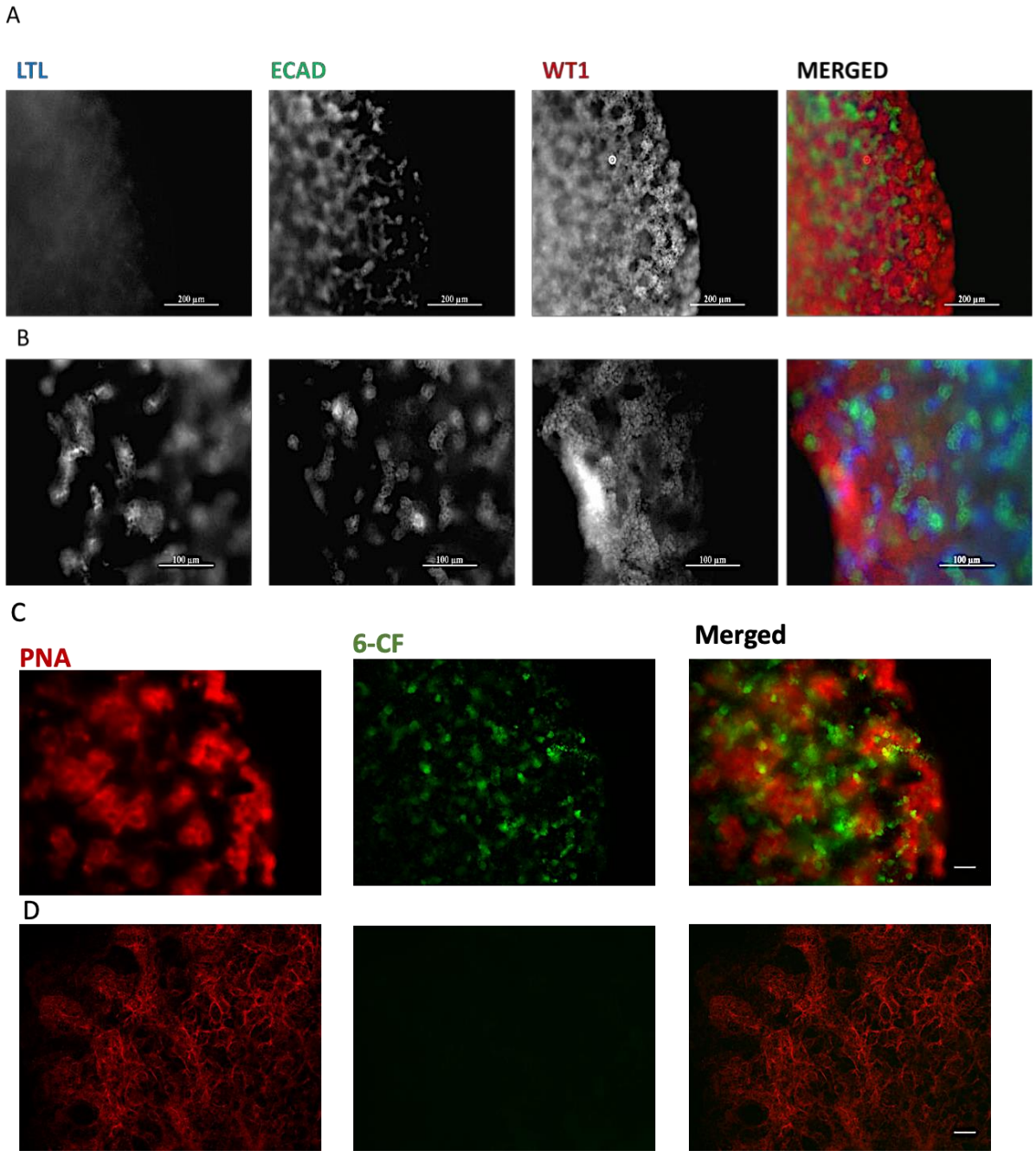

Figure 4.9. Organoids made from cryopreserved cells (cells were differentiated until the end of the differentiation protocol (18 days) then dissociated and cryopreserved). A) Organoid cultured in 3 D culture for 1 day after thawing and removal of the ROK inhibitor. B) Organoids cultured for 3 days after thawing and removal of ROK inhibitor. LTL shown in blue, ECAD shown in green, WT1 shown in red. LTL was negative when organoids were stained after one day of culture. C, D) 6-CF uptake test to 3D organoids made from cryopreserved fully differentiated cells after 4 days of culture post-thawing C) in absence of probenecid, D) in presence of probenecid. Scale bar is 100 µm.

4.4 Discussion:

Proximal tubular secretion and reabsorption are key to the reabsorption of valuable nutrients and solutes, and the clearance of toxins and metabolic waste products, especially for those protein-bound solutes that do not cross the glomerular filtration barrier, and they are of a particular importance in renal drug clearance. Organoids obtained by this protocol have recently been engrafted into animal hosts, either subcutaneous (Bantounas *et al.*, 2018) or under the renal capsule (van den Berg *et al.*, 2018), and were shown to acquire a blood supply from the animal host with some evidence of glomerular perfusion. While glomerular filtration is a crucial aspect of renal function, trans-epithelial tubular transport is another important partner in renal function (Wang and Kestenbaum, 2018). Renal organoids produced using the Takasato protocol of differentiation have not been assessed for their trans-epithelial transport capacity before. Here, I reported the expression OAT1 and OCT2, the major anion and cation transporters on the basolateral membrane of proximal tubular cells. I assessed the function of these transporters and showed that 3D renal organoids can take up 6-CF in an inhibitor-sensitive way suggesting functional anion transporters. Similarly, ASP uptake was seen in proximal tubular structures in the 3D organoids and was inhibited with TPA in a dose dependant manner which reflects physiological function of organic cation transporters in this model.

The presence of functional proximal tubular transporters in renal organoids makes them a promising tool in regenerative medicine; which could probably be used to develop cell-based bioartificial kidney capable of removing anionic and cationic uremic toxins thus improving the currently available dialysis procedures (Jansen *et al.*, 2015; Masereeuw and Stamatialis, 2017a; Oxburgh *et al.*, 2017), or they could be used to engineer human embryonic kidney with one collecting duct tree and organised cortex and medulla which, if achieved, could be transplanted into a host to allow its maturation into a replacement organ (Davies and Chang, 2014), however, in the current situation, the use of hiPSCs-derived renal cells for detecting nephrotoxicity could be more realistic and of a great impact. So, in the next chapter, I aim to evaluate renal-differentiated cells as a potential model to detect nephrotoxicity.

Next, I investigated the possibility of cryopreserving differentiated cells without losing the ability to express key renal proteins and showed that the thawed cells after few

days in culture were able to make renal organoids with positive expression pattern to different segments of the nephron and to the UB/CDs. To my knowledge, the ability to cryopreserve renal differentiated cells has never been investigated before. I reported that treatment with ROCK inhibitor for 24 hrs post thawing was critical for the revival of the cells as cells did not revive in its absence and underwent apoptosis. The importance of ROCK inhibitor to prevent dissociation induced apoptosis has been shown in different applications that involves stem cell dissociation including passaging and cryopreservation (Watanabe *et al*., 2007; Kurosawa, 2012; Claassen, Desler and Rizzino, 2009). It has also been shown to be important for the survival of dissociated renal progenitors cells (Unbekandt and Davies, 2010). Reports have also shown its importance for successful cryopreservation of hiPSC-derived cardiomyocytes (Kim *et al.*, 2011; Xu *et al.*, 2011), hiPSC-derived neural progenitors (Nemati *et al.*, 2011) and hiPSC derived brain endothelial cell progenitors (Wilson *et al.*, 2016). Here, I reported that ROCK inhibitor is similarly important for successful cryopreservation and reviving of hiPSC-derived renal progenitors.

I showed that cells frozen after 12 days of differentiation were able to revive, maintained their capacity to self-organise making tubular structures which showed positive markers for different segments of the nephron and for the collecting ducts, and possessed organic anion and cation transport-ability. Cells were cryopreserved, and successfully revived, for up to one year.

Importantly, organoids made from cryopreserved renal progenitors were able to detect cisplatin toxicity by increasing the apoptotic marker Caspase3; the toxic effect of cisplatin was manifest at 5 µM dose treatment. This was comparable to what other studies have shown (Takasato *et al.*, 2015; Bajaj, A. David Rodrigues, *et al.*, 2018), and was much more sensitive than what has been shown in a recent study performed on hPSC-derived renal organoid and detected cisplatin induced apoptosis at 16 µM dose treatment (Czerniecki *et al.*, 2018). Additionally, I have demonstrated that 18 days differentiated cells could be dissociated and cryopreserved. However, I have to clarify that I investigated cryopreserving the cells after 12 days of differentiation more thoroughly than cryopreserving them after 18 days of differentiation. For the latter, I cryopreserved only one run of differentiated cells and successfully revived them on three different occasions.

Employing cryopreserved cells for nephrotoxicity screening can save time, and effort, allow for high throughput analysis and streamline the use of these cells for drug discovery purposes. Yet, wide scale assessment of the ability of the cryopreserved cells to detect different toxic compounds is still needed.

Chapter 5

5 Use of renal organoids in predicting nephrotoxicity:

5.1 Introduction:

The primary role of renal cells is eliminating various drugs, metabolites and toxins; in addition, the high renal blood flow results in a high rate of toxicant delivery to the kidney, making renal cells highly vulnerable to different forms of injury and toxicity (Perazella, 2009; Pazhayattil and Shirali, 2014). Drug-induced nephrotoxicity is a serious adverse effect of various categories of drugs. Based on the mechanism of toxicity of individual drugs, the damage can affect glomeruli, tubules, vascular cells or interstitial cells and can manifest as acute or chronic functional affection (Awdishu and Mehta, 2017).

Drug research and development goes classically through different steps where the potential compound is first tested in in-vitro 2D cell cultures, then further assessed in experimental animals and finally, it has to proceed through phase I to phase III clinical trials in human before being available for widespread clinical use in markets (Davies, 2018). Until recently, the potential of drug-induced nephrotoxicity has conventionally been tested both in animal models (Gautier *et al.*, 2010, 2016; Harpur *et al.*, 2011) and monolayer cell cultures either of primary cell cultures or cell lines (Huang *et al.*, 2015). Experimental animals for testing toxicity, despite providing an in-vivo multi-organ complex system for assessing drugs, have one major drawback for their use, which is interspecies differences in vulnerability to toxins. Only a small percentage of drugs that reach to phase I clinical trials eventually succeed to proceed to marketing and become available for widespread use (Seruga *et al.*, 2015; Miranda *et al.*, 2018). While cell cultures are an alternative to the use of animals in drug screening, 2D cultures lack the in-vivo complexity where interaction between different types of cells contribute to the effect of the drug (Davies, 2018; Elhendawi and Liu, 2018; Miranda *et al.*, 2018). Also, some of the immortalised proximal tubular cell lines that are used to screen for nephrotoxicity lack certain anion and cation drug transporters (Jenkinson *et al.*, 2012) which makes them less predictive for toxicity.

There is therefore an increasing interest in the use of renal organoids, being a miniature renal tissue, as a model for high throughput compound screening for nephrotoxicity. Some recent reports have demonstrated a predicted response of iPSCs-derived proximal tubules (Kandasamy *et al.*, 2015) or iPSCs-derived

multicellular renal organoids (Bajaj, A David Rodrigues, *et al.*, 2018) to known nephrotoxic compounds.

In this section, I wanted to evaluate the ability of renal-differentiated cells to detect nephrotoxic compounds. Because the anatomical complexity of organoids can be problematic as it makes obtaining a simple quantitative response to toxic stimuli challenging, I address this problem by exploiting a nephrotoxicant-stimulated fluorescent reporter system to screen for toxic compounds in renal organoids.

5.2 Gentamicin treatment and RNA-seq experiment:

The Aminoglycoside family of antibiotics is mainly active against gram-negative bacteria; Gentamicin and Tobramycin are two commonly prescribed members of this family. Nephrotoxicity and ototoxicity are the most serious side effects associated with aminoglycoside exposure; renal injury manifest in the form of non-oliguric acute renal failure with different degrees of tubular dysfunction. Decrease in glomerular filtration rate can occur later after 5-7 days of treatment (Begg and Barclay, 1995).

Aminoglycoside-induced toxicity mainly targets proximal tubular cells (Moestrup *et al.*, 1995). The drug filters freely through the glomeruli then accumulates inside the proximal tubular cells through an apical uptake pathway that is different from the transport via anion and cation transporters. Aminoglycoside drugs are polybasic compounds, they bind to an apical anion phospholipid, Megalin, which is a multi-ligand endocytic receptor that mediates their endocytosis (Moestrup *et al.*, 1995). Physiological Megalin ligands include low molecular weight proteins that filter through the glomeruli such as transthyretin, insulin, vitamin D binding protein, retinol binding protein, α1-microglobulin and β2-microglobulin; it is highly expressed in the proximal tubules and mice deficient in Megalin receptor experience low-molecular-weight proteinuria (Nielsen *et al.*, 1995; Christensen and Willnow, 1999; Leheste *et al.*, 1999; Christensen and Birn, 2001; Schmitz *et al.*, 2002). Schmitz et al demonstrated that Megalin mediated endocytosis is the principal pathway for renal aminoglycoside accumulation and that Megalin knockout mice are protected against renal aminoglycoside accumulation and nephrotoxicity (Schmitz *et al.*, 2002). Inside the cell, the aminoglycoside is translocated into lysosomes where it inhibits the function of

lysosomal enzymes and causes accumulation of damaged organelles and membrane fragments in the form of myeloid bodies (Quiros *et al.*, 2011).

5.2.1 The aim of this experiment was:

- To evaluate the expression of different proximal tubular transporters and receptors. The expression of these transporters and receptors is critical for renal drug uptake and toxic response.

- To test the response of the cells to aminoglycoside and whether that response matches the pre-known nephrotoxic effect of aminoglycoside

- The main aim of this experiment was to find a potential marker that could be used to report toxic insults in renal-differentiated cells through analysing the differentially expressed transcripts, between control untreated renal cells and gentamicin-treated cells, and identifying a highly expressed injury marker. Engineering an iPSC line to report the expression of this marker would enable the production of injury reporting renal cells.

5.3 Results:

In this experiment RNA-seq was performed for three groups of 2D renal-differentiated cells: control group (untreated) and two treated groups of different concentrations; 1 mg/mL (low concentration treated group) and 4 mg/mL (high concentration treated group).

5.3.1 Analysing gene expression data obtained from the control group:

I first used the gene expression data obtained from the control samples to examine the expression of important proximal tubular receptors; the endocytic receptor Megalin and the closely associated receptor Cubilin were both expressed in the untreated samples. Megalin and Cubilin are the main endocytic receptors involved in Gentamicin uptake into proximal tubular cells and the response of the cells to gentamicin is dependent on their expression and function (figure 5.1). I also used the RNA-seq data to examine the expression of the different proximal tubular transporters. *OAT1*, and *3*, were both not detected in the three tested control samples, however, *OATP4C* was

expressed which still could work as an entry site for anionic drugs and toxins. *OCT2* was either not expressed or detected in low levels.

MRP 2 and *4*, which are the major apical transporters that mediate efflux of anions into the urine, were both expressed. *MATE1*, *OCTN1* and *2*, and *P-gp*, the main cation efflux transporters on the apical membrane, were also expressed (figure 5.1).

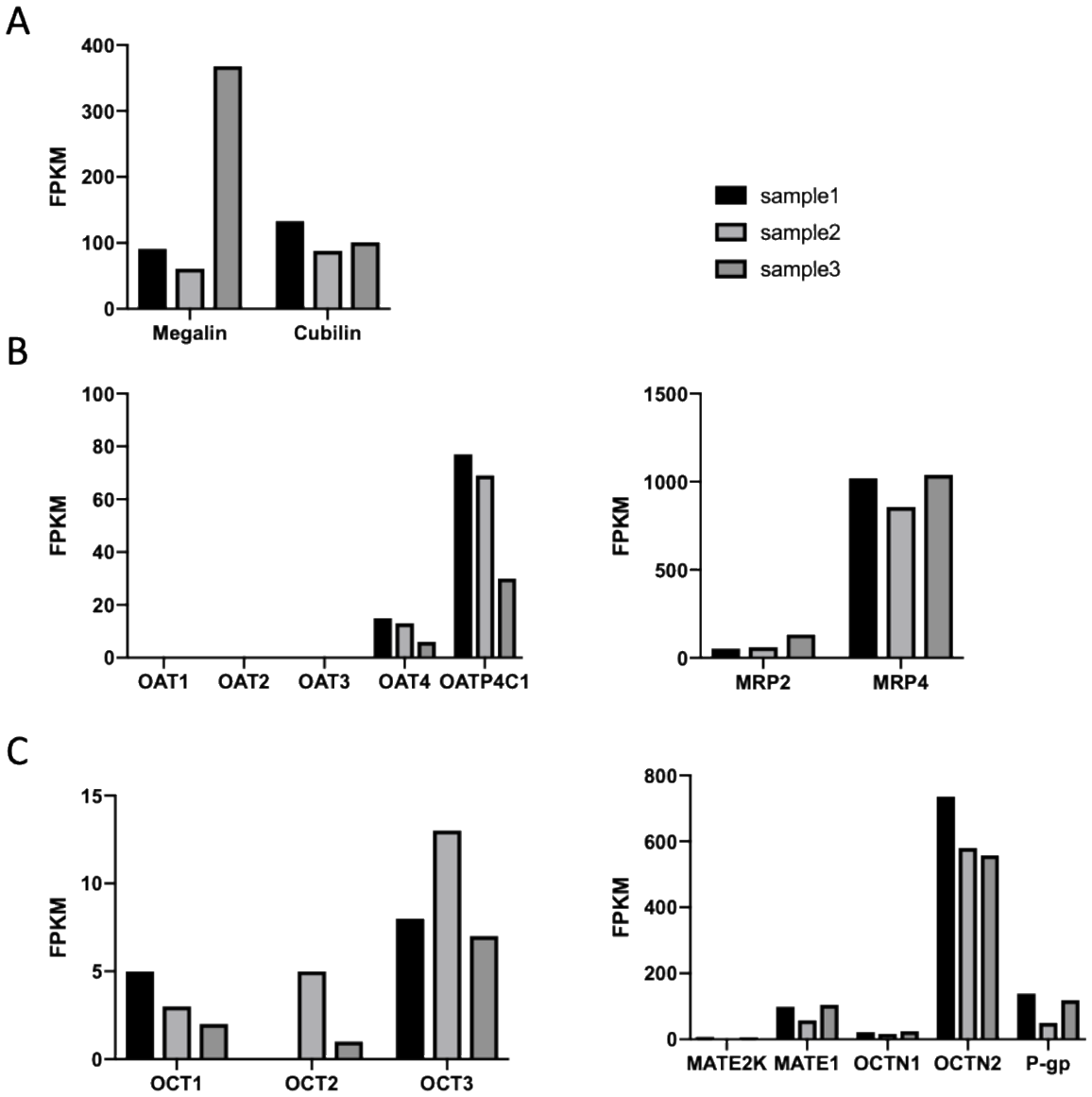

Figure 5.1. The expression of important proximal tubular receptors and transporters in untreated renal-differentiated cells by RNA-seq transcript analyses. A) Expression of the endocytic receptors Megalin and Cubilin. B) Expression of the anion transporters. C) Expression of the cation transporters. FPKM: Fragments Per Kilobase of transcript per Million mapped reads.

My previous RT-PCR results suggested that *OAT1* and *OCT2* were expressed in 3D organoids but not in the 2D differentiated cells; the result of gene expression obtained from the RNA-seq was consistent with the previous RT-PCR results which confirmed the absence of these transporters in the 2D cultures (or, in the case of *OCT2*, presence in low levels in some of the samples). As discussed before *OAT1*, *OAT3* and *OCT1* are the main anion and cation transporters expressed on the basolateral membrane of proximal tubular cells; they mediate the first step of tubular secretion for many drugs, toxins and metabolic waste products by transporting them from the blood to the tubular cells and their absence in the 2D cultures could affect their ability to detect the toxicity of some substrates (for more details see chapter 4). However, the results of the RNA-seq showed that other important renal transporters were detected in the 2D renal-differentiated cells (*OATP4C1*, *MRP2*, *MRP4*, *MATE1*, *OCTN1*, *OCTN2*, *P-gp* and *BCRP1*).

5.3.2 Analysing differentially expressed genes between the control group and the low-dose gentamicin-treated groups:

I next looked at the differentially expressed genes in response to gentamicin treatment in two different contrast groups (the low treated group versus the control group and the high treated group versus the control group). After applying a stringent FDR cut-off of 0.05 there were no genes detected to be expressed significantly different between the low-treated group and the control group. However, when setting a less stringent FDR cut-off, 0.1, there were 14 significantly upregulated genes in that contrast. Setting an FDR cut-off of 0.1 increases the possibility of detecting false positive genes (1.4/14 genes would be expected to be false positive), however, my aim was not to analyse the individual upregulated genes but rather to evaluate the overall response of the treated cells based on a cluster analysis of the upregulated genes; having upregulated cluster of gene involved in particular biological process or molecular function will be more significant than looking at the individual genes.

After endocytosis, aminoglycosides accumulate inside the lysosomes, Golgi apparatus and the endoplasmic reticulum (Silverblatt and Kuehn, 1979; Giurgea-Marion *et al.*, 1986; Sandoval and Molitoris, 2004). The aminoglycoside drug causes lysosomal phospholipidosis as it binds to phospholipids and inhibits the function of the phospholipase enzyme; it also causes deposition and accumulation of polar lipids in a

multi-lamellar way known as myeloid bodies, the enlarged lysosomes then rupture with subsequent release of the myeloid bodies into the cytoplasm (Silverblatt, 1982). The accumulation of the aminoglycoside in the endoplasmic reticulum can cause endoplasmic reticulum stress which initiates unfolded protein response and arrest in the cell cycle (Zhang *et al.*, 2006). It has also been shown that gentamicin binds to calreticulin affecting its chaperon activity for correct protein folding (Horibe *et al.*, 2004). At certain concentration, aminoglycoside leaks outside the lysosomes where it acts on the mitochondria and triggers cytochrome C mediated intrinsic pathway of apoptosis, which disrupts electron transport and ATP production and results in the production of reactive oxygen species (Servais *et al.*, 2006; Morales *et al.*, 2010). Lysosomal cathepsins escape into the cytoplasm and also activate the intrinsic pathway of apoptosis and necrosis in higher concentrations (Schnellmann and Williams, 1998) (Quiros *et al.*, 2011; McWilliam *et al.*, 2017).

When the upregulated genes were used in gene ontology (GO) term analysis, using Panther overrepresentation test (http://www.pantherdb.org), they were linked to relevant GO terms (detoxification of inorganic compounds, response to endoplasmic reticulum stress, response to unfolded protein, protein refolding, cellular response to stress etc) (table 5.1). As shown from the GO term enrichment analysis, there was enrichment in the GO terms linked to endoplasmic reticulum stress and unfolded protein response which suggested an early response to gentamicin detected at this concentration,1 mg/mL. The upregulated genes in the low-treated group versus the control group were further upregulated with higher significance in the high vs control contrast which further suggests the significance and relevance of the upregulated genes (table 5.2).

Table 5.1. Panther Gene Ontology term enrichment analysis for the 14 upregulated genes when comparing the low dose-treated group to the control cells.

GO biological process complete	REFLIST	upregulated genes (14)	expected	fold Enrichment	FDR
chaperone-mediated autophagy (GO:0061684)	4	2	0	> 100	4.41E-03
negative regulation of inclusion body assembly (GO:0090084)	11	2	0.01	> 100	1.74E-02
protein refolding (GO:0042026)	22	4	0.01	> 100	3.18E-06
stress response to metal ion (GO:0097501)	18	3	0.01	> 100	3.48E-04
PERK-mediated unfolded protein response (GO:0036499)	12	2	0.01	> 100	1.96E-02
chaperone cofactor-dependent protein refolding (GO:0051085)	31	5	0.02	> 100	8.54E-08
'de novo' posttranslational protein folding (GO:0051084)	37	5	0.02	> 100	1.54E-07
detoxification of copper ion (GO:0010273)	16	2	0.01	> 100	2.99E-02
stress response to copper ion (GO:1990169)	16	2	0.01	> 100	2.90E-02
'de novo' protein folding (GO:0006458)	41	5	0.03	> 100	1.77E-07
regulation of inclusion body assembly (GO:0090083)	17	2	0.01	> 100	3.15E-02
detoxification of inorganic compound (GO:0061687)	17	2	0.01	> 100	3.06E-02
regulation of cellular response to heat (GO:1900034)	45	5	0.03	> 100	2.39E-07
chaperone-mediated protein folding (GO:0061077)	59	6	0.04	> 100	1.06E-08
cellular response to heat (GO:0034605)	69	4	0.05	87.13	1.57E-04
response to unfolded protein (GO:0006986)	155	8	0.1	77.57	2.47E-10
response to topologically incorrect protein (GO:0035966)	175	9	0.12	77.3	7.43E-12
regulation of response to endoplasmic reticulum stress (GO:1905897)	79	3	0.05	57.08	1.22E-02
Endoplasmic reticulum associated protein degradation pathway (GO:0036503)	82	3	0.05	54.99	1.31E-02
cellular response to unfolded protein (GO:0034620)	119	4	0.08	50.52	9.85E-04
protein folding (GO:0006457)	220	7	0.15	47.82	1.31E-07
positive regulation of cellular protein catabolic process (GO:1903364)	138	3	0.09	32.67	4.32E-02
regulation of protein ubiquitination (GO:0031396)	194	4	0.13	30.99	4.84E-03
regulation of protein modification by small protein conjugation or removal (GO:1903320)	221	4	0.15	27.2	7.68E-03

response to endoplasmic reticulum stress (GO:0034976)	235	4	0.16	25.58	9.35E-03
regulation of cellular response to stress (GO:0080135)	661	8	0.44	18.19	3.99E-06
protein catabolic process (GO:0030163)	649	5	0.43	11.58	2.30E-02
cellular response to stress (GO:0033554)	1609	8	1.07	7.47	1.95E-03
response to organic substance (GO:0010033)	2840	10	1.89	5.29	1.06E-03
cellular response to chemical stimulus (GO:0070887)	2737	8	1.82	4.39	4.95E-02
Response to stress (GO:0006950)	3484	12	2.32	5.17	4.16E-05

Table 5.2. 14 genes significantly upregulated between the low gentamicin treated group and the control group when setting an FDR cut-off of 0.1 and their pattern of expression in the high treated group.

gene_name	Log_2 FC(Low vs Control)	FDR (Low vs Control)	Log_2 FC (High vs Control)	FDR (High vs Control)
INHBE	3.79984787	0.0638602	4.23778322	2.04E-05
MT1F	3.00769486	0.0795063	10.4795115	3.53E-07
MT1G	2.95685361	0.0638602	11.1376446	2.84E-06
HSPA1B	1.56376516	0.0644929	2.88661362	3.26E-05
HSPH1	1.5051937	0.056884	3.25824117	6.97E-05
HERPUD1	1.4915876	0.0739903	2.24188376	0.00013004
HSP90AA1	1.36179404	0.0638602	2.24736257	0.00043464
SLC1A4	1.35630098	0.0976128	2.73449285	2.04E-05
HSPA5	1.33756392	0.0638602	1.17364026	0.00071785
SDF2L1	1.27341455	0.0535053	1.04490022	0.00072075
DNAJB1	1.26359077	0.0646176	2.34979089	2.33E-05
MANF	1.24856294	0.0535053	1.31794135	0.00048054
HSPA8	1.09427653	0.0795063	1.36458984	0.00011121
PDIA4	1.08036286	0.0638602	0.64442267	0.00084008

5.3.3 Analysing differentially expressed genes between the control group and the high-dose gentamicin-treated groups:

Applying an FDR cut-off of 0.05 (for statistical significance) and a fold change cut-off of 2 (for biological importance) there were 2221 upregulated genes and 1770 downregulated genes in the high treated versus the control contrast. To analyse the upregulated genes comparing the high treated group to the control group, I first filtered

the genes by the lowest FDR and then selected the 100 most upregulated genes. I next used these genes to perform GO term enrichment analysis using the PANTHER Over-representation test. The GO terms of the enriched genes included classes highly relevant to toxic insults, including response to toxic substance, detoxification, regulation of cell death, cellular response to stress, response to unfolded and misfolded proteins, chaperone mediated protein folding and chaperone cofactor-dependent protein refolding (table 5.3).

The GO terms linked to the most upregulated genes clearly showed that the cells were exposed to toxic substance that caused injury. *INHBE* gene was one of the most upregulated genes (log fold change = 4.23, FDR = 2.04 -05) it encodes for a member of the *TGF-beta* superfamily. After proteolytic processing it generates inhibin beta subunit; inhibins have a role in regulating numerous processes, including proliferation and apoptosis, and could be upregulated in cases of ER stress (NCBI, 2018). Other genes involved in apoptosis signalling and apoptosis modulation were also highly upregulated including: *LTA*, *JUN, FOS*, *HRK*, *GADD45B*. The oxidative stress marker *HMOX1* was one of the 100 most significant upregulated genes (log fold change: 6.55; FDR: 0.00015) in that contrast (table 5.4).

The expression of *KIM-1*, a biomarker commonly associated with renal tubular necrosis was significantly increased when comparing the high treated group to the control (log fold change: 1.67; FDR: 0.03) and the expression of Megalin was significantly decreased (Log fold change = -3.62, FDR = 0.010) which could be explained as a protective mechanism to decrease the influx of the offending drug (table 5.4).

To find a potential marker that could be used as a reporter for injury and toxicity, I did functional classification, for the same 100 most significant upregulated genes comparing the high treated group to the control group, using PANTHER classification system. The six major gene ontology categories (biological regulation, cellular process, metabolic process, response to stimulus, binding and catalytic activity) were further analysed for the intersection between them to find a marker that can represent most of the toxicity response mechanisms. Two genes were common between the six groups: *TRIB3* (4.4 fold increase; FDR 2.15 x 10^{-5}) and *HMOX1* (93.84 fold increase; FDR 0.00014) (figure 5.2). Although *KIM1* and *NGAL* are highlighted as classical in-

vivo renal injury markers, reports on their suitability for in-vitro nephrotoxicity screening in cell culture model have been mixed. Adler and colleagues reported that KIM1 was not upregulated in response to injury using HPTEC cells in both 2D cultures and 3D microfluidic-based cultures, while according to that study *HMOX1* was a more sensitive marker for predicting nephrotoxicity (Adler *et al.*, 2016). Similar results were obtained by Li et al who also used HPTEC cells and demonstrated either lack of response or low level of upregulation of *KIM1* and *NGAL* respectively (Y. Li *et al.*, 2013a). On the opposite side, Huang et al showed an increase in *KIM1* and other injury markers when exposed HPTEC cells, but not proximal tubular cell lines, to toxic compounds (Huang *et al.*, 2015) .

Table 5.3. Enriched GO terms when comparing the untreated group to the high gentamicin treated group (4 mg/ml) and analysing the 100 most significant upregulated genes.

GO biological process	Ref list	Most significant upreg genes	Expected	Fold Enrichment	FDR
detoxification of copper ion	14	8	0.07	> 100	4.25E-10
detoxification of inorganic compound	15	9	0.08	> 100	3.27E-11
detoxification	110	10	0.57	17.64	5.67E-07
response to toxic substance	482	17	2.48	6.84	5.71E-07
stress response to copper ion	14	8	0.07	> 100	3.40E-10
stress response to metal ion	16	9	0.08	> 100	2.54E-11
response to stress	3290	40	16.95	2.36	3.21E-05
cellular response to zinc ion	22	8	0.11	70.57	3.01E-09
PERK-mediated unfolded protein response	12	3	0.06	48.52	2.34E-03
cellular response to unfolded protein	118	7	0.61	11.51	1.20E-03
response to unfolded protein	154	10	0.79	12.6	9.07E-06
response to topologically incorrect protein	174	10	0.9	11.15	2.28E-05
cellular response to cadmium ion	36	9	0.19	48.52	2.25E-09
chaperone cofactor-dependent protein refolding	28	5	0.14	34.66	2.81E-04
chaperone-mediated protein folding	56	8	0.29	27.72	1.10E-06
'de novo' posttranslational protein folding	33	5	0.17	29.4	5.26E-04
protein refolding	21	4	0.11	36.97	
regulation of cellular response to heat	45	6	0.23	25.88	1.11E-04
regulation of cellular response to stress	654	12	3.37	3.56	3.31E-02
positive regulation of proteasomal ubiquitin-dependent	81	5	0.42	11.98	1.91E-02

protein catabolic process					
positive regulation of proteasomal protein catabolic process	102	5	0.53	9.51	4.72E-02
negative regulation of cell death	999	16	5.15	3.11	1.38E-02

Table 5.4. Important differentially expressed genes between the control and the High gentamicin treated group (4 mg/ml).

Gene name	Log_2 Fold change	FDR
Genes involved in apotosis		
LTA	3.873178046	0.000126499
HSPA1B	2.886613617	3.26E-05
JDP2	1.881787141	7.10E-05
HSPA1A	2.663259915	1.75E-05
HSPA6	5.205504565	3.52E-05
ATF3	3.080254651	0.000376849
FOS	3.87052057	0.00059826
JUN	1.372582654	0.022640799
HRK	3.327710653	0.001257237
The endocytic receptor Megalin		
Megalin	-3.618874339	0.010592678
Important renal injury markers		
KIM1	1.669097501	0.031340852
HMOX1	6.552266071	0.000147085
NGAL	-1.801403278	0.032333098

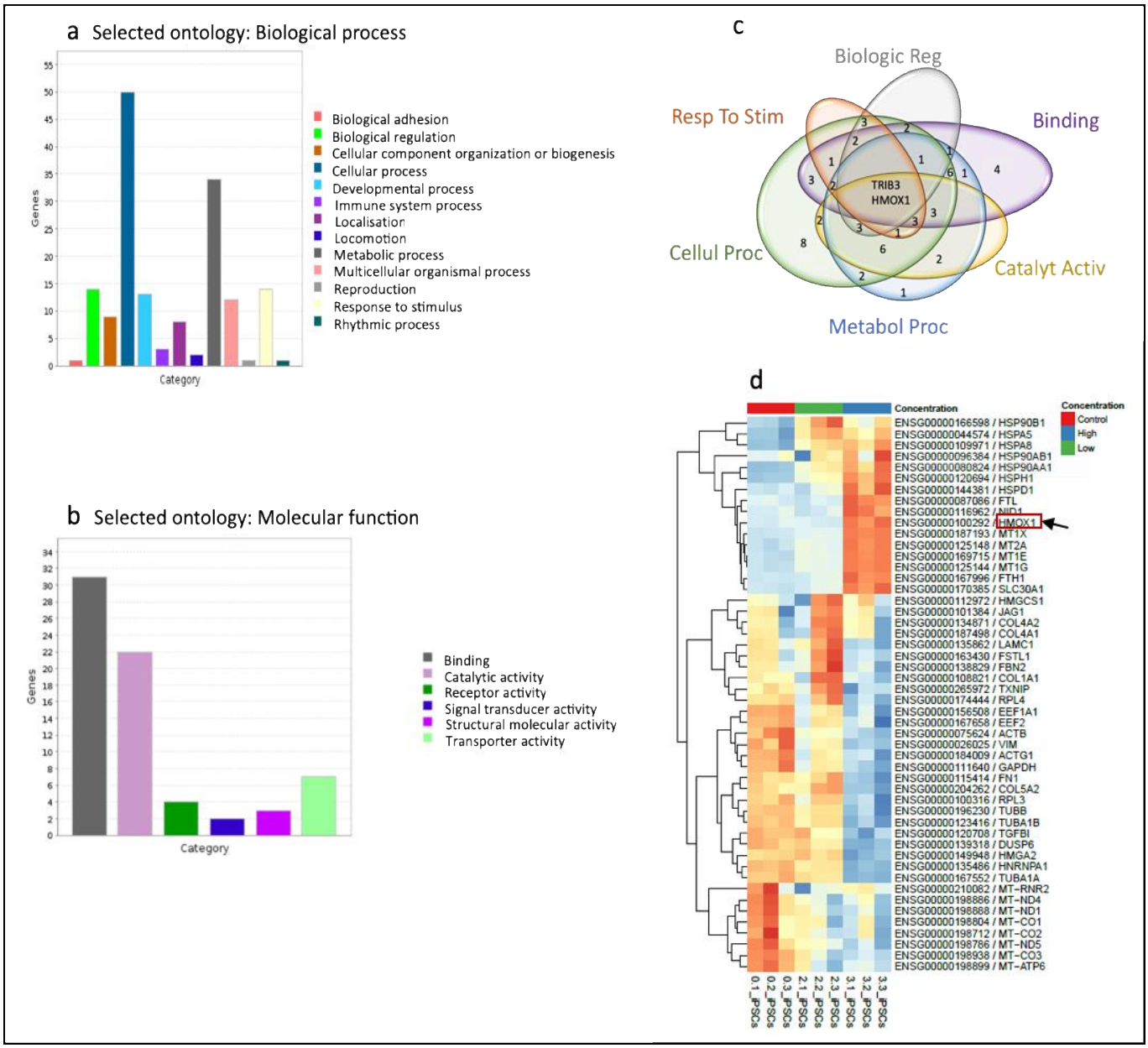

Figure 5.2. RNA-seq analyses of renal-differentiated hiPSCs treated with gentamicin (1mg/ml or 4mg/ml) or left untreated. a,b) Functional classification for the 100 most significant upregulated genes between the high gentamicin treated group and the control group using the biological process ontology (a) and the molecular function ontology (b). c) Venn diagram for the intersection between the six main categories of genes, obtained using the two different ontologies, showing *HMOX1* and *TRIB3* were common between the six groups (full details of the Venn diagram are shown in table 5.5). d) Heat map showing the 50 most variable genes when comparing the three groups together (untreated, low dose-treated and high dose-treated cells); *HMOX1* was one of the 50 most variable genes.

Table 5.5. Shows the detailed intersection between the six main categories of genes using GO classification

Names	total	elements
Binding MF, Biological Regulation BP, Catalytic Activity MF, Cellular Process BP, Metabolic Process BP, Response to Stimulus BP	2	TRIB3, HMOX1
Binding MF, Catalytic Act MF, Cellular Proc BP, Metabolic Process BP, Response to Stimulus BP	3	HSPA6, HSPA1B, HSPA1A
Binding MF, Catalytic Activity MF, Cellular Proc BP, Metabolic Process BP	3	ASNS, FKBP4, TSPYL2
Binding MF, Cellular Process BP, Metabolic Process BP, Response to Stimulus BP	2	INHBE, MSTN
Binding MF, Biological Regulation BP, Cellular Process BP, Metabolic Proc BP	1	HIST1H2AG
Binding MF, Biological Regulation BP, Cellular Process BP, Response to Stimulus BP	2	LRG1, EGF
Catalytic Activity MF, Cellular Process BP, Metabolic Process BP, Response to Stim BP	1	PPP1R15A
Biological Regulation BP, Catalytic Activity MF, Cellular Process BP, Metabolic Process BP	3	DIO3, GCLM, CES1
Binding MF, Cellular Process BP, Metabolic Process BP	6	SFPQ, PSPC1, GCM1, DNAJB1, ATF5, JDP2
Binding MF, Cellular Process BP, Response to Stimulus BP	1	LTA
Binding MF, Biological Regulation BP, Cellular Process BP	2	FTH1, FTL
Binding MF, Biological Regulation BP, Metabolic Process BP	1	ID2
Catalytic Activity MF, Cellular Process BP, Metabolic Process BP	6	UAP1L1, WARS, BAAT, HTRA3, B3GALNT2, ABCC3
Biological Regulation BP, Cellular Process BP, Response to Stimulus BP	3	CASS4, SLC30A2, GABRR2
Binding MF, Cellular Process BP	3	CHORDC1, TUBB3, AVIL
Binding MF, Metabolic Process BP	1	BRPF3
Catalytic Activity MF, Cellular Process BP	2	ME1, NEURL3
Catalytic Act MF, Metabolic Process BP	2	CHKA, ASPRV1
Cellular Process BP, Metabolic Process BP	2	SLC1A4, ZNF425
Binding MF	4	ZFAND2A, CNN1, SQSTM1, MRPL18
Cellular Proc BP	8	SLC38A10, SLC7A11, GATA2, MC1R, RRAD, SCFD2, MYH15, RASL11A
Metab Proc BP	1	ANXA1

5.4 Human iPSC HMOX-1 reporter cell line-derived renal cells to test for nephrotoxic compounds:

The RNA-seq experiment suggested *HMOX1* as a good marker for detecting toxicity, few other studies have also shown *HMOX1* as a sensitive marker for renal toxicity either in HEPTEC cells (Adler et al., 2016) or hiPSCs-derived renal organoids (Bajaj et al., 2018). In collaboration with other members in my lab and an industrial company, I used *HMOX1* reporter hiPCS cell line (the production of this line was done by an MSc student in our lab) that produces mCherry under the control of *HMOX1* promotor to blindly test the response of the renal-differentiated 2D and 3D cell models to different compounds. Before starting the compound screening experiment, the *HMOX1*-mCherry-hiPSC reporter cells were first evaluated for their ability to respond to hydrogen peroxide, an oxidative stress inducer that stimulates the production of HMOX1, both by quantifying the fluorescence, as an indication of mCherry production, and by measuring *HMOX1* expression using qPCR and comparing the results (this evaluation was performed by Dr. Melanie Lawrence; figure 5.3 a-c).

Next, I tested the ability of these cells to differentiate into renal cells, both in 2D and 3D formats, and evaluated the obtained cells for the expression of different specific renal markers using immunofluorescence staining to exclude that *HMOX1* targeting could have affected the ability of these cells to make renal organoids. the differentiated cells showed positive expression of the glomerular markers, WT1 and NPHS1; the proximal tubular markers, Jagged1 and LTL and the distal tubular marker, ECAD. Some of the tubules also showed co-expression of ECAD and GATA3 indicating ureteric epithelial structures (figure 5.3 d-g); collectively the data indicated that the targeting strategy did not affect the ability of the cells to differentiate into renal cells.

Afterwards the differentiated cells were treated with the known nephrotoxicant; cisplatin or gentamicin, in an increasing concentrations and the mCherry fluorescence was quantified and compared to the *HMOX1*-mRNA response to confirm that the reporter response matches the transcript expression response (this evaluation step was performed by Dr. Melanie Lawrence; figure 5.3 h-m).

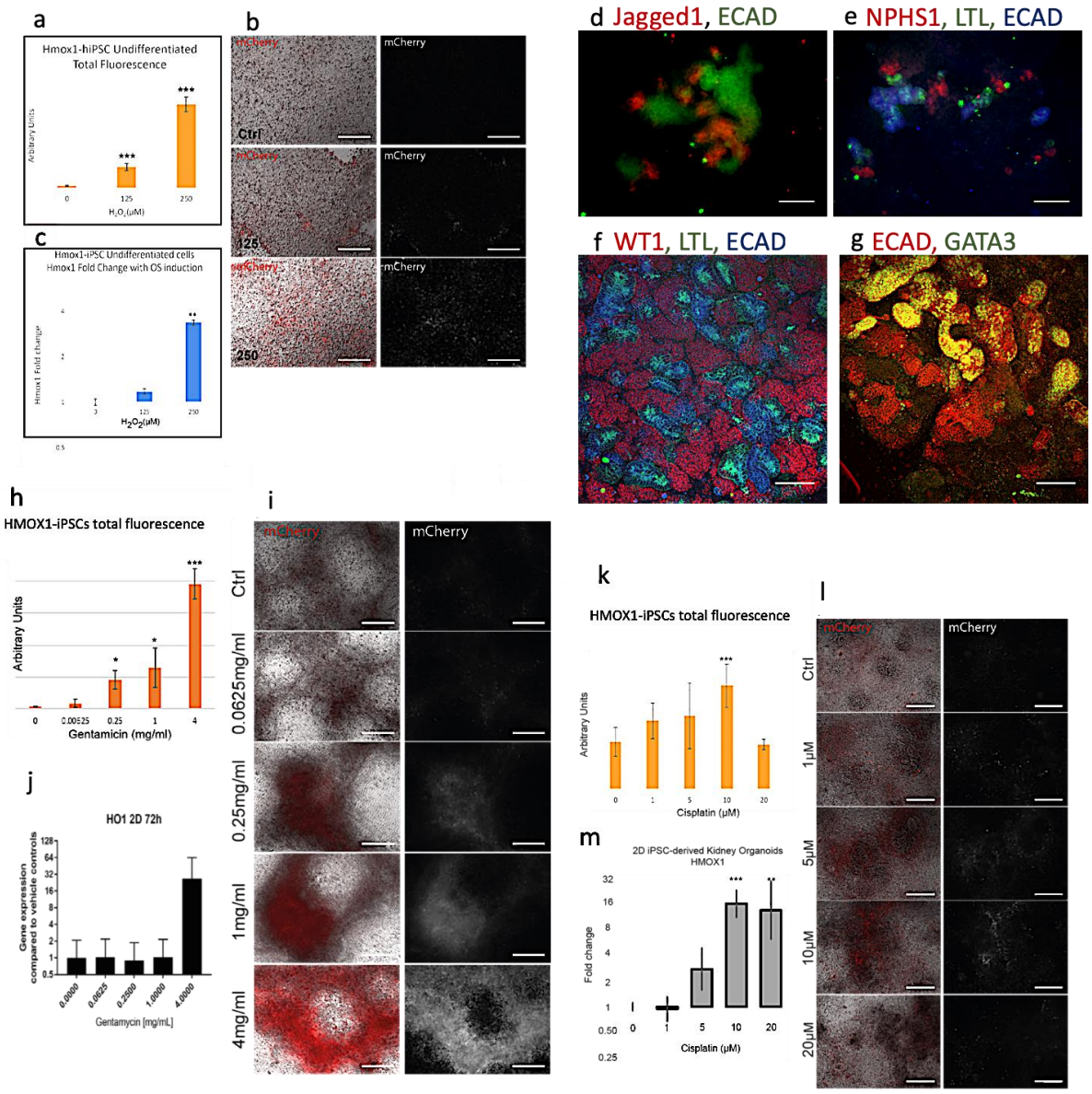

Figure 5.3. Verification of the reporting activity and the renal-differentiation ability of the *HMOX1*-mCherry-hiPSCs. a-c) The response of the undifferentiated *HMOX1*-mCherry-iPSCs to increasing concentrations of the known oxidative stress inducer hydrogen peroxide. a) Shows quantification of the total fluorescence in the treated cells compared to the control; b) representative images for the fluorescing cells; c) shows the fold change of *HMOX1* expression in the treated cells compared to the control using qPCR. d-g) The *HMOX1*-mCherry-iPSC reporter cells are able to differentiate into renal cells, as shown by the expression of renal markers, both in 2D (d, e) and 3D (f, g) differentiation forms. h-j) The response of 2D renal-differentiated cells to increasing concentrations of the known nephrotoxic drug gentamicin. h) The increase in fluorescence in response to the treatment; i) representative images for the treated cells; j) qPCR result showing the fold increase in *HMOX1* transcript level in response to gentamicin. k-m) The increase in *HMOX1* level in response to Cisplatin treatment using total fluorescence quantification of mCherry as an indicator of HMOX1 expression (k) and using qPCR to quantify the transcript level (m); l) representative images for the treated cells. Scale bars are 100 μm for d-g and 200 μm for the rest of the images.

5.4.1 Nephrotoxicity compound screening:

Renal cells derived from the HMOX1 reporter cell line were used to test a panel of blind-coded compounds, supplied by Collaborators in Sweden, for potential nephrotoxicity. *HMOX1*-mCherry-hiPSCs were differentiated for 21 days in two different formats, 2D cultures and 3D organoids. A four-fold dilution series of each compound was prepared, and *HMOX1*-mCherry-hiPS renal cells were incubated in these dilutions for either 24 hrs or 72 hrs (as some of the drugs could induce early toxic response while others could induce toxicity after prolonged exposure), then fluorescent images were taken. The images were quantified for total fluorescence as a measure of HMOX-1 expression in response to the different compounds. Compound screening and analysis of the fluorescent images were completed before revealing the nature of the compounds (figure 5.4 a and 5.4 b).

The 2D and the 3D models were both able to identify Dexamethasone as a benign compound that did not induce significant increase in fluorescence upon exposure to the drug for 24 hrs or 72 hrs.

Ketoprofen is a very widely used non-steroidal anti-inflammatory (NSAID) drug that can have detrimental effect on the renal function mainly through affecting renal blood flow (Catella-Lawson *et al.*, 1999; Whelton *et al.*, 2000; Harirforoosh and Jamali, 2009; Hörl, 2010); increase in fluorescence was detected only in response to the highest concentration tested of Ketoprofen.

Puromycin affects the post-translational modification of glomerular proteoglycans and downregulates its expression hence leads to thinning of the glomerular glycocalyx which affects the glomerular selectivity and leads to proteinuria (Björnson *et al.*, 2005; Jeansson *et al.*, 2009). Puromycin induced increase in fluorescence, both in 2D and 3D cultures, mainly in response to the highest concentration tested.

Cidofovir, an antiviral drug that has wide spectrum activity against DNA viruses, is transported to the proximal tubular cells through OAT1 transporter on the basolateral membrane and causes proximal tubular cell injury, apoptosis and acute renal failure (Ortiz *et al.*, 2005). Cidofovir induced significant increase in fluorescence in response to all tested concentrations after 72 hrs in the 2D model and a significant response

only to the highest concentration tested in the 3D cultures after 24 hrs; no significant response was noticed in the 2D cultures after 24 hrs or in the 3D cultures after 72 hrs.

Cisplatin and Ifosfamide are both taken into the proximal tubular cells through OCT2 transporter. Cisplatin is a chemotherapeutic drug, its enrichment in the proximal tubular cells, caused by the OCT2 transporter activity, leads to tubular cell apoptosis and necrosis (Ban, Hettich and Huguet, 1994); the nephrotoxic effect of Cisplatin is mediated by persistent inhibition of DNA synthesis and depletion of glutathion which results in lipid peroxidation, mitochondrial damage and oxidative stress (Kuhlmann, Burkhardt and Köhler, 1997; Huang *et al.*, 2001). Ifosfamide is an antineoplastic; inside the renal proximal cells Ifosfamide is oxidized into a toxic metabolite; chloroacetaldehyde (CAA) which causes Fanconi syndrome and proximal tubular dysfunction(Aleksa *et al.*, 2005; Nissim *et al.*, 2006). Both Cisplatin and Ifosfamide induced dose dependent increase in fluorescence in the 3D system both after 24 hrs and 72 hrs of exposure. The 2D system showed significant increase in fluorescence only in response to the highest concentration tested after 24 hr treatment of both drugs (384 µM for Cisplatin, 384 and 1536 µM for Ifosfamide); after 72 hrs of treatment the increase of fluorescence was significant for all tested concentrations of Ifosfamide and for the two highest concentrations of Cisplatin (96 and 384 µM). The 3D cultures showed significant increase in fluorescence in response to most of the tested concentrations.

Gentamicin showed increase in fluorescence in response to most of the tested concentrations in 3D cultures at the two evaluated time points; 24 hrs and 72 hrs post exposure. The 2D cultures showed dose related increase in fluorescence after 24 hrs exposure but after 72 hrs exposure the response was only significant in response to the 96 µM concentration.

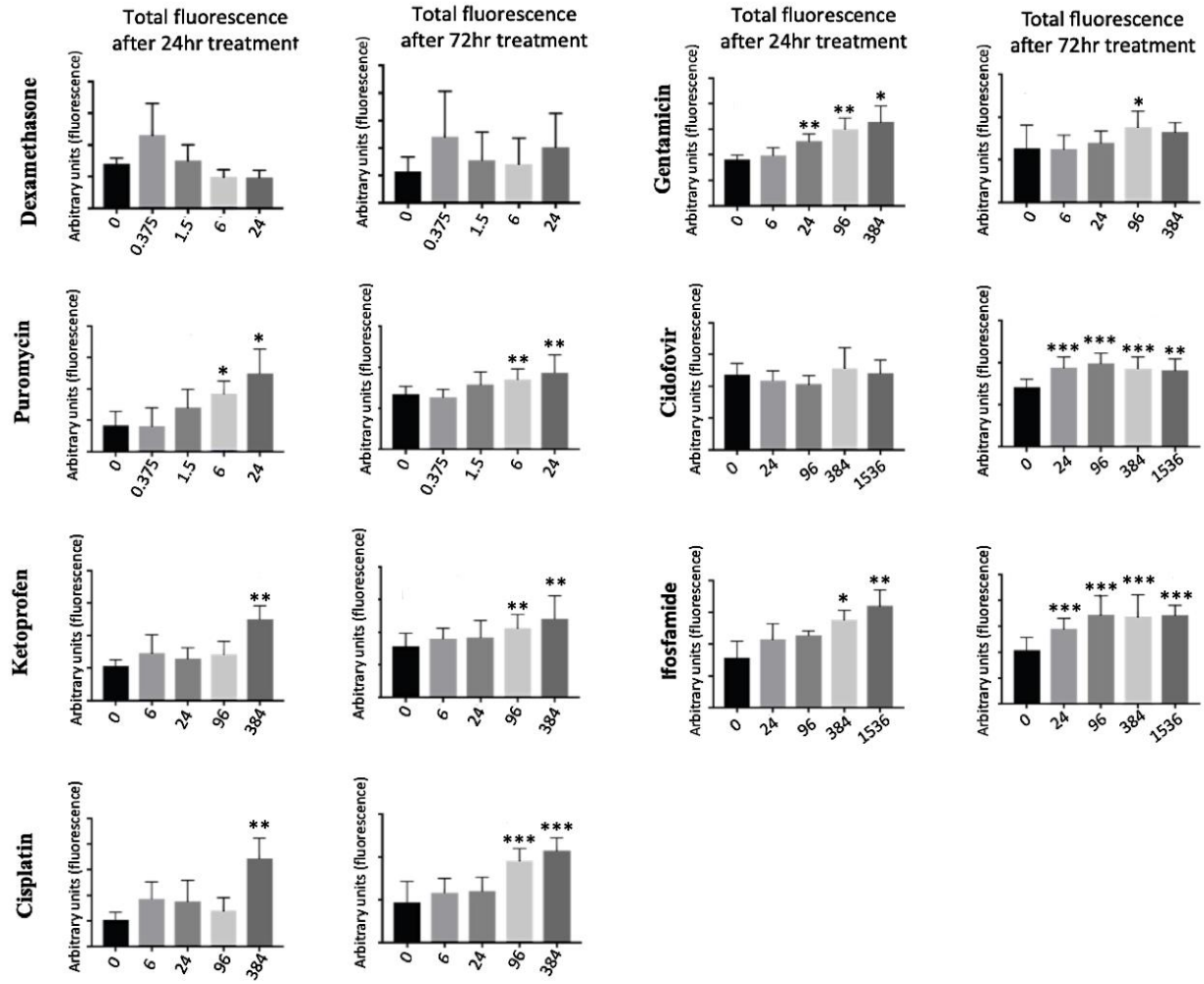

Figure 5.4 a. Compound screening for potential nephrotoxicity using 2D renal-differentiated cells derived from *HMOX1*-mCherry-hiPSC reporter cell line. 2D renal cells were treated with increasing concentrations of the indicated drugs, in a blind-coded way, for either 24 or 72 hrs followed by imaging and quantifying the total fluorescence in the mCherry channel (as an indicator of *HMOX1* expression). Each time-point was carried out as a separated experiment and included an untreated control. Drug concentrations are shown in µM. Significance of fluorescence intensity increase compared to the control was assessed using a T-test with Welch's correction. n=4 for each group in the 24-hr treatment and n= 10 for each group in the 72-hr treatment; data are presented as mean ± SD (p= * <0.05, **<0.01, ***<0.001).

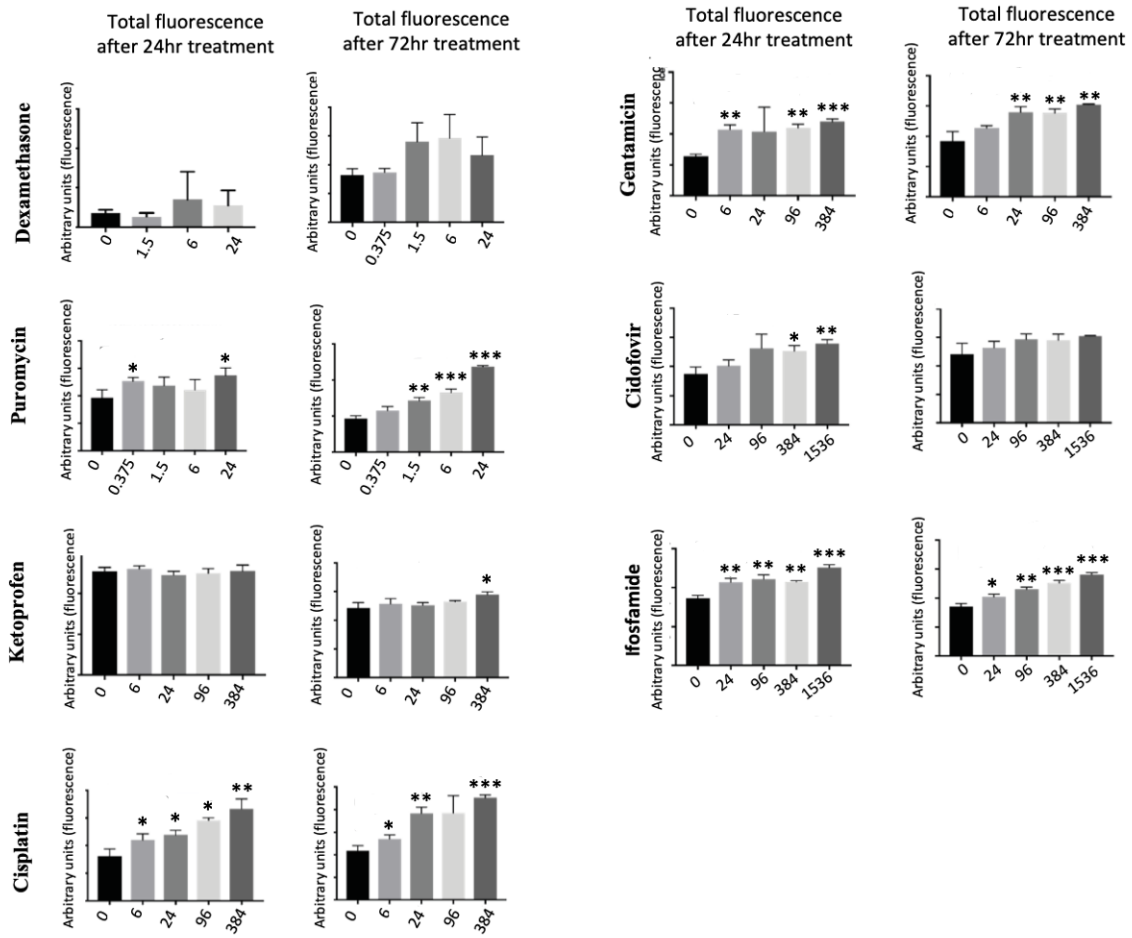

Figure 5.4 b. Compound screening for potential nephrotoxicity using 3D renal-differentiated cells derived from *HMOX1*-mCherry-hiPSC reporter cell line. Renal organoids were treated with increasing concentrations of the indicated drugs, in a blind-coded way, for either 24 or 72 hrs followed by imaging and quantifying the total fluorescence in the mCherry channel (as an indicator of *HMOX1* expression). Each time-point was carried out as a separated experiment; each experiment included an untreated control. Drug concentrations are shown in µM. Significance of fluorescence intensity increase compared to the control was assessed using a T-test with Welch's correction. n=3 for each group; data are presented as mean ± SD (p= * <0.05, **<0.01, ***<0.001).

5.5 Discussion:

Kidneys are at major risk of drug toxicity and so establishing high throughput models that can accurately predict nephrotoxicity is fundamental for drug development. An ideal platform for screening potential drugs and compounds is one that shows structural and functional similarity to human renal tissue (Adler *et al.*, 2016). I have shown in the previous chapters that the iPSCs-derived renal organoids show gene expression pattern similar to the developing human nephrons, I also showed that the 3D organoids expressed OAT1 and OCT2 and were able to transport fluorescent organic anion and cation substrates which suggested that they also share, at least in part, functional similarity to human renal tissue. To test the response of the renal-differentiated cells to detect nephrotoxicity 2D renal-differentiated cells were investigated for their response to gentamicin using RNA-seq. The reason for using 2D cultures in this experiment was that they could be easily adapted to high-throughput applications; in particular, early phases of compound screening necessitate a model that allow testing tens of thousands of compounds (Davies, 2018); in this regards the use of the 2D cultures has the advantage of being less time consuming, less expensive and could be applicable on larger scale compared to the 3D organoids as they could be obtained in 24 wells, 96 wells or even 384 well formats. The 2D cultures start by seeding the iPSCs as monolayers on Matrigel-coated plates, but later, upon differentiation, they develop structures and form tubules and so are not actual monolayers or 2D, but rather, they could be considered as pseudo 2D cultures.

Gene expression data, RT-PCR and RNA-seq, showed absence, or negligible levels, of OAT1 and OCT2 in the 2D renal-differentiated which probably suggests that the 3D cultures offer a better environment for the development of these transporters, however, RNA-seq data showed that other important proximal tubular transporters were detected in the 2D cultures including OCTN2, OAT4, OATP4c1, MATE1, MRP2, 4, and BCRP. In addition to the aforementioned transporters, the 2D cultures also showed expression of the endocytic receptors Megalin and Cubilin, both of which are highly expressed in the renal proximal tubules and have an important role in reabsorbing low molecular weight proteins that can filter through the glomerular barrier; in addition to rescuing the filtered protein these endocytic receptors also play a role in xenobiotic uptake into the proximal tubular cells and the toxic effect of gentamicin is mainly dependent on their expression and function (Christensen and

Birn, 2001; Quiros *et al.*, 2011). The ability of the renal-differentiated cells to detect nephrotoxicity is highly dependent on the expression of these transporters and receptors as they represent the entry site for a lot of drugs and toxic compounds. Although my data showed the detection of many proximal tubular receptors and transporters hiPSC-derived renal cells, performing qPCR to quantify their level of expression and to compare it to the physiological level is still needed.

Analysis of transcriptomic data obtained from gentamicin treated cells showed that cells exposed to 1 mg/ml drug concentration upregulated the expression of genes involved the response to endoplasmic reticulum stress, cellular response to unfolded and topologically incorrect proteins, and in the regulation of cellular response to stress. This reflected a typical image of early gentamicin toxicity. Other publications reported the toxic manifestations of gentamicin to be detected in cultured cells only upon treatment with doses above 1 - 2 mg/ml with apoptosis being the main response (Servais *et al.*, 2006; Pessoa *et al.*, 2009; Quiros *et al.*, 2011; Bajaj, A David Rodrigues, *et al.*, 2018); my results here suggest an early response to gentamicin in my cells, at 1 mg/ml, that mainly involved endoplasmic reticulum stress and unfolded protein response.

GO term enrichment analysis for the most significant most upregulated genes when comparing the high dose treated group (4 mg/ml) to the untreated group showed enrichment of highly relevant GOT: detoxification (18.30 fold enrichment), response to toxic substance (7.29 fold enrichment), PERK-mediated unfolded protein response (52.60 fold enrichment), cellular response to unfolded protein (12.07 fold enrichment), cellular response to topologically incorrect proteins (10.37 fold enrichment). In addition, the high dose treated cells highly upregulated genes involved in apoptosis signalling and regulation. Collectively, the data showed that the cells were able to detect gentamicin as nephrotoxic substance.

The purpose of the RNA-seq experiment was primarily to find a reporter of nephrotoxicity that could be engineered into hiPSCs, and then to assess the performance of that reporter using blind-coded test compounds. In my RNA-seq analyses, *HMOX1* was one of the 50 most variable genes between the three compared groups and functional classification for the most significant upregulated genes, between the 4 mg/mL group and the control group, showed that *HMOX1* could be a

potential useful marker to detect nephrotoxicity. *HMOX1* is ubiquitously expressed in cells but cellular injury caused by oxidative stress, proinflammatory response, exposure to heavy metals, hypoxia, and ischemia highly induces its expression (Agarwal and Bolisetty, 2013; Nath, 2014). Under oxidative stress conditions, hemeproteins release their heme group; free heme catalyses free radical production. *HMOX1* exerts a cytoprotective anti-apoptotic action via catabolizing the free pro-oxidant heme into iron, carbon monoxide and biliverdin thus preventing the free heme from inducing and sensitising cells to undergo apoptosis (Gozzelino, Jeney and Soares, 2010). *HMOX1* inhibition sensitises the cells to damaging agents by decreasing the antioxidative capacity of the cells; this property was used to increase the sensitivity of tumour cells to anti-cancer treatment (P. O. Berberat *et al.*, 2005; Pascal O Berberat *et al.*, 2005). Recent studies have highlighted *HMOX1* as a potential marker for detecting nephrotoxicity; in-vivo studies have shown the upregulation of *HMOX1* in the urine of patients with acute kidney injury and patients with tubulo-interstitial diseases (Yokoyama *et al.*, 2011; Zager, Johnson and Becker, 2012). Adler et al., performed a multiplexed gene expression profiling on HPTECs after exposing them to increasing concentrations of nine different nephrotoxicants plus a control of benign compound and showed that *HMOX1* significantly increased in response to increasing dose of six out of nine tested compounds and it was the marker that was able to detect the most of the nephrotixcants, compared to the other tested markers. The same study also has shown that increase in *HMOX1* in response to tubular toxicity is translatable to animal in-vivo toxicity models through computational digging in tow large rat toxicogenomic databases. Another very recent study has also demonstrated that *HMOX1* is a more sensitive marker for detecting renal tubular toxicity when compared to one of the conventionally used biomarkers; *KIM1*, in hESCs-derived renal cells *(Bajaj et al, 2018)*. Based on the intersection of *HMOX1* in several different toxicity pathways as well as its high level of upregulation, I identified *HMOX1* as a promising toxicity reporter.

An hiPSC-*HMOX1*-reporter cell line was developed and evaluated in our lab with the aim of its use in nephrotoxicity screening; Seven different compounds were used in blind compound screening for nephrotoxicity using 2D and 3D renal organoids that were derived from that cell line. The response to the compounds was evaluated by measuring total fluorescence in response to increasing concentrations of each

compound. Dexamethasone is a benign compound that does not cause nephrotoxicity (Y. Li *et al.*, 2013b; Kandasamy *et al.*, 2015); our model correctly identified it as non-toxic compound that did not induce significant increase in fluorescence. The response to Cisplatin and Ifosfamide was more manifest in the 3D cultures compared to the 2D cultures, which showed delayed response after 72 hrs of exposure or only response to the highest concentrations tested after 24 hr exposure. The uptake of these two drugs is mainly mediated by the OCT2 receptor which was detected in the 3D organoids but not in the 2D cultures; this might explain the earlier and more manifest response in the 3D cultures to these two compounds. The 3D model detected cisplatin toxicity at the first concentration tested (6 µM); that concentration was slightly higher than that shown in other hiPSCs-derived renal cells (Kandasamy *et al.*, 2015) which showed increase in IL6 and IL8 in response to 3.3 µM concentration, but was still either similar to what was used in a recent study that was using hPSCs-derived renal organoids (Bajaj, A David Rodrigues, *et al.*, 2018) or lower than those showed in other studies that used primary human proximal tubular cells (Jang *et al.*, 2013; Adler *et al.*, 2016); likewise the 3D model detected Ifosfamide toxicity at a concentration lower than that reported by a study that used primary human proximal tubular cells (Y. Li *et al.*, 2013a).

The response to the glomerular toxin Puromycin was in accordance to what was reported in Kandasamy et al, 2015 who showed increase in IL6 expression that first appeared in response to 1 ug/mL (3.3 µM) of puromycin and further increased in response to higher concentrations.

The gentamicin toxicity was detected at a lower concentration in this model compared to the gene expression data that were obtained from the RNA-seq experiment in which the response to gentamicin toxicity started to manifest in response to 1 mg/mL treatment. This might be because of the longer half-life of the mCherry protein compared to the *HMOX1* transcript; the mCherry protein reflects the cumulative activity of the promotor and the stability of the fluorescent protein and might not correlate well with the message stability (Snapp, 2009), thus it could accumulate and be detected in response to a lower concentration compared to the transcript.

Ketoprofen causes oxidative gastrointestinal injury and increase the risk of gastrointestinal ulceration (Cheng *et al.*, 2013); reports have also shown that NSAIDs

can rarely cause hepatotoxicity (Agúndez *et al.*, 2011; Sriuttha, Sirichanchuen and Permsuwan, 2018). NSAIDs could have toxic effects on the kidney especially when combined with other toxic compounds or conditions, e.g. their use in elderly, heart failure and diabetic patients, patients complaining of liver cirrhosis, or in combination with renin-angiotensin blockers or diuretics can increase the renal side effects of the drug (Harirforoosh and Jamali, 2009; Hörl, 2010). NSAIDs exert their effect by inhibiting COX1 and 2 enzymes both of which are expressed in the kidney. COX1 has role in controlling renal hemodynamics and GFR, while COX2 is implicated in salt water excretion (Catella-Lawson *et al.*, 1999; Whelton *et al.*, 2000; Weir, 2002). Therefore, inhibition of these enzymes could have adverse effects on the kidney. In our model, Ketoprofen induced increase in fluorescence only in response to the highest concentration tested.

Setting the statistical significance of predicting toxicity to a cut off of $p<0.01$ (considering higher p values to be non-toxic response), the overall performance of the *HMOX1*-mCherry-hiPSC-derived renal cells in predicting nephrotoxicity is summarised in table 5.6. As indicated in the table, no single combination of timing or culture form was completely reliable at predicting toxicity. 3D organoids were in general more sensitive, using them at both 24h and 72h and regarding a positive indication as one that is positive in at least one of these, was sufficient to identify the toxicity of all the blind-coded samples correctly.

Table 5.6. toxicity prediction based on the increase in fluorescence intensity.

Compound	2D 24h	2D 72h	3D 24h	3D 72h
Dexamethasone	N	N	N	N
Ketoprofen	Y	Y	N	N
Puromycin	N	Y	N	Y
Cisplatin	Y	Y	Y	Y
Gentamicin	Y	N	Y	Y
Cidofovir	N	Y	Y	N
Isofamide	Y	Y	Y	Y

Table 5.6: Y = predicted toxicity, N = did not predict toxicity. Green indicates results that are consistent with known clinical data. Prediction score is based on data in Figure 5.4 a and b. A p value of 0.01 or less for one or more of the treatment concentrations is designated as having predicted toxicity.

In conclusion, the reporter-hiPSC-derived renal organoids can predict renal toxicity, however, they are variable in their individual responses to compound treatment and certain culture form (2D or 3D) may be better suited to different classes of drugs. The

inherent variability of the iPSC-derived organoids may also have a role in these results and tackling this will be crucial for the future use of organoids in large scale drug screening. In addition, it is important to note that both the 2D and 3D renal organoids are closer to human embryonic kidneys than adult kidneys (Takasato *et al*., 2015); this immaturity may account for some of the differences between the observed response and the predicted one. Some compounds required longer incubation to induce a significant response via the oxidative stress pathway, this may be due to different mechanisms of toxicity of these compounds. Further investigations to identify the increase in fluorescence in particular renal compartments (podocytes, proximal tubules, distal tubules) may help to explain some differences in compound responses and may also be an additional useful tool to study mechanisms of toxicity. Collectively the data suggest that the *HMOX1*-reporting renal cells could be a promising tool for nephrotoxicity screening, yet further validation and optimisation of this model is required including testing a much larger set of compounds (both nephrotoxic and non-nephrotoxic) for better assessment of the system and its predictive power.

As briefly discussed earlier, renal drug transporters play a pivotal role in handling drugs and uremic toxins. We performed RNA-seq analysis and looked at the expression of the different drug transporters in our 2D differentiated cells. Transcriptomic data showed that 2D renal-differentiated cells expressed important drug transporters including MRP2 and 4, OCTN1 and 2, MATE1, P-gp and OATP4C, in addition to the expression of the important receptors LRP2 and CUBN. However other main transporters were not detected (OAT1 and 3, and OCT2). This matches with a recent study that evaluated transporter expression in renal organoids obtained from hESCs and repoted that OAT1 and 3, OCT2 were very lowly expressed while other tubular transporters were well represented (Bajaj, A. David Rodrigues, *et al.*, 2018). Importantly, OAT1 and OCT2 were both expressed in our 3D renal organoids which suggests that the 3D environment is needed for promoting the expression of these transporters in this culture model of renal cells.

Chapter 6

6 Steps towards organising renal organoids

6.1 Introduction

In 2010, Unbekandt and Davies showed that mouse embryonic kidneys, after being dissociated into single cell suspension and cultured in presence of ROK inhibitor (to inhibit dissociation induced apoptosis), were able to self-organize and form renal structures. Within these re-aggregated cells, UB progenitors developed into multiple collecting duct (CD) trees, around which nephron progenitors condensed and differentiated into different parts of the nephron (Unbekandt and Davies, 2010). While the renal organoids obtained by that way, 'Unbekandt-style renal organoids', are histologically similar to embryonic renal tissue, they lack the anatomical organisation of the kidney which is crucial for proper function; the normal anatomical organisation of the kidney allows a central ramified collecting system to convey urine to a single clear exit. Later on, that technique was modified to produce renal tissue arranged around

central branched collecting duct using a serial re-aggregation technique. This is a two-step process. The first step produces a Unbekandt-style renal organoid, containing multiple collecting ducts, while in the second step, only one of these collecting ducts is dissected and cultured with fresh MM to make engineered kidney tissue arranged around single CD, 'Ganeva-style renal organoid' (Ganeva, Unbekandt and Davies, 2011). More recently, a modification of that technique succeeded in reprograming one of the CD branches into an exit, a ureter-like structure that expresses the ureteric epithelial marker Uroplakin. This step increased the anatomical realism of renal organoids made from dissociated embryonic kidneys and yielded organoids that look much like foetal kidney (Mills *et al.*, 2017) (figure 6.1).

So far, renal organoids that we (or anyone else) can make from hiPSCs are more like Unbekandt-style renal organoids that are composed of multiple dispersed CDs connected to developing nephrons. I wanted to try to make more organised organoids that could be equivalent to Ganeva-style organoids. As explained earlier, a first step towards making this type of renal organoid would necessitate isolating a single UB structure to use it in a second-step aggregation with nephron progenitors, depleted from any other source of UB cells, so that we can obtain renal tissue in which nephrons connect to a single collecting system.

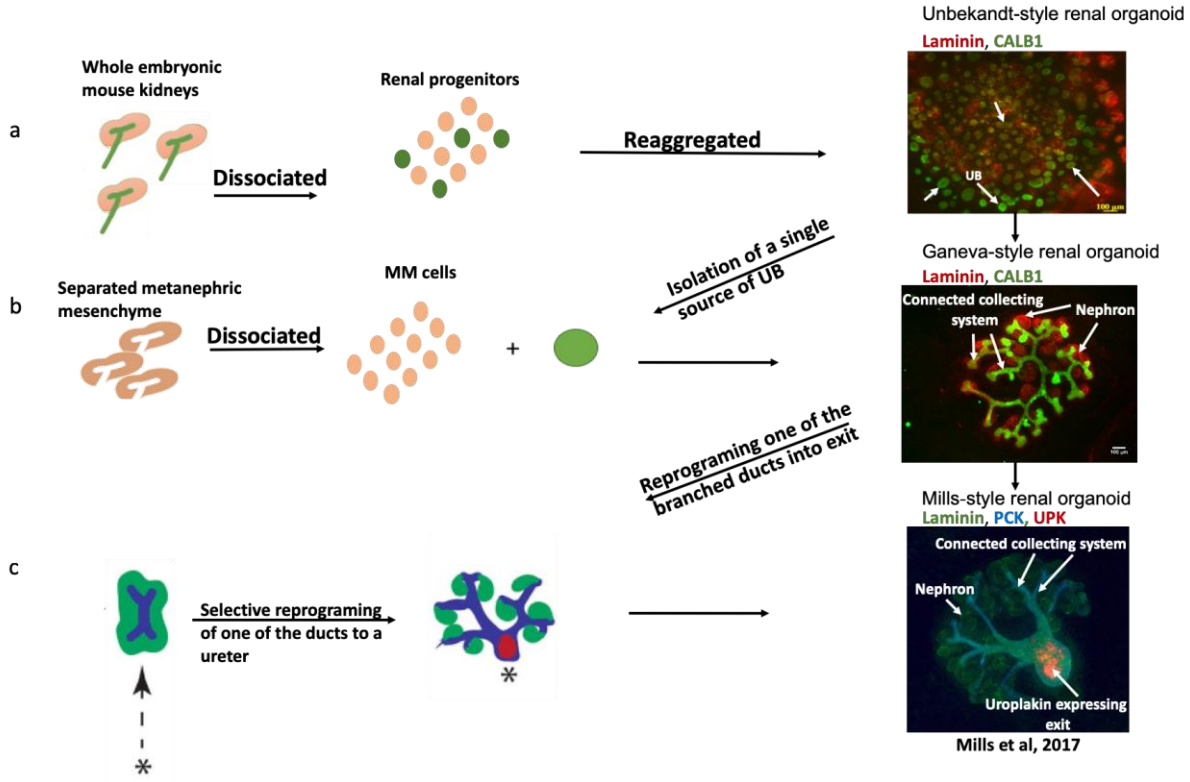

Figure 6.1. Illustrates the sequential steps of engineering organised renal tissue from mouse embryonic kidney cells. a) The first developed method to obtain renal organoids involved dissociation of mouse embryonic kidneys into single cells, re-aggregation of the dissociated cells and culturing them for few days. The result of that culture was renal tissue that has multiple non-connected collecting systems. b) Step 2 in engineering organised kidney tissue; one UB epithelial structure is isolated from the re-aggregates obtained from (a) after few days of culture and re-aggregated with fresh pure MM that has been depleted of its UB cells. That yields renal tissue with single connected collecting tree. C) Step 3 adding a single exit to organoids developed from (b) by reprograming one of the UB branches into ureter-like structure. UB: ureteric bud; MM: metanephric mesenchyme.

Developing more organised renal organoids could be useful for different applications: first, it would offer a model for studying the pathogenesis of different human disorders. Having the advantage that those renal organoids are obtained from the patient's own cells, they could even allow for developing new patient-tailored therapeutic modalities for various disorders. Second, it would provide better organoids for the use in nephrotoxicity screening and drug development. I have shown in the previous section that these organoids can perform some of the physiological function of the kidney and could be a promising tool for screening drugs for nephrotoxicity, yet they are equivalent to embryonic renal tissue, which could make them less predictive of toxic compounds, so finding a suitable environment that could potentiate their maturation is necessary.

A recent study has transplanted foetal human kidneys into adult rats and indicated that the transplanted kidneys showed a dramatic increase in size and maturation of function and were able to support the survival of the nephrectomised rats for an average of 122 days compared to 3 days for rats that did not receive transplant (Chang *et al.*, 2015); if we were able to organise renal organoids derived from hiPSCs and increase their anatomical realism in a way that resembles what we can currently obtain from dissociated mouse embryonic kidneys, Mills-style renal organoids, probably transplanting those organoids in an animal host could also allow for better maturation of the function and increase in the size and could provide an *in-vivo* human kidney model for drug testing and discovery. Third, a long term aimed application could be obtaining larger organised renal tissue that might hopefully, after allowing its maturation in a host, be of a clinical use as a transplantable organ. While this could be a very ambitious application and is quite unclear how feasible it would be, the individual steps towards developing more organised organoids could alternatively be combined with other different *in-vitro* kidney engineering strategies as these steps would involve isolation of pure population of renal cells which means that these cells could be used for populating decellularized scaffolds or bio-printing purposes for which obtaining pure specialised cells is a prerequisite (Kim *et al.*, 2015; Montserrat, Garreta and Izpisua Belmonte, 2016; Hueso *et al.*, 2019).

6.2 Aims:

The main aim of this chapter was to try to engineer an organised human renal tissue arranged around a single collecting tree, similar to Ganeva-style organoids that could be made from dissociated mouse embryonic kidneys but not, so far, possible to make from hiPSCs. To do this I wanted to:

- Develop and optimise a technique to isolate hiPSC-derived UB-like cells from the surrounding cells in renal organoids.

- Try to combine iPSC-derived UB, as a single intact epithelial structure, with nephron progenitors, derived also from hiPSCs, in a trial to obtain renal organoid organised around single ramified CD.

6.3 Engineering iPSCs to report *GATA3* expression using CRISPR-Cas9

One way to isolate the hiPSC-derived UBs would be to tag them using a UB marker in order to discriminate them from the surrounding cell types, thus enabling the use of FACS or manual dissection under a fluorescence microscope to select them. For this purpose, I wanted to engineer an hiPS cell line with a fluorescent reporter inserted into the *GATA3* locus, as a marker of UB structures. This would enable *GATA3* detection once it starts to be expressed and hence allow for the selection of the UB-like structures. A possible way to engineer the reporter cell line was to use the CRISPR-Cas9 technology.

CRISPR-Cas9 is a powerful gene-editing tool that employs the Cas9 nuclease activity under the control of gRNA (Brouns *et al.*, 2008; Marraffini and Sontheimer, 2008) to produce a targeted double-stranded DNA break (DSB) (Cong *et al.*, 2013; Mali *et al.*, 2013). Guide RNA (gRNA) is a short RNA segment composed of two parts: a scaffold sequence which binds to the Cas9 and a targeting guide sequence, also known as spacer sequence, which is specific to the target gene (Mali *et al.*, 2013) (figure 6.2 a). The Cas9 genomic target is identified based on the targeting sequence of its gRNA; after the expression of Cas9 enzyme, it complexes with the gRNA, through an interaction between the Cas9 and the scaffold domain of the gRNA, to make a riboprotein complex. That binding turns the Cas9 nuclease enzyme into its active-DNA binding form. Afterwards, the guide sequence of the gRNA localises the complex to its specific DNA target, via complementary base-pairing with the target sequence (figure 6.2 b). Binding of a protospacer adjacent motif (PAM), immediately adjacent to the genomic DNA target, directs the Cas9 nuclease to cleave the target DNA (Bolotin *et al.*, 2005; Deveau *et al.*, 2008) (figure 6.2 c). The produced targeted DSB stimulates repair mechanisms by one of two general pathways: error-prone Nonhomologous End joining (NHEJ) or Homology Directed Repair (HDR). The latter is used for introducing precise nucleotide changes, such as inserting reporter into the genomic target, by integrating exogenous repair template that contains sequence homology to the target site, via homologous recombination (Jinek *et al.*, 2012, 2013; Cho *et al.*, 2013; Mali *et al.*, 2013). For gene editing purposes using the HDR pathway, DNA repair template which contains the desired change is introduced to the cells together with the Cas9

and the gRNA. The repair template must have homology arms to the DNA target flanking the sought edit sequence. One important thing while designing the repair template is to mutate the PAM sequence, otherwise, the repair template becomes a target for the gRNA-Cas9 cleavage.

I designed the repair template plasmid for my experiment, to introduce a reporter under the control of the *GATA3* promotor, as separate segments that were meant to be assembled via Gibson cloning. Gibson assembly is a method to assemble overlapping DNA fragments through the action of three enzymes (5' exonuclease, DNA polymerase and ligase enzyme) into a one large DNA molecule; this reaction can combine multiple segments in one reaction provided that the segments have homologous overlapping sequences(Gibson *et al.*, 2009) (figure 6.2 d).

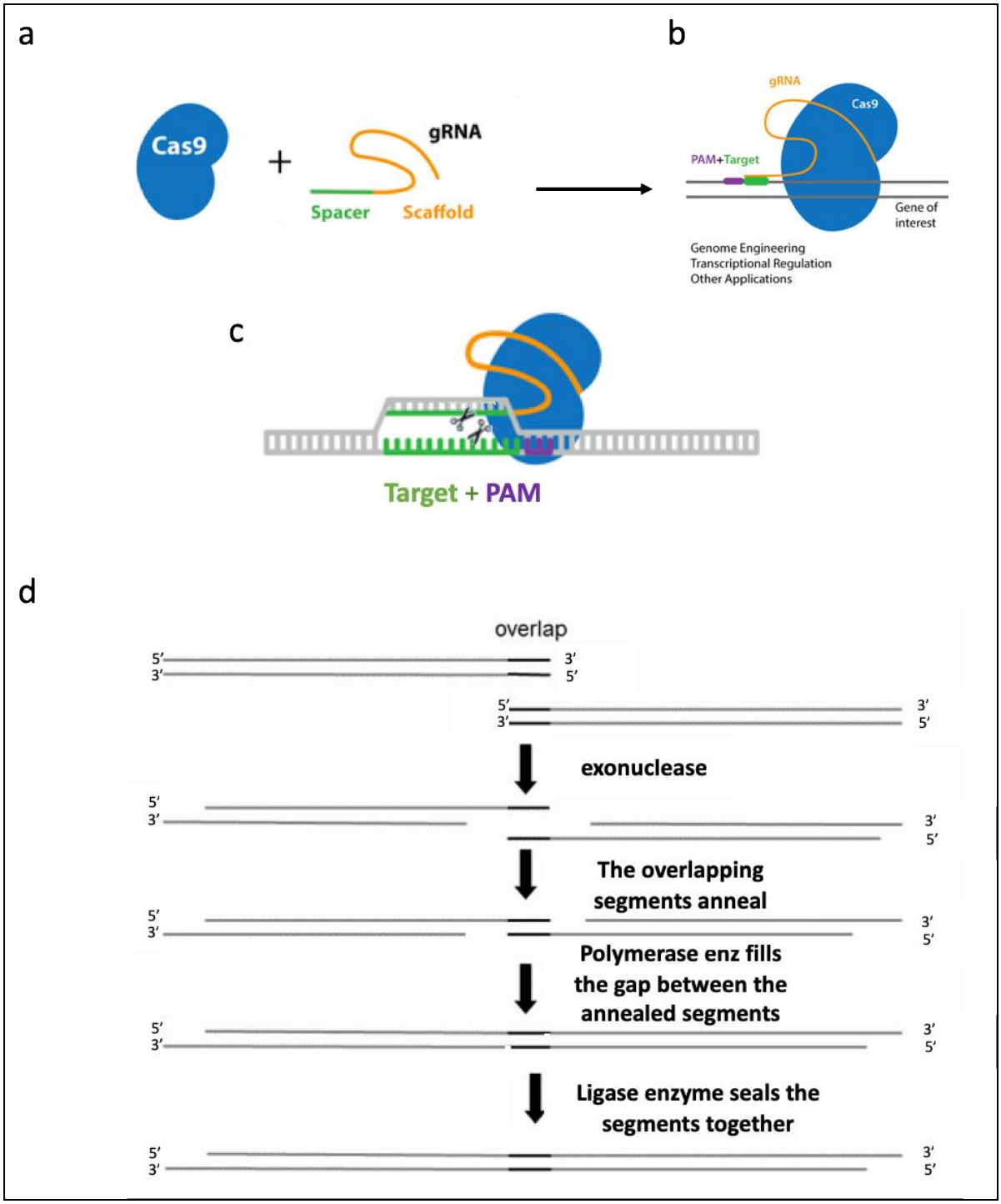

Figure 6.2. a-c) Illustration of the CRISPR/Cas9 targeting technique; the Cas9 enzyme binds to the scaffold sequence of the gRNA which changes the Cas9 into its active-DNA binding state, the target sequence (spacer sequence) of the gRNA then binds to its genomic target which must be immediately adjacent to a PAM sequence; the Cas9 enzyme cuts the DNA 3-4 bp upstream to the PAM; adapted from addgene.org. d) Illustrates Gibson assembly strategy to join segments with overlapping areas. PAM: protospacer adjacent motif.

6.3.1 Results:

6.3.1.1 gRNA design:

Two different gRNAs were designed (to be used separately so that I could choose the one which gives better results) and synthesized as gene blocks by IDT. For designing the gRNA, the *GATA3* genomic coding sequence (CDS) was obtained from Ensemble and 20 base-pair target sequence was selected close to the stop codon of the gene, using Zhang lab gRNA design resources (https://zlab.bio/guide-design-resources). The gRNA sequence was chosen to allow the Cas9 to cleave the *GATA3* genomic area close to the stop codon: 78 bp from the stop codon in case of gRNA1 and 26 bp in case of gRNA2. The chosen sequence was then incorporated into a DNA sequence that contains all components necessary for its expression and function (promotor, scaffold sequence and termination signal) (following the addgene gRNA synthesis protocol, https://media.addgene.org/cms/files/hCRISPR_gRNA_Synthesis.pdf) (Mali *et al.*, 2013); the whole sequence was sent to IDT for synthesis.

6.3.1.2 gRNA cloning and transformation:

The obtained gRNA gene blocks were cloned into a PCR-Blunt II-TOPO plasmid (https://media.addgene.org/cms/files/hCRISP_gRNA_Synthesis) and transformed into TOP10 bacterial strain; single bacterial colonies were selected from overnight-cultured bacterial plates (five single colonies for each of the two gRNAs) and checked for the incorporation of the gRNA gene block inserts by PCR (using M13 primers; their binding sites on the plasmid are indicated in figure 6.3 c) and gel electrophoresis. All selected colonies for gRNA1 and 4 out of 5 colonies for gRNA2 had the correct length segment (698 bp) suggesting successful cloning and transformation (figure 6.3).

One of the tested colonies for each of the two gRNAs was further amplified in an overnight culture and the plasmid DNA was purified, using Maxiprep, and analysed using restriction enzymes (EcoRI, cuts on both sides of the gRNA gene block insert giving 473 bp segment, which represents the gRNA insert, and 3501 bp segment, which represents the backbone; and SalI, which cuts in the plasmid backbone to give 3519 bp linear segment; figure 6.3 c). Gel electrophoresis was then performed, to analyse the restriction enzyme action, which showed the presence of the correct size

segments suggesting incorporation of the gene block insert into the plasmid backbone and successful amplification of the plasmid.

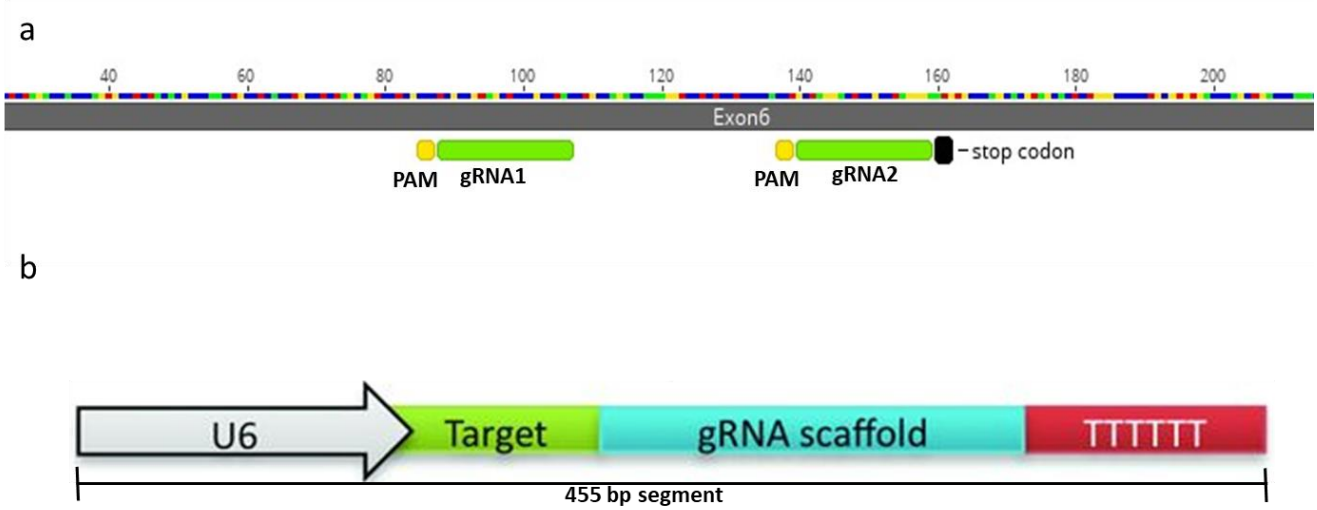

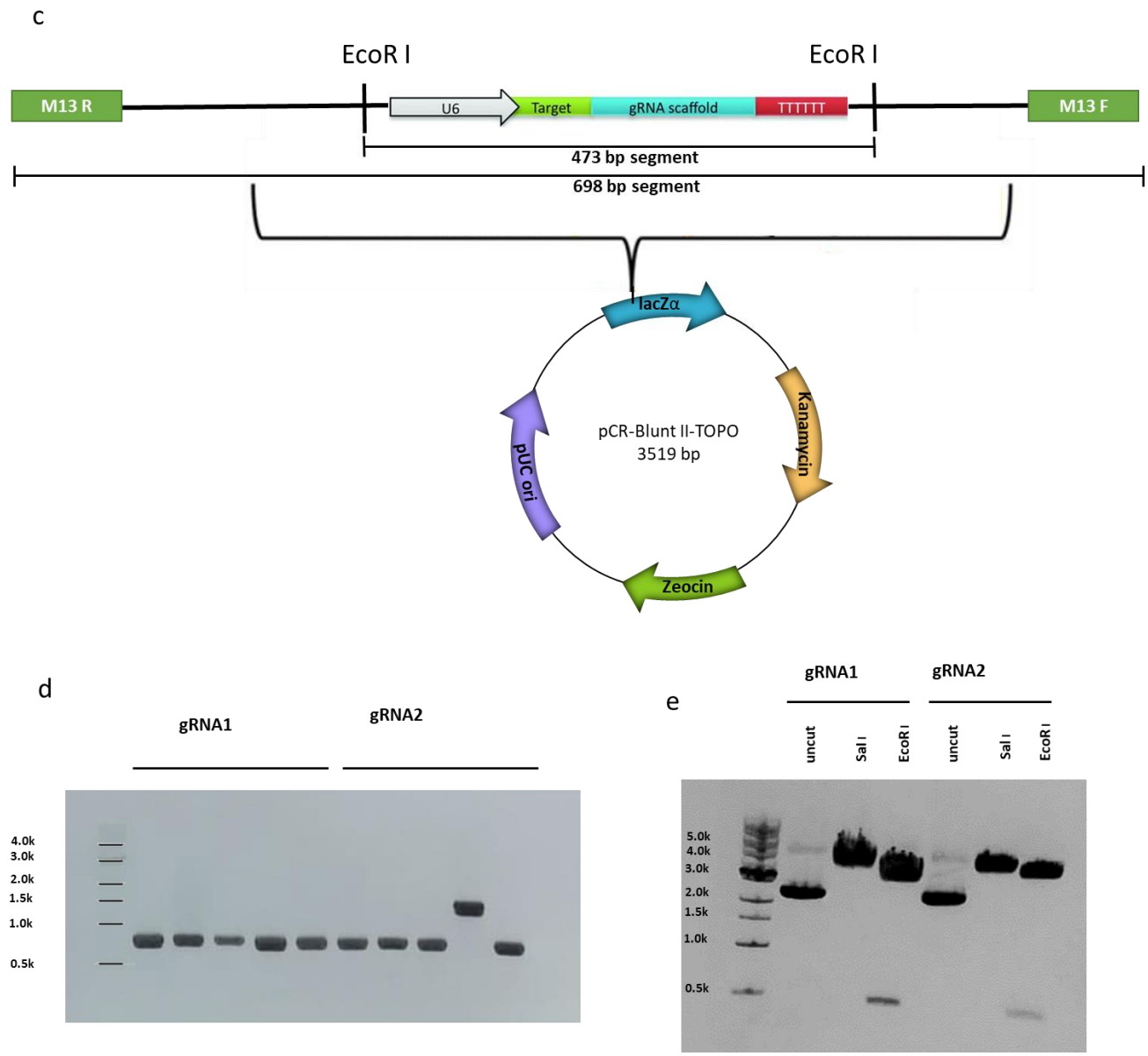

Figure 6.3. gRNA design, cloning and amplification. a) Two gRNAs were selected close to the *GATA3* stop codon (gRNA1 78 bp and gRNA2 23 bp upstream to the stop codon); the PAM sequence for each of the gRNAs is indicated. b) The selected target sequence of each of the gRNAs was incorporated into a DNA fragment to make a 455 bp fragment that codes for a promotor, gRNA target sequence, gRNA scaffold sequence and termination signal (following the gRNA synthesis protocol, Mali et al 2013); the designed fragment was sent for synthesis as a gene block. c) The obtained gene blocks (one for each of the gRNAs) were cloned into a PCR-Blunt-TOPO II plasmid; this plasmid has M13 primers and EcoRI restriction sites on both sides of the insert. d) The plasmid was transformed into Top 10 bacterial cells; five colonies for each gRNA were picked and were first analysed by PCR (using M13 primers). All five colonies for gRNA1 and 4/5 for gRNA2 contained the right size insert (698 bp segment). e) One colony for each gRNA was amplified in an overnight culture and the plasmid DNA was purified, using Maxiprep, and analysed using restriction enzymes: EcoR I cut twice and yielded 473 bp segment, the incorporated insert, and 3501 bp segment, the vector plasmid; Sal I cut once to give a linear plasmid (3947 bp).

6.3.1.3 Repair template plasmid design:

The repair template plasmid was designed to insert a 2A-peptide-mCherry cassette, to report the expression of the *GATA3* gene, and a puʌtk positive/negative selection cassette, placed in a piggybac transposon, flanked by two homologous (5' and 3') arms upstream and downstream to the Cas9 cleavage site in the *GATA3* gene (figure 6.4).

The puʌtk cassette encodes for a bifunctional fusion protein between puromycin N-acetyltransferase (Puro) and a truncated version of the herpes simplex virus type 1 thymidine kinase (ʌTk); cells that incorporate that cassette become resistant to puromycin, and hence cells that incorporate the repair insert could be positively selected using puromycin, but sensitive to 1-(-2-deoxy-2-fluoro-1-b-D-arabino-furanosyl)-5-iodouracil (FIAU) (Chen and Bradley, 2000). The puʌtk cassette was flanked by the piggybac inverted repeats to allow for footprint-free removal, using piggybac transposase, of the cassette after its use in positive selection of the cells that successfully incorporated the insert. After removing the piggybac transposon, cells that did not successfully clear the transposon could be negatively selected using FIAU thus avoiding any possible interference of the antibiotic selection cassette with the expression and function of the *GATA3* gene.

The DNA repair template design was subdivided into five segments (figure 6.4), each of which had 25-40 bp homology to the adjacent segment, to be cloned into a vector plasmid using Gibson assembly. Segment 1 (420 bp) and Segment 5 (480 bp) represented the upstream (5') and downstream (3') homology arms to the cleavage site of the Cas9 respectively. Segment 2 (912 bp) contained the mCherry cassette introduced immediately before the *GATA3*'s stop codon and separated from the end of the *GATA3* gene by a 2A peptide. The small genomic sequence that lies between the site of Cas9 cut and the stop codon was also included in that segment (upstream to the 2A-mCherry cassette). In segment 2, a silent mutation was introduced to one of the guanine nucleotides constituting the PAM sequence of each of the gRNA1 and 2, to avoid cleavage of the repair template by the Cas9. Segment 3 (272 bp) contained the *GATA3* genomic sequence starting from the stop codon to the first TTAA sequence (to ensure footprint-free removal of the piggybac transposon, it should be integrated

into a TTAA chromosomal site). Segment 4 (3276 bp) represented the piggybac transposon with the antibiotic selection cassette.

a

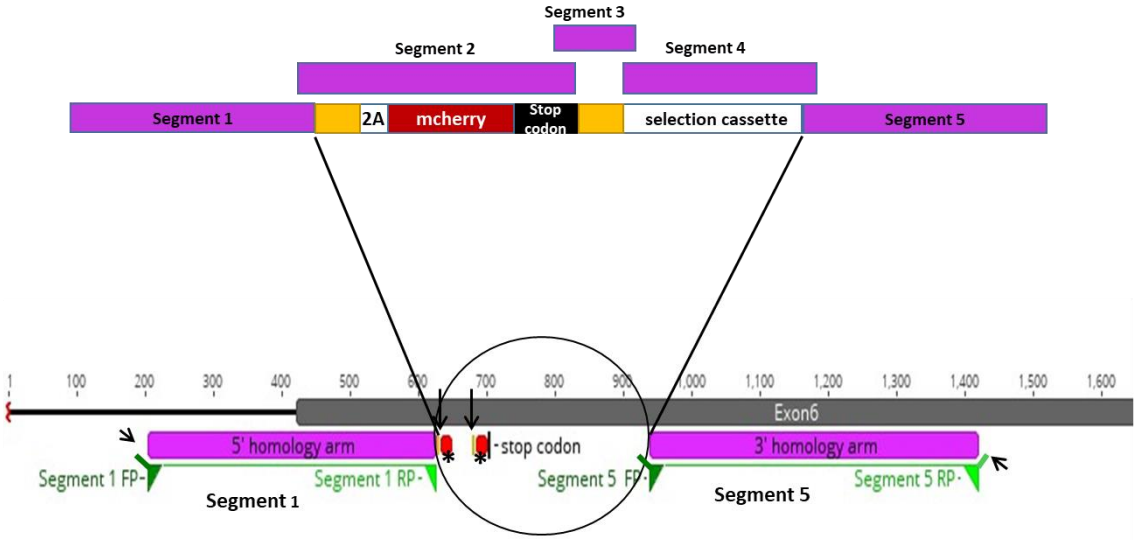

b

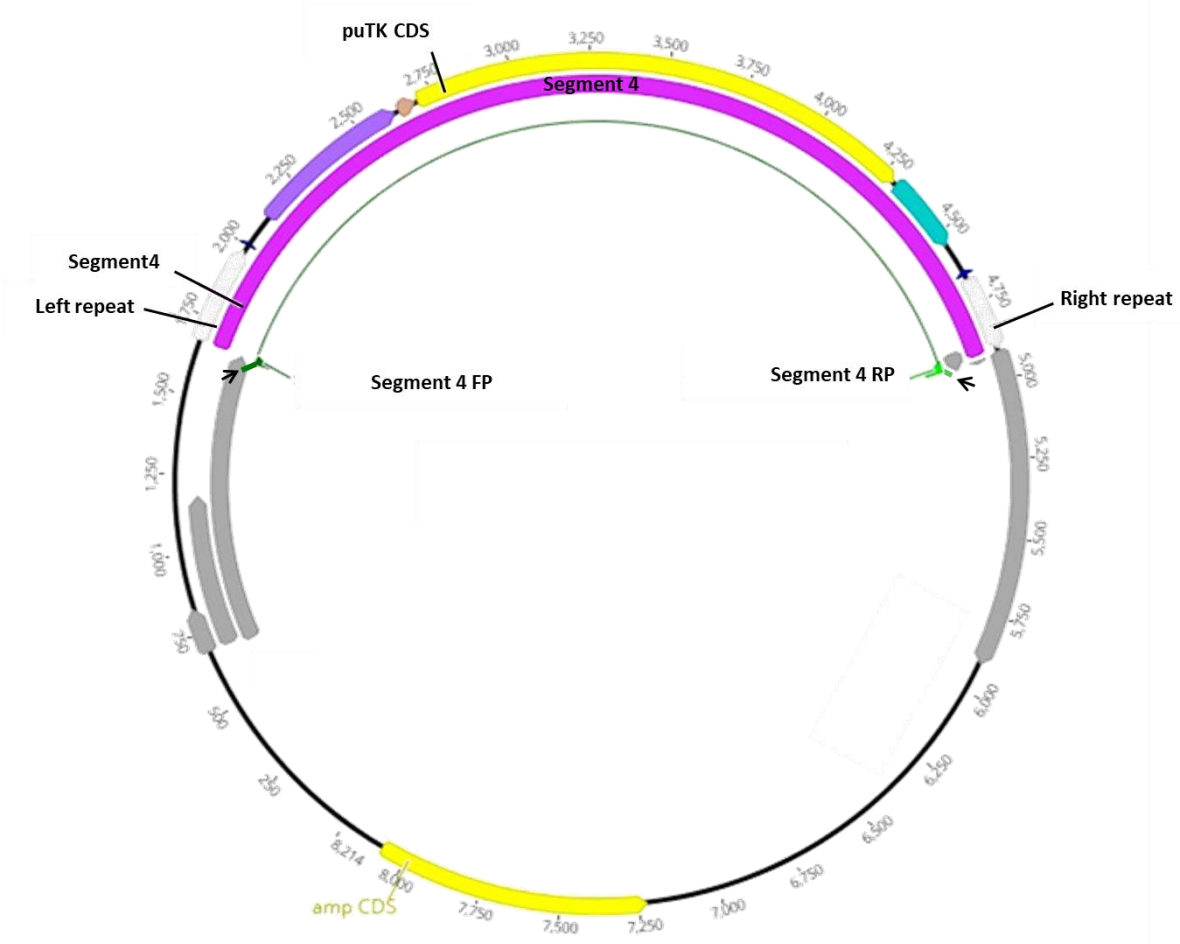

c

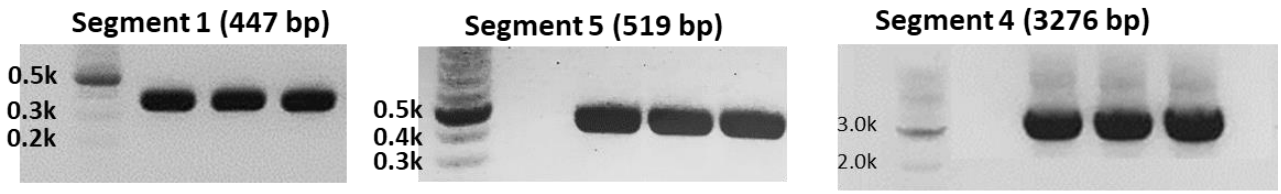
Segment 1 (447 bp)
0.5k
0.3k
0.2k
Segment 5 (519 bp)
0.5k
0.4k
0.3k
Segment 4 (3276 bp)
3.0k
2.0k

d

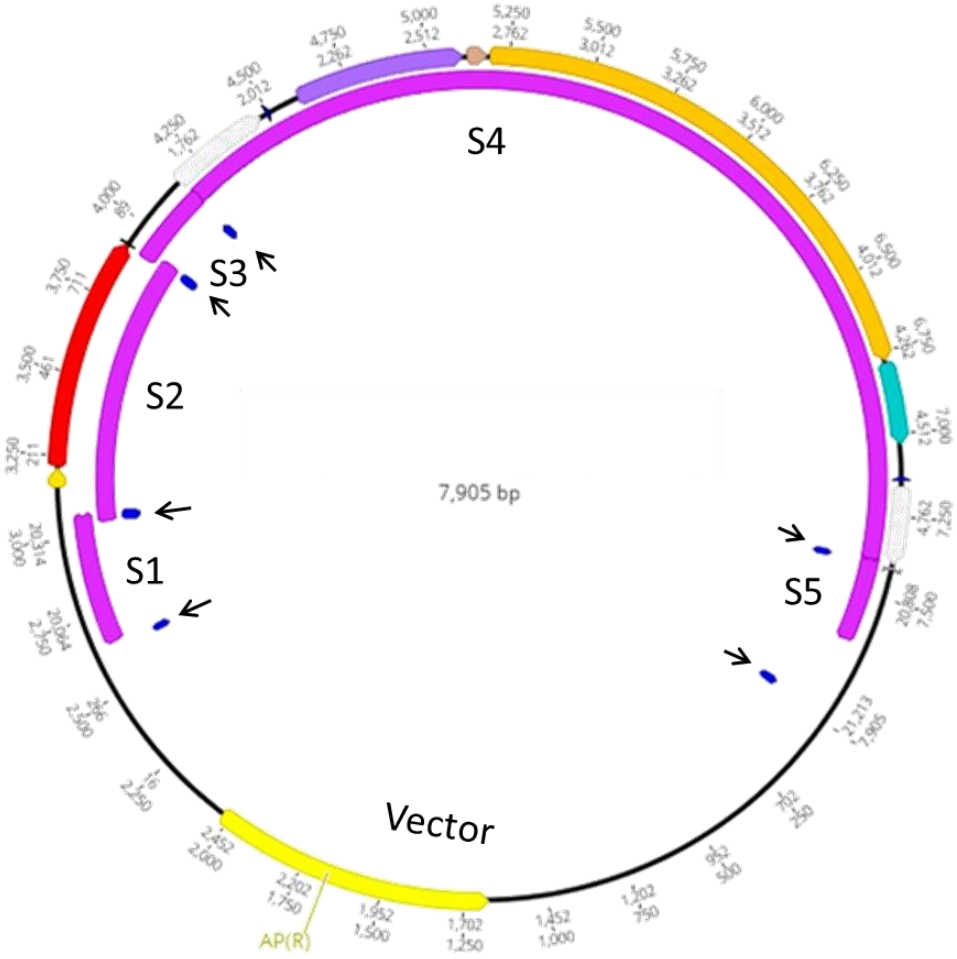
S4
S3
S2
S1
S5
7,905 bp
Vector
AP(R)

e

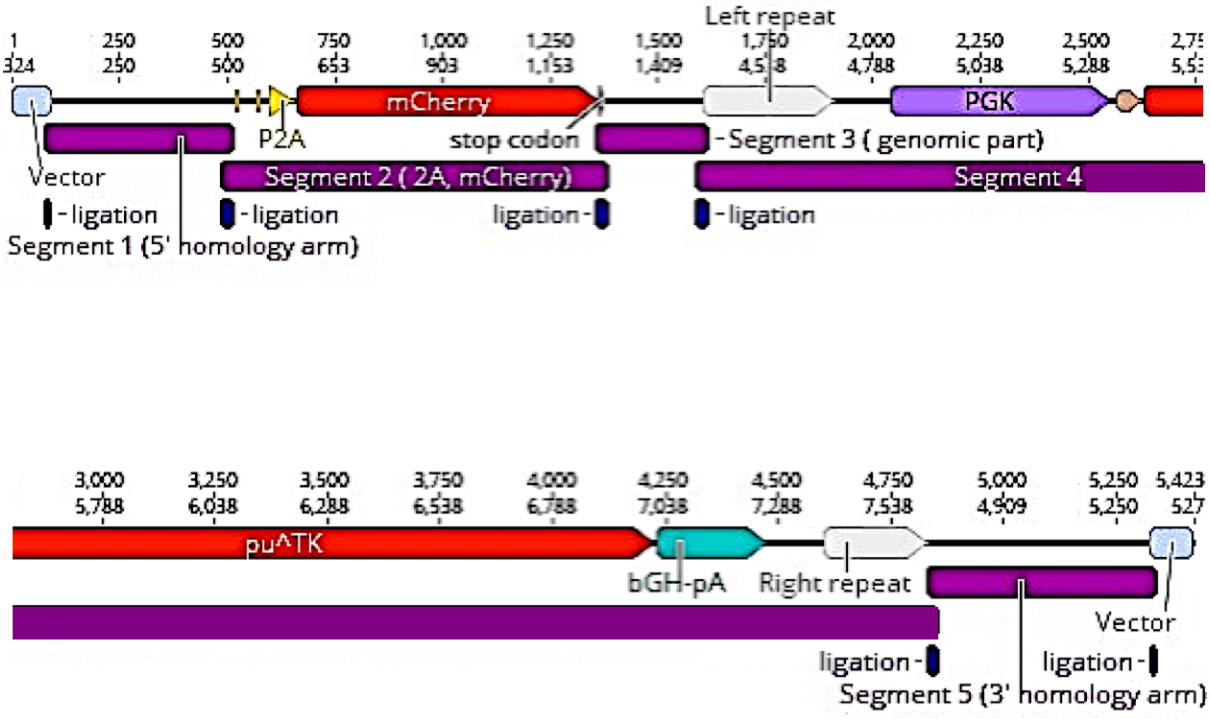

Figure 6.4. Illustrating the *GATA3* targeting plasmid. a) The binding sites of the gRNAs are shown in red and are indicated by asterisks and the arrows indicate the PAM sequences. After Cas9 cleavage, the circled region should be replaced by the repair insert that has two homology arms to the cleavage site. The whole insert was composed of five segments designed to be assembled using Gibson cloning; Segment 1 represents the 5' homology arm and was obtained by PCR amplification from the genomic DNA (the primer binding sites are indicated on the genomic sequence (bottom line)), Segment 2 included the genomic sequence that lies between the cleavage area and the stop codon (75 bp) in addition to a 2A peptide-mCherry-stop sequence, Segment 3 included the genomic sequence starting from the GATA3 gene stop codon to the first TTAA sequence which is necessary to ensure seamless excision of the piggybac (Segment 4) after its use in selecting the successfully edited cells. Segment 2 and 3 were obtained as gene blocks. Segment 4 included positive/negative selection cassette on a transposon and Segment 5 represented the 3' homology arm (obtained by PCR amplification, the primer binding sites are indicated on the genomic sequence). b) Shows the map for pMSC-AAT-PB-PGK plasmid from which Segment 4 was amplified (the primer binding sites are indicated). In a and b) the indented areas on the sides of the primers, indicated by arrow-heads, refer to overhang areas added to the primer sequence to obtain overlapping segments. c) Gel analysis for the amplified segment 1, 4 and 5; segment 2 and 3 were obtained as gene blocks. d) The design for the virtual-cloned repair plasmid with the ligation sites indicated by arrows and blue marks (to be assembled using Gibson assembly). e) Shows the detailed sequence of the repair plasmid; in segment 4: left repeat and right repeat are the recognition sites of the transposase enzyme, PGK is an eukaryotic

promotor, puʌtk is the positive/negative selection cassette and bGH-pA is a poly A signal.

6.3.1.4 Synthesis and cloning of the different segments of the repair plasmid:

Genomic DNA was extracted from hiPSCs and was used to amplify segment 1 and 5 using PCR primers; segment 1 (5' homology arm) forward primer had an overhang area to amplify the segment with homology arm to the vector. Likewise, segment 5 (downstream homology arm) forward and reverse primers were designed with overhang areas to add homology arms to segment 4 and the vector respectively (figure 6.4 a, c). Segment 4 (piggybac transposon with the antibiotic selection cassette) was amplified from the PMSC-AAT-PB-PGK plasmid using primers with overhangs to add homology arms to the adjacent segments (figure 6.4 b, c). The amplified products were gel purified and were sent for sequencing.

Segment 2 and 3 were both obtained as gene blocks from IDT. A PUC18 plasmid, used as a vector, was digested using XbaI enzyme and was gel purified then the enzyme was inactivated by incubating at 62°C for 20 minutes.

The vector and the five segments were used in a Gibson assembly reaction. After running the Gibson cloning, four different sets of primers were used (in four different PCR reactions) to test the assembly of the segments. Primer pairs that bridge over the boundaries of the segments were used: the first primer pair was used to amplify an area between the vector and segment 2, spanning segment 1 (561 bp); the second pair to amplify an area between segment 2 and segment 3 (450 bp); the third pair to amplify an area between segment 3 and segment 4 (487 bp); and the fourth primer pair was used to amplify an area between segment 4 and the vector, spanning segment 5 (958 bp) (figure 6.5 a). The amplified products were run on a gel and all four segments were detected, in the right size, which suggested successful assembly of the different adjacent segments (figure 6.5 b).

The cloning reaction mixture was then transformed into 5-alpha bacterial cells; at the same time control cells were transformed with the PUC18 intact plasmid as a positive control for the transformation step. After an overnight culture, a high number of

colonies were seen in the cells transformed with the intact control plasmid, but very few colonies in the cells transformed with the assembled plasmid (figure 6.5 c, d). I picked single colonies from the transformation plate and first checked the incorporation of my insert by running a PCR reaction which amplifies an area that lies in the middle of my insert (the area between segment 3 and segment 4); 2 out of 12 selected colonies amplified the segment (figure 6.5 e). These two colonies (together with some of the colonies that were negative for the presence of the middle segment in the preliminary PCR) were expanded in an overnight culture, their plasmid DNA was purified, using a miniprep kit, and was analysed using restriction enzymes (NcoI and HpaI), but none of the analysed colonies showed the correct restriction pattern (figure 6.5 f, g).

I repeated the Gibson cloning three times and did two transformations from each cloning reaction and got similar results. One possible solution could be using electrocompetent bacterial cells and electroporation to increase the efficiency of the transformation process. However, I was working to find and optimise a different approach to isolate the differentiated UB structures, in parallel to this technique, and it did show encouraging results (discussed in the following section). I wanted to focus on isolating the UB-like structures and evaluating them so, I did not repeat the transformation. Also, I did not expect to have enough time, even if I managed to clone and purify the repair template plasmid, to transfect the iPSCs, select the correctly edited cells, recover, differentiate them and further analyse and evaluate the reporting cells.

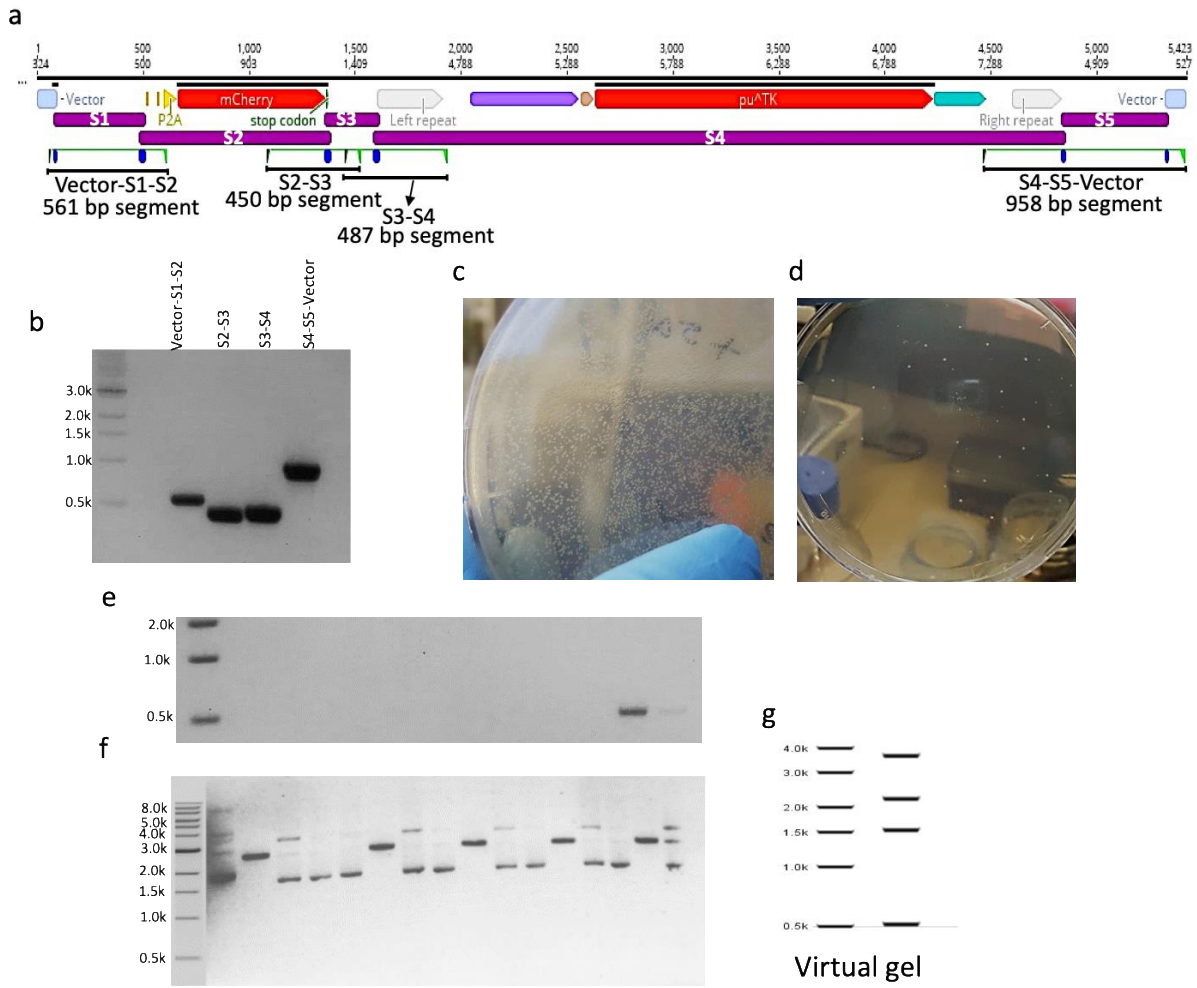

Figure 6.5. a) Illustrates the design for the Gibson cloning and shows the binding sites for the primers that were designed to test the assembly of the different segments after running the Gibson reaction; the primers were designed to span ligation areas and thus ligated segments only should be amplified. b) After running the assembly reaction, the reaction mixture was tested using the four sets of primers shown in (a); all four segments of the correct size were detected suggesting assembly of the adjacent segments. c and d) 5-alpha bacterial cells were transformed with an intact plasmid (c) or cloned plasmid (d); the intact plasmid plate had many colonies, which suggests suitable transformation conditions, while very few colonies grew in the plate of cells transformed with the assembled plasmid. e) 12 colonies were picked from the cells that were transformed with the cloned plasmid and were analysed by PCR (using S3-S4 primers shown in a) as a preliminary check for the incorporation of the assembled insert; only two colonies amplified the correct size segment. f) Those two colonies, together with other colonies picked from the same plate, were amplified in an overnight culture and their plasmid DNA was amplified, using miniprep, and examined by restriction analysis. None of the analysed colonies showed the expected restriction analysis pattern for the correctly assembled plasmid. g) Virtual gel for the restriction analysis expected for the assembled plasmid.

6.4 GDNF conjugation to tag and isolate UB-like structures:

Another possible way to isolate the differentiated UBs, was to employ the interaction between the GDNF protein and its receptor, RET, to live-tag the developing UBs in live-cell cultures and isolate them. GDNF/RET is a critical pathway for the outgrowth and subsequent development and branching of the UB. In the developing kidney, the MM secrets GDNF protein, that stimulates RET receptors in the ND and the UB, first to induce proliferation and outgrowth of the UB from the ND and then after the budding to induce the UB tips to further proliferate and branch (see section 1.2.5 for more details). Labelling RET receptors, through their binding to a fluorescent-tagged GDNF protein, could be one way to isolate iPSC-derived UB-like structures (figure 6.6 a).

6.4.1 Results:

For this experiment, a microscale protein labelling kit was used to conjugate the GDNF protein to a fluorophore; 488 reactive dye. The reactive dye in the labelling kit has a tetrafluorophenyl ester moiety that reacts with primary amines of the protein forming dye-protein conjugate. The protein, 1 mg/ml concentration, was incubated with 488 tetrafluorophenyl esters to allow for the reaction then the formed dye-protein conjugate was purified using a spin filter filled with gel resin to remove the excess dye.

The recovered protein concentration was 400 µg/ml, estimated based on the % yield expected for the protein molecular weight, with a degree of labelling of approximately 2.5 moles of dye/mole of protein.

To test the efficiency of the labelling process, I used mouse embryonic kidneys. E11.5 kidneys that have been cultured for 1.5-3.5 days were treated with the conjugated GDNF (GDNF/488) (100 ng/ml) and were checked for signal after 1 hr, 4 hrs and overnight incubation at 37° C. No signal was detected after 1 or 4 hr of incubation but after overnight incubation, mouse UBs were seen tagged in green (figure 6.6 d, e); the need for the longer incubation period might be because the conjugated protein competes with the normally secreted GDNF from the MM on the receptor binding sites.

In the early stage of metanephric kidney development, E10.5-E11.5, RET expression is detected all-over the WD and the outgrowing UB with higher expression level in the UB tips; by E12.5, Ret expression becomes restricted to the UB tips. Consistent with

that, when E11.5 kidneys that have been cultured *in-vitro* for 1.5 days were treated with the conjugated protein, a bright stain was seen in the branching tips and a less bright signal was seen in stalks (figure 6.6 d) (n=3). However, E11.5 kidneys that were cultured for 3.5 days had only their tips tagged (figure 6. 6 e) (n=3).

Tagging the UB tips confirmed that the protein had successfully been conjugated to the fluorophore without damaging its ability to bind the Ret receptor and suggested that the degree of labelling was enough to be detected under a fluorescence dissecting microscope.

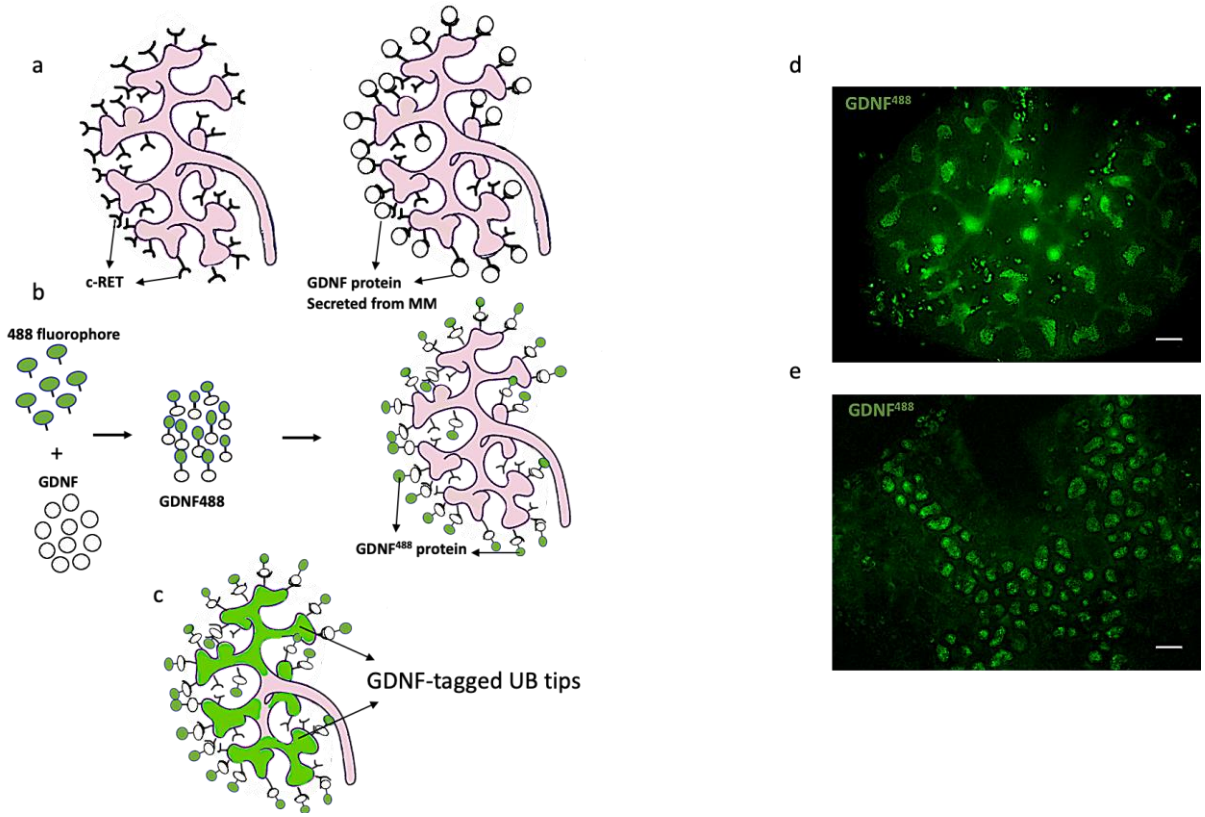

Figure 6.6. a) Schematic for tagging UBs by conjugating the GDNF protein to a fluorophore. RET receptors, expressed on the UB tips, bind to the GDNF protein, secreted from the adjacent MM cells; the MM is not shown. This interaction induces the tip cells to proliferate and undergo branching. b, c) GDNF protein was conjugated to a 488-fluorophore and thus binding of the GDNF/488 to the RET receptors will be marking the UBs with the fluorophore. d, e) Embryonic mouse kidney explants treated with the GDNF/488 to test the efficiency of the conjugation and the efficacy of the tagging process; E11.5 kidneys cultured *in-vitro* for 1.5 days before GDNF/488 treatment had their tips and stalks stained with brighter signal in the tips (d), while E11.5 kidneys that were cultured for 3.5 days before the treatment only showed signal in the UB tips (d). Scale bar is 100 μm.

6.4.1.1 Conjugated GDNF tags UB-like structures in a renal-differentiated mixed population:

I next treated the renal-differentiated cells with the conjugated GDNF protein using the same conditions that were used with mouse embryonic kidneys (overnight incubation; 100 ng/ml concentration); a signal was detected in the terminal ends of some of the tubular structures (figure 6.7a) in a way that suggested UB tip structures.

To further evaluate the live-cell staining process, the cultures were fixed with PFA and stained for GATA3 and CDH1; while the GDNF/488 signal was lost after the fixation, staining and washing process, $GATA3^{+}/CDH1^{+}$ structures were seen in equivalent areas (figure 6.7b) to those that were tagged with the GDNF/488 suggesting that the $GATA3^{+}$/CDH1+ tubular structures, which are expected to be UB-differentiated cells, were expressing functional RET receptors and could be labelled with GDNF/488.

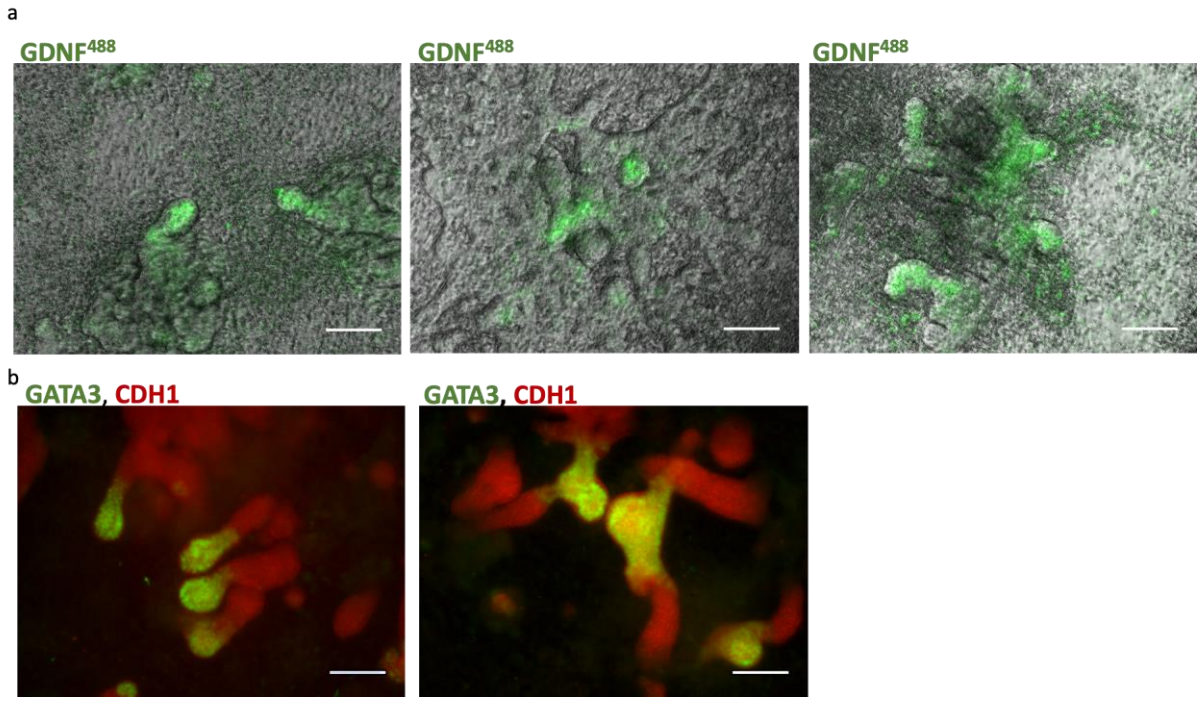

Figure 6.7. a) 20 day-differentiated monolayers that had been treated with the GDNF/488 protein showing bud-like structures labelled with the protein (the three images are for three different samples). b) Same samples shown in a) after fixation and staining for GATA3 and CDH1, UB markers, showing $GATA3^{+}/CDH1^{+}$ structures almost equivalent to those that were stained by the GDNF/488. Scale bar is 100 μm.

6.5 Trial to reconstruct organised renal organoids using the isolated hiPSC-derived UB structures:

We next wanted to combine the isolated iPSC-derived UB structures with a pure nephron progenitor population, sorted from iPSC-derived renal organoids. The aim was to reconstruct an organised renal organoid, equivalent to the Ganeva-style renal tissue that we can achieve from dissociated mouse embryonic kidneys, by adding the UB cells as a single intact epithelial structure and excluding all other UB cells from the culture. Having a single source of UB cells was assumed to develop a single ramified collecting system that induces nephron formation around its growing tips.

This experiment was done in collaboration with another member of the lab, Weijia Liu, who sorted the nephron progenitors using magnetic cell sorting; I will briefly explain the principle that was used for sorting before presenting the results. Dekel and colleagues have performed several studies through which they identified specific surface markers for the different compartments and structures of the human foetal kidney. They identified NCAM1 as a surface marker for the CM, where it is most prominent. NCAM1 is also weakly expressed in early nephron stages (renal vesicle, comma shaped body and S-shaped body) but is completely lost upon further nephron maturation and epithelisation. In contrast, they detected CD133 expression in the mature epithelial structures and to a lesser extent in the comma shaped body and the S-shaped body. CD133 is completely absent from the CM undifferentiated cells. Thus, sorting $NCAM^{+}/CD133^{-}$ cells would be a way for enriching progenitor cells and excluding differentiated cells. In addition, they identified EPCAM as a surface epithelial maker that is expressed brightly in the UB and more mature nephron tubules and less brightly in the early MM-derived epithelial structures, the comma shaped body and the S-shaped body, but is completely absent from the CM. Thus sorting for $NCAM^{+}/CD133^{-}/EPCAM^{-}$ would exclude UB cells and nephron epithelial structures and select only the CM progenitors (Metsuyanim *et al.*, 2009; Harari-Steinberg *et al.*, 2013; Pode-Shakked *et al.*, 2016, 2017).

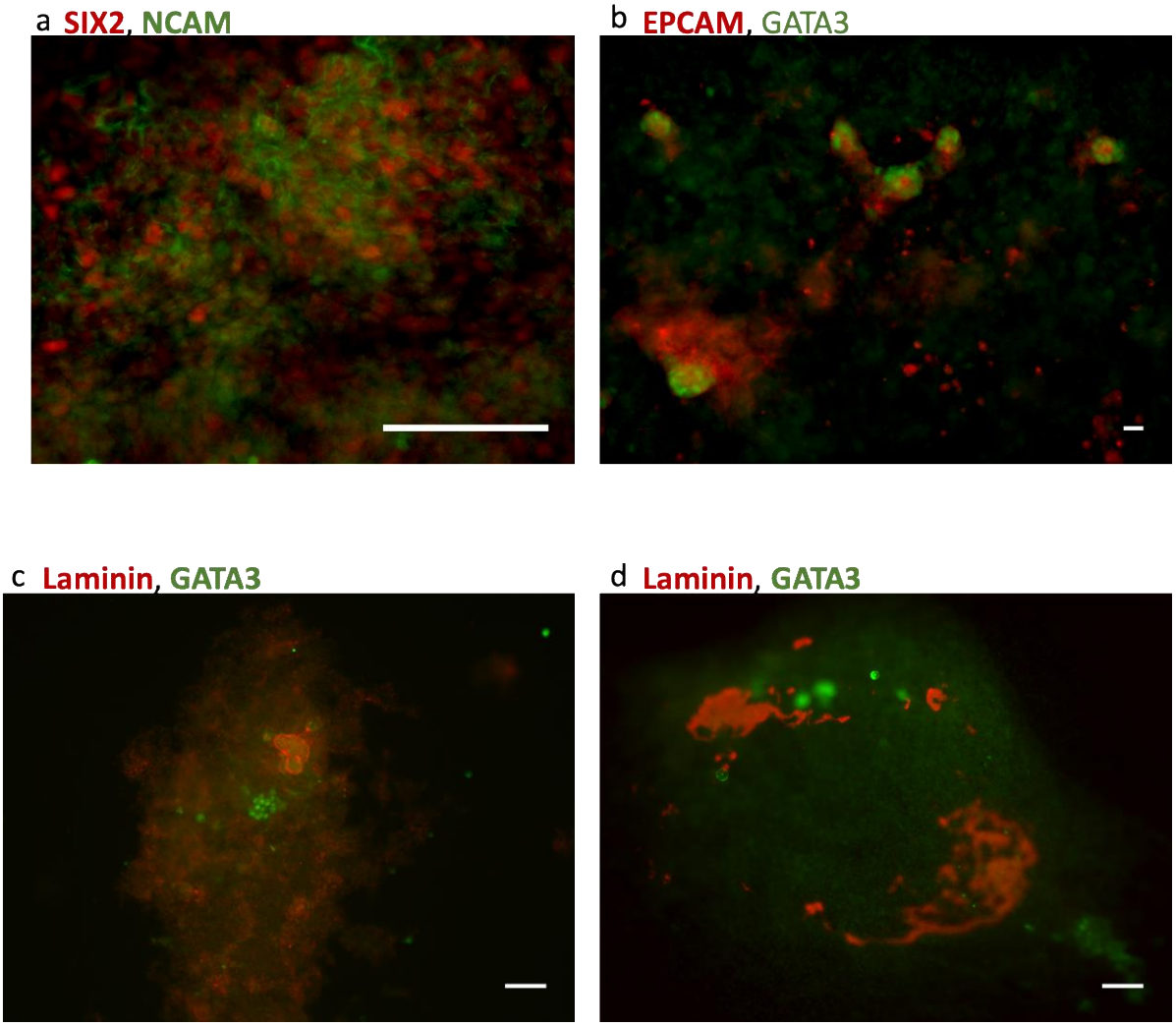

Figure 6.8. a) 12 day-differentiated cells stained for the nephron progenitor marker SIX2 and the surface marker NCAM. b) 17 day-differentiated cells stained for the UB marker GATA3 and the surface marker EPCAM; a, b) were done as an optimisation for the magnetic sorting of the nephron progenitors and were performed by Weijia Liu. c, d) Trial to make organised renal structures by isolating GDNF-tagged UB structures and reaggregating them with sorted nephron progenitors; the reaggregates were kept in culture for 7 days then stained for Laminin (marks the basement membrane for both nephron structures and UBs) and GATA3 (UB and CD marker); no structures were formed. This experiment was done in collaboration with Weijia Liu. Scale bar is 100 μm.

Nephron progenitors were sorted from iPSC-derived renal organoids first by excluding $EPCAM^{+}/CD133^{+}$ cells then selecting NCAM+ cells; the sorted cells were reaggregated with GDNF/488-tagged UBs, which were dissected from a different culture of iPSC-derived renal cells, the re-aggregated cells were kept in culture for seven days but did not develop any structures and neither UB branching nor nephron formation was observed (n=4) (figure 6.8). This might be caused by either the UB,

being unable to branch and induce nephrons, or the NPs, not giving the correct signal for the UB. So, I thought that investigating the ability of the isolated UB-like structures to branch, in a defined system independent of the NPs, would be a logical next step. This will be described in the next chapter.

6.6 Discussion:

Earlier techniques developed in dissociated mouse embryonic kidneys can make organised renal tissue with nephrons arranged around single collecting system (Unbekandt and Davies, 2010; Ganeva, Unbekandt and Davies, 2011; Mills *et al.*, 2017) and containing functional subunits (Lawrence, Chang and Davies, 2015a). More recently, Taguchi and Nishinakamura published a paper in which they managed to make similar organised renal tissue from mESCs, still needed to add stromal progenitors from embryonic kidneys as there is no available protocol for obtaining them from pluripotent cells so far (Taguchi and Nishinakamura, 2017). In this chapter, I wanted to try making a similar organised tissue from hiPSCs as this has never been done so far; for that purpose, a way to isolate the correctly reprogrammed UBs is required. I developed an approach to isolate UB-like structures from iPSC-derived renal organoids as a step towards improving the currently available model of renal organoids.

The central role of the GDNF/RET signalling pathway in inducing UB outgrowth and branching has long been recognised (Moore *et al.*, 1996; Michael and Davies, 2004); specifically, RET is highly expressed in the tips of UBs. Here, I conjugated GDNF protein and used it to label UBs; I showed that mouse embryonic kidney explants that were treated with the conjugated protein had their UBs specifically stained; RET expression, according to the staining results, was detected in both tips and stalks, but was excluded from the main stalk (the extra-renal ureter), in kidney explants that were kept in culture for short period (E11.5 + 1.5 day in culture) but only in the tips of those rudiments that were cultured for longer duration (E11.5+3.5 day in culture); this finding matches earlier studies that show that RET is first detected all over the WD and the whole UB at E11.5 and then becomes restricted to the proliferating tips (Marose *et al.*, 2008).

The pattern of the obtained labelling in iPSC-derived renal cells also suggested successful staining of UB tip structures. Despite losing the fluorescence signal of the live-stain after fixing and washing the samples, immunofluorescence results showed co-expression of GATA3 and CDH1 in roughly equivalent areas, of the developed tubules, to those that were marked by the GDNF/488. The co-localisation of GATA3 and CDH1 as an indicator of successful differentiation towards UBs, however, as I have shown in chapter 3 (section 3.3), results obtained in that context were variable with some differentiation runs that did not yield UB structures. An earlier study has shown the importance of GATA3 in activating and maintaining the expression of RET receptors and that GATA3 inactivation causes loss of RET expression (Grote *et al.*, 2008). It was important to show that GDNF/488 is roughly tagging GATA3 positive structures and not, for example, marking a new population of cells that would be considered non-UB fate according to the previously optimised conditions. Having a marker that can detect UB structures in live culture might be a useful tool for optimising conditions to decrease variability.

I have tried to use the CRISPR/CAS9 gene-editing tool to engineer a reporter cell line for reporting *GATA3* expression as a different strategy to isolate UB structures, but that work was not completed; it would be useful to be able to detect the development of these structures in real-time as this could facilitate tracing the source of variability. It is worth noting that *GATA3* is expressed in different tissues during embryogenesis including the parathyroid gland, the inner ear, the developing kidney (where it is expressed in the ureteric bud, the collecting ducts and the mesangial cells), the central and peripheral nervous system, and the hematopoietic organs (Debacker, Catala and Labastie, 1999; Van Esch and Devriendt, 2001). Hence, the mere expression of *GATA3* in the differentiated hiPSCs doesn't guarantee that these cells are ureteric duct cells. In case of having this reporter cell line working, further assessment of the reporting cells either by testing the co-expression of other UB and CD markers (see chapter 3) or by functional assessment of the reporting structures, through examining their ability to branch and induce nephrons, would be necessary.

Initial result for trying to reconstruct organised renal tissue by reaggregating GDNF/488-tagged UB with sorted nephron progenitors was not successful as no formed structures were seen after 7 days of incubation. This could be due to more

than one reason; one possibility is that the UB and or the nephron progenitors are not mature enough or not fully reprogrammed, so, in the next chapter I set experiments to evaluate the maturity and branching capacity of the isolated UBs. If those UBs proved to be branch-competent and were able to make complex 3D collecting system, then they could be used for making organised kidney tissue by adopting a different strategy; one way might be to induce and allow them to branch before mixing them with nephron progenitors; they might also be used as a cell source for populating scaffolds or 3D bioprinting (Oxburgh *et al*., 2017).

Chapter 7

7 Recapitulating branching morphogenesis using isolated hiPSC-derived structures:

7.1 Introduction:

Branching morphogenesis is the developmental process by which epithelial structures undergo repeated branching into their surrounding mesenchyme thus forming a complex epithelial tree-like structure and shaping the organ geometry (Ochoa-Espinosa and Affolter, 2012; Varner and Nelson, 2014). The ability of the UB tip cells to proliferate and eventually form a ramified collecting system in response to signals emanating from the condensing MM plays a pivotal role in the metanephric kidney development. Indeed, the number of branches produced by the UB is an important determinant of nephron endowment and hence defects in branching morphogenesis are a predisposing factor to renal disease (Shah *et al.*, 2004; Schedl, 2007).

In the previous chapter, I showed that the attempt to reconstruct organised renal organoids by mixing isolated UB structure with sorted nephron progenitors was not successful. One possible explanation could be that the UB and/or the nephron progenitors are not mature enough to induce and respond back to one another. This finding, together with the variability that was sometimes seen in obtaining the UB fate using the Takasato protocol, directed me to further evaluate the obtained UB-like structures and examine their branching capacity, in an MM free condition. In regular 2D and 3D organoid culture conditions no more than one branching event was observed and it was important to investigate if those structures can show higher branching capacity when isolated and induced to branch.

In particular, the variability that this protocol showed in producing UB cells made me also decide to try a different differentiation protocol that directs hiPSCs mainly to UB fate and compare between the UBs obtained from both of them with respect to their efficiency in producing branch-competent UBs. Recently, Taguchi and Nishinakamura published a protocol that aims to differentiate mESCs and hiPSCs towards UBs. To develop their protocol, they first performed a backward *in-vivo* study, using mouse embryos. They started by studying the gene expression pattern in the late maturation stage of WD and UB development, from E9.5 to E11.5, and identified the growth factors that are involved in inducing maturation of E9.5 WD cells into E11.5 UB cells. They then moved a step backward to study an earlier stage of WD development, from E8.75 to E9.5, and in the same way they identified the growth factors that were able to induce maturation of sorted E8.75 WD cells into E9.5 stage. They used the

information obtained from those two steps to delineate a three-day induction protocol that induces the maturation of E8.75 sorted WD cells into UB like structures with similar gene expression pattern to the E11.5 UB. Afterwards, they employed mESCs to define a four-step differentiation protocol that directs the differentiation of mESCs into E8.75 WD precursors. Finally, they combined the information obtained from *in-vivo* analysis of WD and UB progenitor cells with the information obtained from mESC directed differentiation to define an optimised differentiation protocol that derives the differentiation of entities similar to E11.5 UBs from mESCs in 9.25 days (including initial 2 days for embryoid body formation) (Taguchi and Nishinakamura, 2017).

Taguchi and Nishinakamura showed that their induced mESC-derived UBs (miUBs) were able to branch and form ramified trees when cultured isolated in gel upon treatment with specified growth factors. Furthermore, they showed that isolated miUBs were able to branch and induce nephrogenesis forming an organised renal tissue when mixed with mouse embryonic isolated MM. Finally, they transferred their optimised protocol to hiPSCs, with slight modification, and indicated that they obtained UBs with some branching capacities from hiPSCs (hiUBs). The branching that they presented from hiUBs was however obtained from a whole organoid cultured in gel not from isolated UB structures and they commented that the hiUB branching in the gel was significantly slower than that obtained from mouse cells. They also tried to construct an organised renal tissue by mixing hiUB with hiPSC-derived nephron progenitors, but they did not get much success.

7.2 Aims:

I wanted to evaluate and compare the branching capacity of hiUBs obtained from two different differentiation protocols: the Taguchi and Nishinakamura protocol, 2017, and the Takasato et al. protocol, 2015. As discussed earlier, the ability to respond to branching inducing signals to form a ramified three-dimensional network of collecting ducts is an inherent criterion of the normal UBs that is essential for the use of these cells either in therapeutic purposes or in physiological, toxicological or disease modelling studies.

For that purpose, I first used isolated mouse embryonic UBs, as their ability to branch and form collecting duct trees is undoubted (Grobstein, 1955), to optimise culture conditions that can support growth and induce branching in isolated UBs.

7.3 Optimising conditions for evaluating branch-competence using isolated mouse embryonic UBs:

UBs cultured in isolation from the MM cannot branch and eventually die unless they receive external growth factors that can replace the natural presence of the MM (Saxén and Lehtonen, 1987; Qiao, Sakurai and Nigam, 1999; Sakurai, Bush and Nigam, 2001).

Identifying the exact nature of the inducing signals that control UB branching morphogenesis has been deeply investigated over the past few decades using murine embryonic kidney explants. These investigations revealed the importance of extracellular matrices, such as Matrigel, collagen I and IV (Sakurai *et al.*, 1997; Qiao, Sakurai and Nigam, 1999; Sakurai, Bush and Nigam, 2001), and different growth factors with GDNF, signalling through the tyrosine kinase receptor RET and its co-receptor GFRA1, been highlighted as a predominant stimulus of branching (Sainio, Suvanto, *et al.*, 1997); however, GDNF as a single growth factor is not enough to induce branching in UBs isolated from MM and cultured in an extracellular matrix (Sakurai et al. 2001; Yuri et al. 2017, and data in figure 7.1). Other growth factors that were shown to have a role in branching induction include HGF (Cantley *et al.*, 1994), EGF, VEGF-A, Heregulin (Sakurai, Bush and Nigam, 2005) and Pleiotrophin (Sakurai, Bush and Nigam, 2001). In addition, the stromal-derived RA has also been shown to be important for maintaining the expression of RET in the tip cells and thus modulating branching (Mendelsohn *et al.*, 1999; Batourina *et al.*, 2001; Rosselot *et al.*, 2010).

The first trials that aimed to culture UBs in isolation of the MM either used MM-conditioned medium or growth factors purified from the conditioned medium and reported that they were not able to reproduce the same results using commercially available factors (Sakurai, Bush and Nigam, 2001, 2005; Bush *et al.*, 2004; Meyer *et al.*, 2004). A recent study has published a protocol for recapitulating branching morphogenesis from isolated UBs in a completely defined, MM free culture condition (Yuri *et al.*, 2017). That study identified two conditions to maintain the UB tip cell

identity and induce their proliferation and branching, these two conditions were either the combination of GDNF, FGF1, and CHIR99021 (WNT-B catenin signalling) or the combination of GDNF and RA. While any of these two conditions was enough, according to the study, for promoting survival and inducing extensive proliferation in isolated embryonic UBs, they showed that the combination of the four factors, FGF1, GDNF, CHIR99021, RA together with ROCK inhibitor was the optimum condition to prevent apoptosis, promote colony formation and proliferation, and induce branching from dissociated single UB cells (Yuri *et al.*, 2017).

Aim:

I wanted to reproduce and optimise the Yuri protocol in isolated mouse embryonic UBs with the aim of trying to transfer it to hiUBs.

Results:

E11.5 mouse UBs were completely dissected and cleaned from the surrounding MM, then their tips were isolated and cultured suspended in growth factor-reduced Matrigel and the effect of the above-mentioned growth factors (GDNF, FGF1, CHIR, RA) was tested. As expected, GDNF treatment alone was not enough to promote survival and inhibit apoptosis in isolated embryonic UB tips; tips cultured only in presence of GDNF appeared to be dying from the first day of culture and were completely dead by the third day as shown by the uptake of the nuclear dye DAPI or Sytox green (figure 7.1 a, c; n= 6). The addition of FGF1 to GDNF in the culture media that was added to the isolated UB tips inhibited apoptosis and the cultured tips increased in size, probably indicating proliferation of the UB tip cells, but the cultured tips did not show any branching in response to these two factors (figure 7.1 b, d; n= 6).

The combination of GDNF, FGF1 and CHIR induced branching in some, but not all, of the isolated tips (n=11, 5/11 did not branch and 6/11 branched). Some of the isolated UB tips, treated with that combination, increased in size without showing branching. There are usually individual variations in the maturity of embryonic kidneys obtained from the same age, the reason that some of the isolated UB tips did not branch in response to the treatment with GDNF, FGF1 and CHIR could be that these tips were less mature and needed an extra signal to enable them to respond to the growth factors (figure 7.2 a, b).

Adding RA to the previous combination induced robust branching in a very consistent and reproducible way, in addition, the tips of the branching structures showed the characteristic dichotomous tip morphology (figure 7.2 c, d; n=11 for the initial optimisation and was used afterwards as a control for the culture condition with all the following experiments). In contrast, the branching that occurred in response to GDNF, FGF1, and CHIR without RA, in addition to being inconsistent, was slower, limited and showed somehow aberrant tip morphology compared to the branching-response to the same combination plus RA.

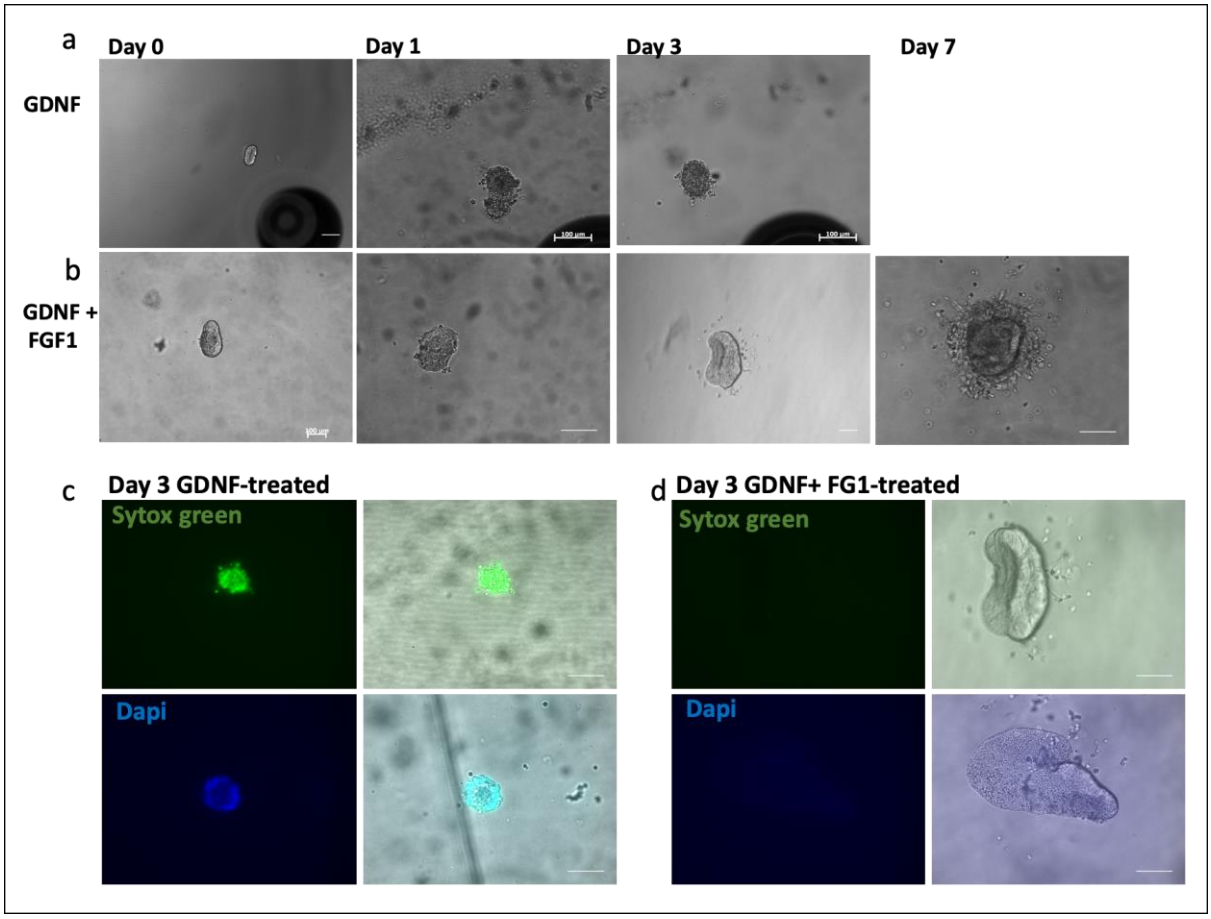

Figure 7.1. Isolated mouse embryonic UBs cultured in Matrigel treated with GDNF (a) or GDNF+ FGF1 (b); none of them branched. c) Isolated UBs that were cultured in the presence of GDNF alone stained positive for sytox green (upper image) or DAPI (lower image) indicating dead cells. d) addition of FGF1 to GDNF inhibited apoptosis. Scale bar is 100 µm.

Therefore, the combination of GDNF, FGF1, CHIR and RA was chosen as a suitable condition for culturing isolated UB tips and inducing branching morphogenesis. I next tried to culture the isolated UB tips on the surface of filter membranes, using trans-wells, instead of being suspended in Matrigel, and treated them with the combination

of GDNF, FGF1, CHIR and RA. UB tips cultured on trans wells did not branch even when 10% Matrigel was added to the culture media, only tips that were suspended in a Matrigel layer were able to branch which probably suggests the importance of the extracellular matrix for UB growth and branching in isolation from the MM.

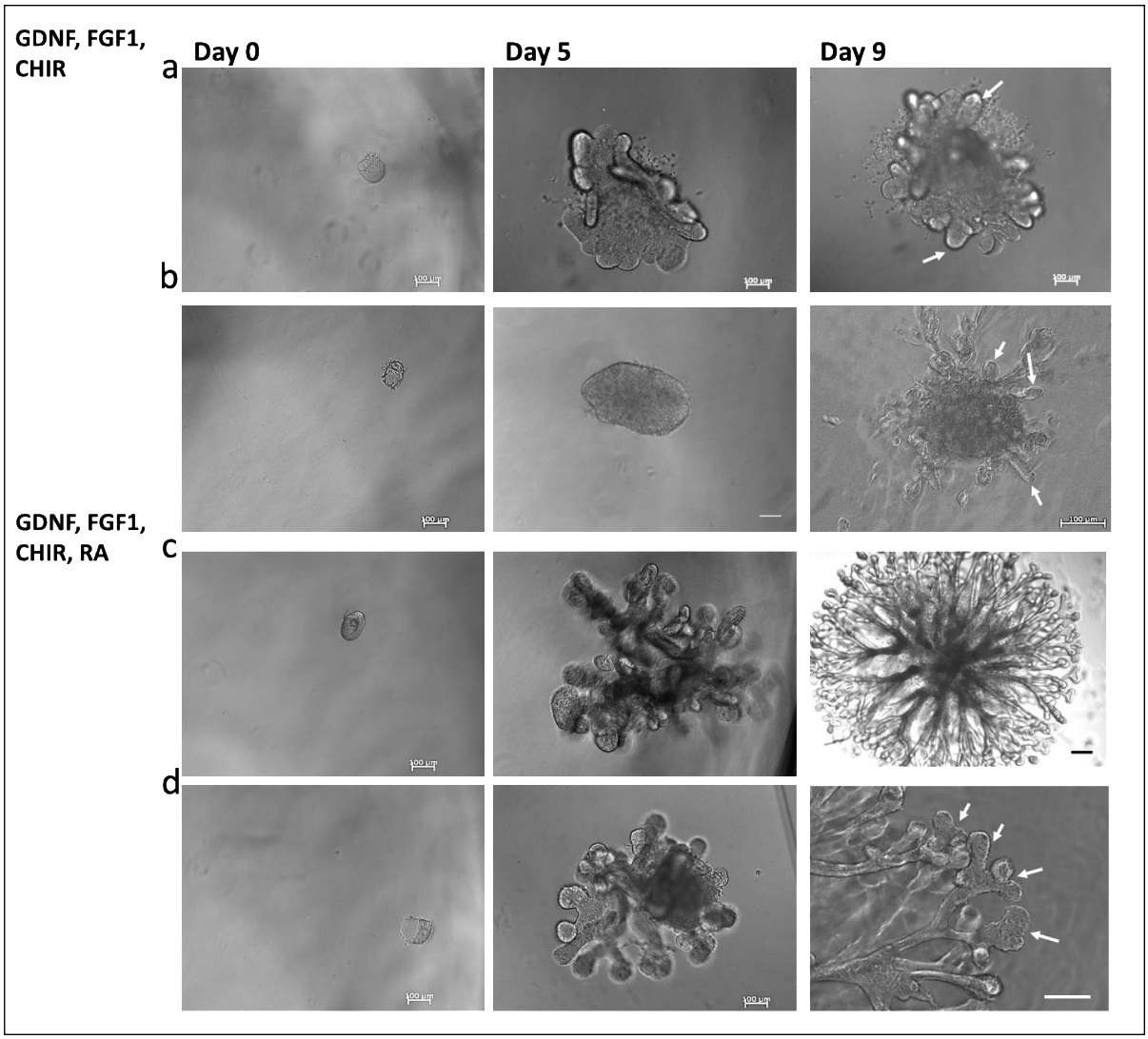

Figure 7.2. a, b) Treatment of the isolated mouse embryonic UBs with a combination of GDNF, FGF1, and CHIR. This combination induced branching in (a) but not in (b) suggesting inconsistency in the response to these factors. b) Showed abnormal projections from the cultured bud on prolonged incubation but not actual branching. c, d) Treatment with GDNF, FGF1, CHIR and RA induced robust branching in a consistent way; arrows in (d, day 9) point to the bifurcating tips. Scale bar is 100 µm.

After optimising a defined condition to examine the branching capacity of isolated UBs, I performed the following experiments to compare between hiUBs obtained from two different differentiation protocols, the Takasato et al protocol and the Taguchi and

Nishinakamura protocol. The obtained UBs were compared for their ability to respond to these defined factors and recapitulate branching morphogenesis. Although these experiments were run in parallel, they are presented here one after the other to avoid confusion.

7.4 Evaluating branch-competence of isolated hiUBs obtained from the Takasato protocol:

Aim:

In this section, I wanted to test the ability of hiPSC-derived UB-like structure to branch forming a ramified tree using the defined culture condition that efficiently induced branching in isolated mouse embryonic UBs . To my knowledge, no other study, so far, has managed to isolate the UB structures obtained using the Takasato protocol of differentiation nor assessed the branching capacity of these structures.

Results:

Renal-differentiated hiPSCs were treated with GDNF/488 to label the hiUB structures, bright-tagged structures were dissected under a fluorescence dissecting microscope, cultured suspended in Matrigel and treated with the combination of GDNF, FGF1, CHIR and RA. The isolated UB-like structures were kept in this culture condition for a total of 14 days. After 4-5 days in culture the isolated structures started to form outgrowing buds that then grew and started to branch; by the end of the treatment duration, the isolated hiUBs, that all started as single spheroid structures, made branched connected epithelial tubules (figure 7.3, n=5, each repeat included a culture of 8-9 individual isolated hiUBs; a total of 44 isolated hiUBs were examined. 32/44 formed ramified trees).

Compared to the mouse embryonic UBs, the branching response of the hiPSCs-derived UBs was slower and the total number of branches was less; this could be due to the inter-species difference as embryogenesis and organogenesis duration is generally much longer in human. The expression of RET in these branching structures was examined by live-treating them with GDNF/488 which showed positive staining especially at the tips. The branched epithelial structures were then extracted from the

Matrigel and stained for different UB markers; they showed expression of GATA3, CDH1, CALB1 and CK8 (figure 7.4).

The ability to branch in response to branching inducing factors, an environment which mimics that created by the MM, and the expression of RET together with other ureteric markers could be considered as a way of functional assessment of the obtained hiUBs.

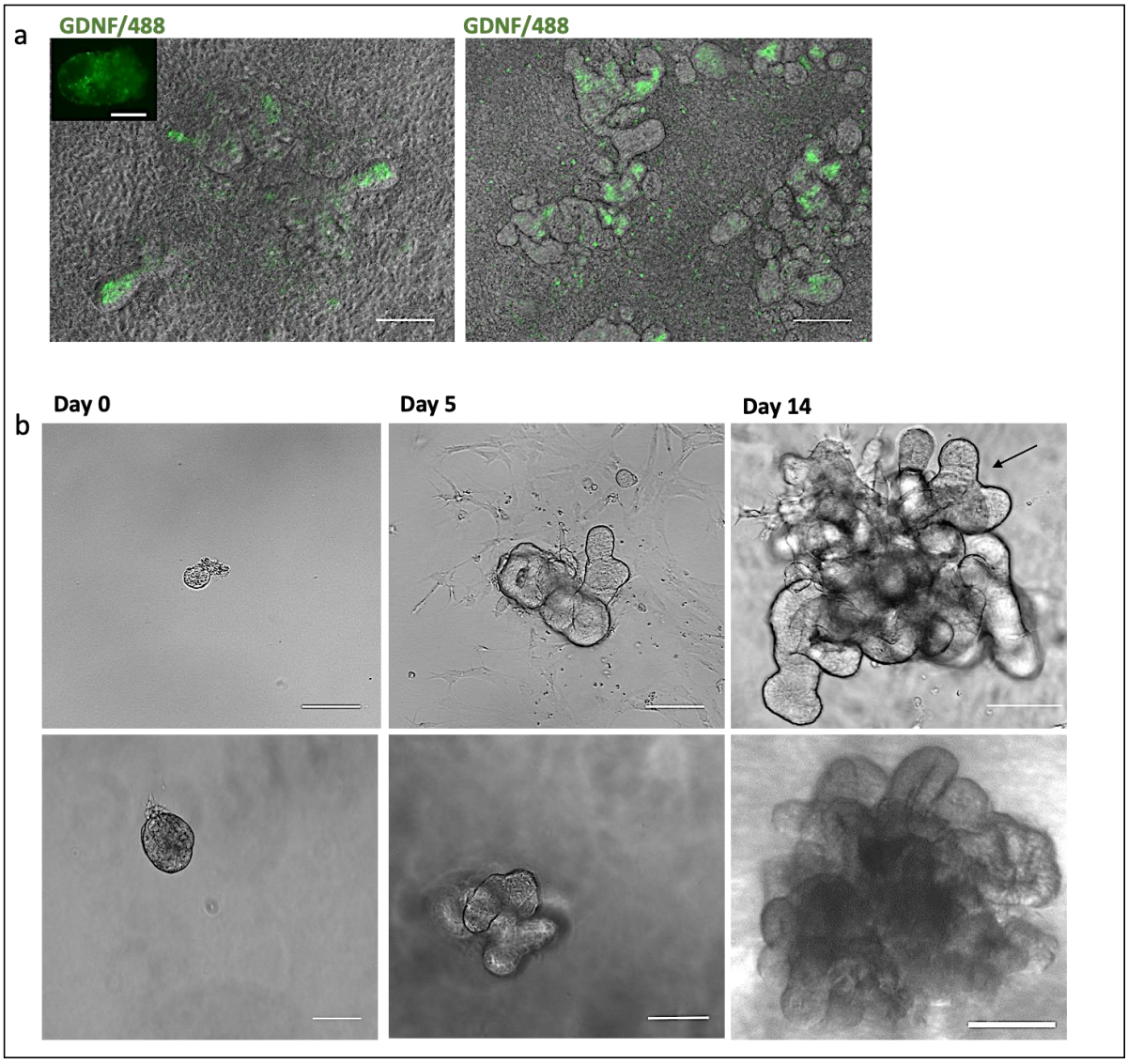

Figure 7.3. a) Differentiated cells using Takasato protocol treated with GDNF/488 to tag the UB structures; the tagged structures were isolated and cultured in Matrigel treated with branching inducing mixture. b) Shows the isolated hiUBs on day 0, 5, and 14 of culture in branching inducing matrix. Scale bar is 100 µm except for the insert in (a), when it is 50 µm.

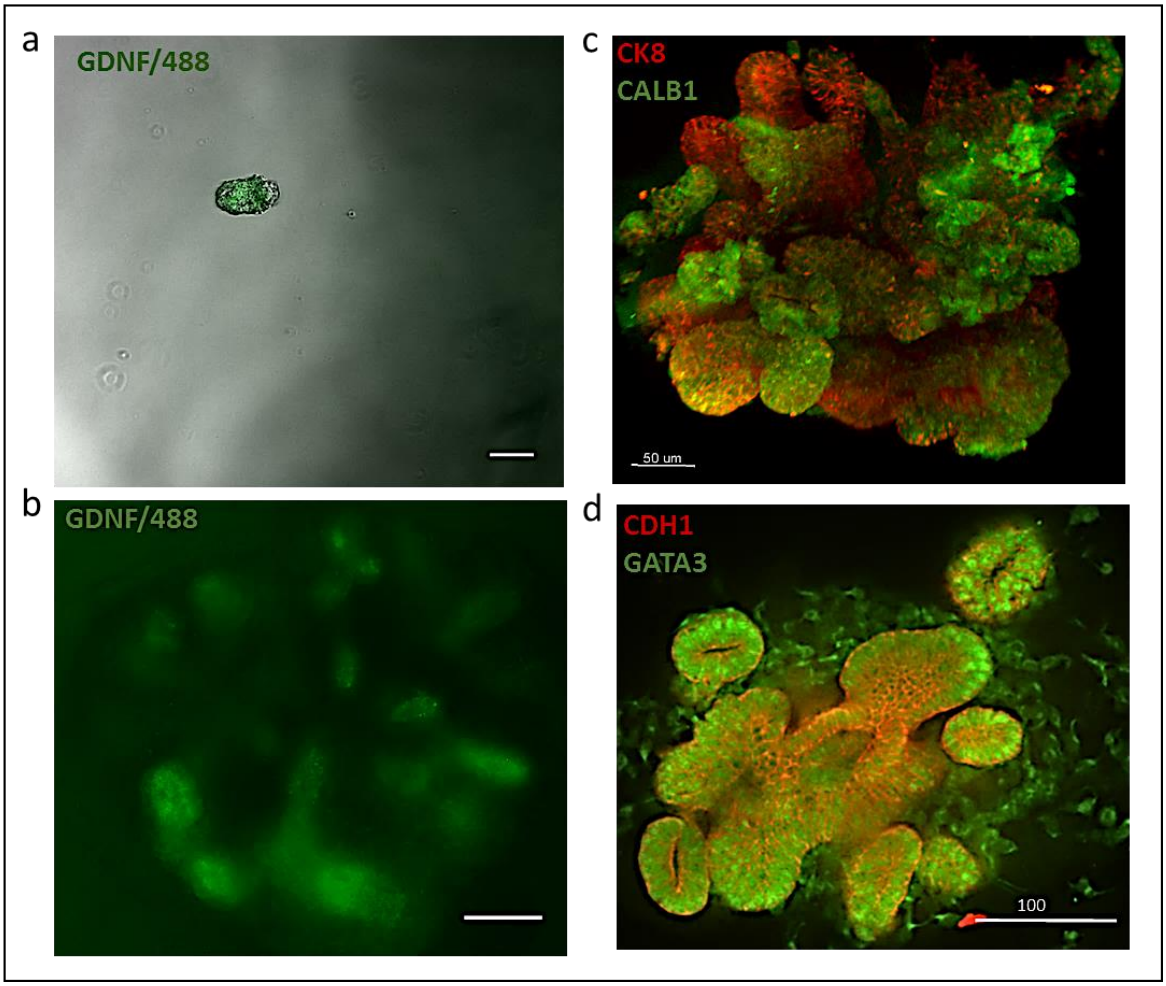

Figure 7.4. a, b) Shows c-RET expression in hiUB obtained using the Takasato protocol (a) hiUB on day 0 of gel-culture and (b) on day 14 of gel-culture showing the ramified structures. c, d) Immunostaining of the branched structures for different UB markers. Scale bar is 100 µm.

7.5 Evaluating branch-competence of isolated hiUBs obtained from the Taguchi and Nishinakamura protocol:

Aim:

In this section, I wanted to reproduce the Taguchi and Nishinakamura protocol for obtaining hiUBs with the aim of comparing between the branch-competence of the hiUBs obtained by this protocol and those obtained by the Takasato protocol.

Results:

hiPSCs were dissociated and reaggregated in the bottom of ultra-low attachment plates to form embryoid bodies in presence the of Activin A and BMP4 for 1 day (step

1) followed by high concentration CHIR treatment in combination with BMP4 for 1.5 days (step 2) to induce nascent mesoderm fate. RA, FGF9, LDN 193189 (to inhibit BMP signalling) and SB 431542 (to inhibit SMAD2/3 signalling) were added for 2 days to induce AIM fate (step 3) then SB431542 was replaced with CHIR and the treatment was continued for 1.75 more days (step 4) to obtain WD progenitors (figure 7.5 a).

After the completion of step 4, the developed spheroids were dissociated and FACS analysed for the co-expression of CXCR4/KIT surface markers, as an indicator of obtaining WD progenitors. An average population of 20% showed positivity to these two markers (n= 3; figure 7.5 b and d). That population was sorted and recovered, then the differentiation protocol was continued to induce maturation of the obtained WD progenitor cells into UB cells as follows: first, WD progenitor cells were treated with a combination of RA, CHIR, FGF9, FGF1 and LDN for 2 days (step 5) then low concentration of GDNF was added to the same combination of growth factors and the treatment was continued for further 2 days (step 6); lastly FGF9 was removed from step 6 factors and treatment was continued for 2 days (step7).

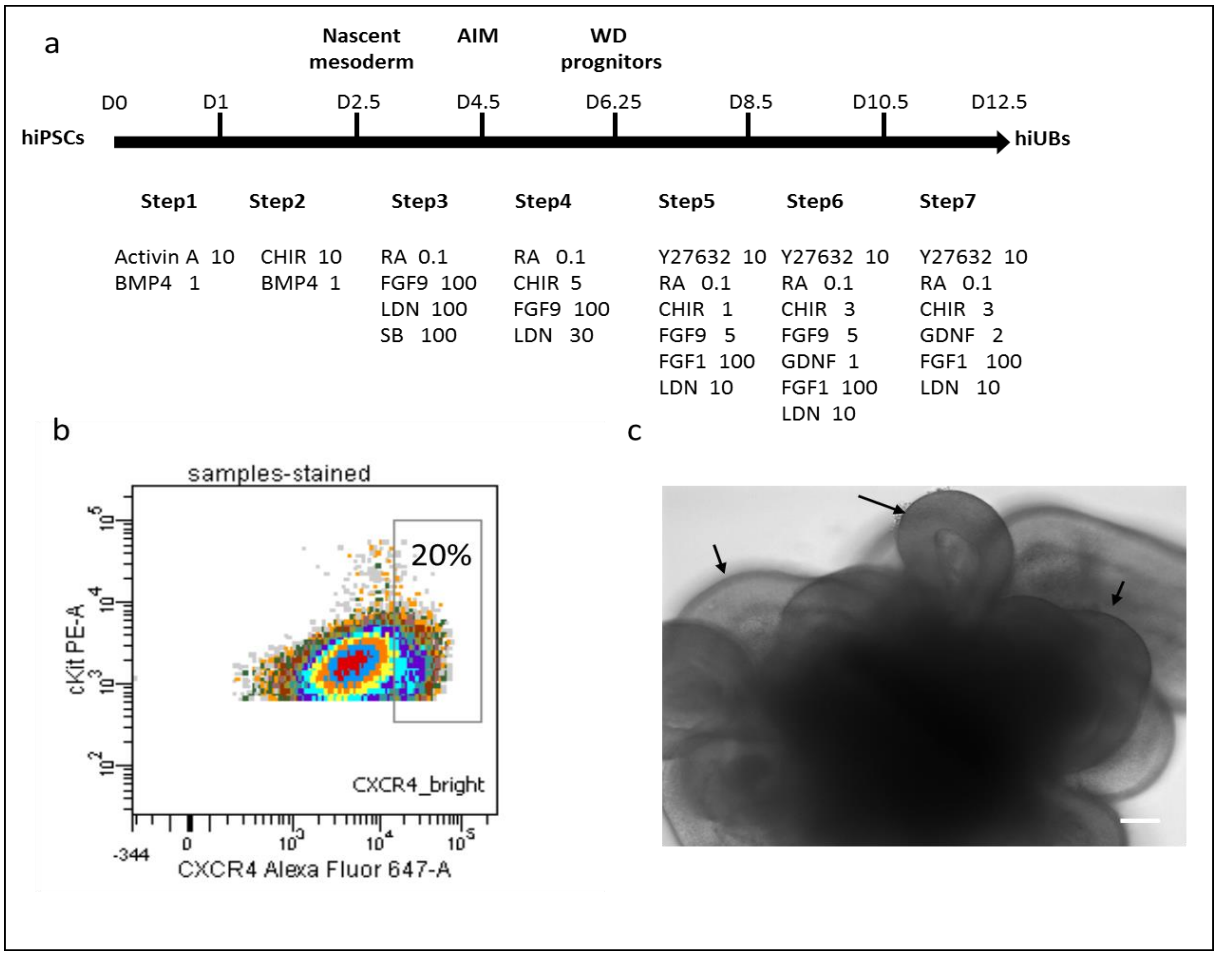

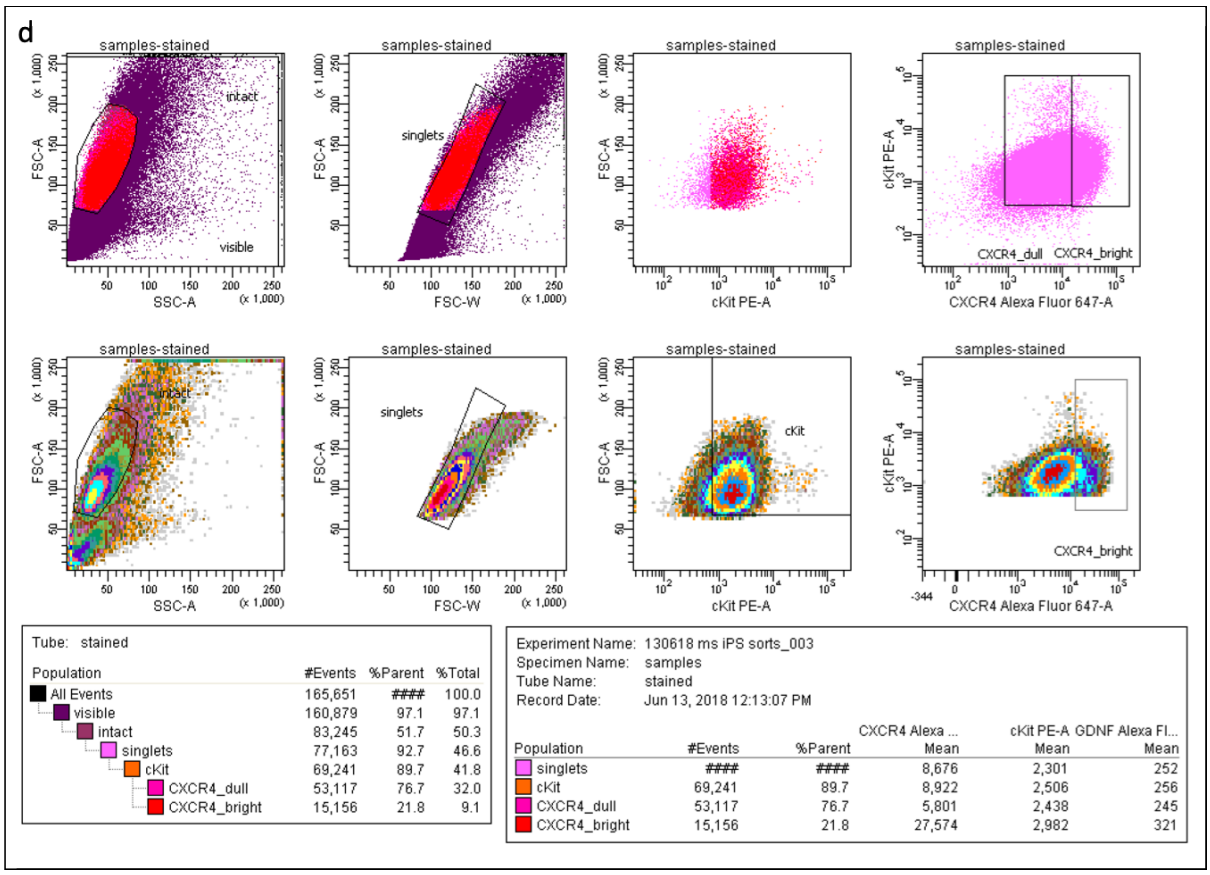

Figure 7.5. Differentiating hiPSCs into UBs using the Taguchi protocol. a) Illustration of the differentiation protocol; the numbers indicate the concentration of the growth factors CHIR, SB, RA and Y27632 are shown in µM concentration, LDN is shown in nM concentration and the rest of the growth factors are indicated in ng/ml. b) FACS results after step 4; $CXCR4^{+}/KIT^{+}$ cells were sorted and recovered. c) Shows a spheroid at the end of the differentiation protocol with buds seen outgrowing from the periphery. Scale bar is 100 µm. d) The gating strategy for Wolffian duct progenitors that were obtained from hiPSCs after applying the Taguchi protocol of differentiation for 6.5 days. Intact singlets represented 46.6% of the total events; 19.6% of these intact singlets (15,156/ 77,163) were $KIT^{+}/CXCR^{++}$. These cells were sorted, recovered and cultured for the end of the differentiation protocol as explained in section 7.5.

At the end of the differentiation protocol (after step 7), the cultured spheroids showed multiple outgrowing buds (figure 7.5 c). Those buds started to appear after step 5 of differentiation and increased afterwards. Obtaining UB fate was evaluated at the end of step 7 by co-staining for CDH1, GATA3 and PAX2; the co-expression of the three of them was detected (n=3; figure 7.6 a, b).

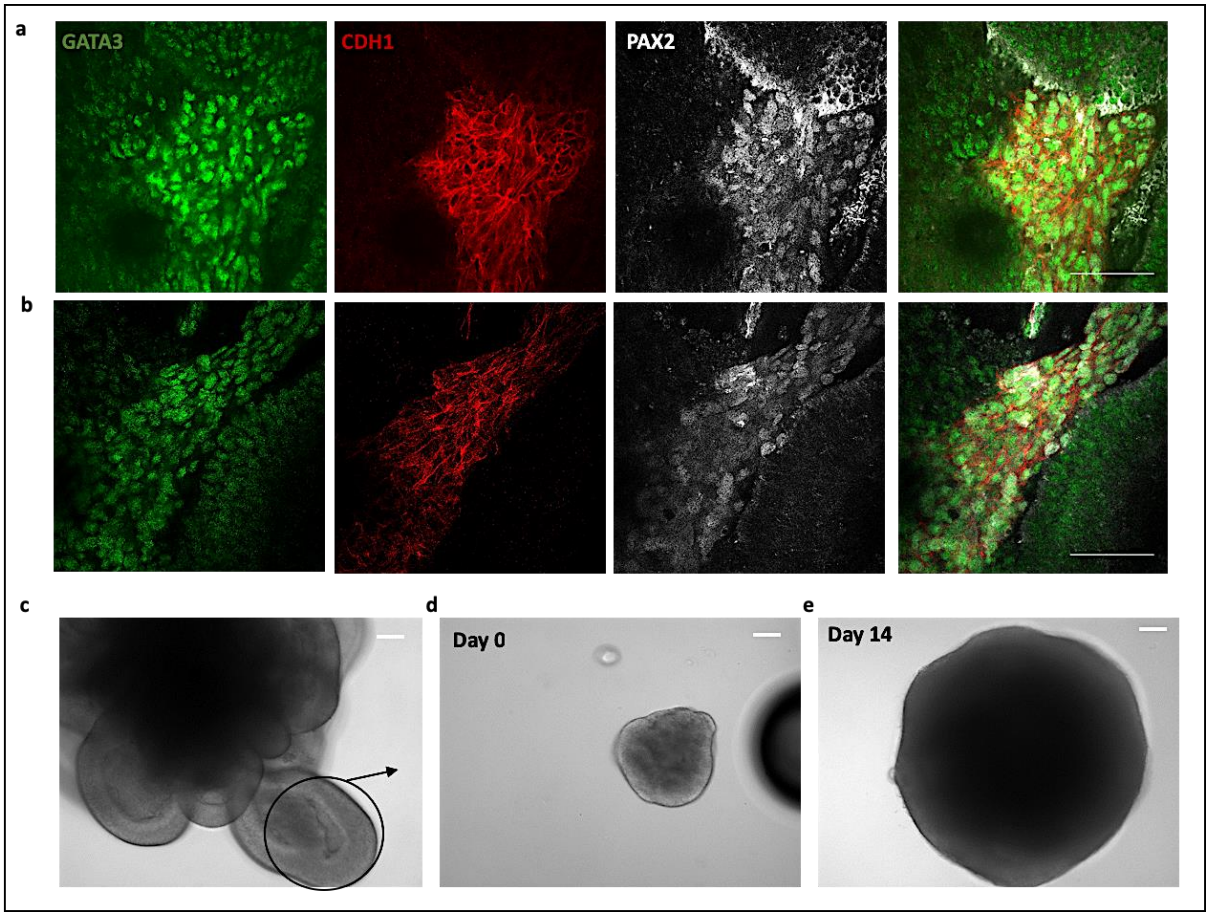

Figure 7.6. a, b) Immunostaining of the spheroids obtained by applying the Taguchi protocol on hiPSCs. At the end of the differentiation protocol, the spheroids showed expression of GATA3, CDH1 and PAX2. c) Single buds were isolated from the spheroids after the end of the differentiation. d) The isolated bud on day 0 of gel culture; e) the same bud after 14 days of gel culture, no branching was seen. Scale bar is 100 µm. NB: PAX2 staining in (a) and (b) is suboptimal; the nuclear PAX2 staining is weak with quite high background. This staining problem is most likely due to the big thickness of the spheroids which might have been problematic for the antibody penetration.

The fully differentiated spheroids were obtained and single buds were dissected from its periphery and cultured in the same conditions that were used to induce branching in embryonic mouse UBs and hiUBs obtained from the Takasato protocol; no branching was observed in these isolated structures until the end of the treatment duration (14 days) (n=3, each repeat contained 10 isolated hiUBs obtained from one run of differentiation; a total of 30 isolated hiUBs were examined; figure 7.6 c-e); hiUBs obtained from Takasato protocol were cultured in parallel and were able to branch which excludes insufficiency of the culture conditions (figure 7.7).

a

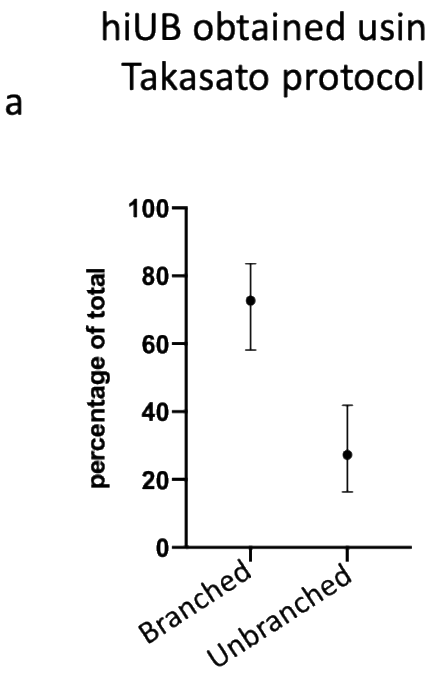

b

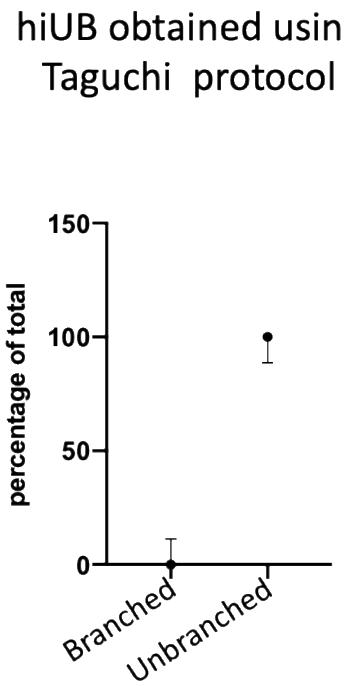

c

	Proportion of positive results (forming ramified tree)	95% confidence interval
hiUB obtained using Takasato protocol	72.7% (32/44)	58.2%, 83.7%
hiUB obtained using Taguchi protocol	0.0% (0/30)	0%, 11.4%

Figure 7.7. a, b) Graph illustrates the 95% confidence interval for obtaining branched (or unbranched) isolated hiUBs in gel a) using the Takasato protocol and b) using the Taguchi protocol; data are presented as mean, upper and lower limits of confidence. c) The table shows the 95% confidence interval (Wilson/Brown; see section 2.16) for obtaining branched tree from isolated hiUB using the two different protocols. n= 44 for hiUBs obtained using the Takasato protocol and 30 for hiUBs obtained using the Taguchi protocol.

7.6 Reproducing Taguchi and Nishinakamura protocol for obtaining miUBs:

The Taguchi protocol was originally developed using mESCs; thorough *in-vivo* and *in-vitro* analyses were employed to develop it with meticulous optimisation to every single step included and then transferred to hiPSCs.

When I tried to recapitulate their human protocol, surprisingly the resulting iUBs did not branch when cultured isolated in Matrigel and treated with branching inducing growth factors. Their experiment to evaluate the branch-competence of the obtained hiUB was set up in a quite different way from what I did. Instead of isolating single hiUBs and inducing them to branch in gel, they transferred the whole spheroid obtained at the end of step 7 of differentiation to Matrigel and treated it with branching inducing factors; they believed that the iUBs underwent initial elongation and bifurcation in the first 7 days of gel culture but that further branching morphogenesis was not observed. Spheroids obtained after step 7 of differentiation show multiple growing buds from all around their peripheries (figure 7.6.b). Transferring the whole spheroid to the branching inducing culture would make spotting and counting branching events confusing; it is hard to tell if there is any new bifurcation points or not in that model. In addition, other populations of cells, within the spheroids, could be supplying undefined additional factors that induce maturation and branching of the tip cells. After considering the difference in the way they evaluated the branch-competence of the hiUB, the branching capacity of the hiUB that they showed was modest, if we were to consider the number of newly formed branches from each individual bud.

In contrast, results obtained from miUBs were way more robust and even very close to what could be obtained from mouse embryonic UB, either in relation to their branching capacity or in their ability to induce nephron formation.

Aim:

I wanted to evaluate the Taguchi mouse protocol for obtaining branch-competent miUBs and organised renal organoids from mESCs. Having the mouse protocol working in the expected way would possibly imply the efficiency of the protocol but the insufficiency of its adaptation to hiPSCs.

The availability of mouse embryonic kidneys would allow for comparing the obtained miUB to their embryonic counterparts but the limited availability of human embryonic tissue, and ethical considerations about their use, leads to extrapolating data from mouse to human which could be unreliable due to the inter-species difference.

7.6.1 Obtaining miUBs using the Taguchi protocol:

E14 mESCs were maintained on the surface of gelatine-coated culture dishes and were tested for the pluripotency markers OCT3/4, Nanog and increased alkaline phosphatase activity (figure 7.8 a-c); to start differentiation cells were dissociated and cultured in U-bottom low attachment plates to allow them to aggregate and form embryoid bodies before starting the differentiation protocol.

The seven steps of the differentiation protocol were applied to the embryoid bodies where the cells were first treated with Activin A for 1 day (step 1) to induce epiblast fate followed by 1.5 day of CHIR treatment (step 2), according to that protocol the duration of CHIR treatment has to be followed strictly to ensure obtaining AIM fate. A combination of RA, FGF9, and SB431542 was then added for 1 day (step 3) to obtain AIM mesoderm which was treated with RA, FGF9 and CHIR for 18 hrs (step 4) to derive $CXCR4^{+}/KIT^{+}$ WD progenitors (figure 7.8 a).

After the end of step 4, the developed spheroids were dissociated and were FACS analysed for the co-expression of CXCR4 and KIT. An average population of 30% was positive for these two surface markers (n=3; figure 7.8 d and g).

The positive population was sorted, and the recovered cells were re-aggregated then the differentiation was continued for further three days to induce maturation of the developed WD progenitors into E11.5 UBs. During these three days, the WD progenitors were first treated with RA, FGF9, CHIR for 1 day (step 5) then GDNF was added to the previous combination of growth factors for 1 day (step 6) and finally a combination of RA, CHIR and GDNF was used for 1 day (step 7).

Similar to the human protocol, after step 5, the spheroids started to show outgrowing buds which increased in size and number after step 6 and 7. It is noteworthy that skipping the sorting step was possible, by shifting the spheroids from step 4 medium to step 5 medium directly, and spheroids still developed outgrowing buds (n= 4, in each repeat six different spheroids were included, all of them showed budding from their periphery without prior FACS); indeed spheroids that were shifted from step 4 to step 5 without sorting developed more buds compared to those seen in sorted re-aggregates probably because sorting involves dissociation of the spheroids which

would cause the sorted re-aggregated cells to take longer time to assemble themselves into structures.

Spheroids obtained at the end of the differentiation protocol (after step7) were examined for the expression of different UB markers and showed positivity to CDH1, PAX2, and GATA3 (n=5) suggesting successful induction of UB fate (figure 7.8 e, f).

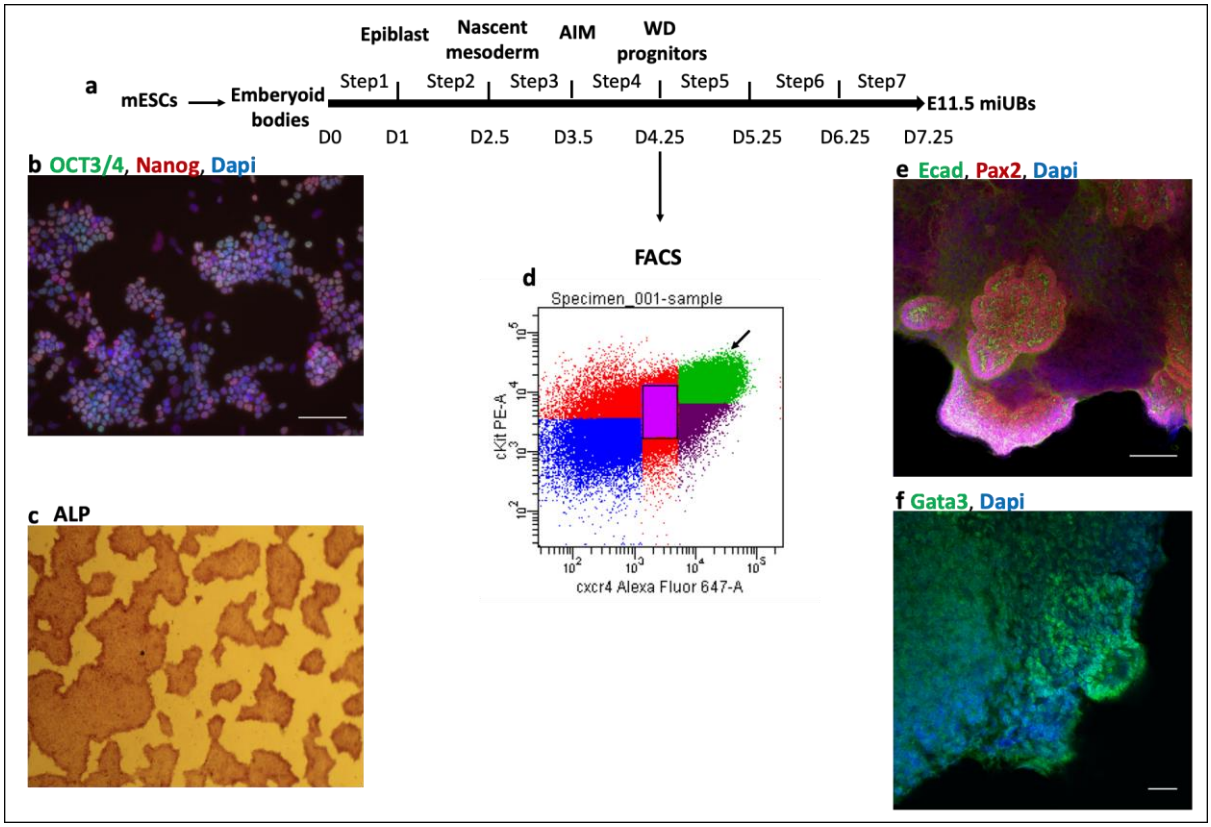

Figure 7.8. Differentiating mESCs into UBs using the mouse Taguchi protocol. a) Outline of the steps of the differentiation protocol. b, c) verification of the mESCs pluripotency by immunostaining for OCT3/4 and Nanog (b) or assessing alkaline phosphatase activity (c). d) FACS analysis of the cells after step 4, CXCR+/KIT+ cells were recovered and the differentiation protocol was continued. e, f) immunostaining of the developed spheroids at the end of differentiation showing positive staining for CDH1 and PAX2 (e) and for GATA3 (f). Scale bar is 100 µm.

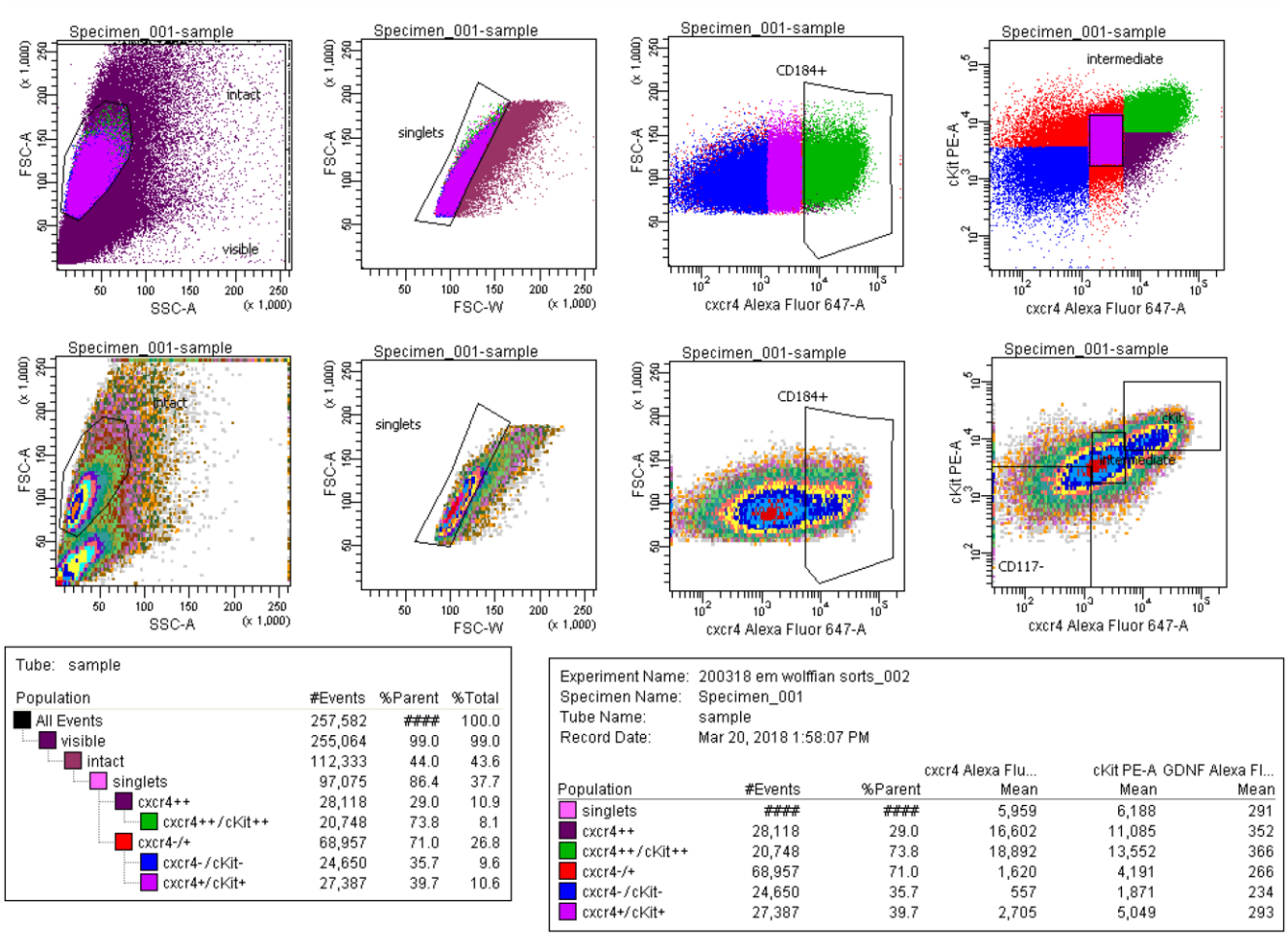

Tube: sample

Population	#Events	%Parent	%Total
All Events	257,582	####	100.0
visible	255,064	99.0	99.0
intact	112,333	44.0	43.6
singlets	97,075	86.4	37.7
cxcr4++	28,118	29.0	10.9
cxcr4++/cKit++	20,748	73.8	8.1
cxcr4-/+	68,957	71.0	26.8
cxcr4-/cKit-	24,650	35.7	9.6
cxcr4+/cKit+	27,387	39.7	10.6

Experiment Name: 200318 em wolffian sorts_002
Specimen Name: Specimen_001
Tube Name: sample
Record Date: Mar 20, 2018 1:58:07 PM

Population	#Events	%Parent	cxcr4 Alexa Flu... Mean	cKit PE-A Mean	GDNF Alexa Fl... Mean
singlets	####	####	5,959	6,188	291
cxcr4++	28,118	29.0	16,602	11,085	352
cxcr4++/cKit++	20,748	73.8	18,892	13,552	366
cxcr4-/+	68,957	71.0	1,620	4,191	266
cxcr4-/cKit-	24,650	35.7	557	1,871	234
cxcr4+/cKit+	27,387	39.7	2,705	5,049	293

figure 7.8.g. Gating strategy for sorting KIT+/CXCR+ cells (Wolffian duct progenitors) after 6.25 days of applying the Taguchi protocol of differentiation to mESCs. The intact singlets represented 37.7% of the total analysed events. Three distinct populations were sorted from these intact singlets: $KIT^{-}/CXCR4^{-}$ (double negative cells 25.4% of the intact singlets; 24,650/97,075), $KIT^{+}/CXCR4^{+}$ (cells with moderate positivity to both markers 28.2%; 27,387/97,075), and $KIT^{++}/CXCR^{++}$ (cells highly positive to both markers 21.4% of the intact singlets; 20,748/97,075). Cells from the three different groups were recovered and cultured separately, and the differentiation protocol was continued. At the end of the differentiation protocol, the $KIT^{+}/CXCR4^{+}$ and the $KIT^{++}/CXCR4^{++}$ cells both formed spheroids with budding UBs from all around. When UBs from the two groups were cultured in branching inducing mixture, they formed branched collecting trees. Thus, these two groups were considered as $KIT^{+}/CXCR^{+}$ (49.6% of the intact singlets) Wolffian duct progenitors. The spheroids formed from the $KIT^{-}/CXCR^{-}$ cells did not show any outgrowing buds; these cells represented the negative population.

7.6.2 Evaluating branch-competence in gel cultures:

To evaluate the capacity of miUB to undergo iterative branching and form ramified inter-connected tree, the spheroids that developed outgrowing buds at the end of step 7 differentiation were obtained and single buds were dissected from its periphery

(figure 7.8 a); the isolated buds were cultured suspended in Matrigel and treated with a combination GDNF, FGF1, CHIR and RA. The isolated miUBs showed branching capacity comparable to what was seen with isolated embryonic UBs. After 7 days in culture, the miUB, which started as single isolated bud, developed into a tree of branched tubules (n= 4, each repeat contained 8 different miUBs; a total of 32 miUBs were examined; 31/32 branched; figure 7.9 b,d).

7.6.3 Testing the possibility of propagating miUBs in gel cultures:

The ability of the obtained miUBs to branch in gel upon treatment with branching inducing factors has been reported in the original protocol, but it has never been investigated if these iUBs could be propagated and expanded for longer periods in gel cultures.

Aim:

Here, I wanted to examine how long could the miUBs keep their branching capacity in gel and to test if I can propagate them in culture for some passages.

Results:

I extracted the branched tree after it has been cultured in the gel for seven days and dissected single tips from its periphery. The newly isolated miUBs were then cultured dipped in Matrigel and treated with the branching inducing mixture of growth factors. I was able to isolate as many as ten new miUBs from one branched miUB-tree, many more could even be dissected but that was enough for my purpose, and passaged them, individually, into new gel cultures, as second-generation miUBs (figure 7.9 d,e). Similar to the 1st generation miUB, originally obtained at the end of the differentiation protocol, the 2nd generation miUB underwent iterative branching forming a whole new branched tree after 7 days in culture (n=4, each repeat included 10 different 2nd generation miUBs all obtained from one 1st generation branched tree; a total of 40 2nd generation miUB were examined; 40/40 branched). The same process was repeated again with the branched 2nd generation miUBs which were extracted, cleaned from the surrounding Matrigel, and new tips were isolated from its periphery for passaging in gel culture (3rd generation miUBs). The isolated 3rd generation miUBs still maintained high capacity of branching and formed branching collecting system after 7 days of

culture under the treatment of branching inducing mixture (n=3, each repeat included 10 different 3rd generation miUBs; a total of 30 2rd generation miUBs were examined; 26/30 branched; figure 7.9 g,f).

When stained for UB markers, the branched trees from the three different generations of miUB showed positive staining for the UB markers PAX2, CADH1, GATA3 and CK8 (figure 7.10).

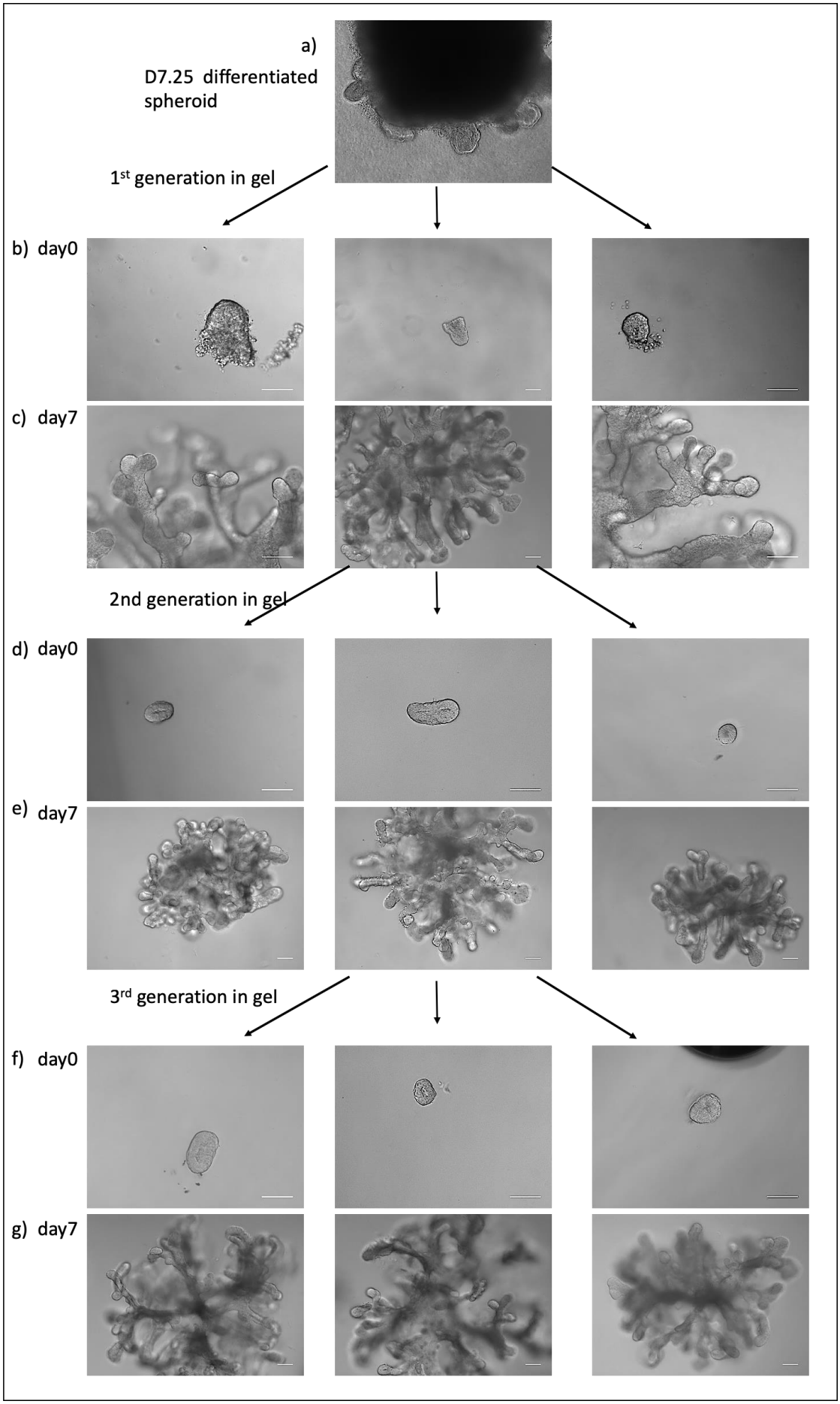
a)
D7.25 differentiated spheroid
1st generation in gel
b) day0
c) day7
2nd generation in gel
d) day0
e) day7
3rd generation in gel
f) day0
g) day7

h

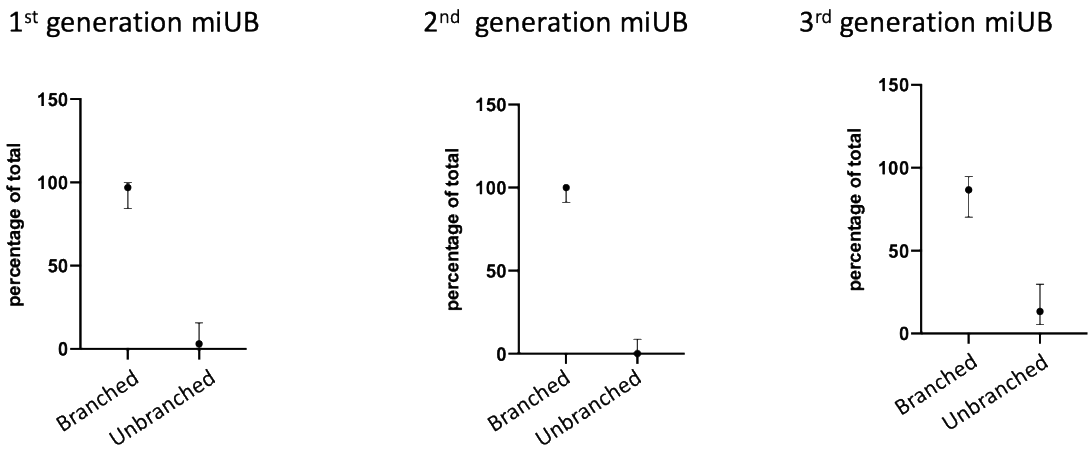

i

	Proportion of positive (formed branched tree)	95% confidence interval
1st generation miUB	96.9% (31/32)	84.3%, 99.8
2nd generation miUB	100% (40/40)	91.2%, 100%
3rd generation miUB	86.7 (26/30)	70.3%, 94.7

Figure 7.9. Illustration of the gel passaging experiment. a) A spheroid obtained from the end of the differentiation protocol was dissected to isolate single UBs. The isolated miUBs were cultured in gel as 1st generation UBs. b, c) Show the isolated miUBs on day 0 (b) and day 7 (c) of gel culture. The ramified structure obtained in (c) was extracted from gel and single miUBs were isolated and passaged in the gel as 2nd generation miUBs, (d) shows day 0 and (e) shows day 7 of gel culture. The process was repeated, structures obtained in (e) were extracted from gel and single miUBs were dissected from the periphery and were cultures as 3rd generation miUBs. f, g) Show the 3rd generation miUBs on day 0 (f) and day 7 (g) of culture. Scale bar is 100 µm. h) Graph shows the proportion of the isolated miUBs that branched and formed ramified trees in gel of the total examined miUBs; data are presented as mean, upper and lower limits of confidence interval. i) The table shows the 95% confidence interval (Wilson/Brown; see section 2.16) for obtaining branched tree from the three different generations of miUB. n= 32 for the 1st generation miUB group, 40 for the 2nd generation miUB group, and 30 for the 3rd generation miUB group.

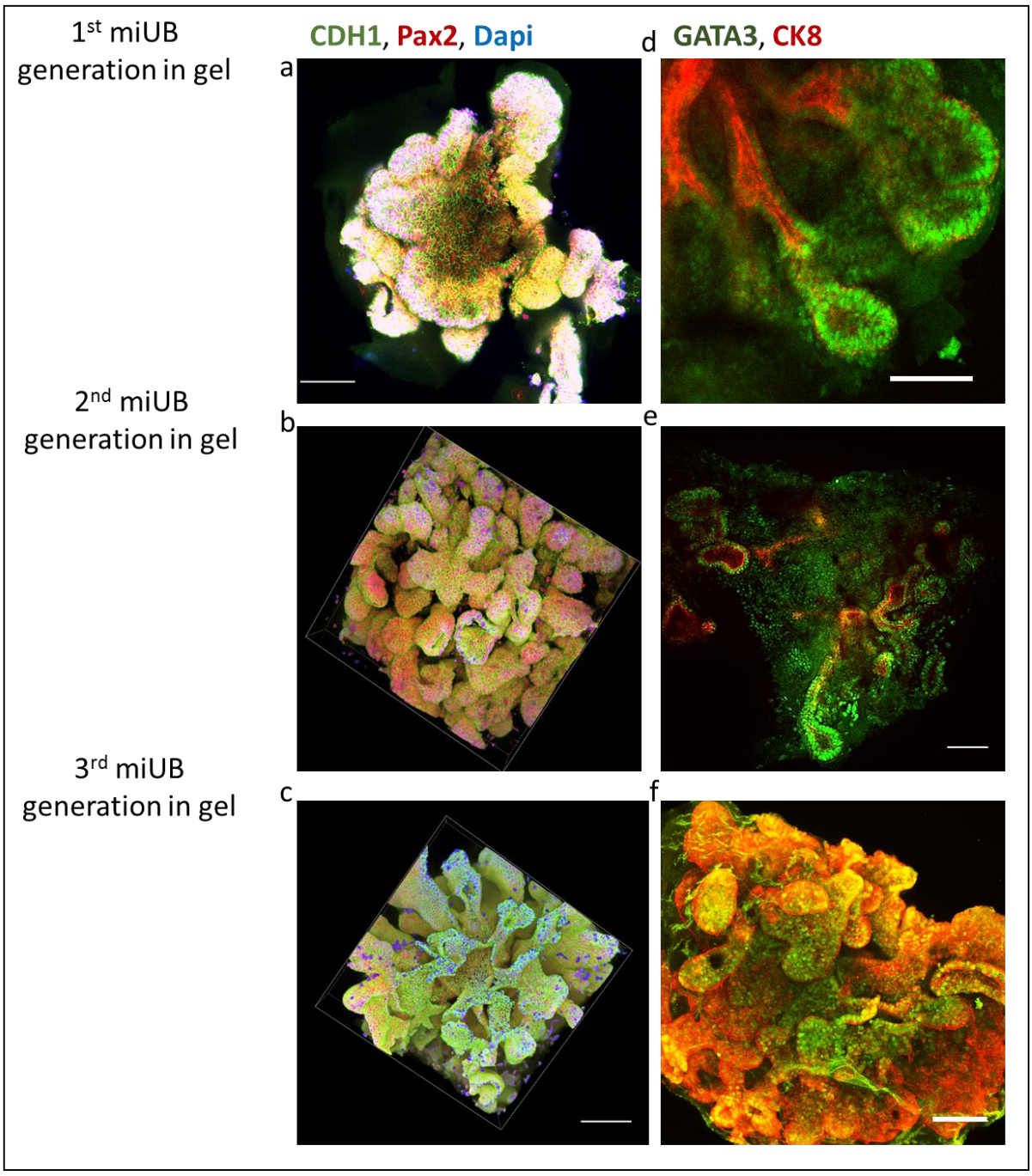

Figure 7.10. Immunostaining results for the ramified trees obtained from the three different generations of miUB cultures a-c) show staining for CDH1, PAX2 and DAPI, d-f) show staining for GATA3 and CK8. Scale bar is 100 µm.

7.6.4 Examining the ability of miUB to induce nephron formation and form organised renal tissue when mixed with embryonic MM:

Next, I wanted to investigate if the obtained miUBs possess the functional capacity to induce nephrogenesis and form complex organised kidney structures arranged around a single collecting system. miUB was obtained by dissection from a spheroid at the

end of the differentiation protocol (after step 7), then aggregated with freshly isolated embryonic MM. Embryonic MM was obtained by microdissection of E11.5 metanephric rudiments to exclude UBs. To ensure that any branching collecting system is originating from the miUB, and not from embryonic UB cells that could be contaminating the MM cells, I first tried to label the miUBs with cell tracker red before mixing it with the MM, however, I noticed that the red label spread from the tagged iUB to the surrounding MM cells after 24 hrs of co-culture. As an alternative strategy to be sure no UB was being carried over with the MM, I used only kidney rudiments from which I was able to remove the embryonic UB intact. In addition, the collected MM was dissociated and passed through a cell strainer to ensure obtaining single cells. In this case, if any UB cells were not excluded during dissection, they would be dispersed into single cells and thus would be unlikely to result in a structure with single collecting system.

The miUB was able to branch and induce nephron formation making an organised renal organoid very similar to Ganeva-style organoids that could be obtained by mixing embryonic MM with embryonic UB (Ganeva, Unbekandt and Davies, 2011); the developed nephrons appeared connected to the central collecting system (n=2; figure 7.11).

I next wanted to test if iUB cultured in a gel and then recovered from it could still maintain its ability to make realistic kidney structures when mixed with embryonic isolated MM; 1st generation branched iUBs were extracted from Matrigel, after 7 days of gel culture, single iUBs were isolated from the branched tree, cleaned as possible from the surrounding gel and were aggregated with freshly isolated embryonic MM cells. The gel-extracted iUBs maintained their ability to induce nephron formation and the re-aggregated cells formed renal organoids with single collecting system (n= 3).

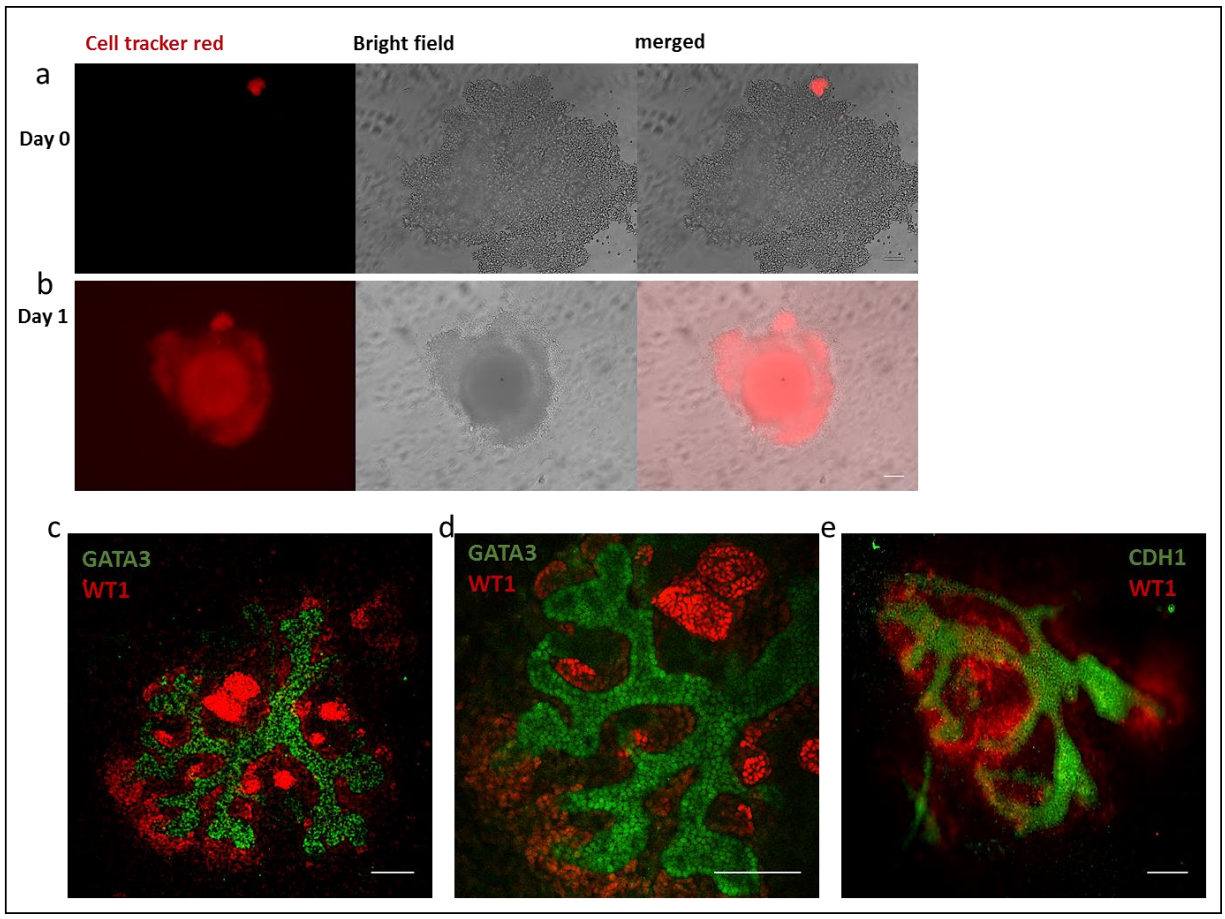

Figure 7.11. Mouse iUBs (obtained by applying the Taguchi protocol to mESCs) induce nephron formation. a,b) Cell tracker red was used to label the isolated miUB before reaggregating it with embryonic MM, on day 0 (a) the red label was confined to the isolated miUB but on Day 1 (b) the whole reaggregated structure was stained with the dye. c, d) Organised kidney tissue constructed by co-culturing miUB and embryonic MM for 7 days. The constructed tissue showed condensed cap mesenchyme around the periphery of the tissue and formed glomeruli towards the centre. e) 4 days cultured miUB with embryonic MM stained for CDH1 and WT1. Scale bar is 100 100 μm.

7.7 Can miUB be reprogramed into Urothelium?

During normal kidney development, after the outgrowth of the UB from the WD and its invasion into the MM, the UB sub-divides into proximal part that invaginates into the MM and undergoes branching morphogenesis to form the intra-renal collecting duct tree, and distal part, the stalk of the ureteric bud, that elongates without branching and develops into the epithelial layer of the definitive ureter (Bohnenpoll and Kispert, 2014).

The type of mesenchyme that surrounds the stalk part of the UB has a distinct developmental origin and distinct fate from that of the MM, which surrounds the tip part. The MM provides all signals necessary for inducing proliferation and branching of the UB tip which eventually form the intra-renal collecting duct tree, at the same time, it responds to inductive signals emanating from the growing tips and undergo mesenchymal to epithelial transition to form nephrons. While the mesenchyme surrounding the UB stalk, tail-bud derived mesenchyme which is characterised by the expression of TBX18, provides signals to elongate without branching and eventually differentiates into smooth muscle cells and fibroblasts which form the smooth muscle layer and the stromal layer surrounding the ureter (Airik *et al.*, 2006; Brenner-Anantharam *et al.*, 2007; Bohnenpoll *et al.*, 2013).

Studies have shown that UB cells are multipotent cells that have the ability to differentiate towards extra-renal ureteric epithelium or intra-renal CD. The stalk part of the UB can branch and induce nephron formation when transplanted into the MM (Sweeney, Lindstrom and Davies, 2008), on the other side, isolated UB tips will stop branching, elongate and express the ureteric epithelium (urothelial) specific marker, Uroplakin, when transplanted into the ureteric mesenchyme (Bohnenpoll and Kispert, 2014; Mills *et al.*, 2017); these findings show that the type of mesenchyme controls the type of UB morphogenesis leading to either branching morphogenesis to form intra-renal collecting system, in the case of the proximal part of the UB, or ureteric morphogenesis, straight unbranched tube lined with highly specialised epithelium, in the case of the distal part of the UB.

BMP4, a member of TGFβ-superfamily, has been shown to play an important role in ureteric morphogenesis and in inducing urothelial differentiation. It is normally

secreted by the peri-Wolffian mesenchyme, the type of mesenchyme that envelops the Wolffian duct, and by the $TBX18^{+}$ mesenchyme surrounding the UB stalk. BMP4 has been shown to inhibit UB outgrowth, budding, and branching morphogenesis. Genetic studies and *in-vitro* studies, performed on metanephric explants, showed that *Bmp4* loss of function or inhibition leads to ectopic budding from the Wolffian duct or branching from the distal UB stalk and disruption of urothelial and smooth muscle differentiation (Miyazaki *et al.*, 2000, 2003; Michos *et al.*, 2007; Wang *et al.*, 2009; Nishinakamura and Sakaguchi, 2014). In addition, exogenous BMP4 treatment has been shown to induce ureteral morphogenesis, to elongate unbranched and express the urothelial marker Uroplakin, in intra-renal UB tips, fated to undergo branching morphogenesis and form collecting tubules, in *in-vitro* cultures of metanephric kidney rudiments (Brenner-Anantharam *et al.*, 2007).

The recent modification that enabled the production of Mills-style renal organoids (see chapter 6 for more details) from mouse embryonic kidneys (equipped with a ureter-like exit) was based on applying a local BMP4 source to re-program one of the ramified UB branches to acquire urothelial fate and serve as an exit while the rest of the tree induces nephrons forming an organised renal tissue (Mills *et al.*, 2017).

Aim:

In the previous section, I showed that isolated miUB could be induced to branch and recapitulate branching morphogenesis, and are able to induce nephron formation if combined with MM. Whether the obtained iUB has the plasticity to develop into urothelium or not has not been investigated before. Here, I wanted to see if the iUBs could be reprogramed into urothelium and recapitulate ureteric morphogenesis if the surrounding environment changed, mimicking what happens during normal development. If this proved to be feasible, a ureter-like exit could be added to the current model of renal organoids obtained from mESCs following the same logic that was developed in Mills et al, 2017 and, in principle, it might be possible to transfer it to hiPSC-derived organoids.

7.7.1 Results:

To examine the ability of miUBs to acquire ureteric fate and express Uroplakin, mESCs were differentiated into miUB (following the 7 steps of differentiation), then single

miUBs were isolated and cultured in Matrigel for 7 days, under the treatment of branching inducing factors. Afterwards, the branched-iUB tree was extracted from the gel and 2nd generation iUBs were isolated from it, as previously described in section 7.6.3, cultured suspended in Matrigel and treated with the branching inducing growth factors in presence of BMP4. The branching inducing growth factors were added to support the growth and prevent apoptosis of the isolated UBs, while BMP4 was added to these growth factors to test the ability to reprogram these structures into ureters that express Uroplakin. At the same time, a control group was cultured under the same conditions but in absence of BMP4.

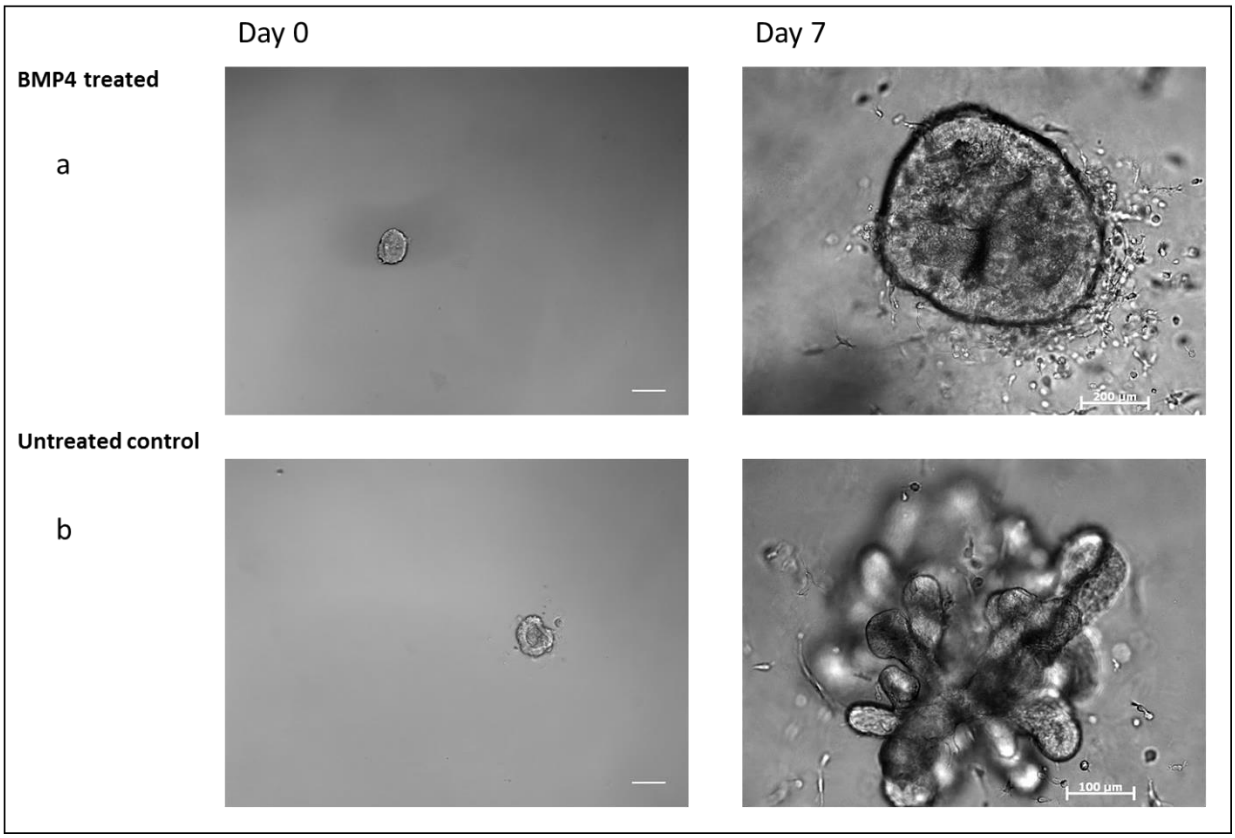

Figure 7.12. Reprograming miUB into extra-renal ureter like structure. mESCs were differentiated into miUBs by applying the Taguchi protocol of differentiation. the plasticity of the obtained miUB to obtain either extra-renal ureter like fate or intra-renal branched tree was examined by culturing isolated miUBs in gel in presence of branching inducing growth factors plus or minus BMP4. a) miUBs treated with BMP4 stopped branching and grew thicker similar to what happens in the extra-renal stalk b) control miUB exposed to the same treatment minus BMP4 formed a branched tree. Scale bar is 100 µm.

The BMP4 treated miUBs grew thicker and stopped branching while the control iUBs branched as usual (n= 3, each repeat included 5 individual miUBs; a total of 15 miUBs were examined; figure 7.12). In addition, Uroplakin expression was highly upregulated in the treated group compared to the non-treated controls suggesting successful reprograming of miUBs into urothelium (n= 5; figure 7.13). This showed that miUB do possess the plasticity to be reprogramed into ureteric epithelium and indicated their close similarity to embryonic UBs as they can efficiently recapitulate the major functional abilities of the embryonic UB: branch and recapitulate branching morphogenesis, induce nephron formation and also can be reprogramed into urothelium and recapitulate ureteric-morphogenesis.

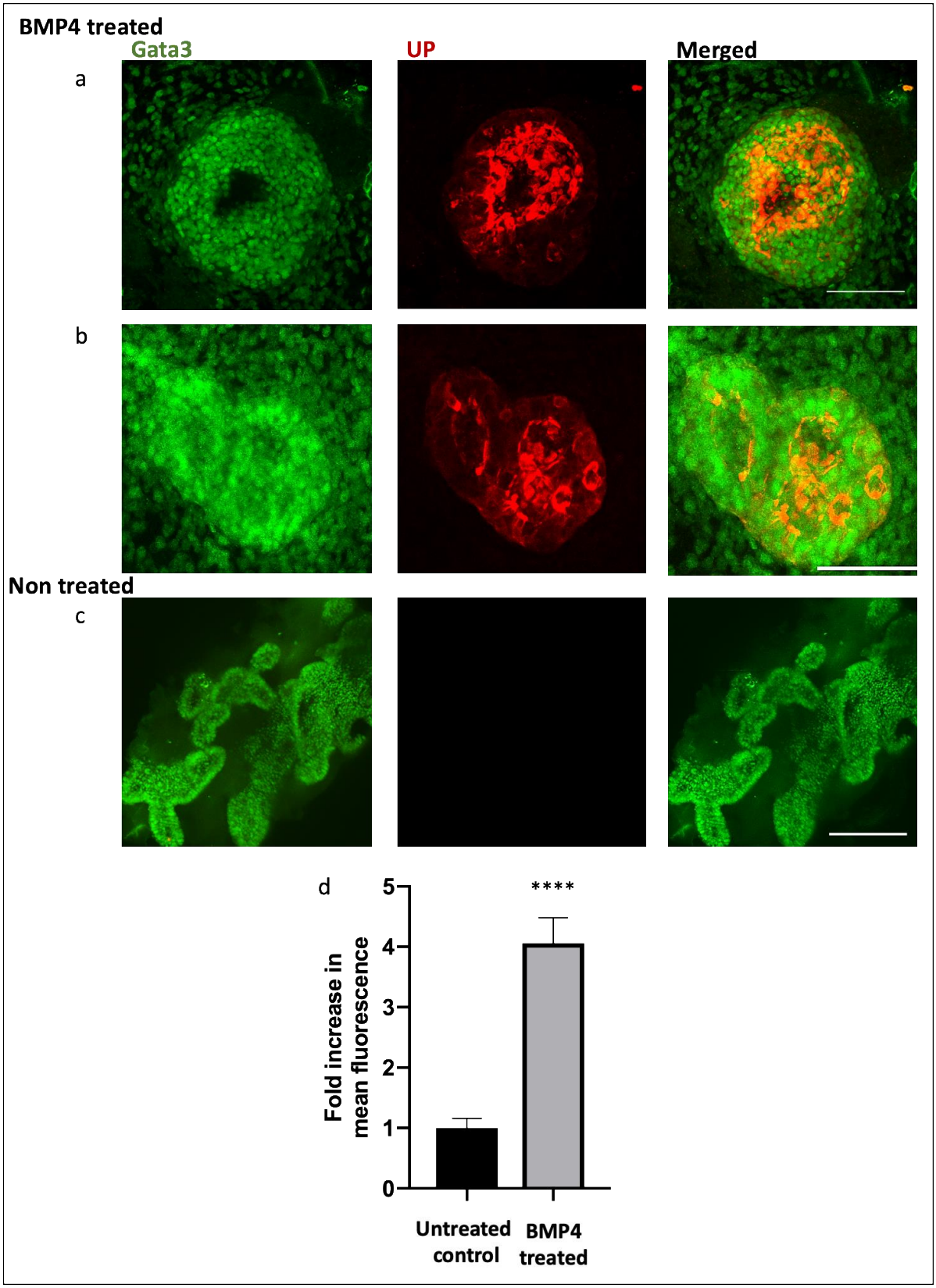

Figure 7.13. a, b) BMP4-treated miUBs expressed the urothelial marker Uroplakin. c) Non-treated control stained negative for Uroplakin; UP: Uroplakin. Scale bar is 100 µm. d) Graph illustrates the increase in Uroplakin mean fluorescence in response to BMP4 treatment; p value <0.0001; n= 5.

7.8 Discussion:

I previously showed that results for obtaining UB fate using the Takasato protocol were variable; I also showed that when hiUBs obtained from that protocol were isolated and re-aggregated with sorted nephron progenitors they failed to branch or induce nephron formation. For these reasons, I wanted to further evaluate these structures and investigate their branching capacity in an MM free culture condition.

I first determined that the combination of GDNF, FGF1, CHIR and RA was optimum for inducing robust branching in isolated embryonic UBs. Yuri et al showed in their study that treatment with GDNF, FGF1 and CHIR was enough to induce “extensive” branching in UBs isolated from mouse embryonic kidneys (Yuri et al, 2017). However, according to my results, in the absence of RA, the branching that was induced in response to this combination of growth factors was inconsistent, slower and limited compared to the treatment with the same plus RA. The importance of RA in maintaining RET expression in the UB tips has been highlighted in previous studies; it has been shown that supplying exogenous RA upregulates RET expression in metanephric kidney explants in a dose dependant manner and enhances branching morphogenesis (Moreau *et al.*, 1998). Another study has shown that blocking RA receptors, via generating dominant-negative mouse models, abolishes RET expression in UBs and hence disturbs ureteric bud formation and branching morphogenesis (Rosselot *et al.*, 2010). The limited and inconsistent branching of the isolated UBs when treated with GDNF, FGF1 and CHIR might be due to loss of RET expression in the absence of RA.

I next showed that isolated hiUBs obtained from the Takasato protocol were able to form ramified structures with expression pattern characteristic to branched collecting tree in response to the treatment with GDNF, FGF1, CHIR and RA, as was optimised in embryonic UBs. Despite the variability in obtaining UB fate using this protocol, these data suggest that the obtained hiUBs are branch-competent. The branching process was, however, slower and the extent of branching was limited compared to mouse embryonic UBs. This could be seen as an interspecies difference. Generally, the human organogenesis period is much longer than that of the mouse. More specifically UB development in human starts at CS13 (28-32 days post ovulation), undergoes 1-2 generations of branching by CS16 (37- 41 days post ovulation) and continues roughly

until weak 37 when nephrogenesis is completed (Lindström *et al.*, 2018; Ryan *et al.*, 2018). This could by no way be compared to that of the mouse. The ramified hiUB tree showed expression of the specific UB markers CK8, CDH1, GATA3 and RET.

In the previous chapter, I tried to construct organised renal tissue by mixing one of the hiUBs with nephron progenitors, but that was not successful. One possible explanation to that might be the absence of stromal renal progenitors from that re-aggregate. Data obtained here from mouse embryonic UBs suggested the importance of RA for proper branching of the isolated UBs and data from other studies also stressed on the importance of RA for RET expression as discussed earlier. RA has been shown to be produced in renal stromal cells by retinaldeyde dehydrogenase 2 and a model has been proposed where RA, secreted from renal stromal cells, signalling through RA receptors, in UB cells, regulates RET expression during both bud formation and branching morphogenesis (Rosselot *et al.*, 2010). Based on this, it is likely that the absence of stromal cells from the re-combination experiment has led to unsuccessful experiment. This also fits with Taguchi and Nishinakamura's results where they showed that mixing miUB with mouse nephron progenitors showed poor development unless stromal progenitors were added to the cultures. It is therefore expected that adding stromal progenitors at the re-aggregation step could improve the result. It is also likely that culturing hiUBs in the branching promoting mixture is inducing further maturation to these cells; it would be interesting to repeat the construction experiment using branched tubule, after an initial treatment with the branching inducing mixture, instead of hiUB that has freshly been isolated from the culture.

I tried to reproduce the Taguchi and Nishinakamura protocol for obtaining hiUBs. I evaluated the differentiated cells at the middle of the differentiation and at the end of the differentiation protocol. Results of the FACS analysis at the middle of the differentiation suggested successful obtaining of WD progenitors (CXCR4+/KIT+ cells) and immunostaining at the end of the differentiation suggested successful obtaining of hiUBs (CDH1+/PAX2+/GATA3+). In addition, morphologically, the obtained spheroids showed multiple outgrowing buds at the end of the differentiation. However, sectioning of the spheroids is recommended for better staining and imaging as the obtained spheroids were very thick. This could help to confirm the expression of the UB markers, especially PAX2, the staining result of which was quite weak. Also, qPCR

would help to confirm and quantify the expression of these markers. When single buds were manually dissected from the periphery of the spheroids, at the end of the differentiation protocol, and cultured separately in branching inducing culture conditions they did not branch.

Using the mouse version of the Taguchi and Nishinakamura protocol, I efficiently obtained branch-competent miUBs. The ability of these miUBs to branch was comparable to their embryonic counterpart; most importantly when those developed miUBs were mixed with embryonic MM they induced nephron formation in an organised renal structure.

Additionally, I showed that miUBs could be propagated in gel for few passages. This could be a powerful tool for providing branched collecting trees that could serve as a model for studying different physiological aspects of the collecting duct cells; it would be interesting to examine if hiUBs could also be propagated in such a way.

Embryonic UBs have the plasticity to acquire extra-renal urothelial fate if surrounded with peri-Wolffian mesenchyme or treated with exogenous BMP4 (Brenner-Anantharam *et al.*, 2007; Bohnenpoll and Kispert, 2014). A distinctive property that has been exploited to add a ureter-like exit to the organoids obtained from dissociated embryonic kidneys (Mills *et al.*, 2017). Here, I showed that the obtained miUBs also possess plasticity to acquire urothelial fate and express UP. This implies that the current model of renal organoids obtained from mESCs could be further improved by locally treating one of the collecting tree branches with BMP4 and inducing it to a urothelial ureter-like exit thus yielding an organised renal tissue equipped with a ureter.

Chapter 8

8 General discussion

Discussion:

Protocols for directed differentiation of hiPSCs towards MM fate (Taguchi *et al.*, 2014; Freedman *et al.*, 2015; Morizane *et al.*, 2015; Garreta *et al.*, 2019), UB fate (Xia, Nivet, Sancho-Martinez, *et al.*, 2013; Taguchi and Nishinakamura, 2017) or the simultaneous production for both of them (Takasato *et al.*, 2013, 2015) have been established and have enabled the generation of renal organoids. The primary goal of this project was to evaluate the currently available model of renal organoids with respect to its efficiency, functional abilities and its suitability to detect nephrotoxicity, then to try to develop techniques to improve it.

8.1 Evaluating renal organoids with respect to the efficiency in nephron formation and functional ability of the formed nephrons:

I successfully reproduced the Takasato protocol for making renal organoids. I obtained renal tubules with gene expression patterns characteristic of the UB and the main renal cell types constituting the nephron. I then moved on to evaluate the functional ability of the obtained organoids. Kidney organoids are potential scaffolds for studying disease pathogenesis and developing new therapeutic options for them (Freedman *et al.*, 2015; Gupta, Susa and Morizane, 2017; Harder *et al.*, 2019). They also represent a possible model for studying drug interactions and testing the toxic potential of substrates in 3D tubular structures with complex multicellular components (Kandasamy *et al.*, 2015; Bajaj *et al.*, 2018) in addition to the increasing hope for their use in regenerative therapy (Kim, Nam and Yang, 2018; Combes *et al.*, 2019; Garreta *et al.*, 2019). Clearly, the potential use of organoids in any of these applications is conditioned by their functional capacity. Using fluorescent substrates, I reported that 3D hiPSCs-derived renal organoids express functional anion and cation transporters, a finding that is of particular importance for the use of these organoids in studying drug interactions and nephrotoxicity screening purposes as they are involved in the pharmacokinetics of wide arrays of drugs (Nigam *et al.*, 2015; Sanjay K. Nigam, 2015). Renal tubular function capacity of the organoid might be exploited to improve quality of the conventional dialysis methods if we were able to fabricate cell-based dialysis membranes that would be able to remove organic cations and anions (Narayanan *et al.*, 2013; Pollock, 2013; Oxburgh *et al*., 2017; Masereeuw and Stamatialis, 2017).

8.2 Cryopreserving renal differentiated cells

I developed and optimised a technique to cryopreserve and revive hiPSC-derived renal cells at two different differentiation points (12 days of differentiation and 18 days of differentiation); I showed that the revived cells possessed organic anion and cation transport-ability and were able to detect Cisplatin toxicity. The possibility of cryopreserving and successfully reviving renal differentiated cells has not been investigated before. Cryopreservation could be a useful tool for different applications of hiPSC-derived renal organoids as it shortens the time needed for obtaining organoids from 20 days to 9 days (or 3 days in the case of cryopreserving 18-day differentiated cells) in addition to saving the time and effort needed to maintain hiPSCs. Collectively the data suggest that cryopreserved renal cells could enable large scale production of renal organoids which could be employed for nephrotoxicity assays. Moreover, a recent study that evaluated variability between different renal organoids concluded that differences in technical parameters, between different runs of differentiation, is the biggest source of variability between renal organoids (Phipson *et al*., 2019). The ability to cryopreserve renal differentiated cells might help to minimise these variations. A cryopreserved stock of renal differentiated cells, that is obtained from the same differentiation runs, from which renal organoids are made on different occasions, to be used in downstream experiments and comparison purposes, could be a way to overcome run-to-run variability between organoids.

8.3 Constructing and evaluating a fluorescent reporter system to screen for nephrotoxic compounds using renal organoids:

Based on analysis of the transcriptomic data obtained from gentamicin treated renal differentiated cells, I identified *HMOX1* as a promising reporter of nephrotoxicity. Findings from other recent studies supported this result; a study performed on HPTEC cells did multiplex gene expression analysis and revealed that *HMOX1* induced the most significant response to increasing doses of the analysed drugs (Adler *et al.*, 2016). Similarly, another recent study, Bajaj et al presented *HMOX1* as a more sensitive indicator of tubular toxicity in hPSC-derived organoids in comparison to the conventional marker KIM1 (Bajaj, A. David Rodrigues, *et al.*, 2018). An *HMOX1*-fluorescent reporter-iPS cell line was constructed in my lab, based on my results. Working in collaboration with other lab members, I showed that organoids made from

the *HMOX1*-reporting-iPSCs can predict nephrotoxicity, at least when used with a range of concentrations and measurements done at more than one time point. We showed that the overall performance of the reporter cells was predictive for renal toxicity (see table 5.6 and the discussion of chapter 5 for more details).

We have assessed the performance of the reporter cells in renal-differentiated organoids but we expect that it could be also used to screen for toxicity in other organoid models since HMOX1 is a global oxidative stress marker and hiPSCs could be differentiated into all specialised cell types in the human body.

8.4 Steps towards improving the current model of renal organoids:

The inherent ability of renal progenitors to self-organise was the base for making renal organoids from hiPSCs, first, by directing the differentiation of hiPSCs into renal progenitors, then, re-aggregating the obtained progenitors and allowing them to self-organise into kidney tissue. However, relying solely on self-assembly lacks control over the spatial organisation of the cells and results in a quite chaotic tissue. Techniques for engineering an anatomically correct renal tissue from the disorganised organoid using dissociated mouse embryonic kidney cells have been developed sequentially (Ganeva, Unbekandt and Davies, 2011; Mills *et al.*, 2017) (see introduction of chapter 6 for more details). These techniques rely on their first step on isolating UB cells from the disorganised tissue. I developed a technique for live-tagging and isolating UB structures from surrounding cells and structures. I showed that conjugating GDNF protein to a fluorophore successfully labelled UBs both in embryonic mouse kidney explants and hiPSC-derived renal tissue and thus enabled their isolation. GDNF/488 could be a useful tool for isolating correctly differentiated UBs from other cell fates in a mixed culture. While I developed this procedure to enable organising renal organoids following steps described in Ganeva et al., 2010, it could equally fit with other *in-vitro* approaches of engineering kidneys as populating decellularized scaffolds and 3D bioprinting strategies, both of which need a source of pure specialised cells (Kim *et al.*, 2015; Montserrat, Garreta and Izpisua Belmonte, 2016; Oxburgh *et al*., 2017; Hueso *et al.*, 2019).

8.5 Comparing two different differentiation protocols with respect to their efficiency in producing branch-competent UBs:

Although the Takasto original protocol described obtaining both UB and MM fate simultaneously (Takasato *et al.*, 2015), I reported a degree of variability in obtaining UB fate using this protocol which led me to evaluate a different protocol that aims to differentiate hiPSCs mainly into UB cells, the Taguchi and Nishinakamura 2017 protocol, and compare between their efficiency in producing branch-competent UBs. I showed that hiUBs that were obtained from the Takasato protocol efficiently branched and formed ramified trees in response to the treatment with branching inducing factors. On the contrary, hiUB obtained from Taguchi and Nishinakamura protocol did not branch under the same culture conditions. Despite the variability seen in obtaining UB fate using Takasato protocol, the ability of the obtained UBs to branch and the pattern of expression seen in the branched structures suggest more mature structures compared to those obtained by the Taguchi and Nishinakamura protocol. In fact, the hiUB branching capacity that Taguchi and Nishinakamura have shown in their study was very limited and inconclusive.

The branched collecting trees that I managed to generate from hiUBs could be used as a model for studying different physiological aspects of collecting ducts and for disease modelling.

8.6 Current situation in renal organoids obtained from mESCs:

I developed a technique to propagate miUBs, obtained by using the Taguchi and Nishinakamura mouse differentiation protocol, in gel cultures for three generations without loosing the expression of different UB markers. This amplification method of miUBs provides ramified branched collecting ducts on a large scale. A quite relevant result has been shown in 2002 using mouse embryonic UBs, but with a different experimental design. In that report, researchers cut one branched tree of embryonic UB into thirds and allowed each third to further branch (Steer *et al.*, 2002). While that has been shown to amplify the obtained UB trees, starting each new generation by single tip structure allows for more robust amplification. Most importantly, there is the difference of applying this to tissue obtained from pluripotent cells rather than embryonic tissue. Encouragingly, when tips were isolated from the 1st generation ramified collecting tree, after its extraction from gel, were aggregated with dissected

embryonic MM it induced nephron formation and produced organised renal tissue. It is still to be evaluated if tips of the 2nd and 3rd generation branched tree would reserve this capacity or not.

Additionally, I successfully reprogramed the obtained miUBs into urothelial fate with positive Uroplakin expression, a characteristic expression marker of the extra-renal ureter. In principle, this would enable the achievement of Mills-style renal organoids, equipped with a ureter-like exit, by inducing ureter-fate in one of the collecting duct branches of the re-aggregated organised organoid that we can now obtain from mESCs.

8.7 Heterogeneity and variability of hiPSC-derived renal cells:

Different protocols have been developed based on recapitulating steps of renal development *in-vitro* to form renal organoids. These protocols agree on the importance of WNT and FGF signalling pathways in deriving the differentiation of renal progenitors, however, they differ in their detailed combination of growth factors, the exact duration of treatment with each growth factor, and the duration of the whole differentiation protocol. In fact, some key findings of these studies are contradictory to one another. For instance, according to Taguchi and colleagues, 2014 and Taguchi and Nishinakamura, 2017 it is not possible to obtain NPs and UB progenitors simultaneously since they develop from different spatial origins. According to these two studies, NPS needs 5-7 days of CHIR treatment while the permissive time window of CHIR treatment for obtaining UBs is restricted to 1.5 days; longer treatments would result in the failure of obtaining UBs. In contrast to these two studies, Takasato and colleagues reported the simultaneous induction of UB progenitors and NPs by adjusting the CHIR treatment to 4 days of differentiation followed by 8 days of FGF9 treatment. Garreta *et al.*, 2019 described a protocol almost similar to the Takasato protocol, with fine-tuning to the extra-cellular environment to allow for better development and maturation of the obtained organoids, and reported the specific derivation of nephron progenitors but not UB cells.

Since those studies were conducted in different laboratories and used different cell lines of hPSCs, mostly generated by different reprograming techniques, the discrepancy in the obtained data well reflects the heterogeneity of the genetic,

epigenetic and transcriptional features of the used cell lines (see section 1.4.3). Genetic heterogeneity could lead to discrepancy in the generated cell types upon differentiation, affect the functionality of the differentiated cells, or completely disrupt the differentiation capacity of the PSCs (Biendarra-Tiegs, Secreto and Nelson, 2019). In my study, I reported variability in obtaining UB fate (see section 3.3), in the percentage of the different nephron specific cell types compared to the total renal organoid (figure 3.13 a), and in the individual responses of organoids to nephrotoxic compounds (figure 5.4). Since my data were all obtained from a single cell line (AD3-01), the variability suggests heterogeneity within one iPSC line (see section 1.4.3). It is important to determine differentiation protocols that are eiffeciently reproducible between different cell lines. Having used only one iPS cell line in this study, reproducing these results in other cell lines might necessitate modifications to the described techniques; it is also possible that obtaining some results might not be achievable.

8.8 Species differences between human and mouse

One major limitation to the field of kidney tissue engineering has always been the paucity of histological and molecular data about human embryogenesis; this has led to the construction of most of the currently available differentiation protocols based on extrapolated data from mouse embryogenesis to human. Although a lot of data are conserved between mammals, there are some distinct molecular features characteristic to each species. An example to this is the difference in SIX1 expression and function between human and mouse (O'Brien *et al*., 2016), the differences in the expression of the anchor genes that have recently been reported (genes expressed in mouse within the nephron lineage and are used to identify key cell types in mouse kidney)(Lindström *et al*., 2018 a), and other differences in regulatory features which might lead to a difference in the process of nephrogenesis (Lindström *et al*., 2018 b). Even when ignoring the histological and the molecular differences, there are obvious anatomical discrepancies between mouse and human kidney including the difference in size, the duration of organogenesis, the timing at which nephrogenesis starts and ends and the UB branching starts and ends, and other features as lobe formation and organisation of the progenitor cells in the nephrogenic niche. In particular, the difference in timing and the duration of organogenesis makes transferring data, without actual defining parallel stages between the two different species, from mouse

to human more like a hit in the dark strategy. This discrepancy between mouse and human kidney development could explain why the Taguchi and Nishinakamura protocol achieved great results in mouse but not in human. Fortunately, recent studies aimed to tackle this problem by performing molecular and cellular characterisation of different stages of human kidney development through immunofluorescence staining, histologic analysis and transcriptomic profiling and contrasting the data to mouse kidney developmental stages (Lindström *et al*., 2018 a,b,c; Ryan *et al*., 2018). It is anticipated that this characterisation would enhance the field of kidney tissue engineering

8.9 Future directions:

My Initial trial to reconstruct an organised, Ganeva-style, renal organoid by re-aggregating sorted nephron progenitors and isolated hiUB did not succeed. However, I expect that culturing hiUBs in branching inducing factors promote their maturation and further differentiation. It worth trying to give hiUB obtained by applying the Takasato protocol an initial induction of branch-promoting growth factors before re-aggregating them with nephron progenitors. I expect a branched UB structure might be more able to induce nephron formation around its branched tips.

It would be interesting to evaluate if hiUBs obtained from Takasato protocol can be reprogrammed into a urothelial fate (as I showed with miUB); initial results show that those hiUBs stop branching, in a ureter-like manner, when treated with BMP4 but further investigation is still needed to confirm the result and assess the expression of Uroplakin. We expect that if we surround hiUB with nephron progenitors and stromal progenitors we might obtain a properly organised kidney structure to which an exit could be added by applying local BMP4 signalling.

The importance of renal stromal progenitors has been highlighted in different studies (Taguchi and Nishinakamura, 2017; Moreau *et al*., 1998; Rosselot *et al*., 2010). In the absence of stromal progenitors, the UB develops fewer and abnormal branches. Currently, there is no available protocol to specifically differentiate hiPSCs into renal stromal progenitors. It is expected that developing a protocol for obtaining stromal progenitors could positively impact the result of specified cell recombination and help

engineering an organised kidney organoid (Davies, 2017; Taguchi and Nishinakamura, 2017).

The robustness of the Taguchi mouse protocol in achieving miUBs with characteristics very close to the embryonic UB, ability to induce nephron formation in an organised renal structure, and plasticity to acquire a urothelial fate suggests that further adjustment to the human version of this protocol could lead to promising results.

9 References

References

Abrahamson, D. R. (1985) *Origin of the Glomerular Basement Membrane Visualized after In Vivo Labeling of Laminin in Newborn Rat Kidneys*, *THE JOURNAL OF CELL BIOLOGY*. Available at: https://www.ncbi.nlm.nih.gov/pmc/articles/PMC2113600/pdf/jc10061988.pdf (Accessed: 3 May 2019).

Abrahamson, D. R. *et al.* (2009) 'Cellular Origins of Type IV Collagen Networks in Developing Glomeruli.', *Journal of the American Society of Nephrology*, 20(7), pp. 1471–1479. doi: 10.1681/ASN.2008101086.

Abyzov, A. *et al*. (2012) 'Somatic copy number mosaicism in human skin revealed by induced pluripotent stem cells.' *Nature*, 492(7429), pp. 438–442. doi: 10.1038/nature11629.

Adler, M. *et al.* (2016) 'A Quantitative Approach to Screen for Nephrotoxic Compounds In Vitro.', *Journal of the American Society of Nephrology : JASN*. American Society of Nephrology, 27(4), pp. 1015–28. doi: 10.1681/ASN.2015010060.

Adler, S. and Chen, X. (1992) 'Anti-Fx1A antibody recognizes a beta 1-integrin on glomerular epithelial cells and inhibits adhesion and growth', *American Journal of Physiology-Renal Physiology*, 262(5), pp. F770–F776. doi: 10.1152/ajprenal.1992.262.5.F770.

Agarwal, A. and Bolisetty, S. (2013) 'Adaptive responses to tissue injury: role of heme oxygenase-1.', *Transactions of the American Clinical and Climatological Association*, 124, pp. 111–22. Available at: http://www.ncbi.nlm.nih.gov/pubmed/23874015 (Accessed: 14 May 2019).

Agúndez, J. A. *et al.* (2011) 'Assessment of nonsteroidal anti-inflammatory drug-induced hepatotoxicity.', *Expert opinion on drug metabolism & toxicology*, 7(7), pp. 817–28. doi: 10.1517/17425255.2011.574613.

Airik, R. *et al.* (2006) 'Tbx18 regulates the development of the ureteral mesenchyme.', *The Journal of clinical investigation*. American Society for Clinical Investigation, 116(3), pp. 663–74. doi: 10.1172/JCI26027.

Al-Awqati, Q. (2013) ‘Cell biology of the intercalated cell in the kidney’, *FEBS Letters*, 587(13), pp. 1911–1914. doi: 10.1016/j.febslet.2013.05.007.

Aleksa, K. *et al.* (2005) ‘Cytochrome P450 3A and 2B6 in the developing kidney: implications for ifosfamide nephrotoxicity’, *Pediatric Nephrology*, 20(7), pp. 872–885. doi: 10.1007/s00467-004-1807-3.

Armstrong, J. F. *et al.* (1993) ‘The expression of the Wilms’ tumour gene, WT1, in the developing mammalian embryo’, *Mechanisms of Development*. Elsevier, 40(1–2), pp. 85–97. doi: 10.1016/0925-4773(93)90090-K.

Atsuta, Y. *et al.* (2013) ‘Transgenesis of the Wolffian duct visualizes dynamic behavior of cells undergoing tubulogenesis *in vivo*’, *Development, Growth & Differentiation*. John Wiley & Sons, Ltd (10.1111), 55(4), pp. 579–590. doi: 10.1111/dgd.12047.

Attia, L. *et al.* (2012) ‘Analysis of nephric duct specification in the avian embryo.’, *Development (Cambridge, England)*. Oxford University Press for The Company of Biologists Limited, 139(22), pp. 4143–51. doi: 10.1242/dev.085258.

Auerbach, R. and Grobstein, C. (1958) ‘Inductive interaction of embryonic tissues after dissociation and reaggregation.’, *Experimental cell research*, 15(2), pp. 384–97. Available at: http://www.ncbi.nlm.nih.gov/pubmed/13597896 (Accessed: 2 May 2019).

Awdishu, L. and Mehta, R. L. (2017) ‘The 6R’s of drug induced nephrotoxicity’, *BMC Nephrology*. BioMed Central, 18(1), pp. 124. doi: 10.1186/s12882-017-0536-3.

Bhutani, K. *et al*. (2016) ‘Whole-genome mutational burden analysis of three pluripotency induction methods.’ *Nat Commun*. Feb 19;7:10536. doi: 10.1038/ncomms10536.

Bajaj, P. *et al.* (2018) ‘Human Pluripotent Stem Cell–Derived Kidney Model for Nephrotoxicity Studies’, *Drug Metabolism and Disposition*, 46(11), pp. 1703–1711. doi: 10.1124/dmd.118.082727.

Ban, M., Hettich, D. and Huguet, N. (1994) ‘Nephrotoxicity mechanism of cis-

platinum (II) diamine dichloride in mice', *Toxicology Letters*. Elsevier, 71(2), pp. 161–168. doi: 10.1016/0378-4274(94)90176-7.

Bantounas, I. *et al.* (2018) 'Generation of Functioning Nephrons by Implanting Human Pluripotent Stem Cell-Derived Kidney Progenitors', *Stem Cell Reports*. Cell Press, 10(3), pp. 766–779. doi: 10.1016/J.STEMCR.2018.01.008.

Barak, H. *et al.* (2012) 'FGF9 and FGF20 Maintain the Stemness of Nephron Progenitors in Mice and Man', *Developmental Cell*, 22(6), pp. 1191–1207. doi: 10.1016/j.devcel.2012.04.018.

Barasch, J. *et al.* (1997) 'Ureteric bud cells secrete multiple factors, including bFGF, which rescue renal progenitors from apoptosis.', *The American journal of physiology*, 273(5 Pt 2), pp. F757-67. Available at: http://www.ncbi.nlm.nih.gov/pubmed/9374839 (Accessed: 1 May 2019).

Barnes, J. D. *et al.* (1994) 'Embryonic Expression of Lim-1, the Mouse Homolog of Xenopus XLim-1, Suggests a Role in Lateral Mesoderm Differentiation and Neurogenesis', *Developmental Biology*, 161(1), pp. 168–178. doi: 10.1006/dbio.1994.1018.

Barresi, G., Tuccari, G. and Arena, F. (1988) 'Peanut and Lotus tetragonolobus binding sites in human kidney from congenital nephrotic syndrome of Finnish type.', *Histochemistry*, 89(2), pp. 117–20. Available at: http://www.ncbi.nlm.nih.gov/pubmed/3397305 (Accessed: 1 May 2019).

Batchelder, C. A. *et al.* (2009) 'Renal Ontogeny in the Rhesus Monkey (Macaca mulatta) and Directed Differentiation of Human Embryonic Stem Cells Towards Kidney Precursors', *Differentiation*, 78(1), pp. 45–56. doi: 10.1016/j.diff.2009.05.001.

Batourina, E. *et al.* (2001) 'Vitamin A controls epithelial/mesenchymal interactions through Ret expression', *Nature Genetics*, 27(1), pp. 74–78. doi: 10.1038/83792.

Bauchet, A. L. *et al.* (2011) 'Immunohistochemical Identification of Kidney Nephron Segments in the Dog, Rat, Mouse, and Cynomolgus Monkey', *Toxicologic Pathology*, 39(7), pp. 1115–1128. doi: 10.1177/0192623311425060.

Beddington, R. S., Rashbass, P. and Wilson, V. (1992) ‘Brachyury--a gene affecting mouse gastrulation and early organogenesis.’, *Development (Cambridge, England). Supplement*, pp. 157–65. Available at: http://www.ncbi.nlm.nih.gov/pubmed/1299362 (Accessed: 8 May 2019).

Begg, E. J. and Barclay, M. L. (1995) *Aminoglycosides-50 years on*, *Br J clin Pharmac*. Available at: https://www.ncbi.nlm.nih.gov/pmc/articles/PMC1365070/pdf/brjclinpharm00008-0014.pdf (Accessed: 5 December 2018).

Berberat, P. O. *et al.* (2005) ‘Heme oxygenase-1-generated biliverdin ameliorates experimental murine colitis.’, *Inflammatory bowel diseases*, 11(4), pp. 350–9. Available at: http://www.ncbi.nlm.nih.gov/pubmed/15803024 (Accessed: 14 May 2019).

Berberat, P. O. *et al.* (2005) ‘Inhibition of Heme Oxygenase-1 Increases Responsiveness of Pancreatic Cancer Cells to Anticancer Treatment’, *Clinical Cancer Research*, 11(10), pp. 3790–3798. doi: 10.1158/1078-0432.CCR-04-2159.

van den Berg, C. W. *et al.* (2018) ‘Renal Subcapsular Transplantation of PSC-Derived Kidney Organoids Induces Neo-vasculogenesis and Significant Glomerular and Tubular Maturation In Vivo.’, *Stem cell reports*. Elsevier, 10(3), pp. 751–765. doi: 10.1016/j.stemcr.2018.01.041.

Bertram, J. F. *et al.* (2011) ‘Human nephron number: Implications for health and disease’, *Pediatric Nephrology*, 26(9), pp. 1529–1533. doi: 10.1007/s00467-011-1843-8.

Berry, R.L. *et al*. (2015) ‘Deducing the stage of origin of Wilms' tumours from a developmental series of Wt1-mutant mice’, *Dis Model Mech*, 1;8(8), pp. 903-17. doi: 10.1242/dmm.018523.

Bhat, P. V. and Manolescu, D.-C. (2008) ‘Role of Vitamin A in Determining Nephron Mass and Possible Relationship to Hypertension’, *The Journal of Nutrition*, 138(8), pp. 1407–1410. doi: 10.1093/jn/138.8.1407.

Biendarra-Tiegs, S.M., Secreto, F.J. and Nelson, T.J. (2019) 'Addressing Variability and Heterogeneity of Induced Pluripotent Stem Cell-Derived Cardiomyocytes.' In: Advances in Experimental Medicine and Biology. Springer, New York, NY. doi: 10.1007/5584_2019_350.

Björnson, A. *et al.* (2005) 'Primary human glomerular endothelial cells produce proteoglycans, and puromycin affects their posttranslational modification', *American Journal of Physiology-Renal Physiology*, 288(4), pp. F748–F756. doi: 10.1152/ajprenal.00202.2004.

Boeuf, H. *et al.* (1997) 'Leukemia inhibitory factor-dependent transcriptional activation in embryonic stem cells.', *The Journal of cell biology*, 138(6), pp. 1207–17. Available at: http://www.ncbi.nlm.nih.gov/pubmed/9298977 (Accessed: 2 May 2019).

Bohnenpoll, T. *et al.* (2013) 'Tbx18 expression demarcates multipotent precursor populations in the developing urogenital system but is exclusively required within the ureteric mesenchymal lineage to suppress a renal stromal fate', *Developmental Biology*. Academic Press, 380(1), pp. 25–36. doi: 10.1016/J.YDBIO.2013.04.036.

Bohnenpoll, T. and Kispert, A. (2014) 'Ureter growth and differentiation', *Seminars in Cell and Developmental Biology*. Elsevier Ltd, 36, pp. 21–30. doi: 10.1016/j.semcdb.2014.07.014.

Boivin, F. J. *et al.* (2015) 'Stromally Expressed β-Catenin Modulates Wnt9b Signaling in the Ureteric Epithelium'. doi: 10.1371/journal.pone.0120347.

Boland, M. J. *et al.* (2012) 'Generation of mice derived from induced pluripotent stem cells.', *Journal of visualized experiments : JoVE*, 2(69), p. e4003. doi: 10.3791/4003.

Bolotin, A. *et al.* (2005) 'Clustered regularly interspaced short palindrome repeats (CRISPRs) have spacers of extrachromosomal origin', *Microbiology*, 151(8), pp. 2551–2561. doi: 10.1099/mic.0.28048-0.

Bouchard, M. *et al.* (2002) 'Nephric lineage specification by Pax2 and Pax8.', *Genes & development*. Cold Spring Harbor Laboratory Press, 16(22), pp. 2958–70. doi: 10.1101/gad.240102.

Braam, S. R. *et al.* (2008) ‘Recombinant Vitronectin Is a Functionally Defined Substrate That Supports Human Embryonic Stem Cell Self-Renewal via V5 Integrin’, *CELLS*, 26, pp. 2257–2265. doi: 10.1634/stemcells.2008-0291.

Bradley, A. *et al.* (1984) ‘Formation of germ-line chimaeras from embryo-derived teratocarcinoma cell lines’, *Nature*. Nature Publishing Group, 309(5965), pp. 255–256. doi: 10.1038/309255a0.

Breen, C. M. *et al.* (2001) ‘Confocal imaging of organic anion transport in intact rat choroid plexus’. doi: 10.1152/ajprenal.00171.

Bremer, J. L. (1916) ‘The interrelations of the mesonephros, kidney and placenta in different classes of animals’, *American Journal of Anatomy*. John Wiley & Sons, Ltd, 19(2), pp. 179–209. doi: 10.1002/aja.1000190203.

Brenner-Anantharam, A. *et al.* (2007) ‘Tailbud-derived mesenchyme promotes urinary tract segmentation via BMP4 signaling’, *Development*, 134(10), pp. 1967–1975. doi: 10.1242/dev.004234.

Bridgewater, D. *et al.* (2008) ‘Canonical WNT/β-catenin signaling is required for ureteric branching’, *Developmental Biology*. Academic Press, 317(1), pp. 83–94. doi: 10.1016/J.YDBIO.2008.02.010.

Brophy, P. D. *et al.* (2001) ‘Regulation of ureteric bud outgrowth by Pax2-dependent activation of the glial derived neurotrophic factor gene’, *Development*, 128(23).

Brouns, S. J. J. *et al.* (2008) ‘Small CRISPR RNAs Guide Antiviral Defense in Prokaryotes’, *Science*, 321(5891), pp. 960–964. doi: 10.1126/science.1159689.

Brown, A. C. *et al.* (2013) ‘Role for compartmentalization in nephron progenitor differentiation.’, *Proceedings of the National Academy of Sciences of the United States of America*. National Academy of Sciences, 110(12), pp. 4640–5. doi: 10.1073/pnas.1213971110.

Brown, L., Cai, T., & DasGupta, A. (2001). 'Interval Estimation for a Binomial Proportion.' *Statistical Science*, 16(2), pp. 101–133.

Bruce, S. J. *et al.* (2007) ‘In vitro differentiation of murine embryonic stem cells toward a renal lineage.’, *Differentiation; research in biological diversity*, 75(5), pp. 337–49. doi: 10.1111/j.1432-0436.2006.00149.x.

Buehr, M., Gu, S. and McLaren, A. (1993) ‘Mesonephric contribution to testis differentiation in the fetal mouse’, *Development*, 117(1).

Bulger, R. E., Cronin, R. E. and Dobyan, D. C. (1979) ‘Survey of the morphology of the dog kidney.’, *The Anatomical record*, 194(1), pp. 41–65. doi: 10.1002/ar.1091940104.

Burckhardt, G. (2012) ‘Drug transport by Organic Anion Transporters (OATs)’, *Pharmacology & Therapeutics*, 136(1), pp. 106–130. doi: 10.1016/j.pharmthera.2012.07.010.

Burckhardt, G., Wolff, N. A. and Bahn, A. (2002) ‘Molecular Characterization of the Renal Organic Anion Transporter 1’, *Cell Biochemistry and Biophysics*. Humana Press, 36(2–3), pp. 169–174. doi: 10.1385/CBB:36:2-3:169.

Burdon, T. *et al.* (1999) ‘Suppression of SHP-2 and ERK signalling promotes self-renewal of mouse embryonic stem cells.’, *Developmental biology*, 210(1), pp. 30–43. doi: 10.1006/dbio.1999.9265.

Bush, K. T. *et al.* (2004) ‘TGF-β superfamily members modulate growth, branching, shaping, and patterning of the ureteric bud’, *Developmental Biology*. Academic Press, 266(2), pp. 285–298. doi: 10.1016/J.YDBIO.2003.10.023.

Cantley, L. G. *et al.* (1994) ‘Regulation of mitogenesis, motogenesis, and tubulogenesis by hepatocyte growth factor in renal collecting duct cells’, *American Journal of Physiology-Renal Physiology*, 267(2), pp. F271–F280. doi: 10.1152/ajprenal.1994.267.2.F271.

Carroll, T. J. *et al.* (2005) ‘Wnt9b Plays a Central Role in the Regulation of Mesenchymal to Epithelial Transitions Underlying Organogenesis of the Mammalian Urogenital System’, *Developmental Cell*, 9(2), pp. 283–292. doi: 10.1016/j.devcel.2005.05.016.

Carroll, T. J. and Vize, P. D. (1999) ‘Synergism between Pax-8 and lim-1 in embryonic kidney development.’, *Developmental biology*, 214(1), pp. 46–59. doi: 10.1006/dbio.1999.9414.

Catella-Lawson, F. *et al.* (1999) ‘Effects of specific inhibition of cyclooxygenase-2 on sodium balance, hemodynamics, and vasoactive eicosanoids.’, *The Journal of pharmacology and experimental therapeutics*, 289(2), pp. 735–41. Available at: http://www.ncbi.nlm.nih.gov/pubmed/10215647 (Accessed: 14 May 2019).

Cebrián, C. *et al.* (2004) ‘Morphometric index of the developing murine kidney’, *Developmental Dynamics*, 231(3), pp. 601–608. doi: 10.1002/dvdy.20143.

Chade, A. R. *et al.* (2009) ‘Endothelial progenitor cells restore renal function in chronic experimental renovascular disease.’, *Circulation*, 119(4), pp. 547–57. doi: 10.1161/CIRCULATIONAHA.108.788653.

Chang, N. K. *et al.* (2015) ‘Arterial Flow Regulator Enables Transplantation and Growth of Human Fetal Kidneys in Rats’, *American Journal of Transplantation*, 15(6), pp. 1692–1700. doi: 10.1111/ajt.13149.

Chen, G. *et al.* (2011) ‘Chemically defined conditions for human iPSC derivation and culture’, *Nature Methods*. NIH Public Access, 8(5), pp. 424–429. doi: 10.1038/nmeth.1593.

Chen, K. G. *et al.* (2014) ‘Human Pluripotent Stem Cell Culture: Considerations for Maintenance, Expansion, and Therapeutics’, *Cell Stem Cell*. Elsevier Inc., 14(1), pp. 13–26. doi: 10.1016/j.stem.2013.12.005.

Chen, Y. T. and Bradley, A. (2000) ‘A new positive/negative selectable marker, puDeltatk, for use in embryonic stem cells.’, *Genesis (New York, N.Y. : 2000)*, 28(1), pp. 31–36. doi: 10.1002/1526-968.

Cheng, H. T. *et al.* (2003) ‘Gamma-secretase activity is dispensable for mesenchyme-to-epithelium transition but required for podocyte and proximal tubule formation in developing mouse kidney’, *Development (Cambridge, England)*, 130(20), pp. 5031–5042. doi: 10.1242/dev.00697.

Cheng, Y. T. *et al.* (2013) ‘Catechin protects against ketoprofen-induced oxidative damage of the gastric mucosa by up-regulating Nrf2 in vitro and in vivo’, *The Journal of Nutritional Biochemistry*, 24(2), pp. 475–483. doi: 10.1016/j.jnutbio.2012.01.010.

Cho, S. W. *et al.* (2013) ‘Targeted genome engineering in human cells with the Cas9 RNA-guided endonuclease’, *Nature Biotechnology*, 31(3), pp. 230–232. doi: 10.1038/nbt.2507.

Christensen, E. I. and Birn, H. (2001) *Megalin and cubilin: synergistic endocytic receptors in renal proximal tubule*. Available at: http://www.ajprenal.org (Accessed: 6 December 2018).

Christensen, E. I. and Willnow, T. E. (1999) ‘Essential role of megalin in renal proximal tubule for vitamin homeostasis.’, *Journal of the American Society of Nephrology : JASN*, 10(10), pp. 2224–36. Available at: http://www.ncbi.nlm.nih.gov/pubmed/10505701 (Accessed: 6 December 2018).

Ciarimboli, G. *et al.* (2010) ‘Organic cation transporter 2 mediates cisplatin-induced oto- and nephrotoxicity and is a target for protective interventions.’, *The American journal of pathology*, 176(3), pp. 1169–80. doi: 10.2353/ajpath.2010.090610.

Ciarimboli, G. *et al.* (2011) ‘New Clues for Nephrotoxicity Induced by Ifosfamide: Preferential Renal Uptake via the Human Organic Cation Transporter 2’, *Molecular Pharmaceutics*, 8(1), pp. 270–279. doi: 10.1021/mp100329u.

Cirio, M. C. *et al.* (2011) ‘Lhx1 Is Required for Specification of the Renal Progenitor Cell Field’, *PLoS ONE*, 6(4), p. 18858. doi: 10.1371/journal.pone.0018858.

Claassen, D. A., Desler, M. M. and Rizzino, A. (2009) ‘ROCK inhibition enhances the recovery and growth of cryopreserved human embryonic stem cells and human induced pluripotent stem cells’, *Molecular Reproduction and Development*, 76(8), pp. 722–732. doi: 10.1002/mrd.21021.

Colvin, J. S. *et al.* (1999) ‘Genomic organization and embryonic expression of the mouse fibroblast growth factor 9 gene’, *Developmental Dynamics*, 216(1), pp. 72–88. doi: 10.1002/(SICI)1097-0177(199909)216:1<72::AID-DVDY9>3.0.CO;2-9.

Combes, A. N. *et al.* (2019) ‘Single-cell analysis reveals congruence between kidney organoids and human fetal kidney’, *Genome Medicine*, 11(1), p. 3. doi: 10.1186/s13073-019-0615-0.

Cong, L. *et al.* (2013) ‘Multiplex Genome Engineering Using CRISPR/Cas Systems’, *Science*, 339(6121), pp. 819–823. doi: 10.1126/science.1231143.

Costantini, F. (2012) ‘Genetic controls and cellular behaviors in branching morphogenesis of the renal collecting system.’, *Wiley interdisciplinary reviews. Developmental biology*, 1(5), pp. 693–713. doi: 10.1002/wdev.52.

Costantini, F. and Kopan, R. (2010) ‘Patterning a complex organ: branching morphogenesis and nephron segmentation in kidney development.’, *Developmental cell*, 18(5), pp. 698–712. doi: 10.1016/j.devcel.2010.04.008.

Costantini, F. and Shakya, R. (2006) ‘GDNF/Ret signaling and the development of the kidney’, *BioEssays*, 28(2), pp. 117–127. doi: 10.1002/bies.20357.

Cowell, J. K. *et al.* (1991) ‘Structural rearrangements of the WT1 gene in Wilms’ tumour cells.’, *Oncogene*, 6(4), pp. 595–9. Available at: http://www.ncbi.nlm.nih.gov/pubmed/1851548 (Accessed: 1 May 2019).

Croisille, Y., Gumpel-Pinot, M. and Martin, C. (1976) ‘[Differentiation of secretory tubes of avian kidney : effect of heterogenous inducers].’, *Comptes rendus hebdomadaires des seances de l’Academie des sciences. Serie D: Sciences naturelles*, 282(22), pp. 1987–90. Available at: http://www.ncbi.nlm.nih.gov/pubmed/821670 (Accessed: 1 May 2019).

Czerniecki, S. M. *et al.* (2018) ‘High-Throughput Screening Enhances Kidney Organoid Differentiation from Human Pluripotent Stem Cells and Enables Automated Multidimensional Phenotyping’, *Cell Stem Cell*. Cell Press, 22(6), pp. 929-940.e4. doi: 10.1016/J.STEM.2018.04.022.

Das, A. *et al.* (2014) ‘Stromal–epithelial crosstalk regulates kidney progenitor cell differentiation’, *Nat Cell Biol. Author manuscript; available in PMC 2014 March 01*. Nature Publishing Group, 15(9), pp. 1035–1044. doi: 10.1038/ncb2828.Stromal-epithelial.

Davidson, A. J. (2008) ‘Mouse kidney development’, in *StemBook*, pp. 1–30. doi: 10.3824/stembook.1.34.1.

Davies, J. (1994) ‘Control of calbindin-D28K expression in developing mouse kidney’, *Developmental Dynamics*. John Wiley & Sons, Ltd, 199(1), pp. 45–51. doi: 10.1002/aja.1001990105.

Davies, J. (2018) ‘Organoids and mini-organs: Introduction, history, and potential’, *Organs and Organoids*. Academic Press, pp. 3–23. doi: 10.1016/B978-0-12-812636-3.00001-8.

Davies, J. A. (2017) ‘Organizing Organoids: Stem Cells Branch Out’, *Cell Stem Cell*, 21(6), pp. 705–706. doi: 10.1016/j.stem.2017.11.011.

Davies, J. A. and Chang, C. H. (2014) ‘Engineering kidneys from simple cell suspensions: An exercise in self-organization’, *Pediatric Nephrology*, 29(4), pp. 519–524. doi: 10.1007/s00467-013-2579-4.

Davies, J. A. and Garrod, D. R. (1995) ‘Induction of early stages of kidney tubule differentiation by lithium ions.’, *Developmental biology*, pp. 50–60. doi: 10.1006/dbio.1995.1006.

Davis, R. P. *et al.* (2008) ‘Targeting a GFP reporter gene to the MIXL1 locus of human embryonic stem cells identifies human primitive streak-like cells and enables isolation of primitive hematopoietic precursors’, *Blood*, 111(4), pp. 1876–1884. doi: 10.1182/blood-2007-06-093609.

Deveau, H. *et al.* (2008) ‘Phage Response to CRISPR-Encoded Resistance in Streptococcus thermophilus’, *Journal of Bacteriology*, 190(4), pp. 1390–1400. doi: 10.1128/JB.01412-07.

Dickson, L. E. *et al.* (2014) ‘BRIEF REVIEW The Proximal Tubule and Albuminuria: Really!’, *J Am Soc Nephrol*, 25, pp. 443–453. doi: 10.1681/ASN.2013090950.

Diwan, S. B. and Stevens, L. C. (1976) ‘Development of teratomas from the ectoderm of mouse egg cylinders.’, *Journal of the National Cancer Institute*, 57(4), pp. 937–42. Available at: http://www.ncbi.nlm.nih.gov/pubmed/1003535 (Accessed: 2

May 2019).

Doble, B. W. and Woodgett, J. R. (2007) ‘Role of Glycogen Synthase Kinase-3 in Cell Fate and Epithelial-Mesenchymal Transitions’, *Cells Tissues Organs*, 185(1–3), pp. 73–84. doi: 10.1159/000101306.

Donovan, M. J. *et al.* (1999) ‘Initial differentiation of the metanephric mesenchyme is independent of WT1 and the ureteric bud’, *Developmental Genetics*, 24(3–4), pp. 252–262. doi: 10.1002/(SICI)1520-6408(1999)24:3/4<252::AID-DVG8>3.0.CO;2-K.

Dressler, G. R. *et al.* (1990) ‘Pax2, a new murine paired-box-containing gene and its expression in the developing excretory system.’, *Development (Cambridge, England)*, 109(4), pp. 787–95. Available at: http://www.ncbi.nlm.nih.gov/pubmed/1977574 (Accessed: 1 May 2019).

Dressler, G. R. (2006) ‘The Cellular Basis of Kidney Development’, *Annu. Rev. Cell Dev. Biol*, 22(1), pp. 509–29. doi: 10.1146/annurev.cellbio.22.010305.104340.

Drummond, I. a *et al.* (1998) ‘Early development of the zebrafish pronephros and analysis of mutations affecting pronephric function.’, *Development (Cambridge, England)*, 125(23), pp. 4655–67. doi: 10.1016/0925-4773(93)90090-k.

Elhendawi, M. and Davies, J. A. (2018) ‘Sebinger Culture: A System Optimized for Morphological Maturation and Imaging of Cultured Mouse Metanephric Primordia.’, *Bio-protocol*, 8(4). doi: 10.21769/BioProtoc.2730.

Elhendawi, M. and Liu, W. (2018) ‘Kidney organoids’, *Organs and Organoids*. Academic Press, pp. 117–143. doi: 10.1016/B978-0-12-812636-3.00006-7.

Van Esch, H. *et al.* (2000) ‘GATA3 haplo-insufficiency causes human HDR syndrome.’, *Nature*, 406(6794), pp. 419–22. doi: 10.1038/35019088.

Van Esch, H. and Devriendt, K. (2001) ‘Transcription factor GATA3 and the human HDR syndrome.’, *Cellular and molecular life sciences : CMLS*, 58(9), pp. 1296–300. Available at: http://www.ncbi.nlm.nih.gov/pubmed/11577985 (Accessed: 1 May 2019).

Essafi, A. *et al.* (2011) ‘A wt1-controlled chromatin switching mechanism underpins

tissue-specific wnt4 activation and repression.', *Developmental cell*. Europe PMC Funders, 21(3), pp. 559–74. doi: 10.1016/j.devcel.2011.07.014.

Evans, M. J. and Kaufman, M. H. (1981) 'Establishment in culture of pluripotential cells from mouse embryos', *Nature*. Nature Publishing Group, 292(5819), pp. 154–156. doi: 10.1038/292154a0.

Fetting, J. L. *et al.* (2014) 'FOXD1 promotes nephron progenitor differentiation by repressing decorin in the embryonic kidney.', *Development (Cambridge, England)*, 141(1), pp. 17–27. doi: 10.1242/dev.089078.

Filipski, K. K. *et al.* (2009) 'Contribution of Organic Cation Transporter 2 (OCT2) to Cisplatin-Induced Nephrotoxicity', *Clinical Pharmacology & Therapeutics*, 86(4), pp. 396–402. doi: 10.1038/clpt.2009.139.

Fraser, E. A. (1920) 'The Pronephros and early Development of the Mesonephros in the Cat.', *Journal of anatomy*, 54(Pt 4), pp. 287-304.7. Available at: http://www.ncbi.nlm.nih.gov/pubmed/17103905 (Accessed: 1 May 2019).

Freedman, B. S. *et al.* (2015) 'Modelling kidney disease with CRISPR-mutant kidney organoids derived from human pluripotent epiblast spheroids', *Nature Communications*. Nature Publishing Group, 6(May), p. 8715. doi: 10.1038/ncomms9715.

Fujii, T. *et al.* (1994) 'Expression patterns of the murine LIM class homeobox gene lim1 in the developing brain and excretory system', *Developmental Dynamics*, 199(1), pp. 73–83. doi: 10.1002/aja.1001990108.

Fujita, T. *et al.* (2006) 'Transport of drugs in the kidney by the human organic cation transporter, OCT2 and its genetic variants.', *Journal of pharmaceutical sciences*, 95(1), pp. 25–36. doi: 10.1002/jps.20536.

Fusaki, N. *et al.* (2009) 'Efficient induction of transgene-free human pluripotent stem cells using a vector based on Sendai virus, an RNA virus that does not integrate into the host genome.', *Proceedings of the Japan Academy. Series B, Physical and biological sciences*. The Japan Academy, 85(8), pp. 348–62. doi: 10.2183/PJAB.85.348.

Gadue, P. *et al.* (2006) 'Wnt and TGF-beta signaling are required for the induction of an in vitro model of primitive streak formation using embryonic stem cells', *Proceedings of the National Academy of Sciences*, 103(45), pp. 16806–16811. doi: 10.1073/pnas.0603916103.

Ganeva, V., Unbekandt, M. and Davies, J. A. (2011) 'An improved kidney dissociation and reaggregation culture system results in nephrons arranged organotypically around a single collecting duct system.', *Organogenesis*, 7(June), pp. 83–87. doi: 10.4161/org.7.2.14881.

Garber, K. (2015) 'RIKEN suspends first clinical trial involving induced pluripotent stem cells.' *Nature Biotechnology*, 33(9), 890–891.

Garreta, E. *et al.* (2019) 'Fine tuning the extracellular environment accelerates the derivation of kidney organoids from human pluripotent stem cells', *Nature Materials*. Nature Publishing Group, 18(4), pp. 397–405. doi: 10.1038/s41563-019-0287-6.

Gautier, J. C. *et al.* (2010) 'Evaluation of Novel Biomarkers of Nephrotoxicity in Two Strains of Rat Treated with Cisplatin', *Toxicologic Pathology*, 38(6), pp. 943–956. doi: 10.1177/0192623310379139.

Gautier, J. C. *et al.* (2016) 'Evaluation of novel biomarkers of nephrotoxicity in Cynomolgus monkeys treated with gentamicin', *Toxicology and Applied Pharmacology*. Academic Press, 303, pp. 1–10. doi: 10.1016/J.TAAP.2016.04.012.

Genbacev, O. *et al.* (2005) 'Serum-free derivation of human embryonic stem cell lines on human placental fibroblast feeders', *Fertility and Sterility*, 83(5), pp. 1517–1529. doi: 10.1016/j.fertnstert.2005.01.086.

Georgas, K. *et al.* (2009) 'Analysis of early nephron patterning reveals a role for distal RV proliferation in fusion to the ureteric tip via a cap mesenchyme-derived connecting segment', *Developmental Biology*. Elsevier Inc., 332(2), pp. 273–286. doi: 10.1016/j.ydbio.2009.05.578.

Gibson, D. G. *et al.* (2009) 'Enzymatic assembly of DNA molecules up to several hundred kilobases', *Nature Methods*. Nature Publishing Group, 6(5), pp. 343–345. doi: 10.1038/nmeth.1318.

Gifford, S. (2015) ‘Recycling organs – growing tailor-made replacement kidneys’, *Regenerative Medicine*, 10, pp. 913–915. doi: 10.2217/rme.15.60.

Giurgea-Marion, L. *et al.* (1986) ‘Impairment of lysosome-pinocytic vesicle fusion in rat kidney proximal tubules after treatment with gentamicin at low doses.’, *Toxicology and applied pharmacology*, 86(2), pp. 271–85. Available at: http://www.ncbi.nlm.nih.gov/pubmed/3787625 (Accessed: 8 December 2018).

Golle, L. *et al.* (2017) ‘Bone marrow-derived cells and their conditioned medium induce microvascular repair in uremic rats by stimulation of endogenous repair mechanisms.’, *Scientific reports*, 7(1), p. 9444. doi: 10.1038/s41598-017-09883-x.

Gore, A. *et al*. (2011). ‘Somatic coding mutations in human induced pluripotent stem cells.’ *Nature*, 471(7336), pp. 63–67. doi: 10.1038/nature09805.

Gozzelino, R., Jeney, V. and Soares, M. P. (2010) ‘Mechanisms of Cell Protection by Heme Oxygenase-1’, *Annual Review of Pharmacology and Toxicology*, 50(1), pp. 323–354. doi: 10.1146/annurev.pharmtox.010909.105600.

Grieshammer, U. *et al.* (2004) ‘SLIT2-mediated ROBO2 signaling restricts kidney induction to a single site.’, *Developmental cell*, 6(5), pp. 709–17. Available at: http://www.ncbi.nlm.nih.gov/pubmed/15130495 (Accessed: 1 May 2019).

Grieshammer, U. *et al.* (2005) ‘FGF8 is required for cell survival at distinct stages of nephrogenesis and for regulation of gene expression in nascent nephrons’, *Development*, 132(17), pp. 3847–3857. doi: 10.1242/dev.01944.

Grobstein, C. (1955) ‘Inductive interaction in the development of the mouse metanephros’, *Journal of Experimental Zoology*. Wiley Subscription Services, Inc., A Wiley Company, 130(2), pp. 319–339. doi: 10.1002/jez.1401300207.

Grobstein, C. (1953) ‘Inductive epitheliomesenchymal interaction in cultured organ rudiments of the mouse.’, *Science (New York, N.Y.)*, 118(3054), pp. 52–5. Available at: http://www.ncbi.nlm.nih.gov/pubmed/13076182 (Accessed: 1 May 2019).

Grote, D. *et al.* (2006) ‘Pax2/8-regulated Gata3 expression is necessary for morphogenesis and guidance of the nephric duct in the developing kidney’,

Development, 133(1), pp. 53–61. doi: 10.1242/dev.02184.

Grote, D. *et al.* (2008) 'Gata3 acts downstream of beta-catenin signaling to prevent ectopic metanephric kidney induction.', *PLoS genetics*. Public Library of Science, 4(12), p. e1000316. doi: 10.1371/journal.pgen.1000316.

Gupta, N. R. and Lam, A. Q. (2016) 'Pluripotent Stem Cells for Kidney Diseases', in. Humana Press, Cham, pp. 69–84. doi: 10.1007/978-3-319-33270-3_4.

Gupta, N., Susa, K. and Morizane, R. (2017) 'Regenerative Medicine , Disease Modelling , and Drug Discovery in Human Pluripotent Stem Cell-Derived Kidney Tissue', (August 2017), pp. 1–3.

Gurdon, J. B. (1962) *The Developmental Capacity of Nuclei taken from Intestinal Epithelium Cells of Feeding Tadpoles*, *Development*. Available at: http://dev.biologists.org/content/develop/10/4/622.full.pdf (Accessed: 27 September 2018).

Haensly, W. E. *et al.* (1982) 'Proximal-tubule-like epithelium in Bowman's capsule in spontaneously hypertensive rats. Changes with age.', *The American journal of pathology*. American Society for Investigative Pathology, 107(1), pp. 92–7. Available at: http://www.ncbi.nlm.nih.gov/pubmed/7065126 (Accessed: 30 April 2019).

Hallgrimsson, B., Benediktsson, H. and Vize, P. D. (2003) *Anatomy and histology of the human urinary system, In The kidney : from normal development to congenital diseases*. Edited by P. D. Vize, A. S. Woolf, and J. B. L. Bard. Academic Press.

Harari-Steinberg, O. *et al.* (2013) 'Identification of human nephron progenitors capable of generation of kidney structures and functional repair of chronic renal disease.', *EMBO molecular medicine*. Wiley-Blackwell, 5(10), pp. 1556–68. doi: 10.1002/emmm.201201584.

Harder, J. L. *et al.* (2019) 'Organoid single cell profiling identifies a transcriptional signature of glomerular disease', *JCI Insight*, 4(1). doi: 10.1172/jci.insight.122697.

Hardy, K. M. *et al.* (2011) 'FGF signalling through RAS/MAPK and PI3K pathways regulates cell movement and gene expression in the chicken primitive streak without

affecting E-cadherin expression', *BMC Developmental Biology*, 11(1), p. 20. doi: 10.1186/1471-213X-11-20.

Harirforoosh, S. and Jamali, F. (2009) 'Renal adverse effects of nonsteroidal anti-inflammatory drugs', *Expert Opinion on Drug Safety*, 8(6), pp. 669–681. doi: 10.1517/14740330903311023.

Harpur, E. *et al.* (2011) 'Biological Qualification of Biomarkers of Chemical-Induced Renal Toxicity in Two Strains of Male Rat', *Toxicological Sciences*, 122(2), pp. 235–252. doi: 10.1093/toxsci/kfr112.

Hediger, M. A. *et al.* (2005) 'Molecular Physiology of Urate Transport', *Physiology*, 20(2), pp. 125–133. doi: 10.1152/physiol.00039.2004.

Heidenhain (1874) 'The physiology of the kidney', *British Medical Journal*, Sept. 19, 1874, pp. 373–374. Available at: https://www.ncbi.nlm.nih.gov/pmc/articles/PMC2294971/pdf/brmedj05162-0013.pdf (Accessed: 8 May 2019).

Heidrich, H. G. *et al.* (1972) 'The polarity of the proximal tubule cell in rat kidney. Different surface charges for the brush-border microvilli and plasma membranes from the basal infoldings.', *The Journal of cell biology*, 54(2), pp. 232–45. Available at: http://www.ncbi.nlm.nih.gov/pubmed/4261147 (Accessed: 1 May 2019).

Hennigar, R. A., Schulte, B. A. and Spicer, S. S. (1985) 'Heterogeneous distribution of glycoconjugates in human kidney tubules.', *The Anatomical record*, 211(4), pp. 376–90. doi: 10.1002/ar.1092110403.

Henry, M. P. *et al*. (2019) 'The Genomic Health of HumanPluripotent Stem Cells: Genomic Instability and the Consequences on Nuclear Organization.', *Front Genet*, 21;9:623. doi:10.3389/fgene.2018.00623.

Hernández, A. M. *et al.* (2007) 'Novel mutation in the gene encoding the GATA3 transcription factor in a Spanish familial case of hypoparathyroidism, deafness, and renal dysplasia (HDR) syndrome with female genital tract malformations.', *American journal of medical genetics. Part A*, 143A(7), pp. 757–62. doi: 10.1002/ajmg.a.31617.

Hohenstein, P. and Hastie, N. D. (2006) ‘The many facets of the Wilms’ tumour gene, WT1.’, *Human molecular genetics*, 15 Spec No 2(suppl_2), pp. R196-201. doi: 10.1093/hmg/ddl196.

Horibe, T. *et al.* (2004) ‘Gentamicin binds to the lectin site of calreticulin and inhibits its chaperone activity’, *Biochemical and Biophysical Research Communications*, 323(1), pp. 281–287. doi: 10.1016/j.bbrc.2004.08.099.

Hörl, W. H. (2010) ‘Nonsteroidal Anti-Inflammatory Drugs and the Kidney.’, *Pharmaceuticals (Basel, Switzerland)*. Multidisciplinary Digital Publishing Institute (MDPI), 3(7), pp. 2291–2321. doi: 10.3390/ph3072291.

http://www.pantherdb.org *PANTHER - Gene List Analysis*. Available at: http://www.pantherdb.org/ (Accessed: 14 May 2019).

Huang, J. X. *et al.* (2015) ‘Evaluation of biomarkers for in vitro prediction of drug-induced nephrotoxicity: comparison of HK-2, immortalized human proximal tubule epithelial, and primary cultures of human proximal tubular cells.’, *Pharmacology research & perspectives*. Wiley-Blackwell, 3(3), p. e00148. doi: 10.1002/prp2.148.

Huang, Q. *et al.* (2001) ‘Assessment of Cisplatin-Induced Nephrotoxicity by Microarray Technology’, *Toxicological Sciences*. Oxford University Press, 63(2), pp. 196–207. doi: 10.1093/toxsci/63.2.196.

Hueso, M. *et al.* (2019) ‘Progress in the Development and Challenges for the Use of Artificial Kidneys and Wearable Dialysis Devices’, *Kidney Diseases*. Karger Publishers, 5(1), pp. 3–10. doi: 10.1159/000492932.

Hughson, M. *et al.* (2003) ‘Glomerular number and size in autopsy kidneys: The relationship to birth weight’, *Kidney International*, 63(6), pp. 2113–2122. doi: 10.1046/j.1523-1755.2003.00018.x.

Hu, P. *et al***.** (2000). ‘Ablation of uroplakin III gene results in small urothelial plaques, urothelial leakage, and vesicoureteral reflux.’ *Urology* 57, 117. *J Cell Biol*, 27;151(5), pp. 961-72.

Huo, X. and Liu, K. (2018) ‘Renal organic anion transporters in drug–drug

interactions and diseases', *European Journal of Pharmaceutical Sciences*, 112, pp. 8–19. doi: 10.1016/j.ejps.2017.11.001.

Imai, M. and Kokko, J. P. (1974) 'Sodium chloride, urea, and water transport in the thin ascending limb of Henle. Generation of osmotic gradients by passive diffusion of solutes.', *Journal of Clinical Investigation*, 53(2), pp. 393–402. doi: 10.1172/JCI107572.

Imai, M. and Kokko, J. P. (1976) 'Mechanism of sodium and chloride transport in the thin ascending limb of Henle.', *Journal of Clinical Investigation*, 58(5), pp. 1054–1060. doi: 10.1172/JCI108556.

Jang, K. J. *et al.* (2013) 'Human kidney proximal tubule-on-a-chip for drug transport and nephrotoxicity assessment', *Integrative Biology*, 5(9), p. 1119. doi: 10.1039/c3ib40049b.

Jansen, J. *et al.* (2015) 'Human proximal tubule epithelial cells cultured on hollow fibers: Living membranes that actively transport organic cations', *Scientific Reports*. Nature Publishing Group, 5(October), pp. 1–12. doi: 10.1038/srep16702.

Jeansson, M. *et al.* (2009) 'Adriamycin alters glomerular endothelium to induce proteinuria.', *Journal of the American Society of Nephrology : JASN*. American Society of Nephrology, 20(1), pp. 114–22. doi: 10.1681/ASN.2007111205.

Jenkinson, S. E. *et al.* (2012) 'The limitations of renal epithelial cell line HK-2 as a model of drug transporter expression and function in the proximal tubule', *Pflügers Archiv - European Journal of Physiology*. Springer-Verlag, 464(6), pp. 601–611. doi: 10.1007/s00424-012-1163-2.

Jinek, M. *et al.* (2012) 'A programmable dual-RNA-guided DNA endonuclease in adaptive bacterial immunity.', *Science (New York, N.Y.)*, 337(6096), pp. 816–21. doi: 10.1126/science.1225829.

Jinek, M. *et al.* (2013) 'RNA-programmed genome editing in human cells.', *eLife*. eLife Sciences Publications, Ltd, 2, p. e00471. doi: 10.7554/eLife.00471.

Jokelainen, P. (1963) *An electron microscope study of the early development of the*

rat metanephric nephron. Basel ;;New York: S. Karger. Available at: https://www.worldcat.org/title/electron-microscope-study-of-the-early-development-of-the-rat-metanephric-nephron/oclc/12824457 (Accessed: 1 May 2019).

Jones, E. A., Clement-Jones, M. and Wilson, D. I. (2000) 'JAGGED1 expression in human embryos: correlation with the Alagille syndrome phenotype.', *Journal of medical genetics*. BMJ Publishing Group, 37(9), pp. 658–62. doi: 10.1136/jmg.37.9.658.

Kaminski, M. M. *et al.* (2016) 'Direct reprogramming of fibroblasts into renal tubular epithelial cells by defined transcription factors', *Nature Cell Biology*. Nature Publishing Group, 18(12), pp. 1269–1280. doi: 10.1038/ncb3437.

Kandasamy, K. *et al.* (2015) 'Prediction of drug-induced nephrotoxicity and injury mechanisms with human induced pluripotent stem cell-derived cells and machine learning methods.', *Scientific reports*. Nature Publishing Group, 5(January), p. 12337. doi: 10.1038/srep12337.

Karavanov, A. A. *et al.* (1998) 'Expression pattern of the rat Lim-1 homeobox gene suggests a dual role during kidney development.', *The International journal of developmental biology*, 42(1), pp. 61–6. Available at: http://www.ncbi.nlm.nih.gov/pubmed/9496787 (Accessed: 1 May 2019).

Kekuda, R. *et al.* (1998) 'Cloning and functional characterization of a potential-sensitive, polyspecific organic cation transporter (OCT3) most abundantly expressed in placenta.', *The Journal of biological chemistry*, 273(26), pp. 15971–9. Available at: http://www.ncbi.nlm.nih.gov/pubmed/9632645 (Accessed: 14 January 2019).

Kerjaschki, D. (1984) 'Identification and characterization of podocalyxin--the major sialoprotein of the renal glomerular epithelial cell', *The Journal of Cell Biology*, 98(4), pp. 1591–1596. doi: 10.1083/jcb.98.4.1591.

Kim, D. and Dressler, G. R. (2005) 'Nephrogenic Factors Promote Differentiation of Mouse Embryonic Stem Cells into Renal Epithelia', *Journal of the American Society of Nephrology*, 16(12), pp. 3527–3534. doi: 10.1681/ASN.2005050544.

Kim, S. *et al.* (2015) 'Current strategies and challenges in engineering a bioartificial

kidney.', *Frontiers in bioscience (Elite edition)*, 7, pp. 215–28. Available at: http://www.ncbi.nlm.nih.gov/pubmed/25553375 (Accessed: 27 April 2019).

Kim, Y. K., Nam, S. A. and Yang, C. W. (2018) 'Applications of kidney organoids derived from human pluripotent stem cells.', *The Korean journal of internal medicine*. Korean Association of Internal Medicine, 33(4), pp. 649–659. doi: 10.3904/kjim.2018.198.

Kim, Y. Y. *et al.* (2011) 'Cryopreservation of Human Embryonic Stem Cells Derived-Cardiomyocytes Induced by BMP2 in Serum-Free Condition', *Reproductive Sciences*, 18(3), pp. 252–260. doi: 10.1177/1933719110385130.

Kinder, S. J., Loebel, D. A. and Tam, P. P. (2001) 'Allocation and early differentiation of cardiovascular progenitors in the mouse embryo.', *Trends in cardiovascular medicine*, 11(5), pp. 177–84. Available at: http://www.ncbi.nlm.nih.gov/pubmed/11597828 (Accessed: 1 May 2019).

Kirk, A. *et al.* (2010) 'Differential expression of claudin tight junction proteins in the human cortical nephron.', *Nephrology, dialysis, transplantation : official publication of the European Dialysis and Transplant Association - European Renal Association*. Oxford University Press, 25(7), pp. 2107–19. doi: 10.1093/ndt/gfq006.

Kispert, A. *et al.* (1996) 'Proteoglycans are required for maintenance of Wnt-11 expression in the ureter tips.', *Development (Cambridge, England)*, 122(11), pp. 3627–37. Available at: http://www.ncbi.nlm.nih.gov/pubmed/8951078 (Accessed: 1 May 2019).

Kispert, A., Vainio, S. and McMahon, A. P. (1998) 'Wnt-4 is a mesenchymal signal for epithelial transformation of metanephric mesenchyme in the developing kidney.', *Development (Cambridge, England)*, 125(21), pp. 4225–34. Available at: http://www.ncbi.nlm.nih.gov/pubmed/9753677 (Accessed: 1 May 2019).

Kitamoto, Y., Tokunaga, H. and Tomita, K. (1997) 'Vascular endothelial growth factor is an essential molecule for mouse kidney development: glomerulogenesis and nephrogenesis.', *The Journal of clinical investigation*, 99(10), pp. 2351–7. doi: 10.1172/JCI119416.

Kleinman, H. K. *et al.* (1982) ‘Isolation and characterization of type IV procollagen, laminin, and heparan sulfate proteoglycan from the EHS sarcoma’, *Biochemistry*. American Chemical Society, 21(24), pp. 6188–6193. doi: 10.1021/bi00267a025.

Kleinsmith, L. J. and Pierce, G. B. (1964) ‘Multipotentiality of single embryonal cacinma cells.’, *Cancer research*, 24, pp. 1544–51. Available at: http://www.ncbi.nlm.nih.gov/pubmed/14234000 (Accessed: 2 May 2019).

Ko, L. J. and Engel, J. D. (1993) ‘DNA-binding specificities of the GATA transcription factor family.’, *Molecular and cellular biology*, 13(7), pp. 4011–22. Available at: http://www.ncbi.nlm.nih.gov/pubmed/8321208 (Accessed: 22 October 2018).

Kobayashi, A. (2005) ‘Distinct and sequential tissue-specific activities of the LIM-class homeobox gene Lim1 for tubular morphogenesis during kidney development’, *Development*. doi: 10.1242/dev.01858.

Kobayashi, A. *et al.* (2008) ‘Six2 Defines and Regulates a Multipotent Self-Renewing Nephron Progenitor Population throughout Mammalian Kidney Development’, *Cell Stem Cell*, 3(2), pp. 169–181. doi: 10.1016/j.stem.2008.05.020.

Koepsell, H. *et al.* (1998) ‘Structure and Function of Renal Organic Cation Transporters’, *Physiology*. American Physiological Society, 13(1), pp. 11–16. doi: 10.1152/physiologyonline.1998.13.1.11.

Koepsell, H. (2013) ‘The SLC22 family with transporters of organic cations, anions and zwitterions q’, *Molecular Aspects of Medicine*, 34, pp. 413–435. doi: 10.1016/j.mam.2012.10.010.

Koepsell, H., Lips, K. and Volk, C. (2007) ‘Expert Review Polyspecific Organic Cation Transporters: Structure, Function, Physiological Roles, and Biopharmaceutical Implications’, *pharmaceutical research*, 24(7), pp. 1227–1251. doi: 10.1007/s11095-007-9254-z.

Kokko, J. P. (1970) ‘Sodium chloride and water transport in the descending limb of Henle.’, *The Journal of clinical investigation*, 49(10), pp. 1838–46. doi: 10.1172/JCI106401.

Kokko, J. P. (1972) ‘Urea transport in proximal tubule and the descending limb of Henle.’, *The Journal of clinical investigation*, 51(8), pp. 1999–2008. doi: 10.1172/JCI107006.

Kolhar, P. *et al.* (2010) ‘Synthetic surfaces for human embryonic stem cell culture.’, *Journal of biotechnology*, 146(3), pp. 143–6. doi: 10.1016/j.jbiotec.2010.01.016.

Koopman, P. and Cotton, R. G. (1984) ‘A factor produced by feeder cells which inhibits embryonal carcinoma cell differentiation. Characterization and partial purification.’, *Experimental cell research*, 154(1), pp. 233–42. Available at: http://www.ncbi.nlm.nih.gov/pubmed/6468525 (Accessed: 2 May 2019).

van Koppen, A. *et al.* (2012) ‘Human embryonic mesenchymal stem cell-derived conditioned medium rescues kidney function in rats with established chronic kidney disease.’, *PloS one*. Edited by J.-C. Dussaule, 7(6), p. e38746. doi: 10.1371/journal.pone.0038746.

Kreidberg, J. A. *et al.* (1993) ‘WT-1 is required for early kidney development’, *Cell*, 74(4), pp. 679–691. doi: 10.1016/0092-8674(93)90515-R.

Kuhlmann, M. K., Burkhardt, G. and Köhler, H. (1997) ‘Insights into potential cellular mechanisms of cisplatin nephrotoxicity and their clinical application.’, *Nephrology, dialysis, transplantation : official publication of the European Dialysis and Transplant Association - European Renal Association*, 12(12), pp. 2478–80. Available at: http://www.ncbi.nlm.nih.gov/pubmed/9430835 (Accessed: 15 November 2018).

Kume, T., Deng, K. and Hogan, B. L. (2000) ‘Murine forkhead/winged helix genes Foxc1 (Mf1) and Foxc2 (Mfh1) are required for the early organogenesis of the kidney and urinary tract’, *Development*, 127(7).

Kunath, T. *et al.* (2007) ‘FGF stimulation of the Erk1/2 signalling cascade triggers transition of pluripotent embryonic stem cells from self-renewal to lineage commitment’, *Development*, 134(16), pp. 2895–2902. doi: 10.1242/dev.02880.

Kurosawa, H. (2012) ‘Application of Rho-associated protein kinase (ROCK) inhibitor to human pluripotent stem cells’, *Journal of Bioscience and Bioengineering*, 114(6), pp. 577–581. doi: 10.1016/j.jbiosc.2012.07.013.

Kusaba, T. *et al.* (2014) ‘Differentiated kidney epithelial cells repair injured proximal tubule’, *Proceedings of the National Academy of Sciences*, 111(4), pp. 1527–1532. doi: 10.1073/pnas.1310653110.

Kwon, E. M. *et al*. (2017) ‘iPSCs and fibroblast subclones from the same fibroblast population contain comparable levels of sequence variations.’, *Proc Natl Acad Sci USA* **114**, pp. 1964–1969. doi: 10.1073/pnas.1616035114.

Labastie, M. C. *et al.* (1995) *The GATA-3 gene is expressed during human kidney embryogenesis*, *Kidney International*. doi: 10.1038/ki.1995.223.

Lagies, S. *et al.* (2018) ‘Metabolic characterization of directly reprogrammed renal tubular epithelial cells (iRECs).’, *Scientific reports*. Nature Publishing Group, 8(1), p. 3878. doi: 10.1038/s41598-018-22073-7.

Lambers, T. T. *et al.* (2006) ‘Calbindin-D28K dynamically controls TRPV5-mediated Ca2+ transport’, *The EMBO Journal*, 25(13), pp. 2978–2988. doi: 10.1038/sj.emboj.7601186.

Lawrence, M. L., Chang, C. H. and Davies, J. A. (2015) ‘Transport of organic anions and cations in murine embryonic kidney development and in serially-reaggregated engineered kidneys.’, *Scientific reports*. Nature Publishing Group, 5(1), p. 9092. doi: 10.1038/srep09092.

Lawrence, M. L., Elhendawi, M. and Davies, J. A. (2019) ‘Investigating Aspects of Renal Physiology and Pharmacology in Organ and Organoid Culture’, in. Humana Press, New York, NY, pp. 127–142. doi: 10.1007/978-1-4939-9021-4_11.

Lee, C. T. *et al.* (2016) ‘The role of calbindin-D28k on renal calcium and magnesium handling during treatment with loop and thiazide diuretics.’, *American journal of physiology. Renal physiology*. American Physiological Society, 310(3), pp. F230-6. doi: 10.1152/ajprenal.00057.2015.

Lee, S. Y. *et al.* (2013) ‘Expression of E-cadherin in pig kidney.’, *Journal of veterinary science*. The Korean Society of Veterinary Science, 14(4), pp. 381–6. doi: 10.4142/JVS.2013.14.4.381.

Leheste, J. R. *et al.* (1999) ‘Megalin Knockout Mice as an Animal Model of Low Molecular Weight Proteinuria’, *The American Journal of Pathology*, 155(4), pp. 1361–1370. doi: 10.1016/S0002-9440(10)65238-8.

Lehtonen, E. *et al.* (1983) ‘Differentiation of metanephric tubules following a short transfilter induction pulse’, *Wilhelm Roux’s Archives of Developmental Biology*, 192(3–4), pp. 145–151. doi: 10.1007/BF00848683.

Li, R. W. *et al.* (2013) ‘Involvement of organic cation transporter-3 and plasma membrane monoamine transporter in serotonin uptake in human brain vascular smooth muscle cells.’, *Frontiers in pharmacology*. Frontiers Media SA, 4, p. 14. doi: 10.3389/fphar.2013.00014.

Li, S. *et al.* (2017) ‘Development and Application of Human Renal Proximal Tubule Epithelial Cells for Assessment of Compound Toxicity.’, *Current chemical genomics and translational medicine*. Bentham Science Publishers, 11, pp. 19–30. doi: 10.2174/2213988501711010019.

Li, X. *et al.* (2008) ‘ROCK inhibitor improves survival of cryopreserved serum/feeder-free single human embryonic stem cells’, *Human Reproduction*, 24(3), pp. 580–589. doi: 10.1093/humrep/den404.

Li, Y. *et al.* (2005) ‘Expansion of human embryonic stem cells in defined serum-free medium devoid of animal-derived products’, *Biotechnology and Bioengineering*, 91(6), pp. 688–698. doi: 10.1002/bit.20536.

Li, Y. *et al.* (2013) ‘An in vitro method for the prediction of renal proximal tubular toxicity in humans’, *Toxicology Research*. The Royal Society of Chemistry, 2(5), p. 352. doi: 10.1039/c3tx50042j.

Lin, Y. *et al.* (2001) ‘Induced repatterning of type XVIII collagen expression in ureter bud from kidney to lung type: association with sonic hedgehog and ectopic surfactant protein C.’, *Development (Cambridge, England)*, 128(9), pp. 1573–85. Available at: http://www.ncbi.nlm.nih.gov/pubmed/11290296 (Accessed: 1 May 2019).

Lin, Y. *et al.* (2003) ‘Patterning parameters associated with the branching of the ureteric bud regulated by epithelial-mesenchymal interactions.’, *The International*

journal of developmental biology, 47(1), pp. 3–13. Available at: http://www.ncbi.nlm.nih.gov/pubmed/12653247 (Accessed: 1 May 2019).

Lindström, N. O. *et al.* (2018 a) 'Conserved and Divergent Features of Human and Mouse Kidney Organogenesis', *Journal of the American Society of Nephrology : JASN*, 29(3), pp. 1–21. doi: 10.1681/ASN.2017080887.

Lindström, N.O. (2018 b)'Conserved and Divergent Features of Mesenchymal Progenitor Cell Types within the Cortical Nephrogenic Niche of the Human and Mouse Kidney.' *J Am Soc Nephrol*, 29(3),pp.806-824. doi:10.1681/ASN.2017080890.

Lindström, N.O. et al., (2018 c) 'Conserved and Divergent Molecular and Anatomic Features of Human and Mouse Nephron Patterning.' *J Am Soc Nephrol*, 29(3),pp.825-840. doi: 10.1681/ASN.2017091036.

Logan, C. Y. and Nusse, R. (2004) 'The WNT signaling pathway in development and disease', *Annual Review of Cell and Developmental Biology*. Annual Reviews, 20(1), pp. 781–810. doi: 10.1146/annurev.cellbio.20.010403.113126.

Loh, Y. H. *et al.* (2006) 'The Oct4 and Nanog transcription network regulates pluripotency in mouse embryonic stem cells', *Nature Genetics*. Nature Publishing Group, 38(4), pp. 431–440. doi: 10.1038/ng1760.

Ludwig, T. E. *et al.* (2006) 'Derivation of human embryonic stem cells in defined conditions'. doi: 10.1038/nbt1177.

Le Scouarnec, S. and Gribble, S. M. (2012) 'Characterising chromosome rearrangements: recent technical advances in molecular cytogenetics.', *Heredity*,108(1), pp. 75–85.

Mackay, A. R. *et al.* (1993) 'Identification of the 72-kDa (MMP-2) and 92-kDa (MMP-9) gelatinase/type IV collagenase in preparations of laminin and Matrigel.', *BioTechniques*, 15(6), pp. 1048–51. Available at: http://www.ncbi.nlm.nih.gov/pubmed/8292337 (Accessed: 2 May 2019).

Maeshima, A. *et al.* (2007) 'Glial cell-derived neurotrophic factor independent

ureteric bud outgrowth from the Wolffian duct.', *Journal of the American Society of Nephrology : JASN*. American Society of Nephrology, 18(12), pp. 3147–55. doi: 10.1681/ASN.2007060642.

Majumdar, A. *et al.* (2003) 'Wnt11 and Ret/Gdnf pathways cooperate in regulating ureteric branching during metanephric kidney development.', *Development (Cambridge, England)*, 130(14), pp. 3175–85. Available at: http://www.ncbi.nlm.nih.gov/pubmed/12783789 (Accessed: 1 May 2019).

Malaguti, M. *et al.* (2013) 'Bone morphogenic protein signalling suppresses differentiation of pluripotent cells by maintaining expression of E-Cadherin.', *eLife*, 2, p. e01197. doi: 10.7554/eLife.01197.

Mali, P. *et al.* (2013) 'RNA-Guided Human Genome Engineering via Cas9', *Science*, 339(6121), pp. 823–826. doi: 10.1126/science.1232033.

Mallon, B. S. *et al.* (2006) 'Toward xeno-free culture of human embryonic stem cells', *The International Journal of Biochemistry & Cell Biology*. Pergamon, 38(7), pp. 1063–1075. doi: 10.1016/J.BIOCEL.2005.12.014.

Marose, T. D. *et al.* (2008) 'Beta-catenin is necessary to keep cells of ureteric bud/Wolffian duct epithelium in a precursor state.', *Developmental biology*, 314(1), pp. 112–26. doi: 10.1016/j.ydbio.2007.11.016.

Marraffini, L. A. and Sontheimer, E. J. (2008) 'CRISPR Interference Limits Horizontal Gene Transfer in Staphylococci by Targeting DNA', *Science*, 322(5909), pp. 1843–1845. doi: 10.1126/science.1165771.

Marshall, Jr, E. and Vickers, J. (1923) 'The mechanism of the elimination of phenolsulphonephthalein by the kidney-a proof of secretion by the convoluted tubules', *Johns Hopkins Hosp (Bull)*, 34, pp. 1–6. Available at: https://ci.nii.ac.jp/naid/10018238662/ (Accessed: 4 November 2018).

Martello, G. and Smith, A. (2014) 'The Nature of Embryonic Stem Cells', *Annual Review of Cell and Developmental Biology*, 30(1), pp. 647–675. doi: 10.1146/annurev-cellbio-100913-013116.

Martin, G. R. (1980) ‘Teratocarcinomas and mammalian embryogenesis.’, *Science (New York, N.Y.)*, 209(4458), pp. 768–76. Available at: http://www.ncbi.nlm.nih.gov/pubmed/6250214 (Accessed: 2 May 2019).

Martin, G. R. (1981) ‘Isolation of a pluripotent cell line from early mouse embryos cultured in medium conditioned by teratocarcinoma stem cells.’, *Proceedings of the National Academy of Sciences of the United States of America*, 78(12), pp. 7634–8. Available at: http://www.ncbi.nlm.nih.gov/pubmed/6950406 (Accessed: 2 May 2019).

Martin, G. R. and Evans, M. J. (1975) ‘Differentiation of clonal lines of teratocarcinoma cells: formation of embryoid bodies in vitro.’, *Proceedings of the National Academy of Sciences of the United States of America*, 72(4), pp. 1441–5. Available at: http://www.ncbi.nlm.nih.gov/pubmed/1055416 (Accessed: 2 May 2019).

Masereeuw, R. *et al.* (1999) ‘Active lucifer yellow secretion in renal proximal tubule: evidence for organic anion transport system crossover.’, *The Journal of pharmacology and experimental therapeutics*, 289(2), pp. 1104–11. Available at: http://www.ncbi.nlm.nih.gov/pubmed/10215693 (Accessed: 20 February 2019).

Masereeuw, R. *et al.* (2014) ‘The Kidney and Uremic Toxin Removal: Glomerulus or Tubule?’, *Seminars in Nephrology*, 34, pp. 191–208. doi: 10.1016/j.semnephrol.2014.02.010.

Masereeuw, R. and Stamatialis, D. (2017) ‘Creating a Bioartificial Kidney’, *The International Journal of Artificial Organs*. SAGE PublicationsSage UK: London, England, 40(7), pp. 323–327. doi: 10.5301/ijao.5000581.

Masuda, S. *et al.* (2006) ‘Identification and Functional Characterization of a New Human Kidney–Specific H $^{+}$ /Organic Cation Antiporter, Kidney-Specific Multidrug and Toxin Extrusion 2’, *Journal of the American Society of Nephrology*, 17(8), pp. 2127–2135. doi: 10.1681/ASN.2006030205.

Matsuda, T. *et al.* (1999) ‘STAT3 activation is sufficient to maintain an undifferentiated state of mouse embryonic stem cells.’, *The EMBO journal*, 18(15), pp. 4261–9. doi: 10.1093/emboj/18.15.4261.

Matsui, Y., Zsebo, K. and Hogan, B. L. (1992) ‘Derivation of pluripotential embryonic

stem cells from murine primordial germ cells in culture.', *Cell*, 70(5), pp. 841–7. Available at: http://www.ncbi.nlm.nih.gov/pubmed/1381289 (Accessed: 2 May 2019).

Mcmahon, A. P. (2016) 'Development of the mammalian kidney', *Current topics in developmental biology*, 117, pp. 31–64. doi: 10.1016/bs.ctdb.2015.10.010.Development.

McTaggart, S. J. *et al.* (2001) 'Clinical spectrum of Denys-Drash and Frasier syndrome.', *Pediatric nephrology (Berlin, Germany)*, 16(4), pp. 335–9. Available at: http://www.ncbi.nlm.nih.gov/pubmed/11354777 (Accessed: 1 May 2019).

McWilliam, S. J. *et al.* (2017) 'Aminoglycoside-induced nephrotoxicity in children', *Pediatric Nephrology*, 32(11), pp. 2015–2025. doi: 10.1007/s00467-016-3533-z.

Meisner, L. F. and Johnson, J. A. (2008) 'Protocols for cytogenetic studies of human embryonic stem cells.' *Methods*, 45(2), pp. 133–141. doi: 10.1016/j.ymeth.2008.03.005.

Melkoumian, Z. *et al.* (2010) 'Synthetic peptide-acrylate surfaces for long-term self-renewal and cardiomyocyte differentiation of human embryonic stem cells.', *Nature biotechnology*, 28(6), pp. 606–10. doi: 10.1038/nbt.1629.

Mendelsohn, C. *et al.* (1999) 'Stromal cells mediate retinoid-dependent functions essential for renal development.', *Development (Cambridge, England)*, 126(6), pp. 1139–1148. Available at: http://www.ncbi.nlm.nih.gov/pubmed/10021334 (Accessed: 21 October 2018).

Menon, M. C., Chuang, P. Y. and He, C. J. (2012) 'The Glomerular Filtration Barrier: Components and Crosstalk', *International Journal of Nephrology*. Hindawi, 2012, pp. 1–9. doi: 10.1155/2012/749010.

Metsuyanim, S. *et al.* (2009) 'Expression of Stem Cell Markers in the Human Fetal Kidney', *PLoS ONE*. Public Library of Science, 4(8). doi: 10.1371/JOURNAL.PONE.0006709.

Meyer, T. N. *et al.* (2004) 'Spatiotemporal regulation of morphogenetic molecules during in vitro branching of the isolated ureteric bud: toward a model of branching

through budding in the developing kidney', *Developmental Biology*, 275(1), pp. 44–67. doi: 10.1016/j.ydbio.2004.07.022.

Michael, L. and Davies, J. A. (2004) 'Pattern and regulation of cell proliferation during murine ureteric bud development', *Journal of Anatomy*, 204(4), pp. 241–255. doi: 10.1111/j.0021-8782.2004.00285.x.

Michos, O. *et al.* (2007) 'Reduction of BMP4 activity by gremlin 1 enables ureteric bud outgrowth and GDNF/WNT11 feedback signalling during kidney branching morphogenesis', *Development*, 134(13), pp. 2397–2405. doi: 10.1242/dev.02861.

Michos, O. (2010) 'Kidney development: from ureteric bud formation to branching morphogenesis', *Curr Opin Genet Dev*, 9(1), pp. 19–22. doi: 10.3816/CLM.2009.n.003.Novel.

Mierau, G. W., Beckwith, J. B. and Weeks, D. A. (1987) 'Ultrastructure and histogenesis of the renal tumors of childhood: an overview.', *Ultrastructural pathology*, 11(2–3), pp. 313–33. Available at: http://www.ncbi.nlm.nih.gov/pubmed/3035769 (Accessed: 1 May 2019).

Miller, D. S., Letcher, S. and Barnes, D. M. (1996) 'Fluorescence imaging study of organic anion transport from renal proximal tubule cell to lumen.', *The American journal of physiology*. American Physiological Society Bethesda, MD , 271(3 Pt 2), pp. F508-20. doi: 10.1152/ajprenal.1996.271.3.F508.

Mills, C. G. *et al.* (2017) 'Asymmetric BMP4 signalling improves the realism of kidney organoids', *Scientific Reports*. Springer US, 7(1), pp. 1–8. doi: 10.1038/s41598-017-14809-8.

Miner, J. H. (2012) 'The glomerular basement membrane.', *Experimental cell research*. NIH Public Access, 318(9), pp. 973–8. doi: 10.1016/j.yexcr.2012.02.031.

Miranda, C. *et al.* (2018) 'Towards Multi-Organoid Systems for Drug Screening Applications', *Bioengineering*, 5(3), p. 49. doi: 10.3390/bioengineering5030049.

Miyazaki, H. *et al.* (2005) 'Modulation of Renal Apical Organic Anion Transporter 4 Function by Two PDZ Domain–Containing Proteins', *Journal of the American Society*

of Nephrology, 16(12), pp. 3498–3506. doi: 10.1681/ASN.2005030306.

Miyazaki, T., Nakatsuji, N. and Suemori, H. (2014) 'Optimization of slow cooling cryopreservation for human pluripotent stem cells', *genesis*, 52(1), pp. 49–55. doi: 10.1002/dvg.22725.

Miyazaki, Y. *et al.* (2000) 'Bone morphogenetic protein 4 regulates the budding site and elongation of the mouse ureter', *Journal of Clinical Investigation*. American Society for Clinical Investigation, 105(7), pp. 863–873. doi: 10.1172/JCI8256.

Miyazaki, Y. *et al.* (2003) 'Evidence that bone morphogenetic protein 4 has multiple biological functions during kidney and urinary tract development', *Kidney International*, 63(3), pp. 835–844. doi: 10.1046/j.1523-1755.2003.00834.x.

Moestrup, S. K. *et al.* (1995) 'Evidence that epithelial glycoprotein 330/megalin mediates uptake of polybasic drugs.', *The Journal of clinical investigation*. American Society for Clinical Investigation, 96(3), pp. 1404–13. doi: 10.1172/JCI118176.

Molitoris, B. A. and Nelson, W. J. (1990) 'Alterations in the establishment and maintenance of epithelial cell polarity as a basis for disease processes.', *The Journal of clinical investigation*. American Society for Clinical Investigation, 85(1), pp. 3–9. doi: 10.1172/JCI114427.

Montserrat, N., Garreta, E. and Izpisua Belmonte, J. C. (2016) 'Regenerative strategies for kidney engineering', *The FEBS Journal*, 283(18), pp. 3303–3324. doi: 10.1111/febs.13704.

Moon, K. H. *et al.* (2016) 'Kidney diseases and tissue engineering', *Methods*, 99, pp. 112–119. doi: 10.1016/j.ymeth.2015.06.020.

Moore, K. L., Persaud, T. V. N. and Torchia, M. G. (2015) '*The developing human : clinically oriented embryology*. '

Moore, M. W. *et al.* (1996) 'Renal and neuronal abnormalities in mice lacking GDNF', *Nature*, 382(6586), pp. 76–79. doi: 10.1038/382076a0.

Morales, A. I. *et al.* (2010) 'Metformin prevents experimental gentamicin-induced nephropathy by a mitochondria-dependent pathway', *Kidney International*, 77(10),

pp. 861–869. doi: 10.1038/ki.2010.11.

More, S. S. *et al.* (2010) ‘Organic Cation Transporters Modulate the Uptake and Cytotoxicity of Picoplatin, a Third-Generation Platinum Analogue’, *Molecular Cancer Therapeutics*, 9(4), pp. 1058–1069. doi: 10.1158/1535-7163.MCT-09-1084.

Moreau, E. *et al.* (1998) ‘Regulation of c-ret expression by retinoic acid in rat metanephros: implication in nephron mass control.’, *The American journal of physiology*, 275(6 Pt 2), pp. F938-45. Available at: http://www.ncbi.nlm.nih.gov/pubmed/9843911 (Accessed: 21 October 2018).

Moriguchi, T. *et al.* (2016) ‘Gata3 Hypomorphic Mutant Mice Rescued with a Yeast Artificial Chromosome Transgene Suffer a Glomerular Mesangial Cell Defect.’, *Molecular and cellular biology*. American Society for Microbiology (ASM), 36(17), pp. 2272–81. doi: 10.1128/MCB.00173-16.

Morizane, R. *et al.* (2015) ‘Nephron organoids derived from human pluripotent stem cells model kidney development and injury’, *Nature Biotechnology*, 33(11), pp. 1193–1200. doi: 10.1038/nbt.3392.

Morizane, R. and Lam, A. Q. (2015) ‘Directed differentiation of pluripotent stem cells into kidney’, *Biomarker Insights*, 2015, pp. 147–152. doi: 10.4137/BMI.S20055.

Morizane, R., Monkawa, T. and Itoh, H. (2009) ‘Differentiation of murine embryonic stem and induced pluripotent stem cells to renal lineage in vitro.’, *Biochemical and biophysical research communications*, 390(4), pp. 1334–9. doi: 10.1016/j.bbrc.2009.10.148.

Moscona, A. and Moscona, H. (1952) ‘The dissociation and aggregation of cells from organ rudiments of the early chick embryo.’, *Journal of anatomy*, 86(3), pp. 287–301. Available at: http://www.ncbi.nlm.nih.gov/pubmed/12980879 (Accessed: 2 May 2019).

Motamedi, F. J. *et al.* (2014) ‘WT1 controls antagonistic FGF and BMP-pSMAD pathways in early renal progenitors’, *Nature Communications*. Nature Publishing Group, 5(1), p. 4444. doi: 10.1038/ncomms5444.

Motohashi, H. *et al.* (2002) ‘Gene expression levels and immunolocalization of organic ion transporters in the human kidney.’, *Journal of the American Society of Nephrology : JASN*, 13(4), pp. 866–74. Available at: http://www.ncbi.nlm.nih.gov/pubmed/11912245 (Accessed: 14 January 2019).

Motohashi, H. *et al.* (2013) ‘Precise comparison of protein localization among OCT, OAT, and MATE in human kidney’, *Journal of Pharmaceutical Sciences*. John Wiley & Sons, Ltd, 102(9), pp. 3302–3308. doi: 10.1002/jps.23567.

Motohashi, H. and Inui, K. (2013) ‘Organic cation transporter OCTs (SLC22) and MATEs (SLC47) in the human kidney’, *The American Association of Pharmaceutical Scientists Journal*. Springer, 15(2), pp. 581–588. doi: 10.1208/s12248-013-9465-7.

Mugford, J. W. *et al.* (2008) ‘Osr1 expression demarcates a multi-potent population of intermediate mesoderm that undergoes progressive restriction to an Osr1-dependent nephron progenitor compartment within the mammalian kidney’, *Developmental Biology*, 324(1), pp. 88–98. doi: 10.1016/j.ydbio.2008.09.010.

Mugford, J. W. *et al.* (2009) ‘High-resolution gene expression analysis of the developing mouse kidney defines novel cellular compartments within the nephron progenitor population.’, *Developmental biology*. NIH Public Access, 333(2), pp. 312–23. doi: 10.1016/j.ydbio.2009.06.043.

Murphy, S. V and Atala, A. (2014) ‘3D bioprinting of tissues and organs.’, *Nature biotechnology*. Nature Publishing Group, 32(8), pp. 773–785. doi: 10.1038/nbt.2958.

Naiman, N. *et al.* (2017) ‘Repression of Interstitial Identity in Nephron Progenitor Cells by Pax2 Establishes the Nephron-Interstitium Boundary during Kidney Development.’, *Developmental cell*. NIH Public Access, 41(4), pp. 349-365.e3. doi: 10.1016/j.devcel.2017.04.022.

Narayanan, K. *et al.* (2013) ‘Human embryonic stem cells differentiate into functional renal proximal tubular–like cells’, *Kidney International*. Elsevier, 83(4), pp. 593–603. doi: 10.1038/KI.2012.442.

Nath, K. A. (2014) ‘Heme oxygenase-1 and acute kidney injury’, *Current Opinion in Nephrology and Hypertension*, 23(1), pp. 17–24. doi:

10.1097/01.mnh.0000437613.88158.d3.

Nemati, S. *et al.* (2011) ‘Long-Term Self-Renewable Feeder-Free Human Induced Pluripotent Stem Cell–Derived Neural Progenitors’, *Stem Cells and Development*, 20(3), pp. 503–514. doi: 10.1089/scd.2010.0143.

NHS (2018) *Transplant activity report - NHS Organ Donation Register | Organ Donation - English*. Available at: https://www.organdonation.nhs.uk/helping-you-to-decide/about-organ-donation/statistics-about-organ-donation/transplant-activity-report/ (Accessed: 3 May 2019).

Nichols, J. and Smith, A. (2009) ‘Naive and Primed Pluripotent States’, *Cell Stem Cell*, 4(6), pp. 487–492. doi: 10.1016/j.stem.2009.05.015.

Nie, X. *et al.* (2011) ‘Six1 regulates Grem1 expression in the metanephric mesenchyme to initiate branching morphogenesis.’, *Developmental biology*, 352(1), pp. 141–51. doi: 10.1016/j.ydbio.2011.01.027.

Nielsen, S. *et al.* (1995) ‘Aquaporin-1 water channels in short and long loop descending thin limbs and in descending vasa recta in rat kidney’, *American Journal of Physiology-Renal Physiology*, 268(6), pp. F1023–F1037. doi: 10.1152/ajprenal.1995.268.6.F1023.

Nies, A. T. *et al.* (2011) ‘Organic Cation Transporters (OCTs, MATEs), In Vitro and In Vivo Evidence for the Importance in Drug Therapy’, in. Springer, Berlin, Heidelberg, pp. 105–167. doi: 10.1007/978-3-642-14541-4_3.

Nigam, S. K. *et al.* (2015) ‘Handling of Drugs, Metabolites, and Uremic Toxins by Kidney Proximal Tubule Drug Transporters’, *Clinical Journal of the American Society of Nephrology*, 10(11), pp. 2039–2049. doi: 10.2215/CJN.02440314.

Nigam, S. K. (2015) ‘What do drug transporters really do?’, *Nature Reviews Drug Discovery*. Nature Publishing Group, 14(1), pp. 29–44. doi: 10.1038/nrd4461.

Nishikawa, M. *et al.* (2012) ‘Stepwise renal lineage differentiation of mouse embryonic stem cells tracing in vivo development.’, *Biochemical and biophysical research communications*, 417(2), pp. 897–902. doi: 10.1016/j.bbrc.2011.12.071.

Nishinakamura, R. and Sakaguchi, M. (2014) ‘BMP signaling and its modifiers in kidney development’, *Pediatric Nephrology*. Springer Berlin Heidelberg, 29(4), pp. 681–686. doi: 10.1007/s00467-013-2671-9.

Nissim, I. *et al.* (2006) ‘Ifosfamide-induced nephrotoxicity: mechanism and prevention.’, *Cancer research*. American Association for Cancer Research, 66(15), pp. 7824–31. doi: 10.1158/0008-5472.CAN-06-1043.

Niwa, H. *et al.* (1998) ‘Self-renewal of pluripotent embryonic stem cells is mediated via activation of STAT3.’, *Genes & development*, 12(13), pp. 2048–60. Available at: http://www.ncbi.nlm.nih.gov/pubmed/9649508 (Accessed: 2 May 2019).

Nouwen, E. J. *et al.* (1993) ‘Stage- and segment-specific expression of cell-adhesion molecules N-CAM, A-CAM, and L-CAM in the kidney.’, *Kidney international*, 44(1), pp. 147–58. Available at: http://www.ncbi.nlm.nih.gov/pubmed/8355456 (Accessed: 1 May 2019).

O’Brien, L. L. *et al.* (2016) ‘Differential regulation of mouse and human nephron progenitors by the Six family of transcriptional regulators.’, *Development (Cambridge, England)*. Company of Biologists, 143(4), pp. 595–608. doi: 10.1242/dev.127175.

Ochoa-Espinosa, A. and Affolter, M. (2012) ‘Branching morphogenesis: from cells to organs and back.’, *Cold Spring Harbor perspectives in biology*, 4(10), pp. a008243–a008243. doi: 10.1101/cshperspect.a008243.

Ohuchi, H. *et al.* (2000) ‘FGF10 Acts as a Major Ligand for FGF Receptor 2 IIIb in Mouse Multi-Organ Development’, *Biochemical and Biophysical Research Communications*, 277(3), pp. 643–649. doi: 10.1006/bbrc.2000.3721.

Okazawa, M. *et al.* (2015) ‘Region-specific regulation of cell proliferation by FGF receptor signaling during the Wolffian duct development’, *Developmental Biology*, 400(1), pp. 139–147. doi: 10.1016/j.ydbio.2015.01.023.

Ortiz, A. *et al.* (2005) ‘Tubular cell apoptosis and cidofovir-induced acute renal failure.’, *Antiviral therapy*, 10(1), pp. 185–90. Available at: http://www.ncbi.nlm.nih.gov/pubmed/15751777 (Accessed: 16 January 2019).

Oxburgh, L. *et al.* (2017) '(Re)Building a Kidney.', *Journal of the American Society of Nephrology : JASN*. American Society of Nephrology, 28(5), pp. 1370–1378. doi: 10.1681/ASN.2016101077.

Pallone, T. L. *et al.* (2003) 'Countercurrent exchange in the renal medulla', *Am J Physiol Regul Integr Comp Physiol*, 284, pp. 1153–1175. doi: 10.1152/ajpregu.00657.2002.-The.

Papaioannou, V. E., Waters, B. K. and Rossant, J. (1984) 'Interactions between diploid embryonal carcinoma cells and early embryonic cells.', *Cell differentiation*, 15(2–4), pp. 175–9. Available at: http://www.ncbi.nlm.nih.gov/pubmed/6535642 (Accessed: 2 May 2019).

Parameswaran, M. and Tam, P. P. L. (1995) 'Regionalisation of cell fate and morphogenetic movement of the mesoderm during mouse gastrulation', *Developmental Genetics*, 17(1), pp. 16–28. doi: 10.1002/dvg.1020170104.

Park, J.-S. *et al.* (2012) 'Six2 and Wnt regulate self-renewal and commitment of nephron progenitors through shared gene regulatory networks', *Dev Cell*, 23(3), pp. 637–651. doi: 10.1016/j.devcel.2012.07.008.

Park, J. S., Valerius, M. T. and McMahon, A. P. (2007) 'Wnt/ -catenin signaling regulates nephron induction during mouse kidney development', *Development*, 134(13), pp. 2533–2539. doi: 10.1242/dev.006155.

Patek, C. E. *et al.* (2003) 'Murine Denys-Drash syndrome: evidence of podocyte de-differentiation and systemic mediation of glomerulosclerosis', *Human Molecular Genetics*. Oxford University Press, 12(18), pp. 2379–2394. doi: 10.1093/hmg/ddg240.

Pazhayattil, G. S. and Shirali, A. C. (2014) 'Drug-induced impairment of renal function.', *International journal of nephrology and renovascular disease*. Dove Press, 7, pp. 457–68. doi: 10.2147/IJNRD.S39747.

Pearce, D. *et al.* (2015) 'Collecting duct principal cell transport processes and their regulation', *Clinical Journal of the American Society of Nephrology*, 10(1), pp. 135–146. doi: 10.2215/CJN.05760513.

Pedersen, A., Skjong, C. and Shawlot, W. (2005) ‘Lim 1 is required for nephric duct extension and ureteric bud morphogenesis.’, *Developmental biology*, 288(2), pp. 571–81. doi: 10.1016/j.ydbio.2005.09.027.

Pepicelli, C. V *et al.* (1997) ‘GDNF induces branching and increased cell proliferation in the ureter of the mouse.’, *Developmental biology*, 192(1), pp. 193–8. doi: 10.1006/dbio.1997.8745.

Perantoni, A. O. *et al.* (2005) ‘Inactivation of FGF8 in early mesoderm reveals an essential role in kidney development.’, *Development (Cambridge, England)*. The Company of Biologists Ltd, 132(17), pp. 3859–71. doi: 10.1242/dev.01945.

Perantoni, A. O., Dove, L. F. and Karavanova, I. (1995) ‘Basic fibroblast growth factor can mediate the early inductive events in renal development.’, *Proceedings of the National Academy of Sciences of the United States of America*. National Academy of Sciences, 92(10), pp. 4696–700. Available at: http://www.ncbi.nlm.nih.gov/pubmed/7753867 (Accessed: 1 May 2019).

Perazella, M. A. (2009) ‘Renal vulnerability to drug toxicity.’, *Clinical journal of the American Society of Nephrology : CJASN*. American Society of Nephrology, 4(7), pp. 1275–83. doi: 10.2215/CJN.02050309.

Pessoa, E. A. *et al.* (2009) ‘Gentamicin-induced preconditioning of proximal tubular LLC-PK1 cells stimulates nitric oxide production but not the synthesis of heat shock protein.’, *Brazilian journal of medical and biological research = Revista brasileira de pesquisas medicas e biologicas*, 42(7), pp. 614–20. Available at: http://www.ncbi.nlm.nih.gov/pubmed/19466282 (Accessed: 14 May 2019).

Phipson, B. *et al*. (2019) ‘Evaluation of variability in human kidney organoids.’, *Nat Methods*. 2019 Jan;16(1), pp.79-87. doi: 10.1038/s41592-018-0253-2.

Piepenhagen, P. A. *et al.* (1995) ‘Differential expression of Na(+)-K(+)-ATPase, ankyrin, fodrin, and E-cadherin along the kidney nephron’, *American Journal of Physiology-Cell Physiology*, 269(6), pp. C1417–C1432. doi: 10.1152/ajpcell.1995.269.6.C1417.

Pietruck, F. *et al.* (2006) ‘Digital Fluorescence Imaging of Organic Cation Transport

in Freshly Isolated Rat Proximal Tubules', *Drug Metabolism and Disposition*, 34(3), pp. 339–342. doi: 10.1124/dmd.105.006403.necessary.

Pode-Shakked, N. *et al.* (2016) 'Dissecting Stages of Human Kidney Development and Tumorigenesis with Surface Markers Affords Simple Prospective Purification of Nephron Stem Cells', *Scientific Reports*. Nature Publishing Group, 6(1), p. 23562. doi: 10.1038/srep23562.

Pode-Shakked, N. *et al.* (2017) 'Evidence of In Vitro Preservation of Human Nephrogenesis at the Single-Cell Level', *Stem Cell Reports*. Cell Press, 9(1), pp. 279–291. Available at: https://www.sciencedirect.com/science/article/pii/S2213671117301807?via%3Dihub (Accessed: 12 April 2019).

Poladia, D. P. *et al.* (2006) 'Role of fibroblast growth factor receptors 1 and 2 in the metanephric mesenchyme', *Developmental Biology*, 291(2), pp. 325–339. doi: 10.1016/j.ydbio.2005.12.034.

Pollock, C. A. (2013) 'Toward a bioartificial kidney: will embryonic stem cells be the answer?', *Kidney international*. Elsevier, 83(4), pp. 543–5. doi: 10.1038/ki.2012.461.

Potter, E. L. (1972) *Normal and abnormal development of the kidney.* Chicago: Year Book Medical Publishers. Available at: https://books.google.co.uk/books/about/Normal_and_abnormal_development_of_the_kidney. (Accessed: 1 May 2019).

Prakash Bangalore, M. *et al.* (2017) 'Genotoxic Effects of Culture Media on Human Pluripotent Stem Cells.', *Scientific reports*, 7(1), p. 42222. doi: 10.1038/srep42222.

Pritchard, J. B. and Miller, D. S. (1996) 'Renal secretion of organic anions and cations', *Kidney International*. Elsevier Masson SAS, 49(6), pp. 1649–1654. doi: 10.1038/ki.1996.240.

Prozialeck, W. C. and Edwards, J. R. (2007) 'Cell Adhesion Molecules in Chemically-Induced Renal Injury', *Pharmacology & therapeutics*. NIH Public Access, 114(1), p. 74. doi: 10.1016/J.PHARMTHERA.2007.01.001.

Prozialeck, W. C., Lamar, P. C. and Appelt, D. M. (2004) ‘Differential expression of E-cadherin, N-cadherin and beta-catenin in proximal and distal segments of the rat nephron.’, *BMC physiology*. BioMed Central, 4, p. 10. doi: 10.1186/1472-6793-4-10.

Qiao, J. *et al.* (1999) ‘FGF-7 modulates ureteric bud growth and nephron number in the developing kidney.’, *Development (Cambridge, England)*, 126, pp. 547–554. doi: 10.1006/dbio.2000.9623.

Qiao, J. *et al.* (2001) ‘Multiple fibroblast growth factors support growth of the ureteric bud but have different effects on branching morphogenesis.’, *Mechanisms of development*, 109(2), pp. 123–35. Available at: http://www.ncbi.nlm.nih.gov/pubmed/11731227 (Accessed: 1 May 2019).

Qiao, J., Sakurai, H. and Nigam, S. K. (1999) ‘Branching morphogenesis independent of mesenchymal–epithelial contact in the developing kidney’, *Proceedings of the National Academy of Sciences of the United States of America*. National Academy of Sciences, 96(13), p. 7330. Available at: https://www.ncbi.nlm.nih.gov/pmc/articles/PMC22085/ (Accessed: 28 April 2019).

Quiros, Y. *et al.* (2011) ‘An Integrative Overview on the Mechanisms Underlying the Renal Tubular Cytotoxicity of Gentamicin’, *Toxicological Sciences*. Oxford University Press, 119(2), pp. 245–256. doi: 10.1093/toxsci/kfq267.

Ranghini, E. J. and Dressler, G. R. (2015) ‘Evidence for intermediate mesoderm and kidney progenitor cell specification by Pax2 and PTIP dependent mechanisms.’, *Developmental biology*, 399(2), pp. 296–305. doi: 10.1016/j.ydbio.2015.01.005.

Ren, J. *et al.* (2015) ‘Role of age-related decrease of renal organic cation transporter 2 in the effect of atenolol on renal excretion of metformin in rats.’, *European journal of drug metabolism and pharmacokinetics*, 40(3), pp. 349–54. doi: 10.1007/s13318-014-0214-9.

Resnick, J. L. *et al.* (1992) ‘Long-term proliferation of mouse primordial germ cells in culture.’, *Nature*, 359(6395), pp. 550–1. doi: 10.1038/359550a0.

Revest, J. M. *et al.* (2001) ‘Fibroblast growth factor receptor 2-IIIb acts upstream of Shh and Fgf4 and is required for limb bud maintenance but not for the induction of

Fgf8, Fgf10, Msx1, or Bmp4.', *Developmental biology*, 231(1), pp. 47–62. doi: 10.1006/dbio.2000.0144.

Richards, M. *et al.* (2002) 'Human feeders support prolonged undifferentiated growth of human inner cell masses and embryonic stem cells', *Nature Biotechnology*, 20(9), pp. 933–936. doi: 10.1038/nbt726.

Richards, M. *et al.* (2003) 'Comparative Evaluation of Various Human Feeders for Prolonged Undifferentiated Growth of Human Embryonic Stem Cells', *Stem Cells*. Wiley-Blackwell, 21(5), pp. 546–556. doi: 10.1634/stemcells.21-5-546.

Rivera-Pérez, J. A. and Magnuson, T. (2005) 'Primitive streak formation in mice is preceded by localized activation of Brachyury and Wnt3', *Developmental Biology*, 288(2), pp. 363–371. doi: 10.1016/j.ydbio.2005.09.012.

Robb, L. and Tam, P. P. . (2004) 'Gastrula organiser and embryonic patterning in the mouse', *Seminars in Cell & Developmental Biology*, 15(5), pp. 543–554. doi: 10.1016/j.semcdb.2004.04.005.

De Robertis, E. M. and Kuroda, H. (2004) 'Dorsal-ventral patterning and neural induction in Xenopus embeyos', *Annual Review of Cell and Developmental Biology*, 20(1), pp. 285–308. doi: 10.1146/annurev.cellbio.20.011403.154124.

Rodin, S. *et al.* (2010) 'Long-term self-renewal of human pluripotent stem cells on human recombinant laminin-511', *Nature Biotechnology*, 28(6), pp. 611–615. doi: 10.1038/nbt.1620.

Rossant, J. and Papaioannou, V. E. (1985) 'Outgrowth of embryonal carcinoma cells from injected blastocysts in vitro correlates with abnormal chimera development in vivo.', *Experimental cell research*, 156(1), pp. 213–20. Available at: http://www.ncbi.nlm.nih.gov/pubmed/3994789 (Accessed: 2 May 2019).

Rosselot, C. *et al.* (2010) 'Non-cell-autonomous retinoid signaling is crucial for renal development.', *Development (Cambridge, England)*. Company of Biologists, 137(2), pp. 283–92. doi: 10.1242/dev.040287.

Ruotsalainen, V. *et al.* (1999) 'Nephrin is specifically located at the slit diaphragm of

glomerular podocytes', *Proc Natl Acad Sci U S A*, 96(14), pp. 7962–7967. doi: 10.1073/pnas.96.14.7962.

Ruxton, G. D. (2006) 'The unequal variance t-test is an underused alternative to Student's t-test and the Mann–Whitney U test', *Behavioral Ecology*. Narnia, 17(4), pp. 688–690. doi: 10.1093/beheco/ark016.

Ryan, D. *et al.* (2018) 'Development of the Human Fetal Kidney from Mid to Late Gestation in Male and Female Infants', *EBioMedicine*, 27, pp. 275–283. doi: 10.1016/j.ebiom.2017.12.016.

Ryan, G. *et al.* (1995) 'Repression of Pax-2 by WT1 during normal kidney development', *Development*, 121(3).

Saha, K. *et al.* (2011) 'Surface-engineered substrates for improved human pluripotent stem cell culture under fully defined conditions', *Proceedings of the National Academy of Sciences*, 108(46), pp. 18714–18719. doi: 10.1073/pnas.1114854108.

Sainio, K., Hellstedt, P., *et al.* (1997) 'Differential regulation of two sets of mesonephric tubules by WT-1.', *Development (Cambridge, England)*, 124(7), pp. 1293–9. Available at: http://www.ncbi.nlm.nih.gov/pubmed/9118800 (Accessed: 1 May 2019).

Sainio, K., Suvanto, P., *et al.* (1997) 'Glial-cell-line-derived neurotrophic factor is required for bud initiation from ureteric epithelium.', *Development (Cambridge, England)*, 124(20), pp. 4077–87. Available at: http://www.ncbi.nlm.nih.gov/pubmed/9374404 (Accessed: 1 May 2019).

Sainio, K. (2003) 'Development of the Mesonephric Kidney', in *The Kidney: From Normal Development to Congenital Disease*, pp. 75–86. doi: 10.1016/B978-012722441-1/50008-7.

Sakurai, H. *et al.* (1997) 'An in vitro tubulogenesis system using cell lines derived from the embryonic kidney shows dependence on multiple soluble growth factors.', *Proceedings of the National Academy of Sciences of the United States of America*. National Academy of Sciences, 94(12), pp. 6279–84. Available at:

http://www.ncbi.nlm.nih.gov/pubmed/9177208 (Accessed: 28 April 2019).

Sakurai, H., Bush, K. T. and Nigam, S. K. (2001) ‘Identification of pleiotrophin as a mesenchymal factor involved in ureteric bud branching morphogenesis.’, *Development (Cambridge, England)*, 128(17), pp. 3283–93. Available at: http://www.ncbi.nlm.nih.gov/pubmed/11546745 (Accessed: 28 April 2019).

Sakurai, H., Bush, K. T. and Nigam, S. K. (2005) ‘Heregulin induces glial cell line-derived neurotrophic growth factor-independent, non-branching growth and differentiation of ureteric bud epithelia.’, *The Journal of biological chemistry*. American Society for Biochemistry and Molecular Biology, 280(51), pp. 42181–7. doi: 10.1074/jbc.M507962200.

Sandoval, R. M. and Molitoris, B. A. (2004) ‘Gentamicin traffics retrograde through the secretory pathway and is released in the cytosol via the endoplasmic reticulum’, *American Journal of Physiology-Renal Physiology*, 286(4), pp. F617–F624. doi: 10.1152/ajprenal.00130.2003.

Sands, J. M. and Layton, H. E. (2009) ‘The Physiology of Urinary Concentration: An Update’, *Seminars in Nephrology*, 29(3), pp. 178–195. doi: 10.1016/j.semnephrol.2009.03.008.

Sands, J. M. and Layton, H. E. (2014) ‘Advances in Understanding the Urine-Concentrating Mechanism’, *Annual Review of Physiology*. Annual Reviews , 76(1), pp. 387–409. doi: 10.1146/annurev-physiol-021113-170350.

Sariola, H. (2002) ‘Nephron induction revisited: from caps to condensates.’, *Current opinion in nephrology and hypertension*, 11(1), pp. 17–21. Available at: http://www.ncbi.nlm.nih.gov/pubmed/11753082 (Accessed: 1 May 2019).

Sariola, H. and Philipson, L. (1999) ‘Bridge over troubled waters’, *Nature Medicine*. Nature Publishing Group, 5(1), pp. 22–23. doi: 10.1038/4700.

Sariola, H. and Saarma, M. (2003) ‘Novel functions and signalling pathways for GDNF’, *Journal of Cell Science*, 116(19), pp. 3855–3862. doi: 10.1242/jcs.00786.

Satchell, S. C. and Braet, F. (2009) ‘Glomerular endothelial cell fenestrations: an

integral component of the glomerular filtration barrier.', *American journal of physiology. Renal physiology*, 296(5), pp. F947-56. doi: 10.1152/ajprenal.90601.2008.

Sato, N. *et al.* (2004) 'Maintenance of pluripotency in human and mouse embryonic stem cells through activation of Wnt signaling by a pharmacological GSK-3-specific inhibitor', *Nature Medicine*, 10(1), pp. 55–63. doi: 10.1038/nm979.

Saxen, L. *et al.* (1965) 'Studies on tubulogenesis of the kidneys. 3. analysis of the early development with the time lapse method.', *Zeitschrift fur Naturforschung. Teil B, Chemie, Biochemie, Biophysik, Biologie und verwandte Gebiete*, 20, pp. 340–3. Available at: http://www.ncbi.nlm.nih.gov/pubmed/14308007 (Accessed: 1 May 2019).

Saxén, L. (1970) 'Failure to demonstrate tubule induction in a heterologous mesenchyme.', *Developmental biology*, 23(4), pp. 511–23. Available at: http://www.ncbi.nlm.nih.gov/pubmed/5500583 (Accessed: 1 May 2019).

Saxén, L. (1987) *Organogenesis of the kidney*. Cambridge University Press. Available at: https://www.cambridge.org/gb/academic/subjects/life-sciences/cell-biology-and-developmental-biology/organogenesis-kidney?format=HB&isbn=9780521301527 (Accessed: 1 May 2019).

Saxén, L. (1999) *What is needed for kidney differentiation and how do we find it? What is needed?*, *Int. J. Dev. Biol*. Available at: www.ehu.es/ijdb (Accessed: 5 September 2018).

Saxén, L. and Lehtonen, E. (1987) 'Embryonic kidney in organ culture.', *Differentiation; research in biological diversity*, 36(1), pp. 2–11. Available at: http://www.ncbi.nlm.nih.gov/pubmed/3328727 (Accessed: 1 May 2019).

Saxén, L. and Sariola, H. (1987) 'Early organogenesis of the kidney.', *Pediatric nephrology (Berlin, Germany)*, 1(3), pp. 385–92. Available at: http://www.ncbi.nlm.nih.gov/pubmed/3153305 (Accessed: 1 May 2019).

Saxen, L. and Wartiovaara, J. (1966) 'Cell contact and cell adhesion during tissue organization.', *International journal of cancer*, 1(3), pp. 271–90. Available at:

http://www.ncbi.nlm.nih.gov/pubmed/5944066 (Accessed: 1 May 2019).

Schedl, A. (2007) ‘Renal abnormalities and their developmental origin.’, *Nature reviews. Genetics*, 8(10), pp. 791–802. doi: 10.1038/nrg2205.

Schmitz, C. *et al.* (2002) ‘Megalin Deficiency Offers Protection from Renal Aminoglycoside Accumulation’, *Journal of Biological Chemistry*, 277(1), pp. 618–622. doi: 10.1074/jbc.M109959200.

Schnellmann, R. G. and Williams, S. W. (1998) ‘Proteases in renal cell death: Calpains mediate cell death produced by diverse toxicants’, *Renal Failure*, 20(5), pp. 679–686. doi: 10.3109/08860229809045162.

Schoenwolf, G. C. *et al.* (2015) *Larsen’s human embryology*. Available at: https://www.worldcat.org/title/larsens-human-embryology/oclc/862800082 (Accessed: 1 May 2019).

Schophuizen, C. M. S. *et al.* (2013) ‘Cationic uremic toxins affect human renal proximal tubule cell functioning through interaction with the organic cation transporter’, *Pflugers Archiv European Journal of Physiology*, 465(12), pp. 1701–1714. doi: 10.1007/s00424-013-1307-z.

Sekine, M. *et al.* (2012) ‘Selective depletion of mouse kidney proximal straight tubule cells causes acute kidney injury’, *Transgenic Research*, 21(1), pp. 51–62. doi: 10.1007/s11248-011-9504-z.

Sekine, T. *et al.* (1997) ‘Expression cloning and characterization of a novel multispecific organic anion transporter.’, *The Journal of biological chemistry*. American Society for Biochemistry and Molecular Biology, 272(30), pp. 18526–9. doi: 10.1074/JBC.272.30.18526.

Self, M. *et al.* (2006) ‘Six2 is required for suppression of nephrogenesis and progenitor renewal in the developing kidney.’, *The EMBO journal*, 25(21), pp. 5214–28. doi: 10.1038/sj.emboj.7601381.

Seruga, B. *et al.* (2015) ‘Failures in Phase III: Causes and Consequences’, *Clinical Cancer Research*, 21(20), pp. 4552–4560. doi: 10.1158/1078-0432.CCR-15-0124.

Servais, H. *et al.* (2006) ‘Gentamicin causes apoptosis at low concentrations in renal LLC-PK1 cells subjected to electroporation.’, *Antimicrobial agents and chemotherapy*. American Society for Microbiology (ASM), 50(4), pp. 1213–21. doi: 10.1128/AAC.50.4.1213-1221.2006.

Shah, M. M. *et al.* (2004) ‘Branching morphogenesis and kidney disease.’, *Development (Cambridge, England)*, 131(7), pp. 1449–1462. doi: 10.1242/dev.01089.

Shakya, R. *et al.* (2005) ‘The role of GDNF in patterning the excretory system’, *Developmental Biology*, 283(1), pp. 70–84. doi: 10.1016/j.ydbio.2005.04.008.

Short, K. M. *et al.* (2014) ‘Global quantification of tissue dynamics in the developing mouse kidney’, *Developmental Cell*. Elsevier Inc., 29(2), pp. 188–202. doi: 10.1016/j.devcel.2014.02.017.

Silva, J. *et al.* (2008) ‘Promotion of Reprogramming to Ground State Pluripotency by Signal Inhibition’, *PLoS Biology*. Edited by M. A. Goodell, 6(10), p. e253. doi: 10.1371/journal.pbio.0060253.

Silva, J. and Smith, A. (2008) ‘Capturing Pluripotency’, *Cell*, 132(4), pp. 532–536. doi: 10.1016/j.cell.2008.02.006.

Silverblatt, F. (1982) ‘Pathogenesis of nephrotoxicity of cephalosporins and aminoglycosides: a review of current concepts.’, *Reviews of infectious diseases*, 4 Suppl, pp. S360-5. Available at: http://www.ncbi.nlm.nih.gov/pubmed/7178755 (Accessed: 13 May 2019).

Silverblatt, F. J. and Kuehn, C. (1979) ‘Autoradiography of gentamicin uptake by the rat proximal tubule cell.’, *Kidney international*, 15(4), pp. 335–45. Available at: http://www.ncbi.nlm.nih.gov/pubmed/513493 (Accessed: 8 December 2018).

Sjögren, A.K. *et al.* (2018) 'A novel multi-parametric high content screening assay in ciPTEC-OAT1 to predict drug-induced nephrotoxicity during drug discovery', *Arch. Toxicol*, 92 (10), pp. 3175–3190. doi: 10.1007/s00204-018-2284-y.

Skromne, I. and Stern, C. D. (2001) ‘Interactions between Wnt and Vg1 signalling

pathways initiate primitive streak formation in the chick embryo.', *Development (Cambridge, England)*, 128(15), pp. 2915–27. Available at: http://www.ncbi.nlm.nih.gov/pubmed/11532915 (Accessed: 8 May 2019).

Smith, A. G. (2001) 'Embryo-Derived Stem Cells: Of Mice and Men', *Annual Review of Cell and Developmental Biology*, 17(1), pp. 435–462. doi: 10.1146/annurev.cellbio.17.1.435.

Smith, A. G. and Hooper, M. L. (1987) 'Buffalo rat liver cells produce a diffusible activity which inhibits the differentiation of murine embryonal carcinoma and embryonic stem cells.', *Developmental biology*, 121(1), pp. 1–9. Available at: http://www.ncbi.nlm.nih.gov/pubmed/3569655 (Accessed: 2 May 2019).

Smith, H. W., Goldring, W. and Chasis, H. (1938) 'The measurment of the tubular excretory mass, effective blood flow and filtration rate in the normal human kidney.', *The Journal of clinical investigation*. American Society for Clinical Investigation, 17(3), pp. 263–78. doi: 10.1172/JCI100950.

Smith, J. L., Gesteland, K. M. and Schoenwolf, G. C. (1994) 'Prospective fate map of the mouse primitive streak at 7.5 days of gestation', *Developmental Dynamics*, 201(3), pp. 279–289. doi: 10.1002/aja.1002010310.

Snapp, E. L. (2009) 'Fluorescent proteins: a cell biologist's user guide.', *Trends in cell biology*. NIH Public Access, 19(11), pp. 649–55. doi: 10.1016/j.tcb.2009.08.002.

Solnica-Krezel, L. and Sepich, D. S. (2012) 'Gastrulation: Making and Shaping Germ Layers', *Annual Review of Cell and Developmental Biology*, 28(1), pp. 687–717. doi: 10.1146/annurev-cellbio-092910-154043.

Soofi, A., Levitan, I. and Dressler, G. R. (2012) 'Two novel EGFP insertion alleles reveal unique aspects of Pax2 function in embryonic and adult kidneys.', *Developmental biology*, 365(1), pp. 241–50. doi: 10.1016/j.ydbio.2012.02.032.

Srichai, M. B. *et al.* (2004) 'A WT1 co-regulator controls podocyte phenotype by shuttling between adhesion structures and nucleus.', *The Journal of biological chemistry*, 279(14), pp. 14398–408. doi: 10.1074/jbc.M314155200.

Srinivas, S. *et al.* (1999) ‘Expression of green fluorescent protein in the ureteric bud of transgenic mice: A new tool for the analysis of ureteric bud morphogenesis’, *Developmental Genetics*, 24(3–4), pp. 241–251. doi: 10.1002/(SICI)1520-6408(1999)24:3/4<241::AID-DVG7>3.0.CO;2-R.

Sriuttha, P., Sirichanchuen, B. and Permsuwan, U. (2018) ‘Hepatotoxicity of Nonsteroidal Anti-Inflammatory Drugs: A Systematic Review of Randomized Controlled Trials.’, *International journal of hepatology*. Hindawi Limited, 2018, p. 5253623. doi: 10.1155/2018/5253623.

Stark, K. *et al.* (1994) ‘Epithelial transformation of metanephric mesenchyme in the developing kidney regulated by Wnt-4.’, *Nature*, 372(6507), pp. 679–683. doi: 10.1038/372679a0.

Steenhard, B. M. *et al.* (2005) ‘Integration of Embryonic Stem Cells in Metanephric Kidney Organ Culture’, *Journal of the American Society of Nephrology*, 16(6), pp. 1623–1631. doi: 10.1681/ASN.2004070584.

Steer, D. L. *et al.* (2002) ‘A strategy for in vitro propagation of rat nephrons’, *Kidney International*. Elsevier, 62(6), pp. 1958–1965. doi: 10.1046/j.1523-1755.2002.00694.x.

Štefková, K., Procházková, J. and Pacherník, J. (2015) ‘Alkaline Phosphatase in Stem Cells’, *Stem Cells International*. Hindawi, 2015, pp. 1–11. doi: 10.1155/2015/628368.

Subramanya, A. R. and Ellison, D. H. (2014) ‘Distal convoluted tubule.’, *Clinical journal of the American Society of Nephrology : CJASN*. American Society of Nephrology, 9(12), pp. 2147–63. doi: 10.2215/CJN.05920613.

Suchy-Dicey, A. M. *et al.* (2016) ‘Tubular Secretion in CKD’, *J Am Soc Nephrol*, 27, pp. 2148–2155. doi: 10.1681/ASN.2014121193.

Sugiura, M. et al. (2014). ‘Induced pluripotent stem cell generation-associated point mutations arise during the initial stages of the conversion of these cells.’ *Stem Cell Reports*, 2(1), pp. 52–63. doi: 10.1016/j.stemcr.2013.11.006.

Sumi, T. *et al.* (2008) 'Defining early lineage specification of human embryonic stem cells by the orchestrated balance of canonical Wnt/ -catenin, Activin/Nodal and BMP signaling', *Development*, 135(17), pp. 2969–2979. doi: 10.1242/dev.021121.

Suzuki, T. *et al.* (2011) 'Transcriptional Regulation of Organic Anion Transporting Polypeptide SLCO4C1 as a New Therapeutic Modality to Prevent Chronic Kidney Disease', *Journal of Pharmaceutical Sciences*. Elsevier, 100(9), pp. 3696–3707. doi: 10.1002/JPS.22641.

Sweeney, D., Lindstrom, N. and Davies, J. A. (2008) 'Developmental plasticity and regenerative capacity in the renal ureteric bud/collecting duct system', *Development*, 135(15), pp. 2505–2510. doi: 10.1242/dev.022145.

Sweet, D. H. *et al.* (2003) 'Organic anion transporter 3 (*Slc22a8*) is a dicarboxylate exchanger indirectly coupled to the Na^+ gradient', *American Journal of Physiology-Renal Physiology*. American Physiological SocietyBethesda, MD , 284(4), pp. F763–F769. doi: 10.1152/ajprenal.00405.2002.

Sweet, D. H. *et al.* (2006) 'Organic anion and cation transporter expression and function during embryonic kidney development and in organ culture models.', *Kidney international*. NIH Public Access, 69(5), pp. 837–45. doi: 10.1038/sj.ki.5000170.

Tada, M. *et al.* (2001) 'Nuclear reprogramming of somatic cells by in vitro hybridization with ES cells.', *Current biology : CB*, 11(19), pp. 1553–8. Available at: http://www.ncbi.nlm.nih.gov/pubmed/11591326 (Accessed: 2 May 2019).

Taguchi, A. *et al.* (2014) 'Redefining the In Vivo Origin of Metanephric Nephron Progenitors Enables Generation of Complex Kidney Structures from Pluripotent Stem Cells', *Cell Stem Cell*, 14(1), pp. 53–67. doi: 10.1016/j.stem.2013.11.010.

Taguchi, A. and Nishinakamura, R. (2017) 'Higher-Order Kidney Organogenesis from Pluripotent Stem Cells', *Cell Stem Cell*. Elsevier Inc., 21(6), pp. 730-746.e6. doi: 10.1016/j.stem.2017.10.011.

Takahashi, K., Tanabe, K., *et al.* (2007) 'Induction of Pluripotent Stem Cells from Adult Human Fibroblasts by Defined Factors', *Cell*, 131(5), pp. 861–872. doi: 10.1016/j.cell.2007.11.019.

Takahashi, K., Okita, K., *et al.* (2007) 'Induction of pluripotent stem cells from fibroblast cultures', *Nature Protocols*, 2(12), pp. 3081–3089. doi: 10.1038/nprot.2007.418.

Takahashi, K. and Yamanaka, S. (2006) 'Induction of Pluripotent Stem Cells from Mouse Embryonic and Adult Fibroblast Cultures by Defined Factors', *Cell*, 126(4), pp. 663–676. doi: 10.1016/j.cell.2006.07.024.

Takasato, M. *et al.* (2013) 'Directing human embryonic stem cell differentiation towards a renal lineage generates a self-organizing kidney', *Nature Cell Biology*. Nature Publishing Group, 16(1), pp. 118–126. doi: 10.1038/ncb2894.

Takasato, M. *et al.* (2014) 'Directing human embryonic stem cell differentiation towards a renal lineage generates a self-organizing kidney', *Nature Cell Biology*, 16(1), pp. 118–126. doi: 10.1038/ncb2894.

Takasato, M. *et al.* (2015) 'Kidney organoids from human iPS cells contain multiple lineages and model human nephrogenesis', *Nature*, 526(7574), pp. 564–568. doi: 10.1038/nature15695.

Takasato, M. *et al.* (2016) 'Generation of kidney organoids from human pluripotent stem cells', *Nature Protocols*. Nature Publishing Group, 11(9), pp. 1681–1692. doi: 10.1038/nprot.2016.098.

Takasato, M. and Little, M. H. (2015) 'The origin of the mammalian kidney: implications for recreating the kidney in vitro', *Development*, 142(11), pp. 1937–1947. doi: 10.1242/dev.104802.

Tang, M. J. *et al.* (1998) 'The RET-glial cell-derived neurotrophic factor (GDNF) pathway stimulates migration and chemoattraction of epithelial cells.', *The Journal of cell biology*, 142(5), pp. 1337–45. Available at: http://www.ncbi.nlm.nih.gov/pubmed/9732293 (Accessed: 1 May 2019).

Tanihara, Y. *et al.* (2007) 'Substrate specificity of MATE1 and MATE2-K, human multidrug and toxin extrusions/H+-organic cation antiporters', *Biochemical Pharmacology*, 74(2), pp. 359–371. doi: 10.1016/j.bcp.2007.04.010.

Thompson, S. *et al.* (1989) ‘Germ line transmission and expression of a corrected HPRT gene produced by gene targeting in embryonic stem cells.’, *Cell*, 56(2), pp. 313–21. Available at: http://www.ncbi.nlm.nih.gov/pubmed/2912572 (Accessed: 2 May 2019).

Thomson, J. A. *et al.* (1998) ‘Embryonic stem cell lines derived from human blastocysts.’, *Science (New York, N.Y.)*. American Association for the Advancement of Science, 282(5391), pp. 1145–7. doi: 10.1126/SCIENCE.282.5391.1145.

Thomson, R. B. and Aronson, P. S. (1999) ‘Immunolocalization of Ksp-cadherin in the adult and developing rabbit kidney.’, *The American journal of physiology*, 277(1), pp. F146-56. doi: 10.1152/ajprenal.1999.277.1.F146.

Torres, M. *et al.* (1995) ‘Pax-2 controls multiple steps of urogenital development.’, *Development (Cambridge, England)*, 121(12), pp. 4057–65. Available at: http://www.ncbi.nlm.nih.gov/pubmed/8575306 (Accessed: 1 May 2019).

Tran, F. H. and Zheng, J. J. (2017) ‘Modulating the wnt signaling pathway with small molecules’, *Protein Science : A Publication of the Protein Society*. Wiley-Blackwell, 26(4), p. 650. doi: 10.1002/PRO.3122.

Tsang, T. E. *et al.* (2000) ‘Lim1 Activity Is Required for Intermediate Mesoderm Differentiation in the Mouse Embryo’, *Developmental Biology*, 223(1), pp. 77–90. doi: 10.1006/dbio.2000.9733.

Unbekandt, M. and Davies, J. a (2010) ‘Dissociation of embryonic kidneys followed by reaggregation allows the formation of renal tissues.’, *Kidney international*. Elsevier Masson SAS, 77(5), pp. 407–416. doi: 10.1038/ki.2009.482.

Urakami, Y. *et al.* (2004) ‘Creatinine transport by basolateral organic cation transporter hOCT2 in the human kidney’, *Pharmaceutical Research*, 21(6), pp. 976–981. doi: 10.1023/B:PHAM.0000029286.45788.ad.

Vallier, L., Alexander, M. and Pedersen, R. A. (2005) ‘Activin/Nodal and FGF pathways cooperate to maintain pluripotency of human embryonic stem cells’, *Journal of Cell Science*, 118(19), pp. 4495–4509. doi: 10.1242/jcs.02553.

Varner, V. D. and Nelson, C. M. (2014) ‘Cellular and physical mechanisms of branching morphogenesis’, *Development*, 141(14), pp. 2750–2759. doi: 10.1242/dev.104794.

Vega, Q. C. *et al.* (1996) ‘Glial cell line-derived neurotrophic factor activates the receptor tyrosine kinase RET and promotes kidney morphogenesis.’, *Proceedings of the National Academy of Sciences of the United States of America*, 93(20), pp. 10657–61. Available at: http://www.ncbi.nlm.nih.gov/pubmed/8855235 (Accessed: 1 May 2019).

Vetter, M. R. and Gibley, C. W. (1966) ‘Morphogenesis and histochemistry of the developing mouse kidney’, *Journal of Morphology*, 120(2), pp. 135–155. doi: 10.1002/jmor.1051200203.

Villa-Diaz, L. G. *et al.* (2010) ‘Synthetic polymer coatings for long-term growth of human embryonic stem cells’, *Nature Biotechnology*. Nature Publishing Group, 28(6), pp. 581–583. doi: 10.1038/nbt.1631.

Villanueva, S., Céspedes, C. and Vio, C. P. (2006) ‘Ischemic acute renal failure induces the expression of a wide range of nephrogenic proteins’, *Am J Physiol Regul Integr Comp Physiol*, 290, pp. 861–870. doi: 10.1152/ajpregu.00384.2005.

Vize, P. D. *et al.* (1997) ‘Model Systems for the Study of Kidney Development: Use of the Pronephros in the Analysis of Organ Induction and Patterning’, *Developmental Biology*, 188, pp. 189–204. doi: 10.1006/dbio.1997.8629.

Volarevic, V. *et al.* (2019) ‘Molecular mechanisms of cisplatin-induced nephrotoxicity: a balance on the knife edge between renoprotection and tumor toxicity.’, *Journal of biomedical science*. BioMed Central, 26(1), p. 25. doi: 10.1186/s12929-019-0518-9.

Walker, K. A. *et al.* (2012) ‘High nephron endowment protects against salt-induced hypertension.’, *American journal of physiology. Renal physiology*, 303(2), pp. F253-8. doi: 10.1152/ajprenal.00028.2012.

Walker, K. A., Sims-Lucas, S. and Bates, C. M. (2016) ‘Fibroblast growth factor receptor signaling in kidney and lower urinary tract development’, *Pediatric Nephrology*, 31(6), pp. 885–895. doi: 10.1007/s00467-015-3151-1.

Wallis, S. A. (2013) 'Binomial confidence intervals and contingency tests: mathematical fundamentals and the evaluation of alternative methods', *Journal of Quantitative Linguistics*. 20 (3), pp. 178-208. doi: 10.1080/09296174.2013.799918.

Wang, G. J. *et al.* (2009) 'Antagonism of BMP4 Signaling Disrupts Smooth Muscle Investment of the Ureter and Ureteropelvic Junction', *Journal of Urology*, 181(1), pp. 401–407. doi: 10.1016/j.juro.2008.08.117.

Wang, K. and Kestenbaum, B. (2018) 'Proximal Tubular Secretory Clearance: A Neglected Partner of Kidney Function.', *Clinical journal of the American Society of Nephrology : CJASN*. American Society of Nephrology, 13(8), pp. 1291–1296. doi: 10.2215/CJN.12001017.

Wartiovaara, J. *et al.* (2004) 'Nephrin strands contribute to a porous slit diaphragm scaffold as revealed by electron tomography.', *The Journal of clinical investigation*. American Society for Clinical Investigation, 114(10), pp. 1475–83. doi: 10.1172/JCI22562.

Watanabe, K. *et al.* (2007) 'A ROCK inhibitor permits survival of dissociated human embryonic stem cells', *Nature Biotechnology*. Nature Publishing Group, 25(6), pp. 681–686. doi: 10.1038/nbt1310.

Watanabe, T. and Costantini, F. (2004) 'Real-time analysis of ureteric bud branching morphogenesis in vitro.', *Developmental biology*, 271(1), pp. 98–108. doi: 10.1016/j.ydbio.2004.03.025.

Weir, M. R. (2002) 'Renal effects of nonselective NSAIDs and coxibs.', *Cleveland Clinic journal of medicine*, 69 Suppl 1, pp. SI53-8. Available at: http://www.ncbi.nlm.nih.gov/pubmed/12086295 (Accessed: 14 May 2019).

Welch, B. L. (1951) 'On the Comparison of Several Mean Values: An Alternative Approach', *Biometrika*. Oxford University PressBiometrika Trust, 38(3/4), pp. 330. doi: 10.2307/2332579.

Whelton, A. *et al.* (2000) 'Renal safety and tolerability of celecoxib, a novel cyclooxygenase-2 inhibitor.', *American journal of therapeutics*, 7(3), pp. 159–75. Available at: http://www.ncbi.nlm.nih.gov/pubmed/11317165 (Accessed: 14 May

2019).

Wilder, P. J. *et al.* (1997) ‘Inactivation of the FGF-4 Gene in Embryonic Stem Cells Alters the Growth and/or the Survival of Their Early Differentiated Progeny’, *Developmental Biology*, 192(2), pp. 614–629. doi: 10.1006/dbio.1997.8777.

Wiles, M. V and Johansson, B. M. (1999) ‘Embryonic stem cell development in a chemically defined medium.’, *Experimental cell research*, 247(1), pp. 241–8. doi: 10.1006/excr.1998.4353.

Wilmut, I. *et al.* (1997) ‘Viable offspring derived from fetal and adult mammalian cells’, *Nature*, 385, pp.810-813. doi: 10.1038/385810a0.

Wilson, H. K. *et al.* (2016) ‘Cryopreservation of Brain Endothelial Cells Derived from Human Induced Pluripotent Stem Cells Is Enhanced by Rho-Associated Coiled Coil-Containing Kinase Inhibition.’, *Tissue engineering. Part C, Methods*, 22(12), pp. 1085–1094. doi: 10.1089/ten.TEC.2016.0345.

Wilson, E. B. (1927) "Probable inference, the law of succession, and statistical inference". J*ournal of the American Statistical Association*, 22 (158), pp. 209–212. doi: 10.2307/2276774.

Wilson, H. V. (1910) ‘A study of some epithelioid membranes in monaxonid sponges’, *Journal of Experimental Zoology*. John Wiley & Sons, Ltd, 9(3), pp. 537–577. doi: 10.1002/jez.1400090305.

Winnier, G. *et al.* (1995) ‘Bone morphogenetic protein-4 is required for mesoderm formation and patterning in the mouse.’, *Genes & development*, 9(17), pp. 2105–16. Available at: http://www.ncbi.nlm.nih.gov/pubmed/7657163 (Accessed: 1 May 2019).

Wu, W., Bush, K. T. and Nigam, S. K. (2017) ‘Key Role for the Organic Anion Transporters, OAT1 and OAT3, in the in vivo Handling of Uremic Toxins and Solutes’, *Scientific Reports*, 7(1), p. 4939. doi: 10.1038/s41598-017-04949-2.

Wu, Y. *et al.* (2015) ‘GSK3 inhibitors CHIR99021 and 6-bromoindirubin-3′-oxime inhibit microRNA maturation in mouse embryonic stem cells’, *Scientific Reports*. Nature Publishing Group, 5(1), p. 8666. doi: 10.1038/srep08666.

Xia, Y. *et al.* (2013) 'Directed differentiation of human pluripotent cells to ureteric bud kidney progenitor-like cells', *Nature Cell Biology*. Nature Publishing Group, 15(12), pp. 1507–1515. doi: 10.1038/ncb2872.

Xia, Y. *et al.* (2014) 'The generation of kidney organoids by differentiation of human pluripotent cells to ureteric bud progenitor–like cells', *Nature Protocols*. Nature Publishing Group, 9(11), pp. 2693–2704. doi: 10.1038/nprot.2014.182.

Xu, C. *et al.* (2011) 'Efficient generation and cryopreservation of cardiomyocytes derived from human embryonic stem cells', *Regenerative Medicine*, 6(1), pp. 53–66. doi: 10.2217/rme.10.91.

Xu, J. and Xu, P.-X. (2015) 'Eya-six are necessary for survival of nephrogenic cord progenitors and inducing nephric duct development before ureteric bud formation', *Developmental Dynamics*, 244(7), pp. 866–873. doi: 10.1002/dvdy.24282.

Xu, P. X. *et al.* (2003) 'Six1 is required for the early organogenesis of mammalian kidney.', *Development (Cambridge, England)*, 130(14), pp. 3085–94. Available at: http://www.ncbi.nlm.nih.gov/pubmed/12783782 (Accessed: 2 May 2019).

Xu, R. H. *et al.* (2002) 'BMP4 initiates human embryonic stem cell differentiation to trophoblast', *Nature Biotechnology*, 20(12), pp. 1261–1264. doi: 10.1038/nbt761.

Yamaguchi, T. P. *et al.* (1994) 'fgfr-1 is required for embryonic growth and mesodermal patterning during mouse gastrulation.', *Genes & development*, 8(24), pp. 3032–44. Available at: http://www.ncbi.nlm.nih.gov/pubmed/8001822 (Accessed: 1 May 2019).

Yamamoto, M. *et al.* (2006) 'Branching ducts similar to mesonephric ducts or ureteric buds in teratomas originating from mouse embryonic stem cells', *American Journal of Physiology-Renal Physiology*, 290(1), pp. F52–F60. doi: 10.1152/ajprenal.00001.2004.

Yamamoto, Y. *et al.* (2018) 'Random migration of induced pluripotent stem cell-derived human gastrulation-stage mesendoderm', *PLOS ONE*. Edited by M. Seno, 13(9), p. e0201960. doi: 10.1371/journal.pone.0201960.

Yamanaka, S. (2012) ‘Induced Pluripotent Stem Cells: Past, Present, and Future’, *Cell Stem Cell*. Cell Press, 10(6), pp. 678–684. doi: 10.1016/J.STEM.2012.05.005.

Yin, J. *et al.* (2015) ‘Atenolol Renal Secretion Is Mediated by Human Organic Cation Transporter 2 and Multidrug and Toxin Extrusion Proteins’, *Drug Metabolism and Disposition*, 43(12), pp. 1872–1881. doi: 10.1124/dmd.115.066175.

Yin, J. and Wang, J. (2016) ‘Renal drug transporters and their significance in drug-drug interactions’, *Acta Pharmaceutica Sinica B*. Elsevier, 6(5), pp. 363–373. doi: 10.1016/j.apsb.2016.07.013.

Ying, Q. L. *et al.* (2008) ‘The ground state of embryonic stem cell self-renewal.’, *Nature*. PMC Canada manuscript submission, 453(7194), pp. 519–23. doi: 10.1038/nature06968.

Ying, Q. L. *et al.* (2003) ‘BMP induction of Id proteins suppresses differentiation and sustains embryonic stem cell self-renewal in collaboration with STAT3.’, *Cell*, 115(3), pp. 281–92. Available at: http://www.ncbi.nlm.nih.gov/pubmed/14636556 (Accessed: 2 May 2019).

Yokoo, T., Kawamura, T. and Kobayashi, E. (2008) ‘Kidney organogenesis and regeneration: A new era in the treatment of chronic renal failure?’, *Clinical and Experimental Nephrology*, 12(5), pp. 326–331. doi: 10.1007/s10157-008-0062-5.

Yokoyama, T. *et al.* (2011) ‘Urinary heme oxygenase-1 as a sensitive indicator of tubulointerstitial inflammatory damage in various renal diseases.’, *American journal of nephrology*, 33(5), pp. 414–20. doi: 10.1159/000327020.

Yonezawa, A. *et al.* (2006) ‘Cisplatin and Oxaliplatin, but Not Carboplatin and Nedaplatin, Are Substrates for Human Organic Cation Transporters (SLC22A1-3 and Multidrug and Toxin Extrusion Family)’, *Journal of Pharmacology and Experimental Therapeutics*, 319(2), pp. 879–886. doi: 10.1124/jpet.106.110346.

Yonezawa, A. and Inui, K. (2011a) ‘Importance of the multidrug and toxin extrusion MATE/SLC47A family to pharmacokinetics, pharmacodynamics/toxicodynamics and pharmacogenomics’, *British Journal of Pharmacology*, 164(7), pp. 1817–1825. doi: 10.1111/j.1476-5381.2011.01394.x.

Yonezawa, A. and Inui, K. (2011b) ‘Organic cation transporter OCT/SLC22A and H+/organic cation antiporter MATE/SLC47A are key molecules for nephrotoxicity of platinum agents’, *Biochemical Pharmacology*. Elsevier, 81(5), pp. 563–568. doi: 10.1016/J.BCP.2010.11.016.

Yoshihara, M., Hayashizaki, Y. and Murakawa Y. (2017) ‘Genomic Instability of iPSCs: Challenges Towards Their Clinical Applications’, *Stem Cell Rev Rep*, 13(1), pp. 7-16. doi: 10.1007/s12015-016-9680-6.

Yoshikawa, Y. *et al.* (1997) ‘Evidence that absence of Wnt-3a signaling promotes neuralization instead of paraxial mesoderm development in the mouse.’, *Developmental biology*, 183(2), pp. 234–42. doi: 10.1006/dbio.1997.8502.

Yu, J. *et al.* (2007) ‘Induced Pluripotent Stem Cell Lines Derived from Human Somatic Cells’, *Science*, 318(5858), pp. 1917–1920. doi: 10.1126/science.1151526.

Yuri, S. *et al.* (2017) ‘In Vitro Propagation and Branching Morphogenesis from Single Ureteric Bud Cells.’, *Stem cell reports*. Elsevier, 8(2), pp. 401–416. doi: 10.1016/j.stemcr.2016.12.011.

Zager, R. A., Johnson, A. C. M. and Becker, K. (2012) ‘Plasma and urinary heme oxygenase-1 in AKI.’, *Journal of the American Society of Nephrology : JASN*, 23(6), pp. 1048–57. doi: 10.1681/ASN.2011121147.

Zhang, F. *et al.* (2006) ‘Ribosomal Stress Couples the Unfolded Protein Response to p53-dependent Cell Cycle Arrest’, *Journal of Biological Chemistry*, 281(40), pp. 30036–30045. doi: 10.1074/jbc.M604674200.

Zhang, L. *et al.* (1997) ‘Cloning and Functional Expression of a Human Liver Organic Cation Transporter’, *Molecular Pharmacology*, 1751(6), pp. 913–21. doi: 10.1038/tpj.2016.78.

Zhao, H. *et al.* (2004) ‘Role of fibroblast growth factor receptors 1 and 2 in the ureteric bud’, *Developmental Biology*. NIH Public Access, 291(2), pp. 325–339. doi: 10.1016/j.ydbio.2005.12.034.

Zhao, X. *et al.* (2010) ‘Viable Fertile Mice Generated from Fully Pluripotent iPS Cells

Derived from Adult Somatic Cells', *Stem Cell Reviews and Reports*. Humana Press Inc, 6(3), pp. 390–397. doi: 10.1007/s12015-010-9160-3.

Zhou, F. and You, G. (2007) 'Molecular insights into the structure-function relationship of organic anion transporters OATs.', *Pharmaceutical research*, 24(1), pp. 28–36. doi: 10.1007/s11095-006-9144-9.

Zhuo, J. L. and Li, X. C. (2013) 'Proximal Nephron', *Comprehensive Physiology*. NIH Public Access, 3(3), p. 1079. doi: 10.1002/CPHY.C110061.

10 Appendix

Segments of the GATA3 targeting plasmid

Segment1 sequence:

AAGCTTGCATGCCTGCAGGTCGACTAGACGGGGCTGTAATCTGGTAACTGTATGT
ATTTTAGTTCTTCAGTCCCTGGGAAGGAGACAGGAGAAGGTGGGAGGGAGGAAG
GGGCCAGCTGAAATGGAAACAGATCCCTGATCCGGGGCGGTCAGTGGAACCCTT
CTTGGTGTGCGAGAGCCTGTGCATTTCAGAGGCAGCAAAAAAGTAAAAAAAAAA
AAAAAAAATTGATCTTTGTTTAGATTAACAGACCCCTGACTATGAAGAAGGAAG
GCATCCAGACCAGAAACCGAAAAATGTCTAGCAAATCCAAAAAGTGCAAAAAA
GTGCATGACTCACTGGAGGACTTCCCCAAGAACAGCTCGTTTAACCCGGCCGCCC
TCTCCAGACACATGTCCTCCCTGAGCCACATCTCGCCCTTCAGCCACTCCAGCCA
CATGCTGACCACG

Ta:

67.8

Segment1 NEB builder primers:

FP (segment1 FP NEB)

AAGCTTGCATGCCTGCAGGTCGACTAGACGGGGCTGTAATCTGG

RP (labelled as ups RP Xbai)

CGTGGTCAGCATGTGGCTG

Segment2 sequence (Gblock1):

CATCTCGCCCTTCAGCCACTCCAGCCACATGCTGACCACGACCACGCCGATGCAC
CCGCCATCCAGCCTGTCCTTTGGACCACACCACCCCTCAAGCATGGTCACCGCCA
TGGGTGGAAGCGGAGCTACTAACTTCAGCCTGCTGAAGCAGGCTGGAGACGTGG
AGGAGAACCCTGGACCTATGGTGAGCAAGGGCGAGGAGGATAACATGGCCATC
ATCAAGGAGTTCATGCGCTTCAAGGTGCACATGGAGGGCTCCGTGAACGGCCAC
GAGTTCGAGATCGAGGGCGAGGGCGAGGGCCGCCCCTACGAGGGCACCCAGAC
CGCCAAGCTGAAGGTGACCAAGGGTGGCCCCCTGCCCTTCGCCTGGGACATCCT
GTCCCCTCAGTTCATGTACGGCTCCAAGGCCTACGTGAAGCACCCCGCCGACATC
CCCGACTACTTGAAGCTGTCCTTCCCCGAGGGCTTCAAGTGGGAGCGCGTGATGA
ACTTCGAGGACGGCGGCGTGGTGACCGTGACCCAGGACTCCTCCCTGCAGGACG
GCGAGTTCATCTACAAGGTGAAGCTGCGCGGCACCAACTTCCCCTCCGACGGCCC
CGTAATGCAGAAGAAGACCATGGGCTGGGAGGCCTCCTCCGAGCGGATGTACCC
CGAGGACGGCGCCCTGAAGGGCGAGATCAAGCAGAGGCTGAAGCTGAAGGACG
GCGGCCACTACGACGCTGAGGTCAAGACCACCTACAAGGCCAAGAAGCCCGTGC
AGCTGCCCGGCGCCTACAACGTCAACATCAAGTTGGACATCACCTCCCACAACG
AGGACTACACCATCGTGGAACAGTACGAACGCGCCGAGGGCCGCCACTCCACCG
GCGGCATGGACGAGCTGTACAAGTAGAGCCCTGCTCGATGCTCACA

Segment3 sequence (Gblock2)

TGGACGAGCTGTACAAGTAGAGCCCTGCTCGATGCTCACAGGGCCCCCAGCGAG
AGTCCCTGCAGTCCCTTTCGACTTGCATTTTTGCAGGAGCAGTATCATGAAGCCT
AAACGCGATGGATATATGTTTTTGAAGGCAGAAAGCAAAATTATGTTTGCCACTT
TGCAAAGGAGCTCACTGTGGTGTCTGTGTTCCAACCACTGAATCTGGACCCCATC
TGTGAATAAGCCATTCTGACTCATATCCCCTATTTAACCCTAGAAAGATAGTC

Segment4 (piggyback):

TCATATCCCCTATTTAACCCTAGAAAGATAGTCTGCGTAAAATTGACGCATGCAT
TCTTGAAATATTGCTCTCTCTTTCTAAATAGCGCGAATCCGTCGCTGTGCATTTAG
GACATCTCAGTCGCCGCTTGGAGCTCCCGTGAGGCGTGCTTGTCAATGCGGTAAG

TGTCACTGATTTTGAACTATAACGACCGCGTGAGTCAAAATGACGCATGATTATC
TTTTACGTGACTTTTAAGATTTAACTCATACGATAATTATATTGTTATTTCATGTT
CTACTTACGTGATAACTTATTATATATATATTTTCTTGTTATAGATATCAACTAGA
ATGCTAGCACAAGTTTGTACAAAAAAGCAGGCTGGCGCCGGAACCAATTCAGTC
GACTGGATCCGGTACCGGGCCCCCCCTCGAGGTCGAGACGGTATCGATAAGCTT
GATATCGAATAATTCTACCGGGTAGGGGAGGCGCTTTTCCCAAGGCAGTCTGGA
GCATGCGCTTTAGCAGCCCCGCTGGGCACTTGGCGCTACACAAGTGGCCTCTGGC
CTCGCACACATTCCACATCCACCGGTAGGCGCCAACCGGCTCCGTTCTTTGGTGG
CCCCTTCGCGCCACCTTCTACTCCTCCCCTAGTCAGGAAGTTCCCCCCCGCCCCGC
AGCTCGCGTCGTGCAGGACGTGACAAATGGAAGTAGCACGTCTCACTAGTCTCG
TGCAGATGGACAGCACCGCTGAGCAATGGAAGCGGGTAGGCCTTTGGGGCAGCG
GCCAATAGCAGCTTTGCTCCTTCGCTTTCTGGGCTCAGAGGCTGGGAAGGGGTGG
GTCCGGGGGCGGGCTCAGGGGCGGGCTCAGGGGCGGGGCGGGCGCCCGAAGGT
CCTCCGGAGGCCCGGCATTCTGCACGCTTCAAAAGCGCACGTCTGCCGCGCTGTT
CTCCTCTTCCTCATCTCCGGGCCTTTCGACCTGCAGCCTGTTGACAATTAATCATC
GGCATAGTATATCGGCATAGTATAATACGACAAGGTGAGGAACTAAACCATGGG
GACCGAGTACAAGCCCACGGTGCGCCTCGCCACCCGCGACGACGTCCCCCGGGC
CGTACGCACCCTCGCCGCCGCGTTCGCCGACTACCCCGCCACGCGCCACACCGTC
GACCCGGACCGCCACATCGAGCGGGTCACCGAGCTGCAAGAACTCTTCCTCACG
CGCGTCGGGCTCGACATCGGCAAGGTGTGGGTCGCGGACGACGGCGCCGCGGTG
GCGGTCTGGACCACGCCGGAGAGCGTCGAAGCGGGGGCGGTGTTCGCCGAGATC
GGCCCGCGCATGGCCGAGTTGAGCGGTTCCCGGCTGGCCGCGCAGCAACAGATG
GAAGGCCTCCTGGCGCCGCACCGGCCCAAGGAGCCCGCGTGGTTCCTGGCCACC
GTCGGCGTCTCGCCCGACCACCAGGGCAAGGGTCTGGGCAGCGCCGTCGTGCTC
CCCGGAGTGGAGGCGGCCGAGCGCGCCGGGGTGCCCGCCTTCCTGGAGACCTCC
GCGCCCCGCAACCTCCCCTTCTACGAGCGGCTCGGCTTCACCGTCACCGCCGACG
TCGAGGTGCCCGAAGGACCGCGCACCTGGTGCATGACCCGCAAGCCCGGTGCCG
GATCCATGCCCACGCTACTGCGGGTTTATATAGACGGTCCTCACGGGATGGGGA
AAACCACCACCACGCAACTGCTGGTGGCCCTGGGTTCGCGCGACGATATCGTCTA
CGTACCCGAGCCGATGACTTACTGGCAGGTGCTGGGGGCTTCCGAGACAATCGC
GAACATCTACACCACACAACACCGCCTCGACCAGGGTGAGATATCGGCCGGGGA
CGCGGCGGTGGTAATGACAAGCGCCCAGATAACAATGGGCATGCCTTATGCCGT
GACCGACGCCGTTCTGGCTCCTCATATCGGGGGGGAGGCTGGGAGCTCACATGC
CCCGCCCCCGGCCCTCACCCTCATCTTCGACCGCCATCCCATCGCCGCCCTCCTGT
GCTACCCGGCCGCGCGATACCTTATGGGCAGCATGACCCCCCAGGCCGTGCTGG
CGTTCGTGGCCCTCATCCCGCCGACCTTGCCCGGCACAAACATCGTGTTGGGGGC
CCTTCCGGAGGACAGACACATCGACCGCCTGGCCAAACGCCAGCGCCCCGGCGA
GCGGCTTGACCTGGCTATGCTGGCCGCGATTCGCCGCGTTTACGGGCTGCTTGCC
AATACGGTGCGGTATCTGCAGGGCGGCGGGTCGTGGCGGGAGGATTGGGGACAG
CTTTCGGGGACGGCCGTGCCGCCCCAGGGTGCCGAGCCCCAGAGCAACGCGGGC
CCACGACCCCATATCGGGGACACGTTATTTACCCTGTTTCGGGCCCCCGAGTTGC
TGGCCCCCAACGGCGACCTGTACAACGTGTTTGCCTGGGCCTTGGACGTCTTGGC
CAAACGCCTCCGTCCCATGCACGTCTTTATCCTGGATTACGACCAATCGCCCGCC
GGCTGCCGGGACGCCCTGCTGCAACTTACCTCCGGGATGGTCCAGACCCACGTCA
CCACCCCCGGCTCCATACCGACGATCTGCGACCTGGCGCGCACGTTTGCCCGGGA
GATGGGGGAGGCTAACTGAGCTCTAGAGCTCGCTGATCAGCCTCGACTGTGCCTT
CTAGTTGCCAGCCATCTGTTGTTTGCCCCTCCCCCGTGCCTTCCTTGACCCTGGAA
GGTGCCACTCCCACTGTCCTTTCCTAATAAAATGAGGAAATTGCATCGCATTGTC
TGAGTAGGTGTCATTCTATTCTGGGGGGTGGGGTGGGGCAGGACAGCAAGGGGG
AGGATTGGGAAGACAATAGCAGGCATGCTGGGGATGCGGTGGGCTCTATGGCTT

CTGAGGCGGAAAGAACCAGCTGGGGCTCGAGATCCACTAGTTCTAGCCTCGAGG
CTAGAGCGGCCGCACTCGAGATATCTAGACCCAGCTTTCTTGTACAAAGTGGTAC
TAGTTAAAAGTTTTGTTACTTTATAGAAGAAATTTTGAGTTTTTGTTTTTTTTTAAT
AAATAAATAAACATAAATAAATTGTTTGTTGAATTTATTATTAGTATGTAAGTGT
AAATATAATAAAACTTAATATCTATTCAAATTAATAAATAAACCTCGATATACAG
ACCGATAAAACACATGCGTCAATTTTACGCATGATTATCTTTAACGTACGTCACA
ATATGATTATCTTTCTAGGGTTAACAGGGTCTCTAGT

Ta:

58.1

FP (piggyback FP NEB)

TCATATCCCCTATTTAACCCTAGAAAGATAGTCTG

RP (piggyback RP NEB)

ACTAGAGACCCTGTTAACCCTAGAAAGATAATCATATTG

Segment5 sequence:

TTTCTAGGGTTAACAGGGTCTCTAGTGCTGTGAAAAAAAAAATGCTGAACATTGC
ATATAACTTATATTGTAAGAAATACTGTACAATGACTTTATTGCATCTGGGTAGC
TGTAAGGCATGAAGGATGCCAAGAAGTTTAAGGAATATGGGAGAAATAGTGTGG
AAATTAAGAAGAAACTAGGTCTGATATTCAAATGGACAAACTGCCAGTTTTGTTT
CCTTTCACTGGCCACAGTTGTTTGATGCATTAAAAGAAAATAAAAAAAAGAAAA
AAGAGAAAAGAAAAAAAAAGAAAAAAGTTGTAGGCGAATCATTTGTTCAAAGC
TGTTGGCCTCTGCAAAGGAAATACCAGTTCTGGGCAATCAGTGTTACCGTTCACC
AGTTGCCATTGAGGGTTTCAGAGAGCCTTTTTCTAGGCCTACATGCTTTGTGAAC
AAGTCCCTGTAATTGTTGTTTGTATGTATAATTCAAAGCACCAAAATAAGAAAAG
ATGAGGATCCCCGGGTACCGAGCTCGAA

Ta**:**

61.4

FP (segment5 FP NEB)

TTTCTAGGGTTAACAGGGTCTCTAGTGCTGTG

RP (segment5 RP NEB)

TTCGAGCTCGGTACCCGGGGATCCTCATCTTTTCTTATTTTGGTGCTTTG

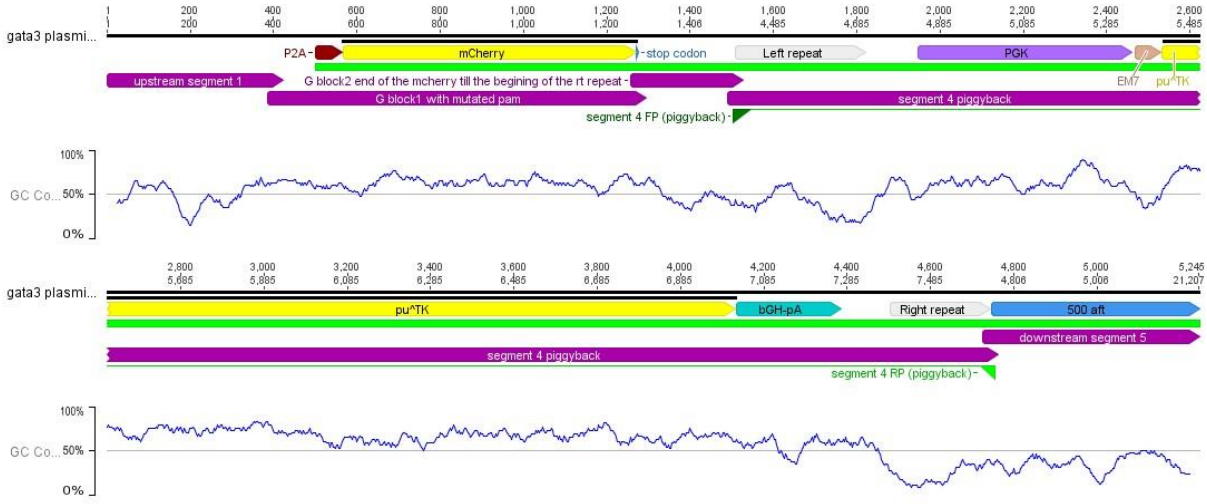

Digested Vector (PUC18 plasmid) sequence (using xbai RE):

CTAGAGGATCCCCGGGTACCGAGCTCGAATTCGTAATCATGGTCATAGCTGTTTC
CTGTGTGAAATTGTTATCCGCTCACAATTCCACACAACATACGAGCCGGAAGCAT
AAAGTGTAAAGCCTGGGGTGCCTAATGAGTGAGCTAACTCACATTAATTGCGTTG
CGCTCACTGCCCGCTTTCCAGTCGGGAAACCTGTCGTGCCAGCTGCATTAATGAA
TCGGCCAACGCGCGGGGAGAGGCGGTTTGCGTATTGGGCGCTCTTCCGCTTCCTC
GCTCACTGACTCGCTGCGCTCGGTCGTTCGGCTGCGGCGAGCGGTATCAGCTCAC
TCAAAGGCGGTAATACGGTTATCCACAGAATCAGGGGATAACGCAGGAAAGAAC
ATGTGAGCAAAAGGCCAGCAAAAGGCCAGGAACCGTAAAAAGGCCGCGTTGCT
GGCGTTTTTCCATAGGCTCCGCCCCCCTGACGAGCATCACAAAAATCGACGCTCA
AGTCAGAGGTGGCGAAACCCGACAGGACTATAAAGATACCAGGCGTTTCCCCCT
GGAAGCTCCCTCGTGCGCTCTCCTGTTCCGACCCTGCCGCTTACCGGATACCTGT
CCGCCTTTCTCCCTTCGGGAAGCGTGGCGCTTTCTCATAGCTCACGCTGTAGGTAT
CTCAGTTCGGTGTAGGTCGTTCGCTCCAAGCTGGGCTGTGTGCACGAACCCCCCG
TTCAGCCCGACCGCTGCGCCTTATCCGGTAACTATCGTCTTGAGTCCAACCCGGT
AAGACACGACTTATCGCCACTGGCAGCAGCCACTGGTAACAGGATTAGCAGAGC
GAGGTATGTAGGCGGTGCTACAGAGTTCTTGAAGTGGTGGCCTAACTACGGCTA
CACTAGAAGGACAGTATTTGGTATCTGCGCTCTGCTGAAGCCAGTTACCTTCGGA
AAAAGAGTTGGTAGCTCTTGATCCGGCAAACAAACCACCGCTGGTAGCGGTGGT
TTTTTTGTTTGCAAGCAGCAGATTACGCGCAGAAAAAAAGGATCTCAAGAAGAT
CCTTTGATCTTTTCTACGGGGTCTGACGCTCAGTGGAACGAAAACTCACGTTAAG
GGATTTTGGTCATGAGATTATCAAAAAGGATCTTCACCTAGATCCTTTTAAATTA
AAAATGAAGTTTTAAATCAATCTAAAGTATATATGAGTAAACTTGGTCTGACAGT
TACCAATGCTTAATCAGTGAGGCACCTATCTCAGCGATCTGTCTATTTCGTTCATC
CATAGTTGCCTGACTCCCCGTCGTGTAGATAACTACGATACGGGAGGGCTTACCA
TCTGGCCCCAGTGCTGCAATGATACCGCGAGACCCACGCTCACCGGCTCCAGATT
TATCAGCAATAAACCAGCCAGCCGGAAGGGCCGAGCGCAGAAGTGGTCCTGCAA
CTTTATCCGCCTCCATCCAGTCTATTAATTGTTGCCGGGAAGCTAGAGTAAGTAG
TTCGCCAGTTAATAGTTTGCGCAACGTTGTTGCCATTGCTACAGGCATCGTGGTG
TCACGCTCGTCGTTTGGTATGGCTTCATTCAGCTCCGGTTCCCAACGATCAAGGC
GAGTTACATGATCCCCCATGTTGTGCAAAAAAGCGGTTAGCTCCTTCGGTCCTCC
GATCGTTGTCAGAAGTAAGTTGGCCGCAGTGTTATCACTCATGGTTATGGCAGCA
CTGCATAATTCTCTTACTGTCATGCCATCCGTAAGATGCTTTTCTGTGACTGGTGA
GTACTCAACCAAGTCATTCTGAGAATAGTGTATGCGGCGACCGAGTTGCTCTTGC
CCGGCGTCAATACGGGATAATACCGCGCCACATAGCAGAACTTTAAAAGTGCTC
ATCATTGGAAAACGTTCTTCGGGGCGAAAACTCTCAAGGATCTTACCGCTGTTGA
GATCCAGTTCGATGTAACCCACTCGTGCACCCAACTGATCTTCAGCATCTTTTACT
TTCACCAGCGTTTCTGGGTGAGCAAAAACAGGAAGGCAAAATGCCGCAAAAAAG
GGAATAAGGGCGACACGGAAATGTTGAATACTCATACTCTTCCTTTTTCAATATT
ATTGAAGCATTTATCAGGGTTATTGTCTCATGAGCGGATACATATTTGAATGTAT
TTAGAAAAATAAACAAATAGGGGTTCCGCGCACATTTCCCCGAAAAGTGCCACC
TGACGTCTAAGAAACCATTATTATCATGACATTAACCTATAAAAATAGGCGTATC
ACGAGGCCCTTTCGTCTCGCGCGTTTCGGTGATGACGGTGAAAACCTCTGACACA
TGCAGCTCCCGGAGACGGTCACAGCTTGTCTGTAAGCGGATGCCGGGAGCAGAC
AAGCCCGTCAGGGCGCGTCAGCGGGTGTTGGCGGGTGTCGGGGCTGGCTTAACT
ATGCGGCATCAGAGCAGATTGTACTGAGAGTGCACCATATGCGGTGTGAAATAC
CGCACAGATGCGTAAGGAGAAAATACCGCATCAGGCGCCATTCGCCATTCAGGC
TGCGCAACTGTTGGGAAGGGCGATCGGTGCGGGCCTCTTCGCTATTACGCCAGCT
GGCGAAAGGGGGATGTGCTGCAAGGCGATTAAGTTGGGTAACGCCAGGGTTTTC
CCAGTCACGACGTTGTAAAACGACGGCCAGTGCCAAGCTTGCATGCCTGCAGGT
CGACTCTAG

The original Vector (PUC18 Plasmid) sequence:

TCGCGCGTTTCGGTGATGACGGTGAAAACCTCTGACACATGCAGCTCCCGGAGA
CGGTCACAGCTTGTCTGTAAGCGGATGCCGGGAGCAGACAAGCCCGTCAGGGCG
CGTCAGCGGGTGTTGGCGGGTGTCGGGGCTGGCTTAACTATGCGGCATCAGAGC
AGATTGTACTGAGAGTGCACCATATGCGGTGTGAAATACCGCACAGATGCGTAA
GGAGAAAATACCGCATCAGGCGCCATTCGCCATTCAGGCTGCGCAACTGTTGGG
AAGGGCGATCGGTGCGGGCCTCTTCGCTATTACGCCAGCTGGCGAAAGGGGGAT
GTGCTGCAAGGCGATTAAGTTGGGTAACGCCAGGGTTTTCCCAGTCACGACGTTG
TAAAACGACGGCCAGTGCCAAGCTTGCATGCCTGCAGGTCGACTCTAGAGGATC
CCCGGGTACCGAGCTCGAATTCGTAATCATGGTCATAGCTGTTTCCTGTGTGAAA
TTGTTATCCGCTCACAATTCCACACAACATACGAGCCGGAAGCATAAAGTGTAA
AGCCTGGGGTGCCTAATGAGTGAGCTAACTCACATTAATTGCGTTGCGCTCACTG
CCCGCTTTCCAGTCGGGAAACCTGTCGTGCCAGCTGCATTAATGAATCGGCCAAC
GCGCGGGGAGAGGCGGTTTGCGTATTGGGCGCTCTTCCGCTTCCTCGCTCACTGA
CTCGCTGCGCTCGGTCGTTCGGCTGCGGCGAGCGGTATCAGCTCACTCAAAGGCG
GTAATACGGTTATCCACAGAATCAGGGGATAACGCAGGAAAGAACATGTGAGCA
AAAGGCCAGCAAAAGGCCAGGAACCGTAAAAAGGCCGCGTTGCTGGCGTTTTTC
CATAGGCTCCGCCCCCCTGACGAGCATCACAAAAATCGACGCTCAAGTCAGAGG
TGGCGAAACCCGACAGGACTATAAAGATACCAGGCGTTTCCCCCTGGAAGCTCC
CTCGTGCGCTCTCCTGTTCCGACCCTGCCGCTTACCGGATACCTGTCCGCCTTTCT
CCCTTCGGGAAGCGTGGCGCTTTCTCATAGCTCACGCTGTAGGTATCTCAGTTCG
GTGTAGGTCGTTCGCTCCAAGCTGGGCTGTGTGCACGAACCCCCCGTTCAGCCCG
ACCGCTGCGCCTTATCCGGTAACTATCGTCTTGAGTCCAACCCGGTAAGACACGA
CTTATCGCCACTGGCAGCAGCCACTGGTAACAGGATTAGCAGAGCGAGGTATGT
AGGCGGTGCTACAGAGTTCTTGAAGTGGTGGCCTAACTACGGCTACACTAGAAG
GACAGTATTTGGTATCTGCGCTCTGCTGAAGCCAGTTACCTTCGGAAAAAGAGTT
GGTAGCTCTTGATCCGGCAAACAAACCACCGCTGGTAGCGGTGGTTTTTTTGTTT
GCAAGCAGCAGATTACGCGCAGAAAAAAAGGATCTCAAGAAGATCCTTTGATCT
TTTCTACGGGGTCTGACGCTCAGTGGAACGAAAACTCACGTTAAGGGATTTTGGT
CATGAGATTATCAAAAAGGATCTTCACCTAGATCCTTTTAAATTAAAAATGAAGT
TTTAAATCAATCTAAAGTATATATGAGTAAACTTGGTCTGACAGTTACCAATGCT
TAATCAGTGAGGCACCTATCTCAGCGATCTGTCTATTTCGTTCATCCATAGTTGCC
TGACTCCCCGTCGTGTAGATAACTACGATACGGGAGGGCTTACCATCTGGCCCCA
GTGCTGCAATGATACCGCGAGACCCACGCTCACCGGCTCCAGATTTATCAGCAAT
AAACCAGCCAGCCGGAAGGGCCGAGCGCAGAAGTGGTCCTGCAACTTTATCCGC
CTCCATCCAGTCTATTAATTGTTGCCGGGAAGCTAGAGTAAGTAGTTCGCCAGTT
AATAGTTTGCGCAACGTTGTTGCCATTGCTACAGGCATCGTGGTGTCACGCTCGT
CGTTTGGTATGGCTTCATTCAGCTCCGGTTCCCAACGATCAAGGCGAGTTACATG
ATCCCCCATGTTGTGCAAAAAAGCGGTTAGCTCCTTCGGTCCTCCGATCGTTGTC
AGAAGTAAGTTGGCCGCAGTGTTATCACTCATGGTTATGGCAGCACTGCATAATT
CTCTTACTGTCATGCCATCCGTAAGATGCTTTTCTGTGACTGGTGAGTACTCAACC
AAGTCATTCTGAGAATAGTGTATGCGGCGACCGAGTTGCTCTTGCCCGGCGTCAA
TACGGGATAATACCGCGCCACATAGCAGAACTTTAAAAGTGCTCATCATTGGAA
AACGTTCTTCGGGGCGAAAACTCTCAAGGATCTTACCGCTGTTGAGATCCAGTTC
GATGTAACCCACTCGTGCACCCAACTGATCTTCAGCATCTTTTACTTTCACCAGC
GTTTCTGGGTGAGCAAAAACAGGAAGGCAAAATGCCGCAAAAAAGGGAATAAG
GGCGACACGGAAATGTTGAATACTCATACTCTTCCTTTTTCAATATTATTGAAGC
ATTTATCAGGGTTATTGTCTCATGAGCGGATACATATTTGAATGTATTTAGAAAA
ATAAACAAATAGGGGTTCCGCGCACATTTCCCCGAAAAGTGCCACCTGACGTCT

AAGAAACCATTATTATCATGACATTAACCTATAAAAATAGGCGTATCACGAGGC
CCTTTCGTC

The PMSC-AAT-PB-PGK plasmid complete sequence:

CTAAATTGTAAGCGTTAATATTTTGTTAAAATTCGCGTTAAATTTTTGTTAAATCA
GCTCATTTTTTAACCAATAGGCCGAAATCGGCAAAATCCCTTATAAATCAAAAGA
ATAGACCGAGATAGGGTTGAGTGTTGTTCCAGTTTGGAACAAGAGTCCACTATTA
AAGAACGTGGACTCCAACGTCAAAGGGCGAAAAACCGTCTATCAGGGCGATGGC
CCACTACGTGAACCATCACCCTAATCAAGTTTTTTGGGGTCGAGGTGCCGTAAAG
CACTAAATCGGAACCCTAAAGGGAGCCCCCGATTTAGAGCTTGACGGGGAAAGC
CGGCGAACGTGGCGAGAAAGGAAGGGAAGAAAGCGAAAGGAGCGGGCGCTAG
GGCGCTGGCAAGTGTAGCGGTCACGCTGCGCGTAACCACCACACCCGCCGCGCT
TAATGCGCCGCTACAGGGCGCGTCCCATTCGCCATTCAGGCTGCGCAACTGTTGG
GAAGGGCGATCGGTGCGGGCCTCTTCGCTATTACGCCAGCTGGCGAAAGGGGGA
TGTGCTGCAAGGCGATTAAGTTGGGTAACGCCAGGGTTTTCCCAGTCACGACGTT
GTAAAACGACGGCCAGTGAGCGCGCGTAATACGACTCACTATAGGGCGAATTGG
AGCTCGTTTAAACGGCGCGCCTCTGCACGACAGGTCTGCCAGCTTACATTTACCC
AAACTGTCCATTACTGGAACCTATGATCTGAAGAGCGTCCTGGGTCAACTGGGCA
TCACTAAGGTCTTCAGCAATGGGGCTGACCTCTCCGGGGTCACAGAGGAGGCAC
CCCTGAAGCTCTCCAAGGTGAGATCACCCTGACGACCTTGTTGCACCCTGGTATC
TGTAGGGAAGAATGTGTGGGGGCTGCAGCTCTGTCCTGAGGCTGAGGAAGGGGC
CGAGGGAAACAAATGAAGACCCAGGCTGAGCTCCTGAAGATGCCCGTGATTCAC
TGACACGGGACGTGGTCAAACAGCAAAGCCAGGCAGGGGACTGCTGTGCAGCTG
GCACTTTCGGGGCCTCCCTTGAGGTTGTGTCACTGACCCTGAATTTCAACTTTGCC
CAAGACCTTCTAGACATTGGGCCTTGATTTATCCATACTGACACAGAAAGGTTTG
GGCTAAGTTGTTTCAAAGGAATTTCTGACTCCTTCGATCTGTGAGATTTGGTGTCT
GAATTAATGAATGATTTCAGCTAAAGATGACACTTATTTTGGAAAACTAAAGGC
GACCAATGAACAACTGCAGTTCCATGAATGGCTGCATTATCTTGGGGTCTGGGCA
CTGTGAAGGTCACTGCCAGGGTCCGTGTCCTCAAGGAGCTTCAAGCCGTGTACTA
GAAAGGAGAGAGCCCTGGAGGCAGACGTGGAGTGACGATGCTCTTCCCTGTTCT
GAGTTGTGGGTGCACCTGAGCAGGGGGAGAGGCGCTTGTCAGGAAGATGGACAG
AGGGGAGCCAGCCCCATCAGCCAAAGCCTTGAGGAGGAGCAAGGCCTATGTGAC
AGGGAGGGAGAGGATGTGCAGGGCCAGGGCCGTCCAGGGGGAGTGAGCGCTTC
CTGGGAGGTGTCCACGTGAGCCTTGCTCGAGGCCTGGGATCAGCCTTACAACGTG
TCTCTGCTTCTCTCCCCTCCAGGCCGTGCATAAGGCTGTGTTAACCCTAGAAAGA
TAGTCTGCGTAAAATTGACGCATGCATTCTTGAAATATTGCTCTCTCTTTCTAAAT
AGCGCGAATCCGTCGCTGTGCATTTAGGACATCTCAGTCGCCGCTTGGAGCTCCC
GTGAGGCGTGCTTGTCAATGCGGTAAGTGTCACTGATTTTGAACTATAACGACCG
CGTGAGTCAAAATGACGCATGATTATCTTTTACGTGACTTTTAAGATTTAACTCA
TACGATAATTATATTGTTATTTCATGTTCTACTTACGTGATAACTTATTATATATA
TATTTTCTTGTTATAGATATCAACTAGAATGCTAGCACAAGTTTGTACAAAAAAG
CAGGCTGGCGCCGGAACCAATTCAGTCGACTGGATCCGGTACCGGGCCCCCCCT
CGAGGTCGAGACGGTATCGATAAGCTTGATATCGAATAATTCTACCGGGTAGGG
GAGGCGCTTTTCCCAAGGCAGTCTGGAGCATGCGCTTTAGCAGCCCCGCTGGGCA
CTTGGCGCTACACAAGTGGCCTCTGGCCTCGCACACATTCCACATCCACCGGTAG
GCGCCAACCGGCTCCGTTCTTTGGTGGCCCCTTCGCGCCACCTTCTACTCCTCCCC
TAGTCAGGAAGTTCCCCCCCGCCCCGCAGCTCGCGTCGTGCAGGACGTGACAAA
TGGAAGTAGCACGTCTCACTAGTCTCGTGCAGATGGACAGCACCGCTGAGCAAT
GGAAGCGGGTAGGCCTTTGGGGCAGCGGCCAATAGCAGCTTTGCTCCTTCGCTTT
CTGGGCTCAGAGGCTGGGAAGGGGTGGGTCCGGGGGCGGGCTCAGGGGCGGGC

TCAGGGGCGGGGCGGGCGCCCGAAGGTCCTCCGGAGGCCCGGCATTCTGCACGC
TTCAAAAGCGCACGTCTGCCGCGCTGTTCTCCTCTTCCTCATCTCCGGGCCTTTCG
ACCTGCAGCCTGTTGACAATTAATCATCGGCATAGTATATCGGCATAGTATAATA
CGACAAGGTGAGGAACTAAACCATGGGGACCGAGTACAAGCCCACGGTGCGCCT
CGCCACCCGCGACGACGTCCCCCGGGCCGTACGCACCCTCGCCGCCGCGTTCGCC
GACTACCCCGCCACGCGCCACACCGTCGACCCGGACCGCCACATCGAGCGGGTC
ACCGAGCTGCAAGAACTCTTCCTCACGCGCGTCGGGCTCGACATCGGCAAGGTG
TGGGTCGCGGACGACGGCGCCGCGGTGGCGGTCTGGACCACGCCGGAGAGCGTC
GAAGCGGGGGCGGTGTTCGCCGAGATCGGCCCGCGCATGGCCGAGTTGAGCGGT
TCCCGGCTGGCCGCGCAGCAACAGATGGAAGGCCTCCTGGCGCCGCACCGGCCC
AAGGAGCCCGCGTGGTTCCTGGCCACCGTCGGCGTCTCGCCCGACCACCAGGGC
AAGGGTCTGGGCAGCGCCGTCGTGCTCCCCGGAGTGGAGGCGGCCGAGCGCGCC
GGGGTGCCCGCCTTCCTGGAGACCTCCGCGCCCCGCAACCTCCCCTTCTACGAGC
GGCTCGGCTTCACCGTCACCGCCGACGTCGAGGTGCCCGAAGGACCGCGCACCT
GGTGCATGACCCGCAAGCCCGGTGCCGGATCCATGCCCACGCTACTGCGGGTTTA
TATAGACGGTCCTCACGGGATGGGGAAAACCACCACCACGCAACTGCTGGTGGC
CCTGGGTTCGCGCGACGATATCGTCTACGTACCCGAGCCGATGACTTACTGGCAG
GTGCTGGGGGCTTCCGAGACAATCGCGAACATCTACACCACACAACACCGCCTC
GACCAGGGTGAGATATCGGCCGGGGACGCGGCGGTGGTAATGACAAGCGCCCA
GATAACAATGGGCATGCCTTATGCCGTGACCGACGCCGTTCTGGCTCCTCATATC
GGGGGGGAGGCTGGGAGCTCACATGCCCCGCCCCCGGCCCTCACCCTCATCTTCG
ACCGCCATCCCATCGCCGCCCTCCTGTGCTACCCGGCCGCGCGATACCTTATGGG
CAGCATGACCCCCCAGGCCGTGCTGGCGTTCGTGGCCCTCATCCCGCCGACCTTG
CCCGGCACAAACATCGTGTTGGGGGCCCTTCCGGAGGACAGACACATCGACCGC
CTGGCCAAACGCCAGCGCCCCGGCGAGCGGCTTGACCTGGCTATGCTGGCCGCG
ATTCGCCGCGTTTACGGGCTGCTTGCCAATACGGTGCGGTATCTGCAGGGCGGCG
GGTCGTGGCGGGAGGATTGGGGACAGCTTTCGGGGACGGCCGTGCCGCCCCAGG
GTGCCGAGCCCCAGAGCAACGCGGGCCCACGACCCCATATCGGGGACACGTTAT
TTACCCTGTTTCGGGCCCCCGAGTTGCTGGCCCCCAACGGCGACCTGTACAACGT
GTTTGCCTGGGCCTTGGACGTCTTGGCCAAACGCCTCCGTCCCATGCACGTCTTT
ATCCTGGATTACGACCAATCGCCCGCCGGCTGCCGGGACGCCCTGCTGCAACTTA
CCTCCGGGATGGTCCAGACCCACGTCACCACCCCCGGCTCCATACCGACGATCTG
CGACCTGGCGCGCACGTTTGCCCGGGAGATGGGGGAGGCTAACTGAGCTCTAGA
GCTCGCTGATCAGCCTCGACTGTGCCTTCTAGTTGCCAGCCATCTGTTGTTTGCCC
CTCCCCCGTGCCTTCCTTGACCCTGGAAGGTGCCACTCCCACTGTCCTTTCCTAAT
AAAATGAGGAAATTGCATCGCATTGTCTGAGTAGGTGTCATTCTATTCTGGGGGG
TGGGGTGGGGCAGGACAGCAAGGGGGAGGATTGGGAAGACAATAGCAGGCATG
CTGGGGATGCGGTGGGCTCTATGGCTTCTGAGGCGGAAAGAACCAGCTGGGGCT
CGAGATCCACTAGTTCTAGCCTCGAGGCTAGAGCGGCCGCACTCGAGATATCTA
GACCCAGCTTTCTTGTACAAAGTGGTACTAGTTAAAAGTTTTGTTACTTTATAGA
AGAAATTTTGAGTTTTTGTTTTTTTTTAATAAATAAATAAACATAAATAAATTGTT
TGTTGAATTTATTATTAGTATGTAAGTGTAAATATAATAAAACTTAATATCTATTC
AAATTAATAAATAAACCTCGATATACAGACCGATAAAACACATGCGTCAATTTT
ACGCATGATTATCTTTAACGTACGTCACAATATGATTATCTTTCTAGGGTTAACC
ATCGACGAGAAAGGGACTGAAGCTGCTGGGGCCATGTTTTTAGAGGCCATACCC
ATGTCTATCCCCCCCGAGGTCAAGTTCAACAAACCCTTTGTCTTCTTAATGATTGA
ACAAAATACCAAGTCTCCCCTCTTCATGGGAAAAGTGGTGAATCCCACCCAAAA
ATAACTGCCTCTCGCTCCTCAACCCCTCCCCTCCATCCCTGGCCCCCTCCCTGGAT
GACATTAAAGAAGGGTTGAGCTGGTCCCTGCCTGCATGTGACTGTAAATCCCTCC
CATGTTTTCTCTGAGTCTCCCTTTGCCTGCTGAGGCTGTATGTGGGCTCCAGGTAA

CAGTGCTGTCTTCGGGCCCCCTGAACTGTGTTCATGGAGCATCTGGCTGGGTAGG
CACATGCTGGGCTTGAATCCAGGGGGGACTGAATCCTCAGCTTACGGACCTGGG
CCCATCTGTTTCTGGAGGGCTCCAGTCTTCCTTGTCCTGTCTTGGAGTCCCCAAGA
AGGAATCACAGGGGAGGAACCAGATACCAGCCATGACCCCAGGCTCCACCAAGC
ATCTTCATGTCCCCCTGCTCATCCCCCACTCCCCCCCACCCAGAGTTGCTCATCCT
GCCAGGGCTGGCTGTGCCCACCCCAAGGCTGCCCTCCTGGGGGCCCCAGAACTG
CCTGATCGTGCCGTGGCCCAGTTTTGTGGCATCTGCAGCAACACAAGAGAGAGG
ACAATGTCCTCCTCTTGACCCGCTGTCACCTAACCAGACTCGGGCCCTGCACCTC
TCAGGCACTTCTGGAAAATGACTGAGGCAGATTCTTCCTGAAGCCCATTCTCCAT
GGGGCAACAAGGACACCTATTCTGTCCTTGTCCTTCCATCGCTGCCCCAGAAAGC
CTCACATATCTCCGTTTAGAATCAGGTCCCTTCTCCCCAGATGAAGAGGAGGGTC
TCTGCTTTGTTTTCTCTATCTCCTCCTCAGACTTGACCAGGCCCAGCAGGCCCCAG
AAGACCATTAATTAAGGCCGGGCCGCTCTAGAACTAGTGGATCCCCCGGGCTGC
AGGAATTCGATATCAAGCTTATCGATACCGTCGACCTCGAGGGGGGGCCCGGTA
CCCAGCTTTTGTTCCCTTTAGTGAGGGTTAATTGCGCGCTTGGCGTAATCATGGTC
ATAGCTGTTTCCTGTGTGAAATTGTTATCCGCTCACAATTCCACACAACATACGA
GCCGGAAGCATAAAGTGTAAAGCCTGGGGTGCCTAATGAGTGAGCTAACTCACA
TTAATTGCGTTGCGCTCACTGCCCGCTTTCCAGTCGGGAAACCTGTCGTGCCAGC
TGCATTAATGAATCGGCCAACGCGCGGGGAGAGGCGGTTTGCGTATTGGGCGCT
CTTCCGCTTCCTCGCTCACTGACTCGCTGCGCTCGGTCGTTCGGCTGCGGCGAGC
GGTATCAGCTCACTCAAAGGCGGTAATACGGTTATCCACAGAATCAGGGGATAA
CGCAGGAAAGAACATGTGAGCAAAAGGCCAGCAAAAGGCCAGGAACCGTAAAA
AGGCCGCGTTGCTGGCGTTTTTCCATAGGCTCCGCCCCCCTGACGAGCATCACAA
AAATCGACGCTCAAGTCAGAGGTGGCGAAACCCGACAGGACTATAAAGATACCA
GGCGTTTCCCCCTGGAAGCTCCCTCGTGCGCTCTCCTGTTCCGACCCTGCCGCTTA
CCGGATACCTGTCCGCCTTTCTCCCTTCGGGAAGCGTGGCGCTTTCTCATAGCTCA
CGCTGTAGGTATCTCAGTTCGGTGTAGGTCGTTCGCTCCAAGCTGGGCTGTGTGC
ACGAACCCCCCGTTCAGCCCGACCGCTGCGCCTTATCCGGTAACTATCGTCTTGA
GTCCAACCCGGTAAGACACGACTTATCGCCACTGGCAGCAGCCACTGGTAACAG
GATTAGCAGAGCGAGGTATGTAGGCGGTGCTACAGAGTTCTTGAAGTGGTGGCC
TAACTACGGCTACACTAGAAGGACAGTATTTGGTATCTGCGCTCTGCTGAAGCCA
GTTACCTTCGGAAAAAGAGTTGGTAGCTCTTGATCCGGCAAACAAACCACCGCT
GGTAGCGGTGGTTTTTTTGTTTGCAAGCAGCAGATTACGCGCAGAAAAAAGGA
TCTCAAGAAGATCCTTTGATCTTTTCTACGGGGTCTGACGCTCAGTGGAACGAAA
ACTCACGTTAAGGGATTTTGGTCATGAGATTATCAAAAAGGATCTTCACCTAGAT
CCTTTTAAATTAAAAATGAAGTTTTAAATCAATCTAAAGTATATATGAGTAAACT
TGGTCTGACAGTTACCAATGCTTAATCAGTGAGGCACCTATCTCAGCGATCTGTC
TATTTCGTTCATCCATAGTTGCCTGACTCCCCGTCGTGTAGATAACTACGATACG
GGAGGGCTTACCATCTGGCCCCAGTGCTGCAATGATACCGCGAGACCCACGCTC
ACCGGCTCCAGATTTATCAGCAATAAACCAGCCAGCCGGAAGGGCCGAGCGCAG
AAGTGGTCCTGCAACTTTATCCGCCTCCATCCAGTCTATTAATTGTTGCCGGGAA
GCTAGAGTAAGTAGTTCGCCAGTTAATAGTTTGCGCAACGTTGTTGCCATTGCTA
CAGGCATCGTGGTGTCACGCTCGTCGTTTGGTATGGCTTCATTCAGCTCCGGTTCC
CAACGATCAAGGCGAGTTACATGATCCCCCATGTTGTGCAAAAAAGCGGTTAGC
TCCTTCGGTCCTCCGATCGTTGTCAGAAGTAAGTTGGCCGCAGTGTTATCACTCA
TGGTTATGGCAGCACTGCATAATTCTCTTACTGTCATGCCATCCGTAAGATGCTTT
TCTGTGACTGGTGAGTACTCAACCAAGTCATTCTGAGAATAGTGTATGCGGCGAC
CGAGTTGCTCTTGCCCGGCGTCAATACGGGATAATACCGCGCCACATAGCAGAA
CTTTAAAAGTGCTCATCATTGGAAAACGTTCTTCGGGGCGAAAACTCTCAAGGAT
CTTACCGCTGTTGAGATCCAGTTCGATGTAACCCACTCGTGCACCCAACTGATCT

TCAGCATCTTTTACTTTCACCAGCGTTTCTGGGTGAGCAAAAACAGGAAGGCAAA
ATGCCGCAAAAAAGGGAATAAGGGCGACACGGAAATGTTGAATACTCATACTCT
TCCTTTTTCAATATTATTGAAGCATTTATCAGGGTTATTGTCTCATGAGCGGATAC
ATATTTGAATGTATTTAGAAAAATAAACAAATAGGGGTTCCGCGCACATTTCCCC
GAAAAGTGCCAC

GATA3 gene CDS:

CTGATTGGTCCCTCCAGGCCCCGCCCCCGCTCGCCCCGCCCCTCTCGCTGGGGCG
CCTCGGAGCCGCGTGCCCTCCGCCCCGGGGTGCCCATTGCGCAGAGCGTGGCCTG
GAGACCCGCGAGCCGGGGAAGGTCGCCGTGGAGTCCCGACCAGAGGCCGGGGTT
GGGGTCGGTGCAGACCGAGGGCTGGTTTCCTTGACTGTGGGAGAAACGCCGGGA
GCCGGAGTAAGTAGGGCTCCGGGCGGGGCGAAAGGAAAAGTTGGGTCCCTAGA
GTGAAGACCGAGTTCTTTCTGTCCGTCTACACTGAGCGTACTCGGGGAATGAGTT
AGAGCCAGTCTCTTCCTCCCCTCCCCCCTTCTCATCCCTCACTGTTGCCACTCAAG
TCAAAAGCACACATTGATTACAAATATTAGGTCTGGAAAGGGCAGCTGCAACAG
CTGAAGCGTGTTCACTCTGGGGGCTTGAGAGCGCAGAAGGCTCGGGAAAGAGGT
GACAATGACAACAAAATTGACGCGGACGCTCCAGTCAAAGGCATCTCCCCTTTA
TCCGATGACTCACCCTCTTAGGAAGTCGGCCCGAGAGGCAAATCTCAAAATACCT
TGACATGAAACATTTTGTTTTTCTGATCAATTTAACGCGCACGTTTCCCCACATCG
ATGCGCTCTCCCAAACACCCTGCATTGGATCCTAATAATGATCCATGCGTGCCTA
TTTTTTAAAAGTCTGAAAAAGAAAATTCTGCCCATCGAAATGAACTTCATGAATG
GGGCAGGCTGGCTGCACCGGGACGGAATCGTCCACCCGACCCGAATGAATTGGC
AGGAGCCGCGGCCACATTTAAAGGGCCAGAGCGCGCGTTCCCTCCCGTCCGCCC
CCAAGCCCCGCGGGCCTCGCCCACCCTGCCCGCCGCCCCTCCGCCGGCGGCCGCC
CTCTGCGGCGCCCCTTTCCGGTCAGTGGAGGGGCGGGAGGAGGGGCGGGGGTGC
GCGGGGCGGGGGGAGAAGTCCTGGAGCGGGTTTGGGTTGCAGTTTCCTTGTGCC
GGGGATCCTGTCCCCTACTCGCCAGCGCCAGGCTCCTCCCCCCCGGCGCGGATGA
CACTAGAACCTCCTTAAGTTGCGTCGCGCCACAGCTGTCTGCGAACACTGAGCTG
CCTGGCGCCGTCTTGATACTTTCAGAAAGAATGCATTCCCTGTAAAAAAAAAAA
AAAAATACTGAGAGAGGGAGAGAGAGAGAGAAGAAGAGAGAGAGACGGAGGG
AGAGCGAGACAGAGCGAGCAACGCAATCTGACCGAGCAGGTCGTACGCCGCCG
CCTCCTCCTCCTCTCTGCTCTTCGCTACCCAGGTTGGTACTGGTGACTTTTTTTTTT
TTTAAGTTTGATTTTTTGCCCCCAACCACTTGGGAGGACCTAAATCAATTTTAAA
AACTCAACTCTCCTCTTTTGGAGGTTTTCTAGGGGCTGAGAGGACGGTCCCGGGA
CCGGTGTCCCCGAGGGAGGGACTTGCCCTCCAAGTCGTAACAGTCAGCCCTGGG
ACTTGCCCTCCAAGTTGCTCAGCCAGCCCCGGCTCCCGCGAGCCGGGCTGCAGGG
ACGTCCCCGAGAGCCCTGCGGGCTCCGCGGCCGTGTCCCCGCGCTCCCGTGCGGG
TCTCGGGTGCGCTGGGCGGGCGGGCGGCGCGAGGGGAGGTTGTGCCACTCCAGC
AACTCAGGGGCTCATCCAGGTCTCCCATTCTCTCCCTTGCAGGTGACCCGAGGAG
GGACTCCGCCTCCGAGCGGCTGAGGACCCCGGTGCAGAGGAGCCTGGCTCGCAG
AATTGCAGAGTCGTCGCCCCTTTTTACAACCTGGTCCCGTTTTATTCTGCCGTACC
CAGTTTTTGGATTTTTGTCTTCCCCTTCTTCTCTTTGCTAAACGACCCCTCCAAGAT
AATTTTTAAAAAACCTTCTCCTTTGCTCACCTTTGCTTCCCAGCCTTCCCATCCCC
CCACCGAAAGCAAATCATTCAACGACCCCCGACCCTCCGACGGCAGGAGCCCCC
CGACCTCCCAGGCGGACCGCCCTCCCTCCCCGCGCGCGGGTTCCGGGCCCGGCG
AGAGGGCGCGAGCACAGCCGAGGCCATGGAGGTGACGGCGGACCAGCCGCGCT
GGGTGAGCCACCACCACCCCGCCGTGCTCAACGGGCAGCACCCGGACACGCACC
ACCCGGGCCTCAGCCACTCCTACATGGACGCGGCGCAGTACCCGCTGCCGGAGG
AGGTGGATGTGCTTTTTAACATCGACGGTCAAGGCAACCACGTCCCGCCCTACTA
CGGAAACTCGGTCAGGGCCACGGTGCAGAGGTACCCTCCGACCCACCACGGTGA

GTGCGCCCGGGGTGCCGGGGCTCCCGCCGGCCGCTTCAGCCGTCCCGGCTCGGG
GAGGTCGGGAGGGACCTGAGGGCGGGGAGAGGTCAAGCGAAAGCCCCCATCTG
CCGTTCCTGGTTCATTTACAAAAAAATTGGGGCCCGGAAATGGGCGAGGAAGGC
CTCTGGCTCGTCGCGAGAGTGTGTTTTGAAAGAGTCGCAGCAGGCGCCTCTCCCG
GCTGGTGGCCCTGGGGCCTGGCGCTCACCTGGCGGGCGCCAGGCCGCAGCCCTC
CGTCTCTGCGCGGCTGCAGGTTTTGGGGTGGGGGGTCTCGGGATGTCCCCAGGCG
CGGGGTGCCCTGGCTCTGCCTCCGCGGGTCCGGGCTCTCTGGGCCCGGTAGCCGG
CGCCGGACAAGCACGGCTGGAACCCGGCTCTTCCAAAAAACCTGGCGTTCCCTG
TTACCCGCTAGCTCTTTCTAGGCGGGTGGGCGGGGTGGAGGGGGCCCTCTGCCAG
CGTCCCTCAATTCGCACATTTTCAGAAAGGCCCCAGAGACCTATTTATTCACACC
CTTCTCCTTGACCTTTTCCCAGAGCTAGTGCCTTTGGTTTTTAGACAGGTCTCTTA
CCTCCTGGCTTCAGGAATGGAATTCTGATGCTGAAGGGGTTTGGGCGGGGAAGA
CCCCTGTCTTAAGTTTGAGGGATCTGAGATTTCCCAGATTCCCGGCTGCACAGAA
TTTTCTTGCGTCTTTGCTTTCAAGTCGCCTCCTTGCCTGCAACTCTTGCCTTACTCT
GTCTCTGGGTACTGCCCTCCATTAGCCTCCCACCTAAGATGTAGGATACACCCCC
GTTTAAATAAAGGCAATTCCAGTACCACCTCTTTCCCCCTTTCACCTGGAGAAGT
TCAGGAGAGTTCTGAAATGTAAAAAAAGAAGACCAGGCCTGTGTAGTTTGAGGA
AAAAAGATCGAACACTTTCCAGCTCTAAGTTTGTTCCTAAAGAAGAAACAGGGG
TAAAACATCGGGCAGAAAAAGTGTGGGGCTTTCTGAGTCCAGCCAGACCGAATT
CTGCCCTGATTCCCCTACTCAGAGCCTGCCTTGACACGGATGACATAGCCCCTCC
GGCAGCAGGCGTCCTCTACCCTGCTGTCGCCAGGTTTTAAACAATCGTTTCTGCG
GATGGGGCGCCCTTTGCCCACGTTCTGTGCGGATCAGCAGTTAGGTGGAAATGCG
GTAGAGGCAGACTTAATATTATTTACTATACTACTTCCTGCATAATATGAATCTT
GACCCTTGGTGTTCAGAGAACTCTCTTTCCCTCTCCACTCCCCTCCCCTTCCTCTC
TCTTAAGATTTTAGTTTCAGTATTGTTCTTAATGGTTGAATCGAATGTCAAATGCT
GAGGCAGGTACTGGCTTTAAAGATCAAGAAGTGTGTGGATTTGCACTTGCTTTTT
AAATGTACCCCTCAGAGTGTATGAGTTACAGCTACCTTAAGATTGTGCGTTTTAA
ATGAAGGCTAATCAGACTCTGTGTCTGAGTCATCTTTCATTTAAAATATACACAT
CAACTGGAATTTTGTGTCTTAGGGGCTCAGGTGAAAATTCACCCATGGCACTGGT
GGGATCATAGCTTTATTGAGGGTGCATGGGGCTTACGTTATCTCCTTCTCCTTTAG
GATTTGGGAGGGTGAGAAAAGCAGAGAAAATGGCCATCCCAGGGTCCAGCCTTG
GGAACTTTCTCCAACAGCCCGAGCAATGAAAACGTCCCTGCAAATCCCATTTTAG
GCCTTTTGCGGGCAGCCTGGCCGTTTCTGAGCAAGCACTGGGTTAGGTTTCCGGA
AACTAACCCTGAAAGTCTCCTGACTTCTGTCCCAAGGCCTCTCCTTCCTGTATTTG
GTGCTGGGAGCTGGGCCTGACTCCAGGGTCGTTTTCTGGTGTGGAGCAGTTGTGT
GGCCGGGCTCCATCCTTCAGGCCTCCTCACTCACAGCCGGCTCTCTTATCAGGCT
GGCTGGGATTAAGTCCGAGTCAGGGAACTCAGGGCCATTGAAGGAAACCCATAA
ATCAAGTCAGGTTCTAGAGAGAGACCTTGGGGAATGTGATTTAGGCGGTGTATCT
GGAGAGGCCAAATAAGCAAAGGGGCCCTTCTCCCCCTCTGCAGCAACCTCTCGG
GTGTCAGCCACAGGCCCTTCATTCTGCTACATTTGATGGGACATCCCTGTGGGAG
AGATGGGTGAAGGATTCTGTCCCCAGCCTGACCCCCAGGTGTGCCAGGCAGGTA
CTCCGGGGACCGCCGGGAATTGAGAGTGGGCCTGAGCCCGGGCTTTTGCTGAAA
AGGAGGCCGATGCGAGGTAGAGATTCCCCAGGTGTCCCTGACGGCCTCCCAGGG
CCACACTCACCCTCCTTCTCTCTCCTGCCCTTTCCCCGTTGCCCCACAGGGAGCCA
GGTGTGCCGCCCGCCTCTGCTTCATGGATCCCTACCCTGGCTGGACGGCGGCAAA
GCCCTGGGCAGCCACCACACCGCCTCCCCCTGGAATCTCAGCCCCTTCTCCAAGA
CGTCCATCCACCACGGCTCCCCGGGGCCCCTCTCCGTCTACCCCCCGGCCTCGTC
CTCCTCCTTGTCGGGGGGCCACGCCAGCCCGCACCTCTTCACCTTCCCGCCCACC
CCGCCGAAGGACGTCTCCCCGGACCCATCGCTGTCCACCCCAGGCTCGGCCGGCT
CGGCCCGGCAGGACGAGAAAGAGTGCCTCAAGTACCAGGTGCCCCTGCCCGACA

GCATGAAGCTGGAGTCGTCCCACTCCCGTGGCAGCATGACCGCCCTGGGTGGAG
CCTCCTCGTCGACCCACCACCCCATCACCACCTACCCGCCCTACGTGCCCGAGTA
CAGCTCCGGACTCTTCCCCCCCAGCAGCCTGCTGGGCGGCTCCCCCACCGGCTTC
GGATGCAAGTCCAGGCCCAAGGCCCGGTCCAGCACAGGTAGGAGCCAGCTCTTC
CCTGGAGCCTTTTCTCCTCCCTCCTCCCCTTTTCCTCAATCCAGGGCCGCACCCAG
AGGGACCCCTCAGGGGAGCCGGGGTGTCCCAAAGCCTGCTGAGATGCCATTCTT
CCCATTCTTCCTGCCGGGAAGGCACTGCATGTCCTCCCATCCTAGCTCACGCCTG
GCCTCGGAAGCAGAGGGGAAGTGGGATCTGATTTAAAACCCCCCAATGAGCTGG
GATAGGAAAAAAGACAAACAAAAACAAAGTCATGCCCTCTTCTGCCTGTCGCAG
GACTTCTGGATTGGGCTGGTAACCTTTAGTCAGTTTCCAAGACCAAATGGAAGGC
CGAGGGAATAATTCTTGAGTGTTTCATGCTAAAACGAAACCTCCTCAAGCCTAAA
CAAACACAGGTCCCTCTATGACCCCTTTGGCCTCTGTCATTCTGACTGTTCCTCTC
GCTCAGCTCAAAGGGGACCACGCAGTGAGGACAGTCCTTTATTAGACGTGTAGA
CACAAAGTGTGTGTGCATGAGCCTGGCCAAAGCTGCACGCATATTCTCTGCGTGG
AAAAGGGGGCTCTCAGCTGAACTGGGAGAAAGCGGTGGCTTTGCATTGGGGAAG
CAGAGTTGAATGAAAATCAAATGTCGCCTGGCCCAGTTAGTTACCTGCAGCGTCT
CCTAGAGCTCTCAGTGCAGTCAGGGGCAGGAAACCGTATTAGGACATATTGCTT
GGCTGAGCTGCAGCCAGAGGAGGTAGAAAGGAACGGAAAAGTGCTCCAGGTGT
GTATCTCAGCTTCCTGTGCTCTGTTCCTTTCCAAAATGCAAACGCTGCCTAGCAGC
ACGCTGCATTTTTATTCAGTTGGTGTCATTACTTGCATGAAGAAAAACCCCACAC
AAAATACTTTGGCTTTAAAAATAAATCGATCTATCACCAATTCCATTTCTAAACA
AAGTAATTGAGTCAAAAGAGAGCTAGGGATTCTCTGATATTGATTTAACTGTATT
ATTAGACAGGGTTTGGTGAAGATTTTGATGTCTCCTTAGGCGTGTCCATTTCAGA
GTGGGCATCTCTTCTCTGATCGGCTCCAGGTATCTTGCCTCCGCTGTCTCTCTACA
GATCCTATATAGAAAGCAATCGTGAAAATCACTTGTCTTTTAGGGATGAGATGAG
CAGCCTTGAAACCGAGCTCCCAAAGCTCCGGTTTGAAAAACTTCAGAGGGAGTA
CTCTGGGAGCCCAGTGACCATGAGATCAGTTTTCAGGGTTTTTTTCCAGGGTGAC
ATTCACTCCGACTGCCTGAGCAGGACTGTCTCTATTTAGTTGATATGTTTTAGCTA
ATCCAATTATTTTCAGACTGCTGCACGCGACAGTTGCATTGTTTATCCTGAGCCA
GGAACTTTAATAGAGTCCGGATGCGGTTAGGCTGACAGAAGAACCCAGACCTGC
ATGTTCAGTACATGAAAGTAGGCAGGAGGGAGAGGGAGGCAGGCTAGCTGGTG
GAGTCAAAAAGAAAGCAAGAGGCCGGGAGAGCTGGAGGCACAAAGTGGCCACG
GTGCCTGGCAGGGGCTGGGCTTGGGGGTGGAGGGAAGGATTAAGAAGTGGGGT
GCAGCTTGACTCAGAAACACAGGCTGGGGAGCTGAATCGAAAGAGAGCAGACCT
ATGCATTTTGAGGTTGTGATGGGATTTCTTTTCTTTTTCTTTTTTTTTTAAAGTTCT
CTTTTCTGGTAAGGCTATGAGGTTGGGGAGAGCTCGTGGTATCTGAGGCCGGCGT
AGTGGTTTGTGCGGGGGGAGGGGACAGAGTGACTTTTCCAAGATACTCTGGTTTC
TTTACCCTCATTTCCGTGTTTGATTTCTCCCCCTCTTGTGCACACTTTCTGCCTTAA
GTTTAGTCTTTTCTTTCCTCTCATTTCTTTCCATAAGACTCTGAACATGGAGGGGA
GAAAGAGAGGGCCGTGGTTTCCCTAAGCCAGAGCTAGGAATACCGATACACCGA
TTTTGGTTTTTTTGGCGAGGAGGAGAGGAGGCCATTTCAATTTGGCCTTTTTACTT
CCTCCTTCTTAATTCCTTTCTCACAGTCGTGAAAACCAAGAACAGCACACCTGGC
AGGGGCGGCGAGCGAGCTGGGACTTTTGGGAGTGTGGAGGGGAAGTTTCGAGAA
GCCCCTCCTTTTGCAGGGGGTGGAGGTGGTGGGAATTCTTCAGGAGGGGATTCTC
TTGGTTTTAGTGGTTGCTCTCTCTCTCTCTCTCTCTCTTTTTTTTCCCCCTTTAACCT
CTTCTTTGCAAATGCATTTGCTGAAGGAGGACACAGAGAAGAGAGAGTTTTTGG
GGTTGTCGCTGGAAACGGTTGAAGTCGTGGTTAGGGCACCTATTGCTGTCTTAAC
GCCTGGGCTTTCGGGGCTGGGACGAAGCTTTTGCAAACAAAAGACAGAGTCTTT
GTGTCCAGGGCCGCTTCTTAGCTCCCCTGCCACCTTTCCAGTTGGGCATCTCCCTC
CACTGTCGTCTGATCGAGCTCCTGCCCTGCTCCCTACCCCCTCCCACAGCCTGGTT

TAAGGGTTTCAGGCCAAGGCGGAGCAAGAGGCATTTGCCAGCAGCTGTTGAATG
TCAAGAGGCCTCGCCGCTCTGTGGTTCTTGTCACCTAAGAGAGAGGTGTCTGCCT
GAGCAGCTCACAACAGGCAGGGGTGAGGAGAGGGGAGGAAAGAAGGCAGGAG
AGAGTCAGGGCCTCCATTAGGAAAACTGGCTGTTTGCTGAAGTCACAGACCAGA
GGCAGCAAGGAAAAAAGAAGAAGAAAAGCCCATAGGAGGCAATGGCAACCTTG
CCGAGTGAATCAAGACAGAAAATTACCCTAGTGTGCAGAACCTTGTTGAAGAGG
TAACCGTTGCTAGCTTTCAAGGTGTTTCTGAAAAGGAAGCTATCACCCTCCCCAC
CACCCTGCAAATGAGAGGAAATCAGACTGATCATGTCAGGCTGGGAGGTCCCCC
AGCACCAGGGTGCCCAGGAGCCGGGTGGCAACCACGCTCCCCGCCTCCAACCAC
AGCGGCCTCTCCTCACACTGCCCTCTGCCCAGTGCCCAAGTAGGGGAGGAGCCC
GAGGGGGTCCCCTGTCTGGGCAGGGTGGGGAGTGGGCCTGCAGTCCTAGCTGGG
ACAGGGCCAGTGCTGCCCCAGAAGGGGCTGACCCAGCAGCTACCAGGGACACAA
AAAGGCAGGCCTGCGGCCTGGCCTGGGCTGCAGCCGGTTACTCGCCCACTCACC
CTTCACTCTTTCCTTCCAGCCTCCCCCACATCCAGTCTGCCACATCCCTCAGGCTT
TTGACCCCAACTGAAAGGTGTCTGGGTGTGATTCAGGCCTGAGCCTTTTTCAAGA
ACTGAGAAGAGCCGTTGGGTACTTAGGAAGGCGCCTTTGGCATGCACTGCAGCG
TGTTTGTGTTTAATCTCAGGGGTTCTGGGGCACAGCAAAGGCTCTCTGGGGACCC
TAGGCTAAGAATCTTTTGGAATGTGGAGCAAAAAAAAAACCTCTCTTACATCCTC
ATTTTTTTTTTTTTTTTAAAAAACAAAGTAGACAAAAACTAGTGGGCACCATCCC
TGACTTTCAAGGGTGCAAGACCCTCTTCCATTTGCAAAAGTCTTTAACTTTCCTGA
AGAACTTACCCCTGGAGAGTATCACAGGCCCCCAAGTGTGAACCCCCCTAGTTCC
CTCCTACTTGATCTGGGGCTTTCCAAAGGCCCAATAGGTCCCATATCTGCCAAGG
CAGATTTTTCCTCCTTTTAGGGGAATCAAAATTCTCAAGCACCCTACTGGGTTCTC
TTCTTCTACCCCAGTGGTCCGGGCAGGTTGGAGGTCATTAATTACTCTCTTAAAA
CAAAACAGTCTTCAGAGCTCATTTTTCTTCCCTACCTACCCTCCGGGGTCCTCCTC
TGGGCCTCCCCTCTCTGGGGGACCAACTTGAGTTAAGCCTCCTGTTCCTGCAAGG
AAGGGGAGTCCTGGCTTTCTCTGGGCACCCAGAGAACTGGGCGCTAGAGACCCG
TGTGTCCCTGGGTCCCCCAAAACCAAGGAGATTCTCCTAGAAAGCATCTTTCTCT
TCCTCTTGCAAAGTTGAAATCAGTTAGCCAACTCCCCCATGTCTTGAAATGGTAA
TTTAAGGGATTCTTCCAAGGAGCTTTCTGGGTGGGTCTGGGTCGCTTTCCAGCCT
GGGCTGAGGGAGTGAATGCTGCTCAGACTTCCTACCGGCCTGGCTGGTTTTTCGT
TTATTTTGTTTGTTTGTGTTTTTGGGAAAAGAGAAACTGTAGGCAGGCCTTGGTTA
CTGAGCAGCCACCCCGCTTTGTTAACTTGCCTCTTCTCCTGATCTTCCTCTGATCG
GCTTCACTCTGTCCTCCCAAACCTTCCCTTTTCCTTTTTCCCTCCCTCCCCCTCTTC
CAGGTTCCCTGCCTAAAGTTTGCATTTCCCCCTTGCACCCCCTGGCTGGGGTCATA
CTTTAACTTCAGTCTCCGTAACAGCGGCTGGAAAGCTATGGAAACCCCTGCTGGG
TCCTAATCGCTTCCTTTCCAGCCAGGGACATTTGCAGTTTGATTGGAAGTAAAAT
CTAAAACCCTAGCTAGTGAAATCAATCAGCCGATTGATCAATCTATGCATCTATT
TATTATCTGTTCACCTATCTAGCCATTGATGAATCCTTCCTTTCCCCCATCCTAAT
CTTCATTATTTAATCAATCTCTATAGACAGACCCATGATGATAATGGGTCACCTTT
GTCTTCCTTTTTTTCCTTTGAGGGAAATGAATGGAATGTTTGCCTTTTGCCACCAT
CCAGGGCTCAGGATTTTCTCAGGGAAGTATTTGTAGCTGGAATCTGCATTCCTCC
TTGGTCCTGCCCGATCTTCTCCATCAAGTCGGGCAAGCCAAGAACAGGGTTCTGT
TGCAACGATGCATCTGCCCCTTCTGCGGGCGCCTCCGTGTGTGTCGGGGGAACGG
TCATGCCAGGACAGCATTCCCCAGCTCAACTTTGGAGCATCTTGGAAAGAGGTG
GGGGTGGACACGCTCCCCAAAAGAGGAGGGAGAAGGAAAAAAGTTCTCCATTTT
ACGTTTCTCCCCCAGTTCCAAATGCTGTCAGCTTTCCTGCGTGTTTTCCTTCCCTA
AGTGGCTTATCTGTGCTTTTGTTTCCAGAAGGCAGGGAGTGTGTGAACTGTGGGG
CAACCTCGACCCCACTGTGGCGGCGAGATGGCACGGGACACTACCTGTGCAACG
CCTGCGGGCTCTATCACAAAATGAACGGACAGAACCGGCCCCTCATTAAGCCCA

AGCGAAGGCTGGTAAGTTCTCGGGAAGGGATGGATTCCATGCTGACCATTCTGG
GTTTCTCATTTCCTCTCTTCCGGAAGGACAGCTTTCTGCAGGAAATTGACAGGAT
AGCCTCCAATCGTGTCAGCTGGCTTGGGACAGTTTTTTTTTTTTTCCTTTTTCTTTC
TTTCTTTTCTTCTTCTTCTTTTTTTTTTTTTTTTTCAAATTTGATACACAGAACAGCT
CTTTTCCCCTCTTTTTCCCCATCCATGTTTCTTAAGTCGCTTGTGAACATTTTAAGG
AGACTGAATTCTTGGTTATCAAATCTGCAGTGTATTCCTGAATAGAATAATGGTA
TGAACAGGACCAGAGCAGCTGGTTTAAGTGCATTGATGAGCACCGTTTGACAGA
TAGAGACATTTAGTATGAGGATGGAATGTTCCAGAAACCATCCAGAATGGGTTC
CTGAAGTTGTGGCGTGTGGCTTCCCAGGAAGGATTACAGACTCAGTGCAATGGA
TGGATTTGTTATGCTAATGCTTCAAAATGGTTGGAGCTGATTAAATGAATTTCAG
AGGCTTCACCAGCAACCAGTGAGCCTAATGCCACTTTCCTCCTTTCTTGGTCTCA
GCCTTTGAGAACTTTCCACAGGCAATTCCTATGGGAAACGTCGTGTGAGTCCTCT
CATACCTGGCATTTGGTCTTCTTTTCTCTTTGAACTACTACCAGTAAGGTGATAGT
TTTTTCTCTCCTCTCTCATTATTCTTTTAAAAACTTTTTAAGCATGAGGGATCCTTG
AGAAAACCTGGCTCTGTCAAGCATTTATAAGGAAGACAACTTATAGGGGACATT
CATTTGCAAGCTCCTCTTTGGAAGTTTGAATAGTGAATGTATGTGACAGACAAAT
AACAACTCTAGCCACAGCTAAGAGATCAAAATGCTTTATGTGGTGCTGACATTCA
CCAAGTCGAGATGGGAGGAGGGGAATTTCCCCACGCAGATTAATGGATAAATTA
GCATCCATCAATTTCTAAGGAAGGAAAAAGAACACCTCTGTATTCTTTTTAAAGA
ATACTTTGCCCTCCCCATCAGATTGTAGTGCAACTCAACACCTTTCACATCCTATT
TTGAAGAAGGAAAAACTTTCTTTTTTTTTTTTTTTTTTTTTTTTGAGACAGAGTCTCA
CTCTGTCACCCAGGCTGGAGTGCAGTGGCACGATCTCGGCTCACTGCAACCTCCA
CCTCCCGGGTTCAAGCAATTCTCCTGTCTCAGCCTCCTGAATAGCTGGGAGTAGG
GACACCCGCCCCCACACCCGGCAAATTTTTGTATTTTCAGTAGAGACAGGGTTTC
GCCTTTTTGGCCAGGCTGGTCTCAAACTCCTGACCTCAGGTGATCCACCGCCTCG
GCCTCCCAGAGTGCTGGGATTACAGGCATGAGCCACCGCTCCCAGCCAAAGAAG
GAAAACTTTCTAGGGATGGAAATGTCCACATGACTTTAATCTTTGACAATCCTGG
ATATCGAGGCTTTATTCTTTCTGATCTTTGCCCCCTTCTCCAACTTTCTCAACCTTC
CCCCACCTCTCCTCCAGCAGTTTGGTTTTTTTTTTTTTTTTTTTTTTTTCCTTTCTC
TCATGTGCAAAGCTGACTTCCTAGGAAAAAGCTGCCGGATATCTGAGCACTGGA
GATAACTCATAAACAACAACTCAGCTTCCCCAACCTAAACACCAAGATGTTTGA
ACGTATCAGAACAAGAAGTGTTTGAAAAAAAAAAAAAAAAAAAGGCTAGAGGTG
TTAGTGCAGAATGAATATGATCACACCACAAAAGAATGTTTTGAATCACTCAAA
AACCTGGCCTTAGTAAAAAAAAAAAAAAAAAAAAGAGAGAGAGAGAGAGAGGA
AAAAAAAACAACAAACAAAAACCTTCTTGTTAAAATGTGTCTTGGTACCATTATA
GTTGTTTTTTTTGTTTTTTCTGTTTTTTTTCTAATAAAAGTAAAGAAGGAAAAAGA
GGGATTAAAAGTCTCAAGGCATGGGCTGATTGGTGAGCAAAAGTTTATTTGACA
TTTTCTTGGGTCTTCTTCCTCTGTCTGGTCAGATTGCAGAGGAGGATCGTAATTCC
ATTTTATGCAATTTTATCTCCACTCACCTTTCATAGGAAATCTCTAGAACTCTGAG
TAATAATTGCTTTGAATTTTAGAGTTCAATGACTGTCACATTTTCATCTCTCTTTT
CTTTCTTAATCATCTGTCTTTGGTGGTTTGATGTTTTTAGTTCTATAGAATTCATAA
GCTACAGGGAGGTAGAACACAGGACACATTCAGATTTCTTTTTCTTTCTTTCTTTC
TTTCTTTTTTTTTTTTTAGCCCTGAGATGTATTTGACTTCTGAACACCTAGAACCCTT
TGTTTTCTTCTTTCCTGTATTCCCTGACCCTTTATTCCAGTTCCAGCTTGCTATTTT
TGTTTGATACATTTGCAGATTCACTGAAGACCACCCAGCCCATATATAGCTAGCT
CTTCTGTGAGATGTGTATTTAACCCTGAAAAAACTAATGCAAGAAATAGGAGAG
ATGACCGAAGGGAAGACTCATAGATTCTTTTCCCCCTGGCATTGCCAGGATTTTC
ATACATCTCACCACTAGTGAGAGGCTGAGCTGCTTGCTTTAATATACTGTACCTC
CTGCTAGTGACCCAAACAGTGTGGCTTTGAGAGACCCTAAGTTCCCATAAAGTTT
GTAGTACTGGAAGCATCTTCCTTTGCTTTTATTTAGATTGCTGTCAATAGACTGCA

AAAGATTACATGCTGTACCTTGTCATCTGGAGCTCTGACTTTACCAGTTGGCATT
ATATGCTTGTACTCTGTACATTCAGAATTGCTGGGCTAGGAAACCCAGGTGCCTG
AGTGATATTAATCTGCTATATCTGAGTAGCTCTTCTAAAAAAAAAAAACACTATA
GGAAGATAATAATCACATATAATTTAATTGTCAAAATCATTAAGCACTGGTTTTA
CGTAGTACTTTCTCCCAAAAAGTACACAAATGAAACAGTTGTTTAAGCATTAAAT
TACCATATTTCATAAAGGCAGTCGGGCAGAGGCATATGGGGTTAGATCAGCACT
CATGGACAATGTGAATTACATTCAAGATGGACAGCAAAAGACTCCCATCTTCTCC
CTTATGATAGGCCAGGGCAGTTTTTAGTTTCCAGTTCCTTAGAACACAGAAAAGA
AAGAATTTTTTTAAAAAGGTCATATATACTCTGTTATTTACATCCCACAGAAGCA
TATCTGTGAAACAATTTAGCAACTTTGAAAGAAAAAGGGTCACTCAGGTTAATTC
AAAATTGTCACTGGGTTCTCCATATCTGGCAGCTTCGGGTGTTGGCTTCAACTTTT
TGCTTGATAAAATATTGATATAAAACTGTACCAGAATCCCAGGCCGGGTGCGGT
GGCTCACTCCTGTAATCCCAGCACTTTGGGAGGCCAAGGCGGGTAGATCATGAG
GTCAGGAGATAGAGACCATCCTGGCTAACACAGGTGAAACCCCGTCTCTACTAA
AAATACAAAAAATTAGCTGGGGCGGTGGCGGGCGCCTGTAGTCTCCAGCTACTT
GGGAGGCTGAGGCAGGAGAATGGTGTGAACCCAGGAGGCGGAGCTTGCAGTGA
GCCGAGATCGCGCCACTGCACTCCAGCCTGGGCGACAGAGCGAGACTCCGTCTC
AGAAACAAAAGAAAACATAACAAAACAAAAAACAAAAAACAAAAAACAAAAC
TGTACCAGGATCCCTATAGTTCTTGTTCTGTGTTCTTATAACCATACCAGAATTTT
CTTCATCACAGACAGAGACTAAACTCTTTCTTCTCTTACCTTTCCTTTGATAATAT
TTTTGATCCAGGAATGGGGATAATTTTGCAGTTAAAATTTTCTTTTTATGATGGAA
GGTGAGGAGGAGAGAGAGGTTTATATTAGAAGTGACCCAACTCCATTTTCTTCCA
ATGGTTTTTTTCAGTTTTATTTTTTTAAAGCGTGAACAGAGAATAGTCACCTGATC
AATTTAAATATGTCAAAAAGTGAAAGAAAAAATCTCTCTTTTAAAGGAAATGAG
GGCAGTAACACAACCAAGGAATCAAAATTCAGGTTGAGGCTGACCTTTGACCTG
CAACTATGCTACTCCATGAACAGCAAGTAGGAAATGGCTGATTTCATGAAGGTG
GACTGGCATCAGAGGAGGCGAGGGATCCAGGGTTCCTGATGAGTGGCAACATTC
CTTGGTCTTTTGAGTTTGTTTGATTGGTGAATCAAATTTAGGTGACAGCCAGCTA
AAGAGAGTGAGGGTGGCTGTCTTGTGAATGGGAAGTGACCAAGCTTGAAAGCAC
AGACTGTGGTGGCTCACGCCTGTAATACCGGCACTTTGGGAGGCCGAGGCAGGT
GGATCACTTGAGGTCAGGAGTTCAAGACCAGCCTGGCCAACATAGTAAAACCCT
GTCTCTACTAAAAATAGAAAAATTAGCCGGGCATGGTGGCAGGTGCTTATAAAT
CCCAGCTACTCGGGAGTGTGAGGCAGGAGAATTGCTTCAAGCCGTGAGGTGGAG
GTTGCAGTGAGCTGAGATCGCACCACTGCACTCCAGCCTGGGTGACAGAGCGAG
ACTCCATCTCAAAACGAGAAAAAAAGAAAGTGCAGGCTGTATAAATTTAGGAGG
TCTTGTTGACCTAGGATGTCCTACTTGGCGCTTCCTCAGGTGTGTCACCCATGTGT
ATGTGCCACACACTTGCACAGACATTCTTTGCAGAATTTGCTGTTGTGTTGGCAC
ACTGTTCTCTTTATAACTCAGCATTTCTTTATTTGCGATCCAGAGTGTTTTTGGTG
CTTGGCTTTGCGCCTCCTTTGCTGTGAATGCATCCTGATGGCTGGAGCCTGTTTGA
GGATGGATATTCTTGGGAGTTGTGTTTGAAAACAACCTCTTGTGGCCCTGGACTT
GGTGAAAAAGGCAACTGAAAGCCCAGTTCCAAAATGAGGCTGGCTAATTCAAAA
TTGCCACCCATAAAAATTAACCCTCTGGTGTACTTTGTGGGTTGAGGGTAGGAGG
CTAAGACTGCCAGGGAGGAGGCCCCGGCTTCCTGCTCCTACCGGGGAGCAGCAG
GTGAAACTCTGACCACGTTACTGCAATCCTGACATGCTCCAGTGGAGTGGCGACA
TTTTTCTTCTCGAGGCAGCTTTTGGGGATCTGTATTACTTTCATGTGGACCACTTG
CTAGTTTTGATTTCAATGATAATTTCTTCCTTCCTTTTTTTTTTTTTCAAGCCTGTC
TTCATAGTGATGACAACACATTTAACATTTGTTTTGATTTTACCCTCTCCTCTCTC
CCCACTCTCAGTCTGCAGCCAGGAGAGCAGGGACGTCCTGTGCGAACTGTCAGA
CCACCACAACCACACTCTGGAGGAGGAATGCCAATGGGGACCCTGTCTGCAATG
CCTGTGGGCTCTACTACAAGCTTCACAATGTAAGTGGACTGGGATCAGCAAGAA

CAGGGCTCGCTTCCTGATGGTGACCAGCAAACAGCGTCACCACCACCCTCTCCAA
GTGAATCGCTCACCATGGGGGCAGATGACAGGTTCCAAATAATTGATGCAATAG
GACCTAGCTTGGAAAACTACTTTGTCTAGCATAGCCGTGCTGAGGCCGAGGGGG
CTCACAGCCTGGCAGCCACACAACCCCCTTGGTATGCATTGGACACTCCACATAC
CATGCAGCAATCCGATGTGCTGAGTGGGCCTGTGTGGTTTATAAGGAAAAAAAA
AAAATCTTCCTTTTGGAAAACAAAAAAAGCCACCGGTCCTATTTTGTTGTTTCCTT
ACATTTTAAACTCTTTGCAGAAAGAGAGAATGAAAGAGAAAGGTAAATAGAATT
GTAATGTGTGGCAGGGGGTCTGGAAACTAAGAGGACCCATTTGGTTACTGAGAG
GTAAAAAGTCTTGGCTAAATCTGTGCTACAAATTTGAAATGGATCCTCTGTATAA
AAGACATGGAAAAAAATGTCTGACAGATTTCGTCTGATGTCTTTGTCCGAACCAA
CTTTCACGTGCAGAGAGCTAGCTCCTGAGGAAGGTGGCTGGCCTGGGGGATGTT
ACCATACCAGGGAAAATAAACTGTCATTTTCTCCTTTTATATCATGTTAGCAGAG
CGGTAATTGCCAGTCACCTGAATTTAGTTGTGTCATTTCTGATCTTTCCATTTGGG
GTCCTCTCATTTTGTAATATATCTTAATCTTAAAAAATTTTTTTTTCAGTTTTTTTT
TTTTCCTGAAATCATTCTGGCTCAGAGGCCATGATTCTAGTGAGGCTTCAAGTTT
ACATTAACTCTAAAGACAAAAATGGTTATTTTGGTCTTTCTCTGTGTTGCTCTCTC
TCTCCTTCCTTTTTAGCTCTTTCTGATTCTCCTAAATTCTCTTGGCCAACCTGACTT
TGGCAAAGTCCGGGGCTGAACAGGGAGGAGACAGGGACTTTTGCTTGCGGCGGT
TCTGGCAATGAACTCATCTTACTCAGGAATACCTGGGAATTGGGGAGGAAGCTTT
TCTGGTTGGATTTTTTGAGTCATAAAGAACTTCTCAGGGTGACCCCAGCACCCTG
CTTCTTTTTCACTTCTTGGGAGCAAGTTGCTGTGATTCCGAGGAGCCCTGTACGCT
CATTCCCTGCCTGTGCCAACTCTCTCGCTGTGGCCCTGGTGCAGTGAATGAAACT
AGAGTCTTACTACGATCCCTTATTCTCCCTTAGGTCCTGGGACTGTGGTCTATATA
CATTTATCAGCAATTCAATCCAAGTTCTATTTTCACTTTGGGGAATTTGCTTGCTG
ACTACAGTAGAGATAGAGATTCGTGATTAAAATCTGGAAGGCTTGGGCTTATAA
GCTATTAGGTTATTAGCATTAGGGTTTATTAGCTATCCAGTCATCAGCACTGCCT
ATGAAATTATTTTTGGGCTGTAATTTATGGATTTCAAAGAACTTTCATGTTACTTG
ATTACATTTGAGCCTGAGATAGTCCCATGATGTAGACAGGGCAGAAATTATTTTT
ATTTCAGTTTTACTTGAGGGAGTTATGACTCAGAAAAGCAAGTCGCTTGCACAAG
GTAACGTGGCTGAGAAAGTATAAGAGTCAGGGCCCATTTCAGAGTCAGGAGGCT
TTCCTGGGAAGTTGGCAGTGTCAGAACTAAGAGGAGAACCAGGGGAAAGGGAA
TGCTCTCTTTTTTTAGAGTATAACAAAATTGTAACAAATTGTGTGTGTATATTT
CATCCCTATATTCGTGGAAGTATAGGAATTATAGGAGATTAACTAGCTATATGTT
TTTTTGAATAGTTAGCTGGGATGAGATATGATCTCACTTGTGTCTGATCACATAT
ATATATATTTCTGAAGAACATGAATTTCTCAAATCAAAGTAAAGCTGAGGAATCC
TCTCCATGGCTCACTTCTACCTCCTCAATCTTAATGAGCTTGGTCTTCATGGCTGG
GCTCCAGTGAATGGGAGACAGAAACTTCCTCATCCTCAAGAGTGGTTTTTCTGTC
TTCTCTGGTTTACCAGGAATTTGTAAAAGGAGGCGATTGATGTGTATTGAACAAT
AAGAGATAATAATCTATTAACATTGTCATCACGTTGCGTTTTGCTCTGCCCTTCCA
GACATCTCTACATGGATGCCATAAGCTCTTTCTTCTTATCTAGGTGTTGAGATAAC
TGCCTACCTCGGTATCAGCATCTCTCAGTGGTGTTGTGACTGGTTATCTGGGGTTG
TGTGGCTACTGGTGTAACTAGATATTATATTTAGATACCTGGCTATGTATAGCTA
GATATCGGCATCAGAGCTGTGTATCTGGACATTATCTTGGTGAAGATTTGATGTG
GGAGTAGATTCCTGTCATCTCTGTAGGCTGCATCTTTATCTTGATGATAACTTTGA
AGAAGGAACCTGGAGATGTTCCTCTGGCAGTGACCTTTCTGGGCTCTCCTGCCAT
CGGTCACGTTGCCTTCCTGGGCTTGGGGAAAATAAGGTCTCAGCTCCAGTGTGGG
GCTTTGTTTCCTTCTCCAGGTGACCTCTCCCAGCTCAGCTTCGGGAAGCTGGGTGT
TGGCTGCTCTCAGCAGGTTGGCCATTTGAATTCTTCCTTTCTTAGCTGTGATTTTC
TGGCTTTGGGAACAGACAGGTAAAACCCAGAGCCAAGGGTTCTCCACCCTTGAG
AACTGTGGCGGAAGGCGATGCTTTCAGCCCGGGAAGTCAGGAATGGCCAGGACA

CTGACATTCACTCCTTGAGTCTGTTTGCCACCCTCCCCTGGGAACATGGCCAGAT
GTGGAGTTTGCTCTTCCGGGCAGATGTCTGCTGTTGGGGTTAATCTGCTTCTGCCT
CCCTGTGGGGAGTAACTTCTGTTTACTTTGTAAAGTTTCCTTTCTTGATTCTGGGC
CCCCAAAGCAAATGTATTTTTAAAGGCAAATGAGGTTTATTAAGAAGAGAGAAA
TGGCAGATGTCTCCGAGACTGAAGTCTCTTGATCTTGAGAGTAGGGTCTGGTCTC
TGTCTCTTTACTCTAGCACATTCTTGGTCTTTCCTTTTCAAGATGAGTGCCCTTTTG
TGCTTTGCACCCCATAGGTGGTTATTAAATACATGTTGATTGGTTGGTTGGCTGTT
TGTCTGGTTAGAAGTGGAGAGTCAGAGCTAGGTGGAAATAGCACTTGCAACCAT
TGCAGCTGCTGTTGGAATGACACAGGCAAGAGATCACTTTTGGGCCAGGCGCGG
TGGCTCATGCCTGCAATTCCAGCACTTTGGGAGGCCGAGGTGGGCAGATCACAA
TGTCGGGAGTTCGAGACCAGCCTGCCCAATATGGTGAAACCCCGTCTCTACTAAA
AATACAAAAATTAGCCAGGTGTGGTGGCAGGCGCCTCTAGTCCCAGCTACTCAG
GAGGCTGAGGCAGGAGAATTGCTTGAACCCGGGAGGCAGAGGTTGCAGTGAGCC
GAGATCGCGCCACTGCACTCCAGCCTGGGCGACAGCGGGAGACTTCGTCTCAAA
AAAAAAAAAAAAAAAAAAAAAAAGATCACCTTTAAGAAAGGCATGGTTTCATA
AAATACAACCCGGCTACATATAAATTCTAGCGGAAGATTTTATGGCACCTCTTAA
AGGCCAGGTAGAAGAGAGGCAACCGAAAGTTACTCAGTAGAACAGTACAGTCCT
CATTTCTTCAAGGCAGACAGCCTTAACCACCTAGAGGCTGATGGCCTGGGGAGT
ACTTTTCAAGTTCTGAAGCAGATTTGTCAAAGTAGCCAAAATGGCATTTCCCTCC
TGAAGATTCTTCACTACCTCGATTCTTATGAAATAGTCTAAGGAAGTTCTAAAGA
AATAAGACAAGTGAATTCTATTTTCGTTACCAGAGAAATACAATCGTACTAGACG
GGGCTGTAATCTGGTAACTGTATGTATTTTAGTTCTTCAGTCCCTGGGAAGGAGA
CAGGAGAAGGTGGGAGGGAGGAAGGGGCCAGCTGAAATGGAAACAGATCCCTG
ATCCGGGGCGGTCAGTGGAACCCTTCTTGGTGTGCGAGAGCCTGTGCATTTCAGA
GGCAGCAAAAAAGTAAAAAAAAAAAAAAAAAATTGATCTTTGTTTAGATTAACA
GACCCCTGACTATGAAGAAGGAAGGCATCCAGACCAGAAACCGAAAAATGTCTA
GCAAATCCAAAAAGTGCAAAAAAGTGCATGACTCACTGGAGGACTTCCCCAAGA
ACAGCTCGTTTAACCCGGCCGCCCTCTCCAGACACATGTCCTCCCTGAGCCACAT
CTCGCCCTTCAGCCACTCCAGCCACATGCTGACCACGCCCACGCCGATGCACCCG
CCATCCAGCCTGTCCTTTGGACCACACCACCCCTCCAGCATGGTCACCGCCATGG
GTTAGAGCCCTGCTCGATGCTCACAGGGCCCCCAGCGAGAGTCCCTGCAGTCCCT
TTCGACTTGCATTTTTGCAGGAGCAGTATCATGAAGCCTAAACGCGATGGATATA
TGTTTTTGAAGGCAGAAAGCAAAATTATGTTTGCCACTTTGCAAAGGAGCTCACT
GTGGTGTCTGTGTTCCAACCACTGAATCTGGACCCCATCTGTGAATAAGCCATTC
TGACTCATATCCCCTATTTAACAGGGTCTCTAGTGCTGTGAAAAAAAAAATGCTG
AACATTGCATATAACTTATATTGTAAGAAATACTGTACAATGACTTTATTGCATC
TGGGTAGCTGTAAGGCATGAAGGATGCCAAGAAGTTTAAGGAATATGGGAGAAA
TAGTGTGGAAATTAAGAAGAAACTAGGTCTGATATTCAAATGGACAAACTGCCA
GTTTTGTTTCCTTTCACTGGCCACAGTTGTTTGATGCATTAAAAGAAAATAAAAA
AAAGAAAAAAGAGAAAAGAAAAAAAAAGAAAAAAGTTGTAGGCGAATCATTTG
TTCAAAGCTGTTGGCCTCTGCAAAGGAAATACCAGTTCTGGGCAATCAGTGTTAC
CGTTCACCAGTTGCCATTGAGGGTTTCAGAGAGCCTTTTTCTAGGCCTACATGCTT
TGTGAACAAGTCCCTGTAATTGTTGTTTGTATGTATAATTCAAAGCACCAAAATA
AGAAAAGATGTAGATTTATTTCATCATATTATACAGACCGAACTGTTGTATAAAT
TTATTTACTGCTAGTCTTAAGAACTGCTTTCTTTCGTTTGTTTGTTTCAATATTTTC
CTTCTCTCTCAATTTTTGGTTGAATAAACTAGATTACATTCAGTTGGCCTAAGGTG
GTTGTGCTCGGAGGGTTTCTTGTTTCTTTTCCATTTTGTTTTTGGATGATATTTATT
AAATAGCTTCTAAGAGTCCGGCGGCATCTGTCTTGTCCCTATTCCTGCAGCCTGT
GCTGAGGGTAGCAGTGTATGAGCTACCAGCGTGCATGTCAGCGACCCTGGCCCG
ACAGGCCACGTCCTGCAATCGGCCCGGCTGCCTCTTCGCCCTGTCGTGTTCTGTG

TTAGTGATCACTGCCTTTAATACAGTCTGTTGGAATAATATTATAAGCATAATAA
TAAAGTGAAAATATTTTAAAACTACAAAATGACATCGTATCCACGTGGTGGCCG
AGCTCTTCTAGAATCTGGTAGCTCTAGCTAATTTCAGAGAAAGGAGTTAAAAGA
AACAACTTAACAACCAGACATGTTAAGTTATTCACTAGGAACCGATGCTAACCCC
AGAGAGTCAACGTCTATTTTGGGGGGAGCTGGGAATATTTGGAGTTCTACATGCG
ACCTGGAGGAATTTATCCTGGGGCCGGGGTGACATCTGGGGTCCCCTAGTGAGT
GGCAGTGTGTCTTCCTGCTCTCCTCCTGCCCTCGAAGGAGGACTGGGAAGATTTC
CACGCTGAGATTCCCAGGCGCAAACTGCAGCTGATGCGTTCCTCGAGGTTCTCTT
TGAGATGGAAACGAGCCGGCTGCTCGTGTTCATTTCTGTTTTGCTTTTCTACTGTT
GAATGAATACCACCACAGTGAAGGGATTATTGGAATGTTTTCGAAACACAAAAT
AACCATTTTGTAACTTCTGCTGTATAGTTTTCTTTTCCTGTGGATGGAGTGTGTAA
CTACAGCACACATTTAAATGAAATCTCTGTTAATCGCCTCTGCACTATCTTAGCA
AATATTTTAAACCTAAAGCTAAATGTTGAAATAAAGGTGTAGAGCATTACTGAG
ATGCAAATGGAGCTCTCTCTGGCTCCTAATTAATGACCTACAACTCGACTGTTGT
TTCCAATTACTTTTGAAACACTGAAGGAAAGAATCACTGCTG